

**SCF-mediated degradation of the two translational regulators,
CPB-3 and GLD-1, during oogenesis in *C. elegans*.**

DISSERTATION

zur Erlangung des akademischen Grades
Doctor rerum naturalium
(Dr. rer. nat.)

vorgelegt

der Fakultät Mathematik und Naturwissenschaften
der Technischen Universität Dresden

von

Edyta Kisielnicka

geboren am 17. Juni 1986 in Sztum, Polen

Gutachter:

Prof. Dr. Christian Dahmann

Prof. Dr. Elisabeth Knust

Eingereicht am 26.01.2017

Tag der Verteidigung:

Summary

The development of an organism and its adult homeostasis rely on regulatory mechanisms that control the underlying gene expression programs. In certain biological contexts, such as germ cell development, gene expression regulation is largely executed at the post-transcriptional level. This relies on RNA-binding proteins (RBPs), whose activity and expression are also heavily controlled. While the RNA-binding potential of RBPs is currently of intense scrutiny, surprisingly little is known to date about the molecular mechanisms that control RNA-binding proteins abundance in the context of germ cell development.

This work identifies the molecular mechanisms that shape expression patterns of two evolutionarily conserved RNA-binding proteins, CPB-3 and GLD-1, which belong to CPEB and STAR protein family, respectively. By focusing on their regulation in the *C. elegans* germ line, this work reveals an involvement of the proteasome in reducing levels of CPB-3/CPEB and GLD-1/STAR at the pachytene-to-diplotene transition during meiotic prophase I. Furthermore, it documents that CPB-3 and GLD-1 are targeted to proteasomal degradation by a conserved SCF ubiquitin ligase complex that utilises SEL-10/Fbxw7 as a substrate recognition subunit. Importantly, destabilisation of both RBPs is likely triggered by their phosphorylation, which is regulated by the mitogen-activated protein kinase, MPK-1, and restricted to the meiotic timepoint of pachytene exit. Lastly, this work investigates the potential consequences of target mRNA regulation upon delayed RBP degradation. Altogether, the collected data characterise a molecular pathway of CPEB and STAR protein turnover, and suggest that MPK-1 signaling may couple RBP-mediated regulation of gene expression to progression through meiosis during oogenesis.

Table of Contents

Summary	3
Table of Contents.....	5
1 Abbreviations	9
2 Introduction	13
2.1 Regulation of gene expression.....	13
2.1.1 Regulation of protein synthesis.....	13
2.1.2 Global regulation of translation	19
2.1.3 Gene-specific regulation of translation	20
2.1.4 Regulation of protein degradation	25
2.2. Meiosis.....	34
2.2.1 Interphase - preparing for the division.....	37
2.2.2 Meiotic division	38
2.2.3 Cytokinesis	40
2.2.4 Meiotic arrest	41
2.3. <i>C. elegans</i> germ line as a model to study translational regulation in oogenesis.	41
2.3.1 The two sexes	42
2.3.2 Germ line development in <i>C. elegans</i> hermaphrodite.....	42
2.3.3 Cellular organisation of the adult hermaphrodite germ line.....	45
2.3.4 Soma-to-germ line communication and key signaling pathways involved..	46
2.3.5 Translational regulation in <i>C. elegans</i> gametogenesis.....	50
2.3.6 Regulated expression of RNA-binding proteins.....	52
2.4 Aim of Thesis	65
3. Results.....	67
3.1 CPB-3 expression is regulated by SCF^{SEL-10} complex and proteasome	67
3.1 Proteasome activity restricts CPB-3 expression	67
3.1.1 Setting up RNAi feeding regimes to inhibit proteasome activity.....	67
3.1.2 Proteasome inhibition by RNAi leads to a partial stabilisation of CPB-3.....	72
3.2 SEL-10 is an F-box-WD40 protein that regulates CPB-3	74
3.2.1 CPB-3 interacts with SEL-10 in heterologous systems	75
3.2.2 CPB-3 is partially stabilised in <i>sel-10(0)</i> animals	79
3.2.3 Phosphorylated CPB-3 accumulates upon <i>cul-1</i> knock-down	80
3.2.4 An additional proteasome-dependent pathway regulates CPB-3 expression	82
3.2.5 Additional pathways mediating CPB-3 degradation may be independent of Cullin-based ubiquitin ligases and APC/cyclosome.....	84
3.3 CPB-3 is phosphorylated <i>in vivo</i>.....	86
3.3.1 Difficulties in detecting phosphorylated CPB-3	86
3.3.2 CPB-3 is phosphorylated in wild-type worms	91
3.3.3 Phosphorylated CPB-3 accumulates in <i>sel-10(0)</i> animals.....	92
3.3.4 Bioinformatic analysis of CPB-3 sequence predicts phosphorylation sites and degrons	95
3.3.5 Identification of phosphorylated residues in CPB-3 by mass spectrometry	99
3.4 Kinase-mediated regulation of CPB-3 stability.....	101

3.4.1	CDK-1 and PLK-1 are probably not involved in regulating CPB-3 stability	102
3.4.2	MAP kinase MPK-1 influences CPB-3 stability.....	104
3.4.3	The MAP kinase MPK-1 regulates CPB-3 phosphorylation.....	104
3.4.4	CPB-3 binds to MPK-1 in yeast	106
3.5	Phosphorylation of CPB-3 links its degradation to meiotic progression	107
3.5.1	Hyperphosphorylated CPB-3 does not accumulate in the pachytene-arrested mutant, <i>daz-1(0)</i>	107
3.5.2	The total amount and activity of MPK-1 are decreased in <i>daz-1(0)</i> mutant germ lines.....	109
3.5.3	Phosphorylated CPB-3 does not accumulate in early- and mid-pachytene	111
3.6	CPB-3 influences the expression of its own regulators.....	114
3.6.1	SEL-10 expression is developmentally regulated	114
3.6.2	<i>cpb-3</i> activity promotes <i>sel-10</i> 3' UTR reporter translation in late pachytene	116
3.6.3	<i>cpb-3</i> activity promotes <i>mpk-1</i> 3' UTR reporter translation in pachytene	118
3.II	GLD-1 expression is regulated by the ubiquitin-proteasome system.....	121
3.7	Regulated protein turnover of GLD-1.....	121
3.7.1	Reduced proteasome activity causes partial stabilisation of GLD-1	121
3.7.2	GLD-1 expression persists longer in oogenesis of <i>sel-10(0)</i> mutant worms	124
3.7.3	<i>sel-10</i> activity regulates the abundance of GLD-1 on the protein level.....	125
3.7.4	SEL-10 likely regulates GLD-1 in context of an SCF E3 ubiquitin ligase.....	131
3.7.5	GLD-1 binds to SEL-10 in yeast	132
3.8	GLD-1 is phosphorylated <i>in vivo</i>	134
3.8.1	Modified GLD-1 accumulates in the absence of <i>sel-10</i> activity	134
3.8.2	Analysis of GLD-1 sequence predicts phosphorylation sites and degrons	135
3.8.3	Identification of phosphorylated residues in GLD-1 by mass spectrometry	139
3.9	GLD-1 is likely regulated by MAP kinase, a master regulator of oogenesis	141
3.9.1	The MAP kinase, MPK-1, regulates GLD-1 phosphorylation.....	141
3.9.2	GLD-1 binds to MPK-1 in yeast.....	143
3.10	Prolonged GLD-1 expression in <i>sel-10(0)</i> mutant changes the expression pattern of GLD-1 mRNA targets modestly	145
3.11	GLD-1 expression in <i>sel-10(0)</i> mutant can be further stabilised by an inhibition of the proteasome	149
3.11.1	Extended GLD-1 expression can be further stabilised by an inhibition of the proteasome in the <i>sel-10(0)</i> mutant germ lines.....	150
3.11.2	A CUL-2-based ubiquitin ligase mediates GLD-1 degradation in late oogenesis	152
4.	Discussion.....	157
4.1	Roles of the ubiquitin-proteasome system (UPS) in regulating RNA-binding proteins in the germ line.....	157
4.1.1	Degradation of CPB-3 and GLD-1 may support oogenic gene expression program.....	161
4.1.2	Expression pattern of CPB-3 and GLD-1 is shaped by translational regulation and proteasomal degradation.....	162
4.1.3	A conserved tumor suppressor, Fbxw7, regulates CPB-3 and GLD-1 stability	163
4.1.4	Additional, yet unidentified E3 ubiquitin ligase may regulate CPB-3 and GLD-1 expression pattern	165

4.2 Phosphorylation of RNA-binding proteins	167
4.2.1 Phosphorylation couples RBPs degradation to meiotic progression.....	167
4.2.2 MPK-1/MAPK regulates phosphorylation of CPB-3 and GLD-1	168
4.2.3 Functional implications of RBPs phosphorylation.....	171
4.2.4 CPB-3 and GLD-1 orthologs are regulated by phosphorylation.....	173
4.3 Consequences of the prolonged expression of CPB-3 and GLD-1 on oogenesis	178
4.4 CPB-3 and GLD-1 may regulate translation of their own degradation machinery.....	181
5. Materials and Methods	187
5.1 Media and solutions	187
5.2 Inhibitors and blocking reagents.	189
5.3 Other chemicals and reagents	190
5.4 Cells.....	190
5.5 Primers	191
5.6 Antibodies	192
5.7 Strains	193
5.8 Worm maintenance, crosses and genotyping.....	193
5.9 Large-scale worm culture.	195
5.10 RNAi feeding.....	196
5.11 Immunocytochemistry.	198
5.12 Gel electrophoresis	199
5.13 Western blotting.....	200
5.14 Protein extracts.....	202
5.15 Protein co-immunoprecipitation (Co-IP) experiments (at 4°C)	206
5.16 Phosphatase assays	207
5.17 Purification of recombinant proteins from insect cells for mass spectrometry analysis	208
5.18 Analysis of fluorescent images.....	209
5.19 Bioinformatic tools	210
References	213
Acknowledgements	237
Declaration.....	239

1 Abbreviations

3' UTR	three prime untranslated region
5' UTR	five prime untranslated region
aa	amino acid
APS	ammonium persulfate
a.u.	arbitrary units
BSA	bovine serum albumin
bp	base pairs
CPEB	cytoplasmic polyadenylation element binding protein
cPAP	cytoplasmic poly(A) polymerase
CRL	Cullin-RING (E3) ligase
Cy3	Cyanine 3
DAPI	4',6-diamidino-2-phenylindole
DNA	deoxyribonucleic acid
DTC	distal tip cell
E1	ubiquitin-activating enzyme
E2	ubiquitin-conjugating enzyme
E3	ubiquitin ligase
eIF	eukaryotic (translation) initiation factor
ER	endoplasmic reticulum
FBF	<i>fem-3</i> binding factor
GLD	germ line development defective
gp	guinea pig
GSC	germline stem cell

Abbreviations

gt	goat
GTP	guanosine-5'-triphosphate
HECT	<u>h</u> omology to <u>E</u> 6-associated protein <u>C</u> -terminus
HEPES	4-(2-hydroxyethyl)-1-piperazineethanesulfonic acid
IP	immunoprecipitation
KH	hnRNP K homology
LB	lysogeny broth
lf	loss of function
λPP	phage lambda protein phosphatase
MAPK	mitogen-activated protein kinase
min	minutes
ml	milliliter
μl	microliter
μm	micrometer
mo	mouse
MR	mitotic region
mRNA	messenger RNA
mRNP	messenger ribonucleoprotein; mRNA-protein complex
NC	nitrocellulose
NGM	nematode growth medium
ORF	open reading frame
PAA	polyacrylamide
PABP	poly(A) binding protein
PAGE	polyacrylamide gel electrophoresis
PAP	poly(A) polymerase
PFA	paraformaldehyde

PIC	pre-initiation complex
PMSF	phenylmethanesulphonyl fluoride
PUF	Pumilio and FBF
PVDF	polyvinylidene difluoride
rb	rabbit
RNA	ribonucleic acid
RNAi	RNA interference
RNP	ribonucleoprotein
rpm	rounds per minute
rt	rat
s	seconds
S	svedberg, sedimentation unit
SCF	(Skp-1, Cullin, F-box)- a type of E3 ligases
siRNA	small interfering RNA
SDS	sodium dodecylsulfate
ss	single stranded
ssDNA	salmon sperm DNA
STAR	signal transduction and activation of RNA
TCA	trichloroacetic acid
TEMED	N,N,N',N'-Tetramethylethylenediamine
TF	transcription factor
tRNA	transfer RNA
TZ	transition zone
Ub	ubiquitin
UPS	ubiquitin proteasome system
X-gal	5-bromo-4-chloro-3-indolyl- β -D-galactopyranoside

2 Introduction

2.1 Regulation of gene expression

Multicellular organisms face the challenge of developing highly organised structures such as organs and body parts. The cells that build up different organs have the same DNA content but express genetic information differently. A great scientific effort is put into investigating mechanisms that make neighbouring clonal cells express genes distinctively.

Reproducible development of the body plan (i.e. the fact that organisms of one species are so similar among themselves) suggests that gene expression is tightly regulated. Different expression programs can result from asymmetric divisions in which certain factors are deposited in one daughter cell but not in the other; thus, sister cells develop further dissimilarly. Alternatively, different gene expression programs can be triggered by a stimulus, e.g. a morphogen or any other signaling molecule. The dynamic changes in gene expression lay the basics of the development.

Most of signaling events and enzymatic activity is executed by proteins. Thus, protein amounts and activities in cells are regulated at multiple levels, starting from their synthesis and ending at their degradation.

2.1.1 Regulation of protein synthesis

Protein synthesis comprises two major steps, which in eukaryotes are spatially separated: transcription of DNA to messenger RNA (mRNA) in the nucleus, and translation of mRNA to a polypeptide chain in the cytoplasm (Figure 2.1.1)(summarised from Alberts et al., 2014). Newly synthesised mRNA undergoes multiple modifications to mature into a template for protein synthesis; this includes intron excision, exons joining, and an attachment of structural elements not encoded in the DNA: methylguanosine cap at 5'-end (referred to as 5' cap) end and poly-adenosine tail at the 3'-end (poly(A) tail)(Alberts et al., 2014). From the beginning of its life, mRNA is associated with various proteins forming ribonucleoprotein complexes (RNPs; reviewed in Singh

et al., 2015). Such complexes are translocated through the nuclear pore to the cytoplasm. There, mRNA is immediately translated or kept translationally silent until transported to a target location and/or re-activated in response to a stimulus. Eventually, mRNA undergoes degradation. All the above-mentioned steps of mRNA life are regulated by a number of mechanisms. The following sections will briefly discuss some of these mechanisms focusing on eukaryotic ones and disregarding differences to prokaryotic system.

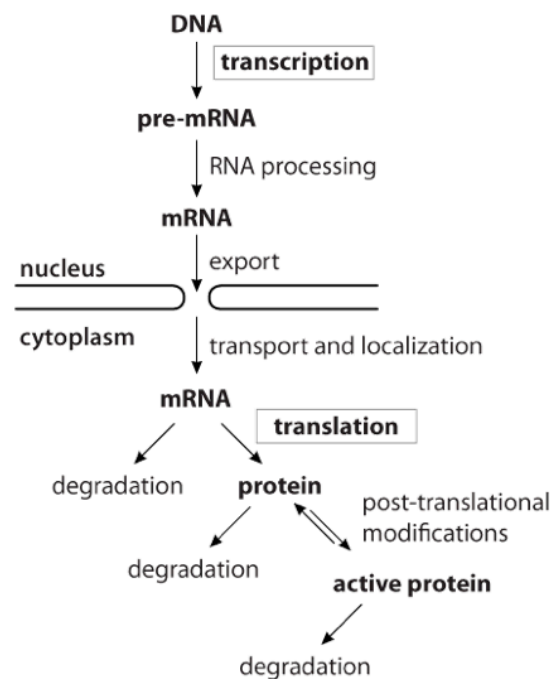


Figure 2.1.1. Gene expression pathway.

Overview of molecular processes that regulate protein synthesis and activity.
Figure adapted from Alberts, (2008).

2.1.1.1 Regulation of mRNA in the nucleus

During transcription, information about protein sequence encoded in DNA is copied onto a less stable molecule - mRNA. Several aspects of this process are regulated: the number of copies (pre-mRNA molecules) produced, excision of transcript fragments (splicing), and incorporation of non-coding sequences (alternative termination site choice)(Alberts et al., 2014).

The number of transcripts produced is determined by regulatory elements in the DNA, such as promoters, enhancers and silencers. These sequences are recognised by specific proteins, transcription factors (TFs; reviewed in Spitz and Furlong, 2012). Transcription factors assemble complexes

that influence the rate of transcription initiation, either promoting (activators) or blocking (repressors) transcription. Their abundance and ability of binding to DNA is a key to the regulation of transcription rate.

pre-mRNA editing may also be regulated. Exon skipping, intron inclusion, and alternative splice site choice, are several best-known demonstrations of alternative splicing. Distinct composition of mRNA coding sequence results in the synthesis of different proteins (isoforms) from one gene. Isoforms may have different properties, such as affinity to interacting proteins or subcellular localisation. Alternative splicing plays a key role in sex determination in the fly, *Drosophila sp.* (Salz and Erickson, 2010).

In addition to differences in the coding sequence, transcripts from the same gene can differ in regard to the 5'- and 3'-untranslated regions (UTRs). Alternative 5' and 3' UTRs originate from an alternative choice of a transcription start site and a transcription termination site, respectively (reviewed in Hinnebusch et al., 2016; Curran and Weiss, 2016; Elkon et al., 2013; Tian and Manley, 2016). UTRs often contain sequences that influence translation rate. Longer UTRs can accommodate more regulatory elements. Hence, the choice of transcription start and termination site may influence the translation rate of mRNA. The length of the UTRs of some genes is regulated during development (reviewed in Davuluri et al., 2008; Kuersten and Goodwin, 2003).

A variety of pathways exist to regulate the abovementioned aspects of transcription. These regulatory mechanisms allow cells to respond to changing conditions, such as stress, growth needs, or signals from other cells.

2.1.1.2 Regulation of mRNA in the cytoplasm

After translocation to the cytoplasm, mRNA may serve as a template for protein synthesis. Multiple mechanisms control the amount of the protein synthesised from a particular mRNA. Two aspects are regulated: mRNA stability and translatability (reviewed in Kong and Lasko, 2012; Garneau et al., 2007). An unstable mRNA gives rise to few protein molecules before it is degraded. Next round of transcription is required to produce more protein. By contrast, stable mRNA can serve longer as a template. This does not necessarily mean that it will give rise to higher number of protein molecules than an unstable mRNA.

Translation of stable mRNAs is often heavily regulated and to date we know more proteins involved in translational repression than activation.

Regulation of stability and translatability is largely mediated by two generic elements of mRNA: the 5' cap and 3' poly(A) tail (Figure 2.1.2). These two stability determinants protect mRNA from digestion by cytoplasmic exonucleases and synergistically enhance translation. Poly(A) tail is bound by poly(A)-binding protein (PABP), which interacts with 5' cap-bound eIF4E (reviewed in Wigington et al., 2014). These interactions result in pseudo-circularisation of mRNA molecules and promote ribosome recruitment. Compromising any of involved elements, which would disrupt circular structure, decrease translation initiation rate and direct mRNA to decay. Thus, regulation of mRNA stability and translatability are difficult to separate as many mechanisms affect both features. The following sections will focus on mechanisms regulating translation.

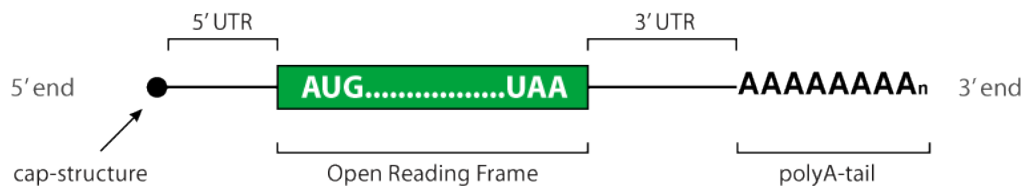


Figure 2.1.2 Schematic drawing of mRNA.

Stick diagram showing mRNA generic features: cap-structure, 5' UTR, Open Reading Frame (ORF), 3' UTR, and poly(A) tail. poly(A) tail is a dynamic element; its length changes during mRNAs lifetime, hence the designation A_n .

Regulation of translation allows the cell to adjust protein production to the needs, without increasing the number of mRNAs copies in the cell, i.e. independently of transcription. Post-transcriptional regulation of gene expression has several advantages. First, it allows localised production of protein. For instance, neurons permit translation of certain mRNAs in dendritic spines of stimulated synapses, while repressing it in non-stimulated dendritic spines and in the cell body. This localised expression functions in strengthening or weakening synaptic connections (reviewed in Costa-Mattioli et al., 2009). Secondly, advantage of translational regulation is that it enables the control of gene expression when transcription is blocked, e.g. in late meiosis, when

chromatin is highly condensed, or in early embryogenesis, when cells undergo very fast division before starting differentiation (reviewed in Richter, 2007). Third, translational regulation facilitates a fast reaction to a stimulus, as mRNAs encoding response proteins can be accumulated in the cytoplasm in translationally repressed state and quickly activated. An example here is frog or mammalian oocytes, which initiate meiosis and morphological development but then arrest their growth, only to resume it upon the reception of a hormonal signal (reviewed in Radford et al., 2008). Lastly, translational regulation can serve to fine-tune transcriptional regulation, as it happens e.g. for a number of genes whose expression oscillates in circadian cycles (Kojima et al., 2012).

The process of translation involves three phases: initiation, elongation and termination (summarised from Aitken and Lorsch, 2012; Gebauer and Hentze, 2004; Kong and Lasko, 2012). The initiation phase comprise events that lead to the assembly of an elongation-competent 80S ribosome. Over 20 proteins participate in the formation of this complex creating multiple possibilities for regulation events (summarised in figure 2.1.3). GTP-bound eukaryotic initiation factor 2 (eIF2) specifically recognises methionine-loaded initiator tRNA (Met-tRNA_i^{Met}), forming a ternary complex (eIF2-TC). The ternary complex associates with the eIF3-, eIF1-, and eIF1A-bound 40S ribosomal subunit, to form an assembly called 43S pre-initiation complex (PIC). A set of three additional initiation factors, eIF4A, eIF4B and eIF4F, unwinds the secondary structures in the 5' region of capped mRNAs. Unwinding allows PIC to bind mRNA and to initiate 5' to 3' scanning in search of the start codon. Base pairing between the start codon and the anticodon triggers a displacement of eIF1, the eIF5-mediated hydrolysis of eIF2-bound GTP, and results in the formation of the 48S initiation complex. The association of the 48S complex with 60S ribosomal subunit triggers displacement of eIFs, which is mediated by eIF5B. Finally, eIF5B-bound GTP is hydrolysed, eIF5B and eIF1A are released and the 80S initiation complex is ready for translation.

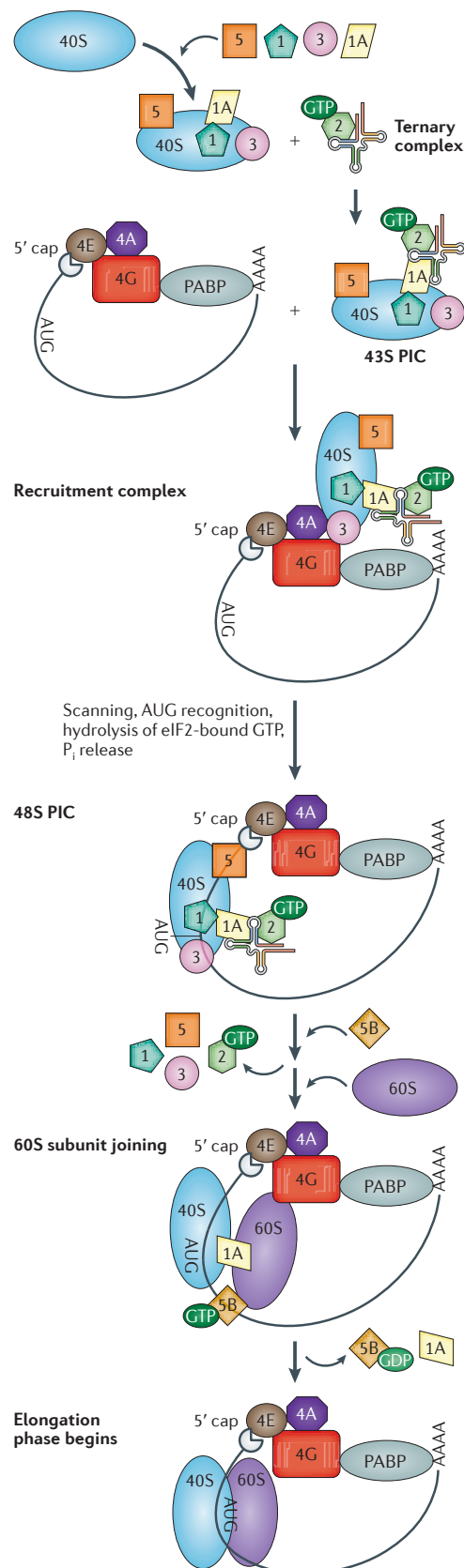


Figure 2.1.3. Cap-dependent translation initiation.

Overview of consecutive steps that lead to the assembly of a translating 80S ribosome.

In the cytoplasm, a free 40S ribosomal subunit is bound by several translation initiation factors (eIFs), which prevent its association with the 60S subunit.

Association of the 40S subunit with the ternary complex (Met-tRNA, eIF2 and GTP) results in a formation of the 43S pre-initiation complex (43S PIC).

43S PIC binds to an mRNA circularised by interactions between 5' cap, eIF4F (consisting of eIF4E, eIF4G and eIF4A), poly(A)-binding protein (PABP), and poly(A) tail. 43S subunit starts scanning mRNA for the AUG start codon.

Recognition of AUG via Met-tRNA is followed by GTP hydrolysis, binding of the large ribosomal subunit, and dissociation of majority of eIFs. At this point, the elongation phase starts.

Figure taken from Kong and Lasko (2012).

In contrast to the initiation, the subsequent steps, i.e. elongation and termination, are mechanistically rather simple. Elongation is stimulated by two elongation factors, EF1 and EF2, which deliver aminoacyl-tRNAs to the codon, hydrolyse GTP, promote ribosome translocation and contribute to proofreading by stabilising perfect matching between codons and anticodons. Due to EFs activity, a ribosome synthesises a polypeptide at a speed of ~ 0.67 amino acids per second, with an accuracy of 99,99% (Alberts et al., 2008; Yan et al., 2016). Translation terminates when a release factor recognises a STOP codon, drives an addition of water molecule to the growing polypeptide, releases the polypeptide from tRNA and causes ribosome disassembly.

Multiple mechanisms exist to regulate translation. The initiation phase, which is mechanistically the most complex, is the principal target of regulation but mechanisms affecting elongation phase have also been identified (Darnell et al., 2011). Regulation may affect translation factors (e.g. their covalent modifications or sequestration in protein complexes) or mRNAs (restricting mRNA access to ribosomes or triggering mRNA degradation). Translational regulation mechanisms are divided into global- and gene-specific ones, depending on whether they affect a majority or only a subset of mRNAs in the cell.

2.1.2 Global regulation of translation

Global mechanisms generally involve changes in the abundance, availability or the activity of translation initiation factors (eIFs; reviewed in Jackson et al., 2010). Various stress conditions, such as starvation, viral infection, or heat shock, usually trigger global translational shut-off (Mathews and Sonenberg, 2007).

A canonical example for the regulation of initiation factor availability is the interaction between eIF4E and the eIF4E-binding protein (4EBP). 4EBP binds to 5' cap-associated eIF4E, thereby blocking access of eIF4G to eIF4E and preventing the ribosome recruitment. 4EBP interaction with eIF4E can be disrupted by phosphorylation of 4EBP. In mammals and *Drosophila*, 4EBP is phosphorylated by a highly conserved kinase, TOR, which becomes activated in response to growth factors. In this way, bulk translational activity in a cell is

regulated by nutritional status and signaling molecules (Dowling et al., 2010; Hay and Sonenberg, 2004; Topisirovic et al., 2010).

Some translation initiation factors (eIFs) are targets of regulatory phosphorylation. For instance, the α subunit of eIF2 (eIF2 α) becomes phosphorylated in response to various conditions, including viral infection, endoplasmic reticulum stress or amino acid starvation. Phosphorylated eIF2 α is fully capable of forming a ternary complex. However, after eIF2-GDP release from the initiation complex, the phosphorylation of eIF2 α blocks the GDP to GTP exchange. As a result, the amount of available eIF2-GTP in the cell drops, which globally inhibits translation (Alberts et al., 2008; Clemens, 2001; Raught and Gingras, 2007).

Although translational regulation affects predominantly the initiation phase, mechanisms affecting elongation have also been unraveled. The activity of elongation factors can be affected by their phosphorylation. The elongation factor-2 (EF2) is phosphorylated and thus inactivated in cells treated with hormones, mitogens and growth factors that increase intracellular calcium levels (Kaul et al., 2011; Ryazanov and Davydova, 1989). Raf-mediated phosphorylation of another factor, EF1A, was shown to decrease its stability and regulate proliferation and apoptosis in cancer cells (Sanges et al., 2012). Interestingly, phosphorylation of an elongation factor has been also described in prokaryotes. Phosphorylation of EF-Tu, which is induced by starvation, globally inhibits protein synthesis (Pereira et al., 2015). Since the identified phosphorylation site is conserved in eukaryotes, the finding raises a possibility that the two domains of life may share some translation-regulating mechanisms.

2.1.3 Gene-specific regulation of translation

In contrast to mechanisms that affect translation globally, gene-specific regulation affects usually a small group of mRNAs and is triggered by RNA sequence. Sequences that influence mRNA stability or translatability are referred to as '*cis*-elements'. They are usually localised in 5' and/or 3' untranslated regions (5' and 3' UTR) of mRNA (Figure 2.1.2). *cis*-elements are recognised by *trans*-acting factors: microRNAs (miRNAs) or RNA-binding proteins (RBPs). These factors recruit proteins that act on generic elements of mRNA (5' cap

structure or 3' poly(A) tail) to modify their interactions with translation initiation machinery or to alter mRNA stability. In addition, RNA-binding proteins often regulate the localisation of mRNA.

Multiple functions of methylguanosine cap and poly(A) tail

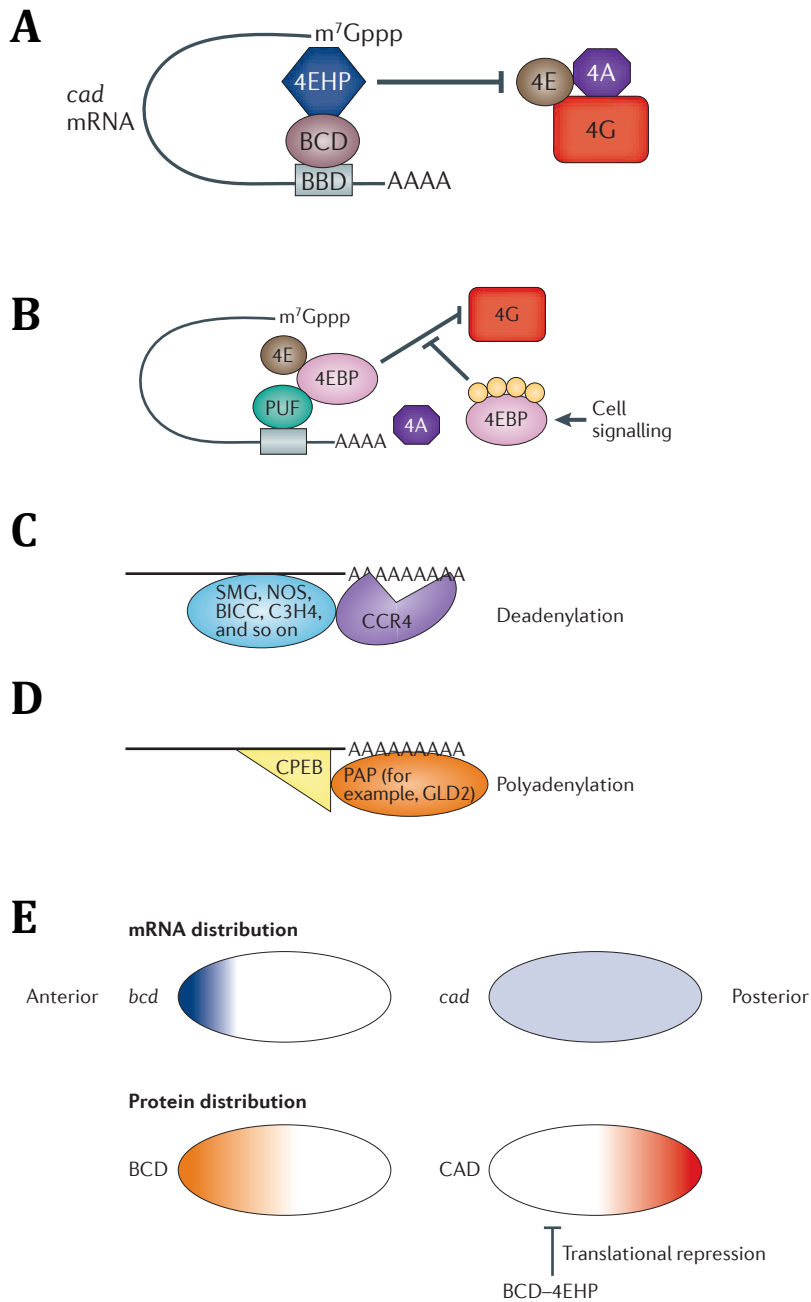
5' cap and 3' poly(A) tail are generic features present on the majority of mRNAs. Both structures are involved in mRNA circularisation, which promotes translation (reviewed in Gebauer and Hentze, 2004; Kong and Lasko, 2012). Additionally, they are important determinants of mRNA stability (reviewed in Garneau et al., 2007; Jalkanen et al., 2014). The 5' cap promotes translation by serving as a binding site for eIF4E; moreover, it regulates mRNA stability by protecting it from digestion by 5'-3' exonucleases. Removal of the 5' cap structure was for a long time considered to irreversibly trigger mRNA degradation. However, re-capping pathways were described recently (Ignatochkina et al., 2015; Mukherjee et al., 2012). The poly(A) tail has a similar, but somewhat more complex role than a cap in regulating mRNA. Whereas the cap structure consists of a single nucleotide, poly(A) tail lengths are different between different mRNAs, cell types and species. Long poly(A) tails correlate with efficient translation and mRNA stability, whereas short poly(A) tails are observed in poorly translated and unstable mRNAs (Jalkanen et al., 2014). These correlations are particularly strong in certain biological contexts, such as gametogenesis or early embryogenesis (Eichhorn et al., 2016; Subtelny et al., 2014; Weill et al., 2012). The length of the poly(A) tail is reversibly regulated by deadenylases (a class of 3'-5' exonucleases) and poly(A) polymerases. The poly(A) tail-mediated regulation of mRNA involves binding of poly(A)-binding protein (PABP), which not only supports an assembly of the initiation complex, but also protects mRNAs from digestion by 3'-5' exonucleases. Together, 5' cap and the poly(A) tail are important "effector structures", through which *trans*-factors, miRNAs and RBPs, regulate mRNAs translation.

Masking the 5'-cap (preventing 4E-cap interaction)

Since the 5' cap is extremely important for mRNA stability, mechanisms that regulate translation do not remove the cap but rather act on the accessibility of the cap structure to translation initiation factors (reviewed in Topisirovic et al., 2010). One mechanism involves binding the cap by a protein similar to eIF4E, such as 4E-homologous protein (4EHP; also known as eIF4E2) (Figure 2.1.4 A). In contrast to eIF4E, 4EHP cannot bind eIF4G, and therefore hinders the association of the pre-initiation complex (PIC) with mRNA. In *Drosophila* embryogenesis, 4EHP is recruited by Bicoid (BCD) protein to the caudal (*cad*) mRNA (Cho et al., 2005). Inhibition of *cad* translation occurs only in the anterior part of the embryo, permitting *cad* translation in the posterior, which plays an important role in establishing a polarity axis (Figure 2.1.4 E). Similarly, Prep1 protein expressed in mammalian oocytes was suggested to bind 4EHP to regulate Hoxb4 mRNA translation and oocyte development (Villaescusa et al., 2009).

Masking the 4EF-bound cap (preventing 4E-4G interaction)

A variation of the cap-dependent mode of regulation is an inhibition of eIF4G association with mRNA by masking the 5' cap-bound eIF4E (Figure 2.1.4 B). The masking is done by eIF4E-binding proteins (4EBPs) (Topisirovic et al., 2010). 4EBPs regulate cell cycle and proliferation in response to environmental cues or signaling molecules (e.g. nutrients availability, growth factors). In this context, 4EBP acts rather as a global regulator of translation. However, 4EBP regulates also developmental processes, such as patterning of *Drosophila* embryo, where specific 4EBPs affect mRNAs more selectively. For example, the *Drosophila* 4EBP, CUP, is recruited to *oskar* (*osk*) and *nanos* (*nos*) mRNAs by RBPs Bruno (BRU) and Smaug (SMG), respectively (Nakamura et al., 2004; Nelson et al., 2004). As a consequence, Oskar and Nanos proteins are synthesised only in the posterior cytoplasm of the developing syncytial embryo. Interestingly, the mechanism of CUP-mediated translational repression does not require its eIF4E-binding activity but acts through deadenylation of target mRNAs (Igreja and Izaurralde, 2011; Jeske et al., 2010).



2.1.4. Gene-specific translational regulation.

Overview of mechanisms regulating translation rate from specific mRNA.

(A) eIF4E homolog proteins (4EHP) bind to the 5' cap (m⁷Gppp) preventing cap interaction with eIF4E (4E). In case of caudal (*cad*) mRNA, 4EHP is recruited by Bicoid (BCD) RNA-binding protein. 4G - eIF4G; 4A - eIF4A.

(B) eIF4E-binding proteins (4EBP) bind to the 5' cap-associated eIF4E protein to prevent its interaction with eIF4G (4G). 4EBP may be recruited to mRNA by PUF (Pumilio and FBF) protein. For instance, yeast 4EBP, Caf20p, is recruited by Puf4/Puf5 to the G1 cyclin, CLN3. Association between eIF4E and 4EBP is disrupted by a modification of the 4EBP by phosphorylation.

(C) Shortening of the poly(A) tail destabilises mRNAs and reduces their translation. Shortening is mediated by deadenylases (such as CCR4), which are recruited by a range of RBPs (such as SMG - Smaug, NOS - Nanos, BICC - Bicaudal C, C3H4 - CCCH zinc finger protein C3H-4).

Figure 2.1.4 - continued.

(D) Extension of poly(A) tails by poly(A) polymerases (PAPs) stabilises mRNAs and promotes their translation. Germ Line Development-defective-2 (GLD-2), a non-canonical cytoplasmic poly(A) polymerase, which elongates poly(A) tails but requires RNA-binding proteins (such as CPEB; cytoplasmic polyadenylation element-binding protein) to efficiently interact with mRNAs.

For simplicity, additional RNA-associated proteins that mediate or stabilise interactions between depicted RBPs and effector proteins are omitted from the picture.

(E) Example of translational control in *Drosophila* early embryo. Translation of anteriorly localised *bicoid* (*bcd*) mRNA results in a formation of Bicoid (BCD) protein gradient along anterior-posterior axis of an embryo. One of the functions of BCD is the recruitment of 4EHP and translational inhibition of *caudal* (*cad*) mRNA. The repression is strong in the anterior and weak in posterior of the embryo, which results in generation of caudal protein (CAD) gradient. BCD and CAD function as morphogens regulating transcription of developmental genes.

Figure adapted from Kong and Lasko, (2012).

Shortening the poly(A) tail

Whereas multiple poly(A)-binding proteins (PABPs) associate with long poly(A) tails to prevent mRNA degradation and promote translation, only few PABPs associate with short tails, which leads to translational repression and sometimes degradation of mRNA (reviewed in Eckmann et al., 2011; Villalba et al., 2011; Weill et al., 2012). Poly(A) tail shortening is mediated by deadenylases, such as the CCR4-NOT complex (Figure 2.1.4 C). Multiple examples of deadenylases activity during gametogenesis and early embryogenesis have been described, which illustrates the importance of poly(A) tail metabolism in these biological contexts. In *Drosophila* embryo, CCR4 is recruited by aforementioned Nanos protein to *cyclin B* mRNA to regulate cell cycle progression (Kadyrova et al., 2007). Furthermore, CCR4 is recruited by SMG to multiple maternal mRNAs to mediate their degradation at the maternal-to-zygotic (oocyte-to-embryo) transition (Tadros et al., 2007). In *Xenopus* oogenesis, different deadenylases are recruited to different mRNAs that control meiotic division. The zinc finger protein C3H-4 recruits the CCR4-NOT complex to such mRNAs as *emi1* and *emi2* (Belloc and Mendez, 2008), whereas another deadenylase, PARN, recruited by CPEB1, represses *cyclin B* mRNAs (Kim and Richter, 2006).

Lengthening the poly(A) tail

Lengthening of a poly(A) tail, which leads to stabilisation of mRNAs and their translational activation, is mediated by cytoplasmic poly(A) polymerases (cytoPAPs) (Eckmann et al., 2011; Villalba et al., 2011; Weill et al., 2012) (Figure 2.1.4 D). In *Xenopus* oocytes, cytoPAP Gld2 is recruited to *cyclin B* or *mos* mRNA by CPEB1, the same protein that recruits deadenylase PARN (Kim and Richter, 2006). The regulation of polyadenylation status of CPEB1 target mRNAs was suggested to depend on the phosphorylation status of CPEB1. Unphosphorylated CPEB associates with both PARN and Gld2 and its mRNA targets remain translationally silent. Phosphorylation of CPEB results in an expulsion of PARN from the complex, Gld2-mediated extension of poly(A) tails and translational activation of mRNAs (Kim and Richter, 2006). Interestingly, a similar mechanism was identified in mouse neurons. Stimulation of dendrites induced CPEB phosphorylation, which resulted in remodeling of a regulatory complex on *NR2A* mRNA, which encodes a subunit of NMDA receptor. CPEB phosphorylation and mRNP remodelling increased *NR2A* translation (Udagawa et al., 2012). Although cases of CPEB-independent cytoplasmic polyadenylation were reported (Charlesworth et al., 2006; Vishnu et al., 2011; Wu et al., 1997), CPEB proteins have long remained the only known factor able to recruit cytoPAPs. Recently, however, Gld2 was shown to be recruited to mRNAs by an RNA-binding protein Musashi in *Xenopus* oocytes (Cragle and MacNicol, 2014) and by a STAR protein family member, QKI-7, in human somatic cells (Yamagishi et al., 2016).

Altogether, several mechanisms exist to regulate the translatability and stability of an mRNA in the cytoplasm. The triggers for those mechanisms are elements of the mRNA sequence, which help to regulate the amount of synthesised proteins.

2.1.4 Regulation of protein degradation

The abundance of regulatory proteins is tightly controlled and limited in time and space. In addition to multiple pathways that restrict protein synthesis, a number of molecular mechanisms regulate protein activity post-translationally. Having fulfilled its function, a protein needs to be removed from the cell. Without

degradation, unnecessary or damaged proteins would accumulate, and their excess could interrupt proper functioning of a cell. Especially in unidirectional processes, such as cell division, mis-expression of a protein can cause re-iteration of a stage. A perfect example for such a situation is the persistence of katanin after meiosis. Katanin is a microtubule-severing protein. Its activity contributes to the formation of an acentriolar and anastral spindle that drives chromosomes segregation during meiosis. Normally, katanin is degraded after meiosis. Its persistence impairs formation and positioning of the centriolar, astral spindle in zygotic division (Srayko et al., 2000).

In order to prevent ectopic activity of proteins, cells have a range of pathways to specifically recognise and degrade obsolete proteins. The main proteolytic systems in the cell are the lysosomal pathway and the proteasome machinery.

2.1.4.1 Lysosomes

Lysosomes are membrane-bound vesicular organelles, which degrade a great variety of compounds. Lysosomes fuse with other vesicles, such as autophagosomes or endosomes, and hydrolyse their content with an array of lysosomal enzymes (Alberts et al., 2014).

Autophagosomes are vesicles that contain cells own organelles and bulk proteins. It was long thought that the cytosolic proteins they contain were taken up non-specifically; however, accumulating evidence suggests that some proteins, such as maternally contributed P granule component, PGL-3, in the *C. elegans* embryo, are deliberately targeted to autophagosomes (Kaushik and Cuervo, 2012; Zhang et al., 2009).

Endosomes, in turn, have a well-established function in specific protein degradation as they regulate the number of cell surface receptors. Internalised receptors can be recycled to the cell membrane or degraded in endolysosomes. Interestingly, also some cytosolic proteins, including cell cycle regulator p27 or a small GTPase RhoB, were reported to be targeted to the endolysosomal pathway for degradation (Fuster et al., 2010; Pérez-Sala et al., 2009).

Currently, a global understanding of how cytoplasmic proteins are recruited to lysosomal degradation pathway remains rather poor. Research can

be complicated by the fact that some investigated proteins are in parallel degraded by the ubiquitin-proteasome system.

2.1.4.2 The ubiquitin-proteasome system (UPS)

The majority of cytosolic proteins are degraded in a controlled manner by a multi-subunit molecular machine - the proteasome (Alberts et al., 2014). To become recognised by the proteasome, target proteins require a post-translational modification - a covalent attachment of the small protein, ubiquitin (Ub) (Figure 2.1.5). Ligation of ubiquitin to target proteins is a highly regulated process performed by specialised enzymes - ubiquitin ligases. Eukaryotes encode hundreds of ubiquitin ligases in order to target proteins specifically and achieve proper time and localisation of their degradation. The proteasome and enzymes that regulate ubiquitination form the ubiquitin-proteasome system (UPS).

2.1.4.3 Structure and activity of the proteasome

The proteasome is a large assembly of proteins, containing up to 66 subunits, with a sedimentation constant of 26S. It consists of a tunnel-like core particle (20S), where proteolysis occurs, and a regulatory particle (19S), which assists in substrate binding and performs several regulatory functions (Chen et al., 2016; Finley et al., 2016; Huang et al., 2016; Jackson et al., 2000; Schweitzer et al., 2016; Willems et al., 2004). Substrates bind to the 19S regulatory particle through their polyubiquitin chain. A predominant notion is that a minimal degradation signal consists of four linked ubiquitin molecules (Thrower et al., 2000). However, a single ubiquitin is sufficient to destabilise 150 amino acids-long oligopeptide chains (Shabek et al., 2012). While several subunits of the regulatory particle serve to bind the ubiquitin tag, others partially unfold the substrate protein to allow its entrance into the tunnel of the proteasomal core (Finley, 2009). Target protein is cleaved into ~3-30 amino acids long oligopeptides (Kisselev et al., 1998), which are later degraded to amino acids by cytosolic endopeptidases (Saric et al., 2004). Ubiquitin is usually saved from degradation by the activity of deubiquitinating enzymes, which are components of the 19S subunit. Noteworthy, there is also a plethora of cytosolic de-

ubiquitinating enzymes, which counteract the activity of ubiquitin ligases (Eletr and Wilkinson, 2014; Komander et al., 2009).

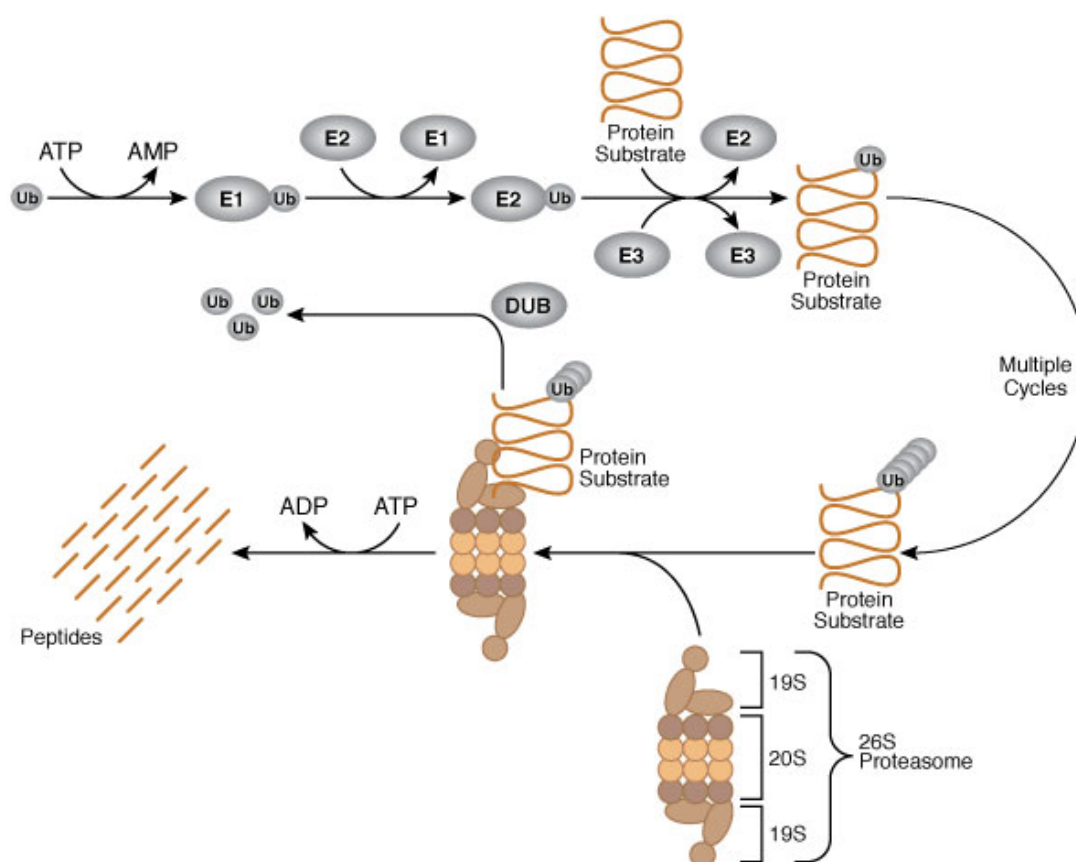


Figure 2.1.5 Mechanism of protein degradation by the Ubiquitin-Proteasome System (UPS).

In a sequence of reactions, three types of enzymes, designated E1, E2, E3, covalently attach ubiquitin molecules to the target protein. Ubiquitinated proteins bind to the 19S regulatory particle of the 26S proteasome. Ubiquitin moieties are removed from the protein by de-ubiquitinases (DUB) and can be used in another ubiquitination cycle. The 19S particle unfolds the protein substrate and assists its entry into the 20S core of the proteasome, where proteolytic cleavage occurs. The degradation products of 3-30 amino acid-long peptides are further digested to individual amino acids by cytoplasmic endopeptidases (not shown). Figure adapted from

https://media.cellsignal.com/www/pdfs/science/pathways/Ubiquitin_Proteasome.pdf

2.1.4.4 Ubiquitination

Ubiquitin (Ub) is a highly conserved, 76 amino acid long protein. It is attached to target proteins by forming an isopeptide bond between the C-terminal glycine of Ub and the amino group of a lysine in a target protein. This covalent attachment is performed in a cascade of reactions involving three different enzymes (Figure 2.1.5).

First, the C-terminal glycine of the ubiquitin polypeptide forms a high-energy thiol-ester bond with a ubiquitin-activating enzyme, generally referred to as E1. This step is associated with ATP hydrolysis. Subsequently, ubiquitin is transferred to a ubiquitin-conjugating enzyme, termed E2, and then to a target substrate selected by a ubiquitin ligase, known as E3 (Alberts et al., 2014).

Since E3 ubiquitin ligases provide specificity of substrate recognition, they are the most numerous and diversified components of the ubiquitination pathways. This is reflected in the number of human genes encoding enzymes in each category: while there are only two genes coding for E1 enzymes and ~30 for E2, ~600 genes are estimated to encode E3 ubiquitin ligases (Komander, 2009).

Based on the sequence similarity and catalytic properties, E3 ubiquitin ligases can be divided into two major classes: HECT-domain and RING-domain (Berndsen and Wolberger, 2014; Fang and Weissman, 2004; Komander, 2009). A characteristic feature of HECT-domain E3s is that they form a thiol-ester bond with ubiquitin and subsequently catalyse ubiquitin transfer onto the substrate. By contrast, RING-domain E3 ubiquitin ligases do not form a covalent bond with ubiquitin. Instead, a RING domain recruits an E2 enzyme, and ubiquitin is directly transferred from E2 onto the substrate protein. RING-domain E3s are a very large group of proteins. Some of them act as a single polypeptide that recruits both the E2 and a substrate. The canonical example is Mdm2, a monomeric RING-E3, whose N-terminal part recognises the substrate, p53, a well-known transcription factor and proto-oncogene. The C-terminally localised RING finger in Mdm2 recruits an E2, which performs a ubiquitin transfer onto p53 (Fang et al., 2000; Haupt et al., 1997; Spratt et al., 2014). However, the majority of RING-domain E3 ubiquitin ligases do not act as a single polypeptide, like Mdm2, but rather assembly multi-subunit complexes. Since they have been the objects of research in this thesis work, they will be discussed in closer detail.

Multisubunit RING-finger E3s

Multimeric RING-domain ubiquitin ligases belong to the best-characterised E3s (reviewed in Berndsen and Wolberger, 2014; Cardozo and Pagano, 2004; Jackson et al., 2000). The scientific interest in these complexes can be largely attributed to their essential roles in the regulation of the cell cycle. Two classes are particularly important: the anaphase promoting complex/cyclosome (APC/C) and the cullin-RING ligases (CRL) (Figure 2.1.6). Both classes show a similar molecular architecture: the substrate recognition module is connected to the E2-containing module by a scaffold protein (Figure 2.1.6 A). This scaffold protein is cullin in CRLs (such as SCF and CRL2) and a cullin homolog, Apc2, in APC/C. The C-terminus of cullin binds a RING-domain protein, which in turn recruits an E2-ubiquitin conjugate. N-terminus of cullin associates with a substrate adaptor module, which usually consists of at least two components: a substrate recognition subunit (SRS) that specifically recognises the target protein, and a second protein, which mediates SRS binding to cullin (Willems et al., 2004).

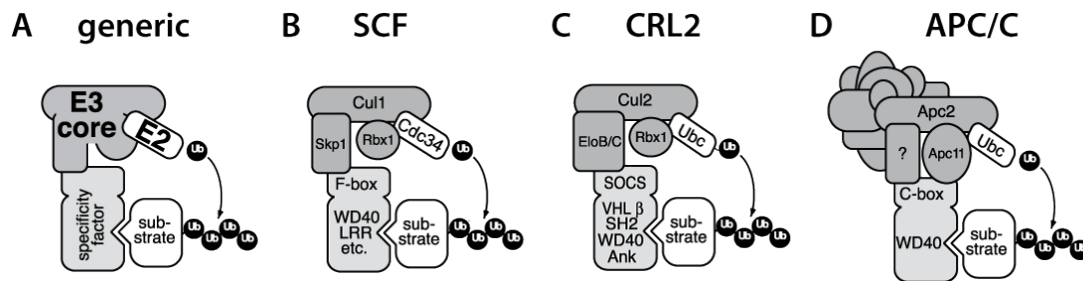


Figure 2.1.6. Schemes of selected multisubunit RING-domain E3 ubiquitin ligases.

(A) A generic scheme of a Cullin-RING ubiquitin ligase. Its E3 core brings together a ubiquitin-conjugated E2 enzyme and a substrate-recognising specificity factor. Ubiquitin is transferred from E2 directly onto a substrate protein.

(B) Composition of an SCF complex. Cullin1 serves as a scaffold protein. Rbx1 is a RING-domain protein that recruits an E2 enzyme (e.g. Cdc34). Skp1 serves as an adaptor to bind different F-box proteins, which function as substrate recognition subunits (SRS).

(C) Composition of a Cullin2-based ubiquitin ligase (CRL2). Similarly to Cullin1, Cullin2 interacts with Rbx1, but instead of Skp1, Cullin2 utilises an ElonginB/C dimer to recruit SOCS-domain SRSs.

(D) Overall architecture of APC/C is similar to CRLs. A cullin-like subunit Apc2 serves as a scaffold; RING domain-containing Apc11 recruits an E2. At least 11 additional proteins are found in an APC/C complex; their functions, however, remain rather poorly characterised. Figure adapted from Willems et al. (2004).

A C-terminally located cullin-homology domain characterises cullin protein family (Sarikas et al., 2011). Eight family members were identified in the human genome; six - in *C. elegans* (Sarikas et al., 2011). Different cullins associate with different substrate adaptors. For instance, Cullin1-based complexes, denoted sometimes as CRL1, but better known as SCF complexes, utilise Skp1 protein to bind a wide range of substrate recognition subunits (Figure 2.1.6 B). Culin2-based complexes do not associate with Skp1. Instead they utilise ElonginB/ElonginC dimers to tether SRSs, which are also distinct from proteins involved in SCF complexes (Figure 2.1.6 C). The modular setup of CRLs allows the same core machinery (Cullin-RING-E2 modules) to associate with multiple substrate recognition subunits and to mediate ubiquitination of a wide range of proteins (Bosu and Kipreos, 2008; Petroski and Deshaies, 2005).

SCF complexes belong to the first E3s ever described because of their essential role in cell cycle progression (reviewed in Nakayama and Nakayama, 2006; Teixeira and Reed, 2013). In addition to degrading cell cycle regulators, such as Sic1 or cyclin E, SCF complexes were found to regulate signaling pathways, e.g. by mediating ubiquitination of NF- κ B. Furthermore, they have developmental roles, such as regulating Hedgehog signaling pathway during *Drosophila* organogenesis and Ras/MAPK signaling in vulva formation in *C. elegans* (de la Cova and Greenwald, 2012; Ou, 2002). The name SCF derives from three main components of the complex: Skp1, Cullin1 and F-box protein. Skp1 is an adaptor protein that bridges Cullin1 to an F-box protein, and the F-box protein is the actual substrate recognition subunit (SRS), which recognises target protein.

2.1.4.5 F-box proteins

F-box proteins are a diversified group of polypeptides, which have in common a ~50 amino acid long domain, called F-box domain (reviewed thoroughly in Skaar et al., 2013; Wang et al., 2014; Zheng et al., 2016a). The domain was identified as a homology region of Skp1-binding proteins, among which was the name-giving protein, cyclin F. Consistently with the ability to bind Skp1, the majority of investigated F-box proteins function in the context of ubiquitin ligases. Recognition of the substrate is mediated by a C-terminally

located protein-protein interaction domain. Most common are WD40 repeats or leucine-rich repeat (LRR) domains but other domains (e.g. Kelch, CASH, proline-rich) were also identified.

The nomenclature of mammalian F-box proteins has been standardised and is based on the domain composition, with Fbxw, FbxL and FbxO standing for F-box proteins with WD40, LRR or other domain, respectively. However, many traditional protein names are still in use, especially in non-mammalian systems (Jin et al., 2004).

Importantly, F-box proteins appear to be intrinsically unstable. Half-lives of three yeast F-box proteins regulating cell cycle and amino acid synthesis, Cdc4, Grr1 and Met30, were estimated to be 5 min, 15 min and 30 min, respectively (Galan and Peter, 1999). Further experiments implied that F-box proteins undergo autoubiquitination in the context of their own SCF complex. Autoubiquitination stimulates their removal from SCF and subsequent proteasomal degradation. This mechanism may have an important biological role. Presumably, it facilitates the exchange of a substrate recognition subunit in SCF ubiquitin ligase complexes. This in turn limits the time window for degradation of particular substrates and therefore allows the ubiquitination machinery to adjust to particular needs of a cell in given conditions (Galan and Peter, 1999).

2.1.4.6 Comparison between phosphorylation and ubiquitination

Due to the high specificity of substrate recognition and the variety of physiological contexts of action, ubiquitination is often likened to phosphorylation (Hunter, 2007; Komander and Rape, 2012; Seet et al., 2006). The similarity between the two modification systems is also visible at the genomic level, as the number of genes encoding modifiers is in ~5-fold excess over the de-modifiers (Figure 2.1.7). Activity of over 500 kinases in human cells is counteracted by ~120 phosphatases, whereas the activity of ~600 ubiquitin ligases is counteracted by ~85 deubiquitinases. However, the complexity of the ubiquitination system is much higher than the complexity of phosphorylation-mediated signaling. In contrast to a single phosphate group, ubiquitin can form an array of polymers (Figure 2.1.8). Each ubiquitin molecule contains seven lysine residues and thus can be modified in different ways. Usually, homogenous

unbranched chains are synthesised. For instance, K48-linked chains are a canonical degradation signal, while K63-linked chains are involved in non-degradative functions, such as endocytosis, DNA damage response and cell signaling. The picture that emerged in the last few years is that ubiquitination is a signaling code involved in regulation of various cellular processes, by modulating protein localisation, activity and stability (reviewed in Komander, 2009; Komander and Rape, 2012).

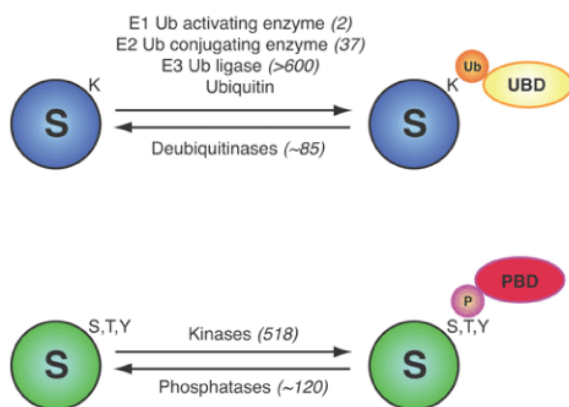


Figure 2.1.7 Comparison between ubiquitination and phosphorylation.

Both types of modification are performed by highly selective enzymes and affect protein function. Both modifications are reversible. The group of enzymes removing the modification is ~5 times smaller than a corresponding group of modifiers.

Figure taken from Komander (2009).

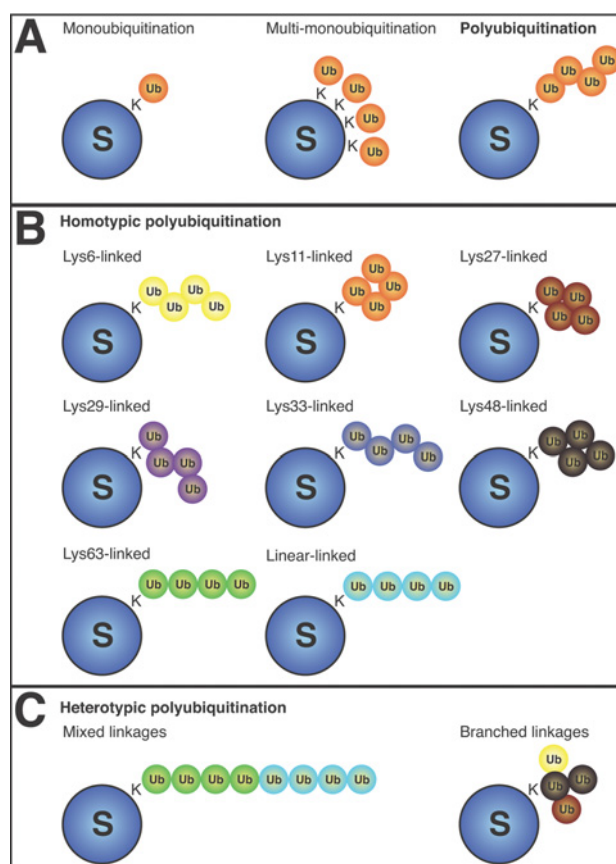


Figure 2.1.8

Various forms of ubiquitination.

(A) Three general layouts of ubiquitination: monoubiquitination, multi-monoubiquitination and polyubiquitination.

(B) Seven lysine residues in ubiquitin allow the formation of differently linked polyubiquitin chains, which form distinct 3D-structures. Particular types of chains serve particular cellular processes.

(C) A polyubiquitin chain can contain diverse types of bonds. Branched chains are also possible.

Figure taken from Komander (2009)

2.1.4.7 Expansion of Skp1- and F-box-related genes in *C. elegans*

The *C. elegans* genome contains an unusually high number of genes encoding F-box proteins and Skp1-related proteins, dubbed SKR (Kipreos and Pagano, 2000; Nayak et al., 2002; Yamanaka et al., 2002). Whereas yeast and human contain only one Skp1 gene, 21 *skr* genes were identified in *C. elegans*. Seven of them (*skr-1*, -2, -3, -7, -8, -9, -10) encode proteins that interact with worm Cullin1 (CUL-1) and thus are expected to function in protein degradation (Nayak et al., 2002; Yamanaka et al., 2002).

Among all Skp1-related proteins, SKR-1 is the most similar to human and yeast Skp1. Genetic analyses support *skr-1* interaction with *cul-1* and F-box protein-encoding *sel-10* gene. *C. elegans skr-1* and -2 share 83% nucleotide identity and 81% amino acid identity, suggesting they may work redundantly (Nayak et al., 2002). The role of the remaining *skr* gene products remains poorly characterised.

F-box genes are also particularly expanded in *C. elegans* (Kipreos and Pagano, 2000; Jin et al., 2004; Thomas, 2006). While 13 F-box proteins were identified in yeast, 27 in *Drosophila*, and 69 in humans, *C. elegans* encodes 326 F-box proteins. Peculiarly, only three predicted F-box proteins in *C. elegans* contain C-terminally located WD40 repeats (Fbxw) and three other, leucine-rich repeats (Fbxl), the two domains most often encountered in substrate recognition subunits of E3s. The majority contains uncharacterised domains and is likely to function outside the context of protein degradation (Kipreos and Pagano, 2000).

2.2. Meiosis

Meiosis is a special type of cell division, which occurs in sexually reproducing eukaryotes. In animals and plants, sexual reproduction involves formation of gametes - cells generated in a process called gametogenesis. Fusion of gametes during fertilisation initiates development of a new organism. Owing to meiosis, the number of chromosomes in gametes is reduced by half compared to parental cells (Figure 2.2.1). Fertilisation restores the normal number of chromosomes (summarised from Alberts et al., 2014; Gilbert, 2006).

In animals, gametes develop from a special cell lineage, the germ line. During gametogenesis, germ cells undergo meiosis and differentiation, which gives them morphological features characteristic for their sexual identity. Male gametes, termed sperm, are usually small and motile, whereas female gametes, called egg cells or ova, are usually large and motionless.

In contrast to clonal reproduction, sexual reproduction generates progeny that is genetically different from parents. The diversity is introduced in three ways. First, fertilisation usually involves gametes coming from two different organisms, male and female. Secondly, segregation of homologs during meiosis I is random (Figure 2.2.2 A). Thirdly, genetic variability is brought about by genetic recombination, which is an essential part of meiosis. Recombination, an exchange of DNA segments between homologous chromosomes, occurs during preparation for meiotic division. Recombination generates new combinations of alleles on chromosomes and increases the diversity of produced gametes (Figure 2.2.2 B). New combinations of genes can therefore be generated and transmitted to the progeny even in species that produce two types of gametes and use them for self-fertilisation ("selfing"). Creating genetic diversity is considered beneficial from the evolutionary point of view, as it can give some offspring a fitness advantage. This prospective evolutionary benefit ("Red Queen hypothesis") and possibility of eliminating deleterious mutations from a population (Miller's ratchet) are two proposed explanations to the observation that majority of eukaryotes reproduce sexually (reviewed in Charlesworth, 2006; Kondrashov, 1993).

Aside from providing evolutionary advantage, recombination provides mechanistic basics for chromosome segregation during meiotic division I (MI). A recombination event generates a physical linkage between homologous chromosomes (a cross over, or CO), which holds chromosomes together during their alignment in a metaphase plate before MI. Recombination is one of the major aspects in which meiosis differs from mitosis. As it involves unique chromatin events, meiosis is significantly longer than mitosis.

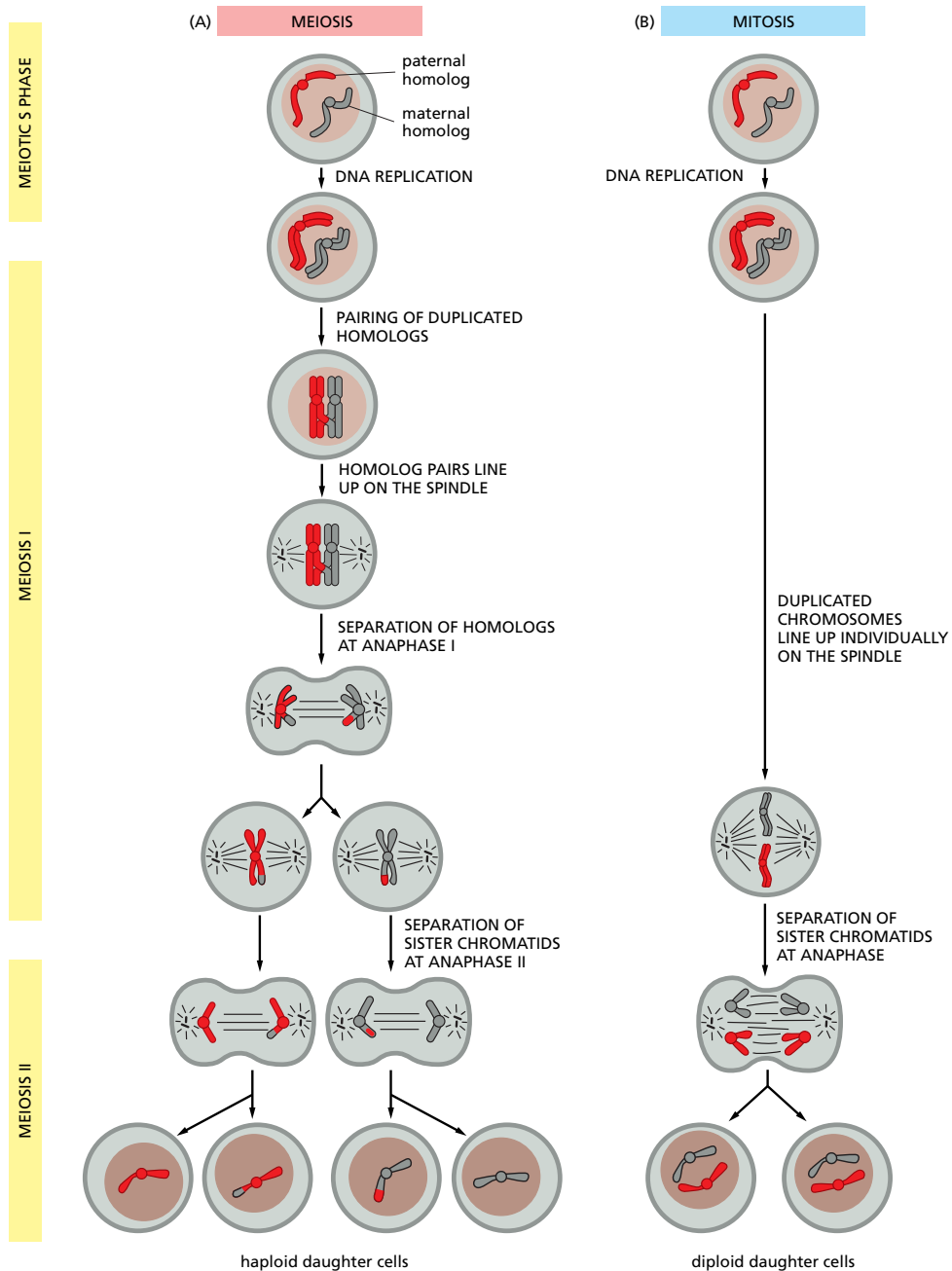


Figure 2.2.1 Comparison between meiotic and mitotic cell division.

For clarity, only one pair of homologous chromosomes (homologs) is shown.

(A) In meiosis, after DNA replication, two nuclear divisions lead to a generation of haploid gametes. As indicated by the formation of chromosomes that are partly red and partly gray, homolog pairing in meiosis is followed by genetic recombination (crossing-over) during meiosis I. The duplicated homologs pair up and segregate into different daughter cells in meiosis I. The sister chromatids separate only in meiosis II.

(B) In mitosis, by contrast, homologs do not pair up, and the sister chromatids separate during the single division. Thus, each cell that divides by mitosis produces two genetically identical daughter cells.

Figure taken from Alberts (2008).

Similarly to mitosis, meiosis is divided into four stages: prophase, metaphase, anaphase and telophase. Since meiosis comprises *de facto* two divisions, meiotic phases are often numbered in order to specify whether they refer to the first (MI) or the second division (MII). The following paragraph will discuss chromatin events in closer detail, focusing on the first phase of meiosis, prophase I, which is usually the longest one and is most relevant to this thesis.

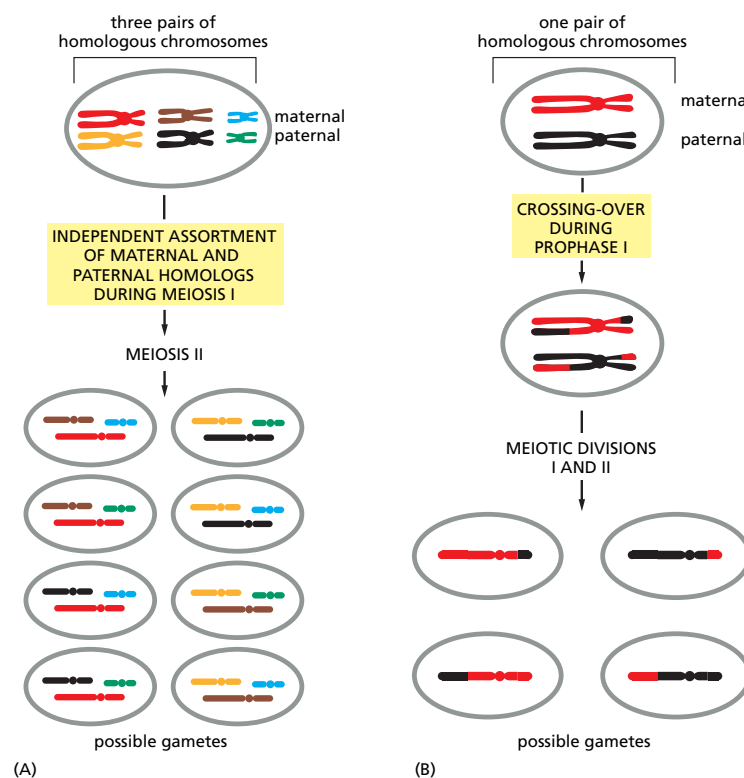


Figure 2.2.2. Two major contributions to the reassortment of genetic material that occurs in the production of gametes during meiosis.

(A) The independent assortment of the maternal and paternal homologs during meiosis. For three homologous pairs there are eight different gametes possible.

(B) Recombination (crossing-over) during prophase I exchanges DNA segments between homologous chromosomes and thereby re-assorts genes on individual chromosomes, increasing the number of possible different gametes.

Figure taken from Alberts (2008).

2.2.1 Interphase - preparing for the division

Similarly to mitosis, meiosis is preceded by a preparatory step, referred to as an interphase, which consists of Gap 1 (G1) phase, Synthesis (S) phase, and Gap 2 (G2) phase. Whereas meiotic G1 and S phases largely resemble mitotic

counterparts, G2 phase is barely noticeable. In G1, cell synthesises a vast array of proteins that will be required at later stages. In pre-meiotic S-phase, DNA replication generates an exact copy of each chromosome. The two copies, called sister chromatids, are held together by the sister chromatid cohesion complex. Some meiosis-specific proteins (specific kleisins) are incorporated into pre-meiotic chromosomes. The presence of special kleisins helps to maintain the sister chromatids cohesion during the first meiotic division (MI) and restrict separation of sister chromatids to the second meiotic division (MII) (Peters et al., 2008; Schvarzstein et al., 2010).

2.2.2 Meiotic division

Following DNA replication, meiotic cells enter a long prophase, during which homologous chromosomes recombine. Based on specific chromosomal events, meiotic prophase is divided into five stages: leptotene, zygotene, pachytene, diplotene and diakinesis (Figure 2.2.3)(summarised from Hillers et al., 2015; Alberts et al., 2014; Lui and Colaiácovo, 2012).

In **leptotene**, chromosomes condense and become visible as thin threads in the nucleus. Two sister chromatids are closely attached to each other and appear as a single thread. In **zygotene**, chromosomes find their homologous counterparts and line up with them. This process involves gross chromatin movements, in which chromosomes often become clustered in one region of a nucleus; this physical proximity is believed to help in identifying a homologue. Paired chromosomes become physically connected to one another by proteinaceous complexes called synaptonemal complexes (SCs). Axial elements of SCs align along chromosome axes, whereas lateral elements form bridges between homologs. The paired (synapsed) chromosomes are called bivalents or tetrads. In **pachytene**, chromosomes are visible as thick threads and the recombination takes place. To this end, multiple double strand breaks are introduced into the DNA, some of which will be repaired by connecting a broken strand to a homologous strand. Such events lead to an exchange of DNA between homologs. The sites where the exchange occurs are referred to as chiasmata. In **diplotene**, synaptonemal complexes start disassembling, homologous chromosomes separate a bit from one another and partially uncoil. This gives

chromosomes a somewhat fuzzier appearance and visualises chiasmata as spots where chromosomes remain tightly condensed. Chiasmata will hold the chromosomes together until their separation in meiosis I. During **diakinesis**, several intracellular changes can be observed in a preparation for the next meiotic phase, metaphase I. This includes strong condensation of chromosomes, disappearance of nucleoli, initiation of meiotic spindle formation, and initiation of nuclear envelope disassembly (nuclear envelope breakdown, NEBD).

By **metaphase**, the nuclear envelope has dispersed and microtubules have formed a meiotic spindle. Microtubules attach to bivalents and align them between the two spindle poles. Bivalents are held together by chiasmata, which in the meantime have moved to the ends of chromosomes. In **anaphase**, microtubules shorten, pulling chromosomes towards the poles. Chiasmata are resolved and two sets of homologous chromosomes are segregated to opposite poles. Segregation is completed in **telophase**, when chromosomes are clearly separated and the nuclear envelope re-forms around each daughter nucleus. Therefore, meiosis I is a reducing division, as daughter cells get only one set of chromosomes. Owing to DNA replication that precedes meiosis, each daughter cell contains two sister chromatids. The sisters are not identical, because of the crossing over, which occurred during prophase I. There is no DNA replication step between meiosis I (MI) and meiosis II (MII). Thus, after telophase I, cells continue their division, by executing a program that largely resembles mitosis.

In prophase II, the nuclear envelope breaks down and a new spindle forms. In metaphase II, spindle fibers connect to kinetochores, proteinaceous structures in the regions that held sister chromatids together. In anaphase II, contraction of spindle fibers separates sister chromatids and drags them to the opposite poles. Meiosis II ends with telophase, when nuclear membrane re-forms around daughter nuclei.

Meiotic division generates four cells with a reduced number of chromosome sets. Moreover, no two daughters are alike due to the recombination. As chromosomes recombine mostly at apparently random sites and are randomly segregated during MI and MII, a single organism produces a great variety of gametes (Alberts et al., 2014).

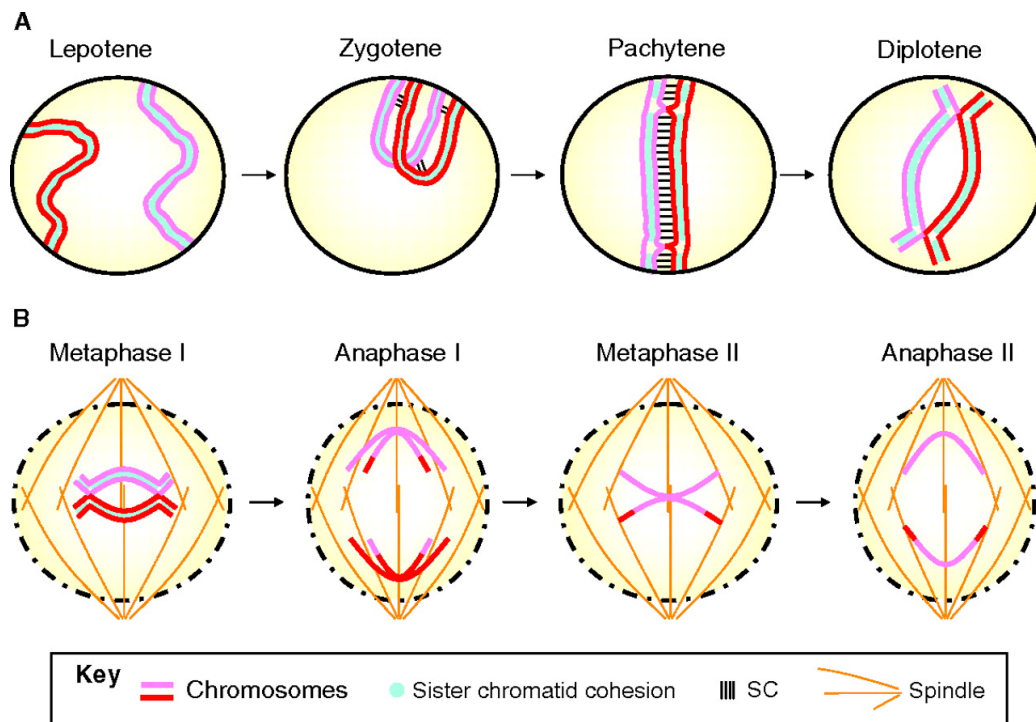


Figure 2.2.3 General model of homologous pairing and segregating in meiosis.

Red and pink lines depict one pair of homologous chromosomes. Sister chromatids are connected by sister chromatid cohesion (blue).

(A) At leptotene, telomeres attach to the nuclear envelope and chromosomes search for homologous sequences. At zygotene, chromosomes align to their homologs and initiate formation of synaptonemal complexes (SC). During pachytene, high levels of homologue alignment are achieved along the entire length, and chromosomes are visible as thick threads under the microscope. Paired homologs recombine. At diplotene, recombination is completed and SCs disassemble, giving the chromosomes more diffuse appearance. During the diakinesis stage, chromosomes strongly condense.

(B) At metaphase I, paired homologous chromosomes line up on the metaphase plate. At anaphase I, homologous chromosomes are segregated to opposite poles. Only one cell containing one pair of sister chromatids is shown for meiosis II. Sister chromatids align on the center plate at metaphase II and segregate to opposite poles at anaphase II.

Figure taken from Tsai et al., (2011).

2.2.3 Cytokinesis

The final steps of meiotic cytokinesis, i.e. dividing the cytoplasm and producing individual cells, contain sex- and species-specific features. Male meiosis leads to the formation of four sperm cells, whereas the number of egg cells resulting from female meiosis depends on the reproductive strategy of a species (Bell, 1982; Gilbert, 2006; Parker et al., 1972). In isogamic species, male and female gametes are very similar, and female meiosis generates four gametes, like male meiosis does. By contrast, in anisogamic species, a strong sexual dimorphism between gametes is observed; female meiosis gives rise to only one

egg cell, which inherits nearly whole cytoplasmic content of an oocyte. The rest of the DNA, equivalent to three sister cells, is extruded from the egg cell in form of so-called polar bodies.

2.2.4 Meiotic arrest

It is difficult to give a general timeline of meiotic events as timing differs largely in different species. However, common themes are that cells arrest in meiosis at certain stages and require signals from other cells to resume the division (reviewed in Stetina and Orr-Weaver, 2011). For instance, mammalian oocytes develop in fetal ovaries until the diplotene stage, at which they arrest. In response to a hormonal stimulation, oocytes resume meiosis, execute MI, and arrest again in metaphase of MII until fertilisation. A similar arrest-and-progression pattern exists in most vertebrates and insects. However, the second arrest in insects is observed in MI rather than MII. In the nematode *C. elegans*, cells appear to progress without break until diakinesis, when they await fertilisation. Maturation of a *C. elegans* oocyte, i.e. resumption of meiosis, is induced by a sperm-derived signal. Sperm triggers entry into meiosis, which proceeds rapidly (within 30 min from nuclear envelope breakdown) without any intervening pauses (McCarter et al., 1999).

2.3. *C. elegans* germ line as a model to study translational regulation in oogenesis.

Caenorhabditis elegans was established as a model organism to study development, cellular interactions, and neurological basis of behaviour (Brenner, 1974; Hirsh et al., 1976; Sulston and Horvitz, 1977). With invariant 959 somatic cells, short generation time, large brood size, and a transparent body, the worm provides a relatively simple and convenient system to investigate complex biological processes. *C. elegans* is easy to maintain as it grows at ambient temperatures (16-25°C) and feeds on bacteria. Strains can be frozen and thawed when needed, which additionally alleviates maintenance burden and facilitates creating large collections of mutant and transgenic strains. Mutations can be easily generated with use of chemical mutagens, transposons or ionising

radiation (Corsi et al., 2015; Wood, 1988). A broad range of available techniques for generating transgenic worms exists (e.g. Mos-mediated single copy insertion (MosSCI); Frokjaer-Jensen et al., 2012) and has recently been widened further by the introduction of CRISPR/Cas9 technology (Dickinson and Goldstein, 2016). The genome sequences of *C. elegans* and closely related *C. brenneri*, *C. briggsae*, *C. remanei* and *C. japonica* are available, and can be useful for analysing evolutionary conservation of molecular mechanisms (Coghlan, 2005; Corsi et al., 2015).

2.3.1 The two sexes

C. elegans population is composed of self-fertile hermaphrodites and males. Hermaphrodites are far more abundant than males (~99.9% under laboratory conditions; Hodgkin et al., 1979). They are in fact specialised females, as they have a female soma, and their germ line produces oocytes throughout their adult life. Spermatogenesis in hermaphrodites occurs only during larval development, giving rise to ~320 sperm cells, which are used by adult worms to fertilise oocytes. Hermaphrodites develop from embryos carrying two sex chromosomes (XX). When one X chromosome is missing, e.g. due to chromosomes nondisjunction during gametogenesis, the resulting XO embryo develops into a male. The percentage of males in the population can increase up to ~40% by mutations in genes affecting disjunction of X chromosome (high incidence of males phenotype, Him; Hodgkin et al., 1979), and up to 50% by mating hermaphrodites with males.

2.3.2 Germ line development in *C. elegans* hermaphrodite

Approximately two thirds of all *C. elegans* cells are germ cells - gametes and their precursors. In adult animals, germ cells are arranged in a spatiotemporal gradient of maturation; thus the position of a germ cell in the gonad normally corresponds to a particular meiotic stage. Transparency of an animal allows observing germ cell development *in situ*, without extruding gonads. Together, these features make *C. elegans* an exceptionally good system for investigating germ cell biology (summarised from Kimble and Crittenden, 2007; Kimble and Ward, 1988; Lints and Hall; Pazdernik and Schedl, 2012).

Germ line specification in *C. elegans* happens during embryonic development (Wang and Seydoux, 2012; and references therein). A single germ line precursor cell, P4, arises from a series of four asymmetric divisions that starts in the zygote, P0 (Figure 2.3.1). Each of these divisions generates a germline blastomere (P1, P2, P3, P4) and a corresponding somatic sister blastomere (AB, EMS, C, and D). P4 blastomere divides symmetrically at approximately 100-cell stage, generating two primordial germ cells, Z2 and Z3. Further development of the germ line is postembryonic.

At hatching, the reproductive organ of the first *C. elegans* larva consists of 4 cells: two primordial germ cells Z2 and Z3, and two somatic gonad precursors Z1 and Z4 (Figure 2.3.2) (Hubbard and Greenstein, 2005; Kimble and Crittenden, 2007; Kimble and Hirsh, 1979; Lints and Hall). If food is available, germ cells initiate mitotic divisions to build a stem cell population. The two somatic gonad precursors Z1 and Z4 cells also divide, giving rise to 12 cells. During L2, germ cells continue divisions, and cells of the somatic gonad primordium grow and change their positions. At the transition from L2 to L3, ten somatic gonad primordium cells move to the center of the gonad, displacing germ cells from the central region. At later larval stages, these ten primordial cells give rise to somatic structures, such as sheath cells, the spermatheca and the uterus. The two somatic gonad primordium cells that are located most distally (distal tip cells, DTCs) lead the migration of proliferating germ cells during L3 and L4 stages and serve as a germline stem cell niche in adulthood. At L3 stage, germ cells continue proliferating, which causes rapid growth of the gonadal arms. Germ cells most proximal to the developing spermatheca initiate male meiosis. At L4 stage, the gonad still expands in size; germ cells initiating meiosis at this and later stages follow the program of oogenesis. In adulthood, after completing its development, the germline tissue enters the maintenance phase. The DTCs finish their migration, bringing distal ends of gonads close together. The adult germ line occupies two U-shaped gonadal arms, which are connected through the sperm storage organ, spermatheca, to the centrally located uterus (Hubbard and Greenstein, 2005; Kimble and Crittenden, 2007; Lints and Hall).

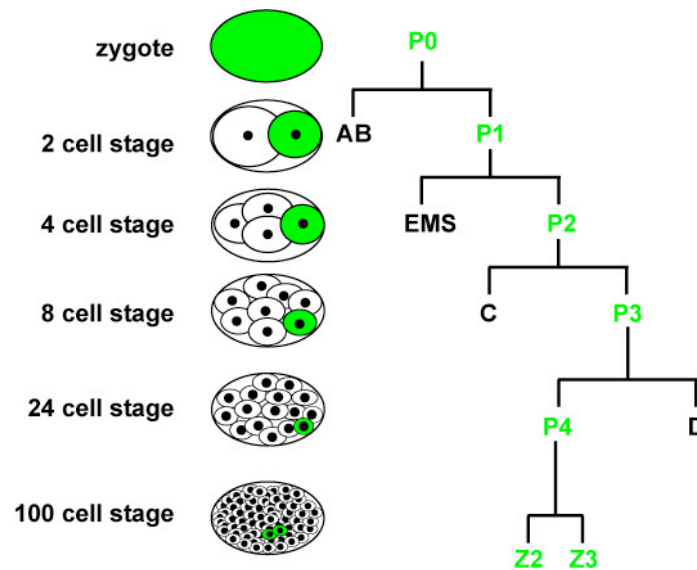


Figure 2.3.1 Embryonic development of the *C. elegans* germ line.

Cytoplasmic germline determinants are segregated during four asymmetric divisions of the P lineage cells. At ~100 cell stage, P4 blastomere divides symmetrically, giving rise to two primordial germ cells - Z2 and Z3.

Figure taken from Kupinski (2009).

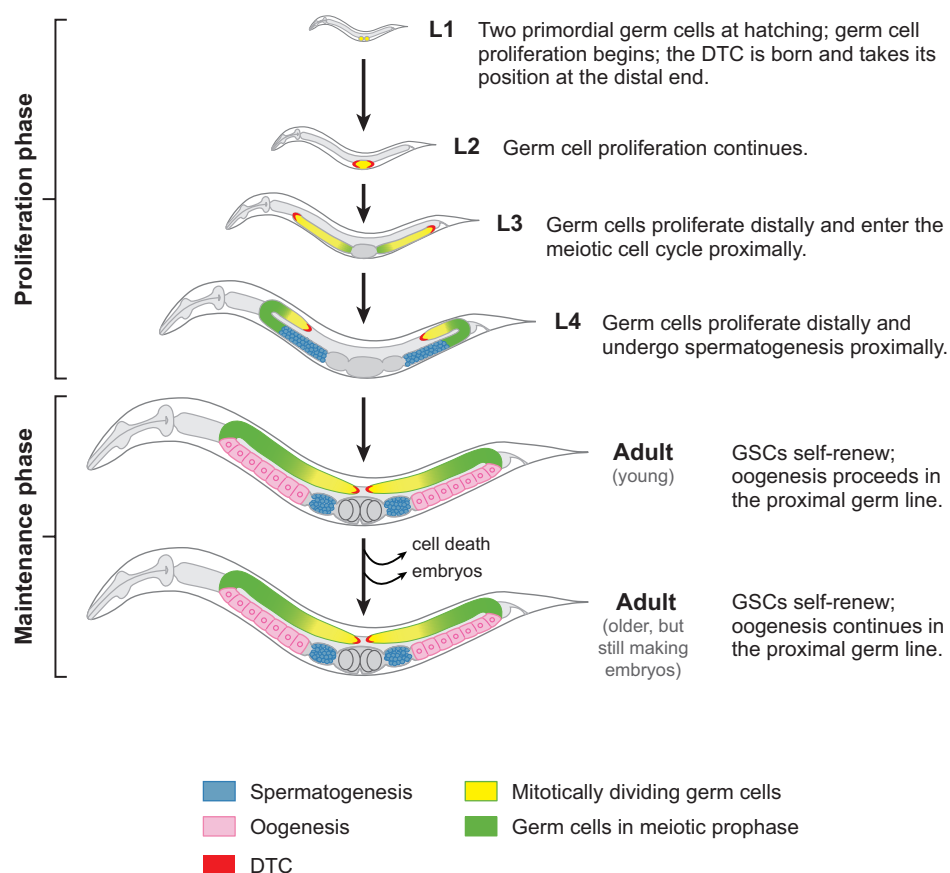


Figure 2.3.2 Post-embryonic development of the *C. elegans* germ line.

Figure taken from Kimble and Crittenden (2007).

2.3.3 Cellular organisation of the adult hermaphrodite germ line

A single adult hermaphrodite gonad is a tubular structure, in which germ cells are spatially arranged in a temporal order of the development (Figure 2.3.3) (Lints and Hall; Lui and Colaiácovo, 2012; Pazdernik and Schedl, 2012). Its distal end is filled with undifferentiated, mitotically dividing germ cells. At a certain distance from the distal tip, germ cells enter the meiotic program to differentiate into gametes. They progress through five consecutive stages of meiotic prophase I and simultaneously move toward the proximal end of the gonad. Meiotic divisions are executed as the oocyte is ovulated from the gonad, passes through the spermatheca, and reaches the uterus (Kimble and Crittenden, 2007; Lints and Hall; Pazdernik and Schedl, 2012).

Visualisation of chromatin (e.g. with DAPI) allows distinguishing different stages of germ cell development. Proliferating germline stem cells (GSCs) and cells in pre-meiotic S-phase reside in the most distal part of the gonad, called the mitotic region (MR) (Crittenden et al., 2006; Fox et al., 2011; Jaramillo-Lambert et al., 2007). In the wild type, this region accommodates ~230 cells arranged in ~20 cell rows. Cells in the proximally adjacent region execute the initial stages of meiosis, leptotene and zygotene (Dernburg et al., 1998; Hirsh et al., 1976). Together with occasionally interspersed pre-meiotic S-phase cells, this region is termed the transition zone (TZ). During zygotene, homologous chromosomes align, which process requires extensive chromatin movements. The nucleolus moves to one side of the nucleus, giving the DAPI-stained chromatin a characteristic shape of a crescent. During the next stage of prophase I, pachytene, chromosomes exchange fragments of DNA by homologous recombination (Dernburg et al., 1998; Villeneuve and Hillers, 2001). Nuclei at this stage have a characteristic appearance of a "bowl of spaghetti" and they fill the distal part of the gonad nearly to the bend region. Shortly before the bend, DNA threads loosen, as cells transit to diplotene and the synaptonemal complexes (SCs) partially disassemble (Lints and Hall). Concomitantly, in diakinesis, the last stage of prophase I, the chromatin strongly condenses, giving six bivalents a dot-like appearance. The nuclei align in a single row, and germ cells grow in size, so that each single oocyte occupies the whole diameter of the proximal gonad. At this stage oocytes arrest, awaiting signals for maturation and ovulation. In the presence of sperm, an event of meiotic resumption and ovulation is observed in

each gonadal arm every ~23 min. In the absence of sperm, diakinesis-arrested oocytes accumulate and stack in the proximal gonad (McCarter et al., 1999).

Despite the spatial distance, cells in the germline tissue remain connected through most of their development. Although the term 'germ cells' is widely used, the germline tissue is in fact a syncytium, as the membranes surrounding the nuclei maintain large openings to the common cytoplasm (Hirsh et al., 1976). Pachytene cells are regularly distributed right beneath the surface of the tube, whose inner, nucleus-free part is filled with the cytoplasm, referred to as rachis or cytoplasmic core. Around the gonadal turn the rachis starts narrowing and oocytes start growing. In the proximal part, oocytes span the whole diameter of the gonad and fully cellularise.

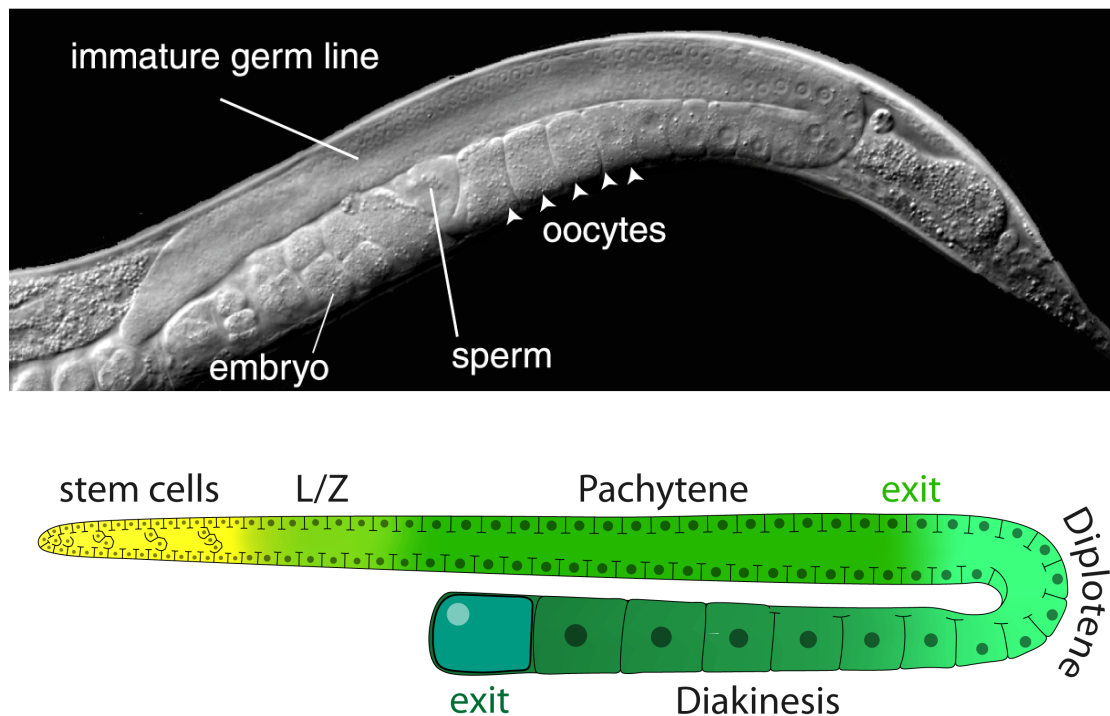


Figure 2.3.3. Gonad of *C. elegans* adult hermaphrodite.

(Top) Nomarski optics microscope image showing posterior half of an adult hermaphrodite. The gonad is a U-shaped tubular structure, in which germ cells are arranged in a gradient of maturation. Figure taken from Kimble and Crittenden (2007).

(Bottom) A cartoon schematically representing germ cells visible in the top image. The position of cells in a gonad corresponds to their meiotic and developmental stage. Yellow region indicates cells that express GLP-1/Notch receptor and thus are responsive to the mitosis-promoting signaling from the distal tip cell (not shown).

2.3.4 Soma-to-germ line communication and key signaling pathways involved

Development of germ cells is not a cell-autonomous process. *C. elegans* germ cells maintain a dialog with the soma from embryogenesis till the end of a

worm's life. The most prominent interactions are that between germline stem cells (Figure 2.3.3 bottom) and their somatic stem cell niche, as well as between developing oocytes and surrounding gonadal sheath cells (Kim et al., 2012; McCarter et al., 1997).

The niche for germline stem cells (GSCs) is formed by a single somatic cell, the distal tip cell (DTC). Laser ablation of the DTC causes all proliferative germ cells to leave mitosis and enter meiosis, which eventually leads to the loss of the germ line (Kimble and White, 1981). Signaling between the DTC and germ cells utilises the Delta/Notch pathway (Austin and Kimble, 1987; Berry et al., 1997; Hansen and Schedl, 2012). Each DTC produces a Delta-like ligand (LAG-2 or APX-2) (Henderson et al., 1994; Nadarajan et al., 2016), which activates the Notch receptor, GLP-1, that is strongly expressed by germ cells in the mitotic region (Crittenden et al., 1994). Activation of the receptor results in a signal transduction cascade that activates a transcriptional program to promote self-renewal and inhibit differentiation (Hansen and Schedl, 2012).

Exemplifying the prominent role of translational regulation in the germ line, the synthesis of GLP-1 receptor is regulated post-transcriptionally. A STAR-family protein GLD-1 represses *glp-1* mRNA in proximal mitotic and early meiotic cells (Marin and Evans, 2003). Reduced levels of GLP-1 protein downregulate Delta/Notch signaling, and promote entry into and maintenance of meiosis. Additionally, as cells move away from the distal tip cell, they lose an access to the Delta/Notch ligand, which further reduces their proliferative potential (Hansen and Schedl, 2012; Kimble and Crittenden, 2007).

Spatial restriction of an interaction between proliferating germ cells and cells expressing Delta-like ligands is particularly important during larval stages (Killian and Hubbard, 2005; Seydoux et al., 1990). If meiotic entry is delayed at L3/L4 stage, proximally located proliferating germ cells come in contact with proximal sheath cells. These sheath cells express Notch ligands but they contact only non-responsive, meiotic cells during normal development. The interaction between the sheath cells and proliferative cells results in activating GLP-1/Notch signaling in the latter, which promotes mitotic divisions, ultimately leading to the formation of a proximal tumor (McGovern et al., 2009). Thus, GLP-1/Notch signaling that occurs between the somatic and germ cells serves as a good

example of an interaction that is essential for proper functioning of an organism but must be tightly control to prevent pathologies.

Another occurrence of soma-to-germ cell communication supports oogenesis during adulthood and this function is largely mediated by MAPK signaling (reviewed in Sundaram, 2013). As pachytene cells approach the bend region, they contact sheath cells, which surround the proximal part of gonadal tube (Lints and Hall). Sheath cells activate a conserved RAS-RAF-MEK-ERK (*let-60*, *lin-45*, *mek-2*, *mpk-1*) signaling pathway in germ cells (Sundaram, 2013). The extracellular signal-regulated kinase, ERK, belongs to the highly conserved family of mitogen-activated protein kinases, MAPKs, which drive cellular responses to a variety of stimuli. In the female germ line, MPK-1 phosphorylates at least 30 proteins and regulates several biological processes, such as organisation of germ cells in the gonad and meiotic progression (Arur et al., 2009). Germline expression pattern of MPK-1 protein is rather uniform (type U in figure 2.3.5) (Lee et al., 2007a; Lee et al., 2007b), except for the distal region, where MPK-1 levels are low due to translational repression of *mpk-1* mRNA by FBF-1 and FBF-2 proteins (Lee et al., 2007a). Additionally, MPK-1 activity in meiotic cells is tightly regulated and restricted to two regions: zone 1, which is the proximal half of the distal gonad, and zone 2, which comprises a few most proximal oocytes (Lee et al., 2007b; Lee et al., 2007a).

In zone 1, MPK-1 activity is required to maintain regular organisation of germ cells in the gonadal tube (Arur et al., 2009; Church et al., 1995), promote transition from mid-pachytene to late-pachytene (Lee et al., 2007b), and to support cell growth (Arur et al., 2011). Accordingly, *mpk-1(0)* mutants fail to form a regular array of germ cells, and their germ cells arrest in pachytene, which results in sterility (Church et al., 1995). Additionally, MPK-1 signaling in zone 1 couples oogenesis to a nutritional status of the worm. Upon starvation, the insulin-like receptor DAF-2 downregulates the Ras-Raf-ERK signaling pathway, which reduces the rate of pachytene exit events (Lopez et al., 2013). This limits the number of oocytes produced and allows deposition of scarce nutrients into fewer cells, increasing the chance of producing high-quality oocytes despite unfavorable conditions. The ligand and the receptor that initiate the activation of MPK-1 in zone 1 are unknown, but laser ablation studies

suggested that sheath cells are involved in triggering ERK signaling (Kuwabara, 2003; McCarter et al., 1999).

In zone 2, high MPK-1 activity correlates with the presence of sperm. Major sperm protein (MSP) secreted by sperm triggers meiotic maturation (i.e. transition from diakinesis to metaphase of meiosis I) in the most proximal oocyte. Simultaneously MSP induces sheath cell contractions, which are required for ovulation (Kim et al., 2012). The signaling pathways that activate MPK-1 in oocytes are unknown but it was discovered that in the absence of sperm, oocyte surface receptors trigger an inhibition of MPK-1 activity. MSP relieves this inhibition by binding to the ephrin receptor, VAB-1, which is localised on the oocyte surface. Furthermore, MPK-1 activity in oocytes is additionally regulated by sheath cells. MSP binding to a yet unidentified receptor on sheath cells inhibits innexin-mediated inhibition of MPK-1 in oocytes (Sundaram, 2013). The importance of sheath cells in regulating MPK-1 activity in oocytes is underlined by the phenotype of *ceh-18(loss-of-function)* mutants. *ceh-18* encodes a POU-homeobox protein, required for proper differentiation and function of sheath cells. Oocytes of *ceh-18(lf)* worms exhibit defect in meiotic arrest and undergo MAPK activation, meiotic maturation and ovulation in the absence of sperm (Greenstein et al., 1994; Kim et al., 2012; Rose et al., 1997), which reveals the importance of sheath cells in regulating processes in gametes.

Altogether, several important cell fate decisions of germ cell development, such as proliferation versus differentiation decision or the stepwise progression through certain meiotic stages, are regulated in communication with the soma. Through signaling from somatic cells, germ line responds to environmental clues and adjusts numerous developmental parameters, such as proliferation rate, growth rate and apoptosis, to optimise animal fertility. The two main signaling pathways that transduce the signal from the initial stimuli are GLP-1/Notch and MPK-1/MAPK. Interestingly, some components of these pathways are translationally regulated, which generates opportunities to investigate crossroads between translational and post-translational regulatory mechanisms in driving biological processes.

2.3.5 Translational regulation in *C. elegans* gametogenesis

Regulation of gene expression during oogenesis relies heavily on post-transcriptional mechanisms. Oogenesis is a multi-step process that requires synchronising nuclear and cytoplasmic events, i.e. coupling of meiotic division and cell differentiation. The outcome of this process is a cell that is competent for fusing with another cell and able to support the development of a new organism. Assuming that all mRNAs required for the execution of meiosis, oocyte differentiation and early embryogenesis are present in developing female germ cells, a complex network of mRNA regulators is expected to exist, to confer the synthesis of required proteins at proper developmental stages. Studies in *C. elegans* revealed a number of regulatory networks composed of RNA-binding proteins, which regulate various aspects of gametogenesis, such as sexual fate specification or meiotic entry.

2.3.5.1 Sex determination in germ cells

In majority of animals, sexual identity of germ cells is a consequence of somatic sex determination. Somatic sex, in turn, is chromosomally established, either by a ratio of X chromosomes to autosomes, or by the presence of a dominant-acting sex chromosome. *C. elegans* is exceptional, as in hermaphrodites, which are somatically females, male gametes are transiently produced during larval development. Thus, chromosomal signals have to be overridden to allow a switch between sexual fates (reviewed in Zanetti and Puoti, 2012).

The core sex determination pathway, which operates predominantly on the transcriptional level, is in the germ line modulated by multiple additional factors. Many of these factors are RNA-binding proteins belonging to different families, e.g. FOG-1/CPEB, FOG-3/Tob/BTG, FBF/PUF proteins, LAF-1/Vasa. FOG-1 and FOG-3 are considered terminal determinants of germ cell sexual identity. They act downstream of the transcription factor TRA-1, which is important in germ line and in soma. FOG-1 and FOG-3 modulate the impact of TRA-1 on gene expression. Other proteins form a complex regulatory network that modulates activity of TRA-1, FOG-1 and FOG-3 to allow sex fate change in a

germ line and its synchronisation with somatic development (Zanetti and Puoti, 2012).

2.3.5.2 Proliferation versus differentiation decision

C. elegans produces germ cells throughout its adult life and thus has to maintain the homeostasis of the germline tissue. Excessive divisions of germline stem cells (GSCs) with seldom events of meiotic entry may result in a formation of a tumor. On the other hand, slow proliferation and frequent meiotic initiation events may deplete the pool of GSCs. In both cases, the fertility of a worm is affected. Hence, striking the balance between mitotic and meiotic divisions, or in other words - proliferation and differentiation, is essential for *C. elegans* fitness.

Probably the best-characterised aspect of regulation is the relationship between GLD-1 and GLP-1. GLP-1 signaling is essential to maintain proliferation in the mitotic region and it inhibits the activity of two meiosis-promoting pathways (reviewed in Hansen and Schedl, 2012; Kimble and Crittenden, 2007). GLD-1 is barely detectable in the most distal cells but its levels gradually increase, to reach maximum in meiotic cells (Jones et al., 1996). Elimination of GLP-1 signaling increases GLD-1 levels in the distal end nearly ten fold. Thus, it has been suggested that GLP-1 signaling inhibits GLD-1 accumulation (Hansen et al., 2004). Since GLD-1 represses *glp-1* mRNA (Marin and Evans, 2003), counteracting activities of the two proteins seem to generate a negative feedback loop, in which levels of GLD-1 determine the outcome.

RNA-binding proteins also regulate GLD-1 accumulation. Two largely redundant translational regulators belonging to PUF family, FBF-1 and FBF-2, bind to *gld-1* mRNA and repress its translation in mitotic cells (Figure 2.3.4) (Crittenden et al., 2002). FBF-1 and FBF-2, collectively referred to as FBF, repress also GLD-3 accumulation, at least in larvae (Eckmann et al., 2004). Consistently with their function, FBFs levels in the distal end of the gonad are high, whereas the levels of GLD-1 and GLD-3 are low (Crittenden et al., 2002; Eckmann et al., 2002; Jones et al., 1996; Lamont et al., 2004).

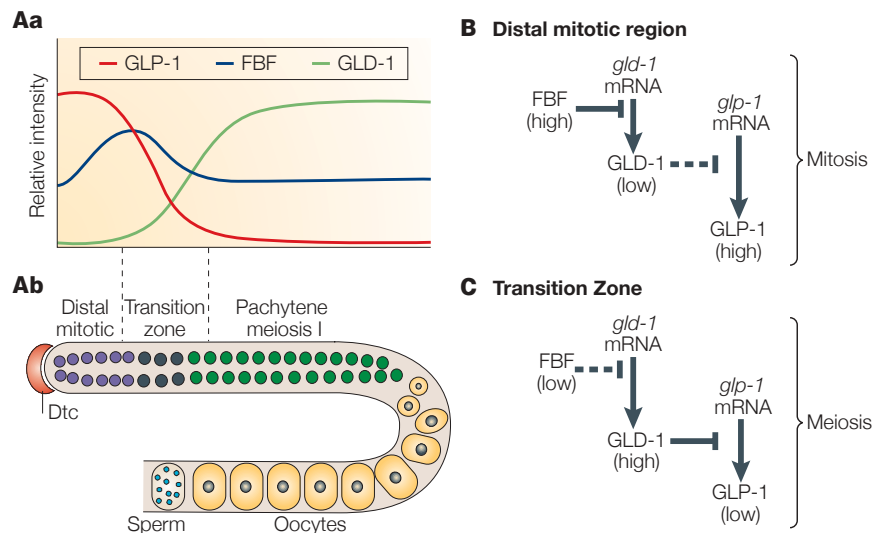


Figure 2.3.4. Levels of RNA-binding proteins regulate gametogenesis.

(Aa) Relative expression levels of a Notch receptor, GLP-1, and two translational repressors, FBF and GLD-1, which regulate mitosis-meiosis decision.

(Ab) Schematic representation of a hermaphrodite germ line. Cell fates in the distal part correlate with protein levels depicted in panel Aa.

(B,C) Interaction network of meiotic entry regulators. Repressive interactions dominate the regulatory mechanism. (B) In the mitotic region, high FBF levels efficiently repress translation of *gld-1* mRNA, and low GLD-1 levels permit expression of GLP-1 receptor. Activity of GLP-1 promotes mitotic divisions. (C) In the transition zone, lower FBF levels permit *gld-1* translation. GLD-1 protein acts as a translational repressor of *glp-1* mRNA. Low GLP-1 activity promotes entry into meiosis.

Figure taken from Kuersten and Goodwin (2003).

2.3.6 Regulated expression of RNA-binding proteins

Activities of distinct RBPs are required at different stages of oogenesis. Surprisingly, multiple RNA *in situ* hybridisation data suggest that most mRNAs expressed in *C. elegans* female germ line are present at low levels in the distal gonad but quickly increase in abundance before the bend region and accumulate to high levels in oocytes (Figure 2.3.5, top). By contrast, at least five prevailing protein expression patterns can be distinguished (types A-D and U, Figure 2.3.5; Nousch and Eckmann, 2013).

The discrepancy between the stereotyped mRNA expression pattern and complex protein expression patterns poses the question, how these diverse expression patterns of RBPs are established? Much insight into this problem was provided by G. Seydoux group in Merritt et al. (2008). The group generated a number of transgenic worms that expressed a reporter protein under the control

of different gene-specific regulatory elements. Promoter fusions were usually expressed uniformly in the germ line and did not recapitulate known gene-specific protein expression patterns. By contrast, upon combining a common permissive promoter with the reporter ORF and a gene-specific 3' UTR, protein expression patterns were largely recapitulated (Merritt et al., 2008). Thus, the majority of expression patterns of RBPs in the female germ line likely arise from the post-transcriptional regulation of their mRNAs, which is driven by elements in 3' UTRs.

Based on a sheer number of translational regulators in the germ line, one could hypothesise that a sequential repression mechanism operates to shape protein expression in the germ line. However, the existence of complex expression patterns, such as types B and C in figure 2.3.5, and the importance of the two translational activators, GLD-2 and GLD-4, for oogenesis (Kadyk and Kimble, 1998; Schmid et al., 2009; Wang et al., 2002) argue that the regulatory network is much more complex.

This work focuses on two proteins, CPB-3 and GLD-1, whose expression in the gonad is restricted to the distal arm. So far, these are the only proteins known to have expression pattern B in the hermaphrodite germ line (Figure 2.3.5). This expression pattern is characterised by low protein levels in the distal end of the germ line, in the closest proximity to the distal tip cell. Nonetheless, type B-proteins are already detectable in the proximal part of the mitotic region (MR), and their levels increase further as germ cells enter meiotic prophase. The levels stay high through the leptotene, zygotene and most of the pachytene. Close to the transition from pachytene to diplotene, which takes place shortly before the bend of the gonad, levels of type B-proteins decrease, and in the diakineti cells that occupy the proximal gonad these proteins are not detectable.

CPB-3 and GLD-1 are the members of conserved RNA-binding protein families, CPEB and STAR, respectively. Both proteins support oogenesis and therefore are important for *C. elegans* reproductive success.

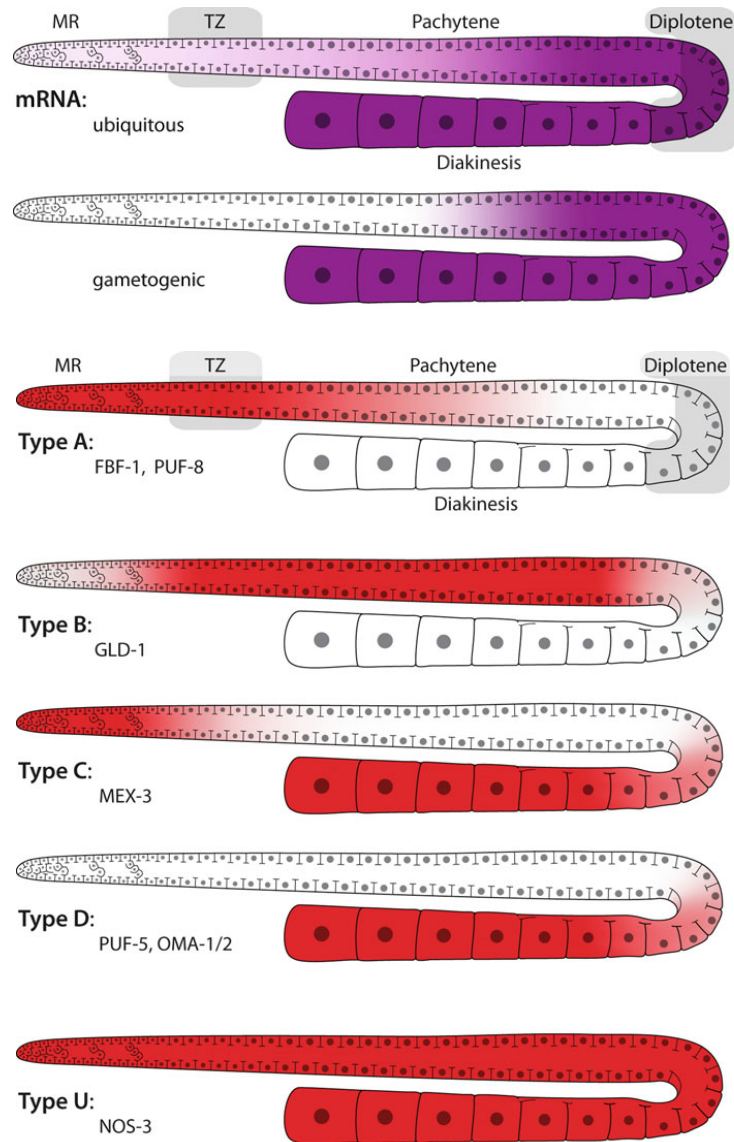


Figure 2.3.5. mRNA and protein expression patterns in female germ line.

(Violet) Majority of mRNAs are weakly expressed in the distal end of the gonad, comprising mitotic cells and early meiosis till mid-pachytene. From mid pachytene, mRNA levels quickly increase to reach maximum abundance in oocytes.

(Red) RNA-binding proteins have different expression patterns in the germ line, which parallel their functions in gametogenesis. Five main expression patterns can be distinguished: A - mainly restricted to mitotic region, B - mainly restricted to early meiosis (leptotene, zygotene, pachytene), C - combination between A and D, D - mainly restricted to developing oocytes in diplotene and diakinesis, U - ubiquitous expression.

Figures adapted from Nousch and Eckmann (2013).

CPB-3

CPB-3 belongs to the cytoplasmic polyadenylation element (CPE)-binding proteins, CPEBs (Figure 2.3.6)(Ivshina et al., 2014; Luitjens et al., 2000). Four genes encoding CPEB proteins were found in vertebrates (CPEBs 1-4), two in *Drosophila* (Oo18-RNA binding protein (Orb), and Orb2) and other invertebrates investigated so far (Figure 2.3.6)(Ivshina et al., 2014). All CPEB proteins have C-terminally located two RNA recognition motifs (RRMs) and two zinc fingers; both domains are important for CPEB functions. RRM1 provide RNA-binding specificity, whereas two zinc fingers were suggested to stabilise protein folding and mediate protein-protein interactions (Afroz et al., 2014; Merkel et al., 2013). The N-terminal part in most homologs does not contain any predicted domains.

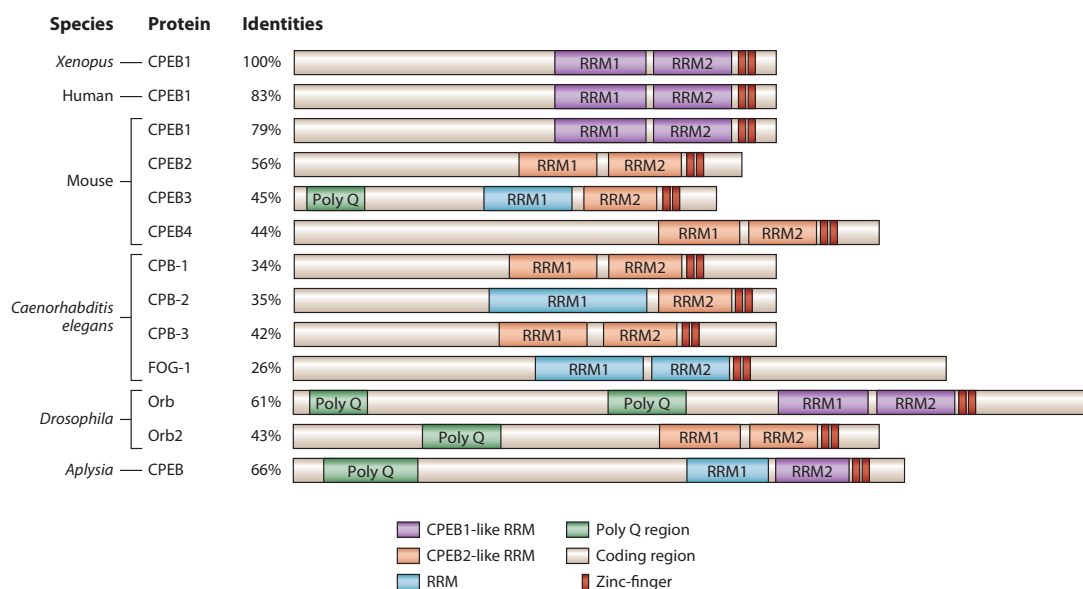


Figure 2.3.6. Evolutional conservation of CPEBs.

C-terminally localised two RNA recognition motives (RRMs) and two zinc-fingers (red rectangles) are common features of all CPEBs. N-terminal region, by contrast, is very weakly conserved and free of predicted domains, except for sporadically occurring polyglutamine-rich region. Figure taken from Ivshina et al. (2014).

Some CPEB proteins, such as mouse CPEB3, *Drosophila* Orb2 and *Aplysia* CPEB, contain N-terminally located poly-glutamine region (Figure 2.3.6), which was shown to promote protein aggregation and to be crucial for protein function in synaptic plasticity and memory formation (Heinrich and Lindquist, 2011; Khan et al., 2015; Krüttner et al., 2012; Majumdar et al., 2012). By contrast, poly-glutamine regions do not occur in CPEB proteins that function in oogenesis (*Xenopus* CPEB1, mouse CPEB1, *Drosophila* Orb, and *C. elegans* CPB-3),

suggesting that activity of "oogenic" CPEBs is regulated differently than amyloidogenic CPEBs (Ivshina et al., 2014).

The first detailed characterisation of CPEB function and activity comes from studies in African claw frog, *Xenopus laevis* (reviewed in Radford et al., 2008). Thanks to its large oocytes, *Xenopus* provided an excellent system for studying biochemistry of meiosis and early embryogenesis. CPEB1 was found to be an essential factor for meiotic progression, particularly for meiotic maturation.

While growing to a size of over 1 mm, *Xenopus* oocytes accumulate yolk, tRNAs, mRNAs, and ribosomes to support the development of an embryo. Multiple mRNAs remain translationally inactive during oogenesis. However, after meiotic progression resumed in response to hormonal stimulation, a subset of mRNAs becomes translationally activated and serves as templates for fast protein synthesis. Translational activation depends on U-rich sequence elements located in the 3' UTRs of mRNAs, which are dubbed cytoplasmic polyadenylation elements (CPEs). CPEB is the *trans*-acting factor that recognises these *cis*-elements and regulates translation (Radford et al., 2008).

Interestingly, CPEB1 is associated with its mRNA targets in growing oocytes, where it mediates translational repression, and in progesterone-stimulated oocytes, where it promotes mRNA polyadenylation and translational activation. CPEB1 interacts with two enzymes that regulate mRNA poly(A) tail length: a cytoplasmic poly(A) polymerase (cytoPAP) Gld2, and a poly(A)-specific ribonuclease, PARN. Both enzymes, Gld2 and PARN, were proposed to co-exist in an mRNA-associated complex (Figure 2.3.7) (Kim and Richter, 2006). Due to the robust activity of PARN and weak activity of Gld2, the poly(A) tail of bound mRNA would remain short and translationally repressed in growing oocytes. Progesterone stimulation induces signaling cascades, which lead to phosphorylation of CPEB1 on serine S174 (Mendez et al., 2000). This phosphorylation is considered to act as a molecular switch of CPEB1 activity. Upon phosphorylation, PARN is expelled from the complex (Kim and Richter, 2006), and Gld2 activity extends the poly(A) tail, leading to the translational activation of mRNA (Barnard et al., 2004). As meiosis progresses, CPEB1 is phosphorylated on six additional sites by cyclin-dependent kinase, Cdk1. This

phosphorylation is believed to reduce CPEB1 affinity to embryonic poly(A)-binding protein, ePAB. Released ePAB associates with extended poly(A) tail and promotes mRNA circularisation and translation initiation (Kim and Richter, 2007). Eventually, an additional phosphorylation by polo-like kinase, Plk1, triggers degradation of CPEB1 (Setoyama et al., 2007).

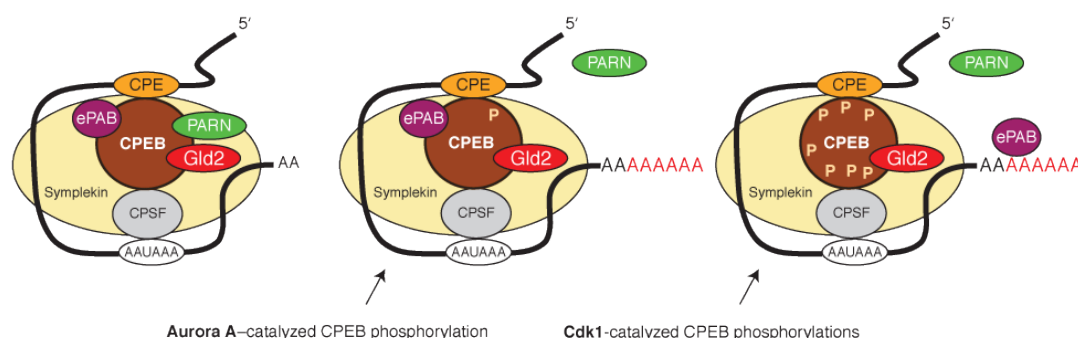


Figure 2.3.7. Mechanisms of CPEB-mediated translational activation.

Phosphorylation of CPEB regulates its interactions with poly(A) tail-modifying enzymes (Gld2 and PARN) and with polyA binding protein (ePAB). Aurora A-mediated phosphorylation promotes dissociation of PARN from the complex, which results in an elongation of poly(A) tail. Additional phosphorylations introduced by Cdk1 promote the release of ePAB, its binding to the poly(A) tail, and promoting translation.

Figure adapted from Richter and Lasko (2011).

The sudden decrease in the amount of CPEB1 drives another wave of the cytoplasmic polyadenylation and the translational activation of a different subset of mRNAs (Belloc et al., 2008; Igea and Mendez, 2010). Although some protein-protein interactions in this model are still questioned, the model provides an elegant reconciliation of CPEB1 presence in translationally silent mRNPs in fully-grown *Xenopus* oocytes and in translationally active mRNPs during meiotic maturation. Moreover, CPEB1 phosphorylation suggests a simple mechanism for coupling translational regulation with cell cycle progression.

Mouse CPEB1 is required early during oogenesis, as germ cells of *cpb-3*^{-/-} (homozygous knock-out) mice arrest at the pachytene stage (Tay and Richter, 2001). Similarly to *Xenopus*, mouse CPEB1 is post-translationally regulated. Phosphorylation of CPEB1 at embryonic day E16.5 is required for the synthesis of synaptonemal complex proteins and progression through pachytene. At embryonic day E18.5 CPEB1 is dephosphorylated, which is considered to render it inactive as a translational activator until meiotic division in adulthood (Tay et

al., 2003). Thus, mouse system provides a support for the hypothesis of a switch-like function of CPEB phosphorylation.

Drosophila homolog of CPEB1, Orb, is required for oocyte formation and establishment of polarity in an embryo (Christerson and Mckearin, 1994; Lantz et al., 1994). Orb is required for the localisation and efficient translation of *oskar* (*osk*) and *gurken* (*grk*) mRNAs (Chang et al., 1999; Chang et al., 2001). Oskar and Gurken are crucial to appropriate anterior-posterior and dorso-ventral patterning (Christerson and Mckearin, 1994; reviewed in Moussian and Roth, 2005). It has been proposed that the mechanism of Orb-mediated translational regulation in *Drosophila* is similar to that of CPEB1 in *Xenopus* (Chang et al., 1999). Indeed, the interaction between Orb and the cytoplasmic poly(A) polymerase homologous to Gld2, Wispy (Wisp), has been reported (Norvell et al., 2015). Furthermore, Orb was found to be heavily phosphorylated and the phosphorylation is essential for its function (Wong et al., 2011). Altogether, CPEB function in regulating translation by interacting with polyadenylation machinery, as well as regulation of CPEB function by phosphorylation, seem to be conserved.

C. elegans encodes four CPEBs: FOG-1, CPB-1, CPB-2, and CPB-3 (Luitjens et al., 2000). FOG-1 is a terminal factor in the germ cell sex determination pathway and acts as a translational regulator to repress oogenic mRNAs (Ellis and Schedl, 2007; Noble et al., 2016). CPB-1 is required for the progression of spermatogenesis in males (Luitjens et al., 2000). CPB-2 function has not been described so far, but its expression pattern in male germ line suggests a function in late spermatogenesis (Ryuji Minasaki, unpublished). CPB-3 is the only *C. elegans* CPEB with a reported role in oogenesis (Hasegawa et al., 2006).

The most thorough analysis of *C. elegans* *cpb-3* function has been reported by Hasegawa et al. (2006). Deficiency in *cpb-3* reduces hermaphrodite fertility and this phenotype is more strongly pronounced at elevated temperatures (25°C). Two alleles have been characterised, *cpb-3(tm1746)* and *cpb-3(bt17)*. *cpb-3(tm1746)* is a ~500 bp deletion, whereas *cpb-3(bt17)* is a deletion in the 3' end of the gene, which removes almost entirely the functional domains of CPEB proteins: the two RRM and the zinc-finger domain. The two mutations bring about very similar phenotypes. However, in contrast to *cpb-3(tm1746)*, the

protein product of *cpb-3(bt17)* is detectable by immunoblotting and in immunofluorescently stained germ lines (Hasegawa et al., 2006; Ryuji Minasaki, unpublished).

The development of germline tissue in *cpb-3(tm1746)* and *cpb-3(bt17)* hermaphrodites proceeds similarly to the wild type until adulthood. From the last molt onwards, i.e. in adult animals, progressive germ line deterioration is observed: the total number of germ cells decreases in *cpb-3(loss of function)* mutants in comparison to wild type. Furthermore, fewer oocytes are observed, and pachytene-like cells are present in the proximal gonad almost till its end. Consistently with apparent oogenesis defects, *cpb-3(lf)* mutants lay significantly fewer embryos than wild type (158 ± 48 vs. 276 ± 44 at 20°C ; 26 ± 14 vs. 166 ± 22 at 25°C , for *cpb-3(tm1746)* allele; Hasegawa et al., 2006). Moreover, a large fraction of embryos ($\sim 50\%$ at 25°C) fails to develop, suggesting reduced quality of oocytes or a requirement for the functional *cpb-3* during embryonic development.

In addition to its function in promoting oogenesis, *cpb-3* likely promotes mitotic divisions, as judged by reduced number of germ cells in the gonads of loss of function mutants and inducing overproliferation synthetically with other mutations (e.g. tumour formation in *cpb-3(bt17)*; *gld-3(ok308)*). Furthermore, combinations of *cpb-3* loss with other mutant backgrounds revealed its non-essential function in regulating sperm-to-oocyte switch (Hasegawa et al., 2006).

The molecular aspects of CPB-3 functions have not been characterised so far. CPB-3 was identified as an interactor of DAZ-1 (deleted in azoospermia), a conserved RNA-binding protein, essential for gametogenesis in multiple systems (Smorag et al., 2014). *C. elegans daz-1(0)* mutants are sterile because their germ cells arrest in meiosis (Karashima et al., 2000). DAZ-1 protein is expressed in the distal gonad: in the mitotic region and in early-to-mid pachytene (Maruyama et al., 2005). Thus, there is an overlap in the germline regions where DAZ-1 and CPB-3 are expressed (Hasegawa et al., 2006). However, the function of the complex is not known.

The molecular characterisation of CPB-3 has not been reported so far. However, due to the sequence similarity between CPB-3 and other CPEBs, interaction partners and activity of CPB-3 might be hypothesised. Similarly to

other systems, CPB-3 forms a complex with the cytoplasmic poly(A) polymerase GLD-2 (Jedamzik, 2009), which argues that CPB-3 may regulate polyadenylation and translational activation of selected mRNAs during oogenesis. The restricted expression pattern in the germ line, suggests that CPB-3 function needs to be terminated at a certain stage of meiosis.

GLD-1

The other protein of B-type expression pattern in *C. elegans* germ line (Figure 2.3.5) is GLD-1, a member of signal transduction and activation of RNA (STAR) family of proteins (Jones and Schedl, 1995; Jones et al., 1996). The family owes its name to the ability of its members to bind RNA and link signal transduction with RNA metabolism (Vernet and Artzt, 1997). STAR proteins are required for a multitude of developmental processes, thus strong loss of function mutations are usually lethal (reviewed in Artzt and Wu, 2010). Weak loss of function mutations manifest themselves by a wide range of neuromuscular defects, such as tremors observed in mice carrying hypomorphic mutation *quaking*^{viable} or horizontally extended posture of wings in *Drosophila* mutants of *how* (*held out wing*) gene (Artzt and Wu, 2010).

Members of STAR protein family have various molecular activities: some serve as translational regulators, while others regulate such aspects of RNA metabolism as pre-mRNA splicing, mRNA transport, or mRNA stability. STAR proteins are characterised by a single KH (hnRNP K-homology) domain and two flanking homology regions, QUA1 and QUA2. Whereas QUA1 domain mediates dimerisation of STAR proteins, KH domain together with QUA1 form an RNA-binding platform (Ryder and Massi, 2010). Several studies aimed at revealing the consensus RNA sequence that is recognised by STAR proteins (Galarneau and Richard, 2009; Carmel et al., 2010; Jungkamp et al., 2011; Wright et al., 2010). Although no simple consensus has been found, several models have been proposed to predict STAR proteins binding to mRNAs (Brummer et al., 2013).

C. elegans has two genes encoding STAR proteins: *asd-2* and *gld-1* (Francis et al., 1995a; Lee and Schedl, 2010; Ohno et al., 2008). *asd-2* is similar to its counterparts in vertebrates and flies, as it functions in developmentally regulated mRNA splicing in the nervous system, like mouse *Quaking5* (QKI5) and

Drosophila How (Artzt and Wu, 2010; Ohno et al., 2008). *gld-1* is more distantly related to those genes by sequence and function; it encodes a translational repressor that is essential for the fertility of hermaphrodite worms. A range of *gld-1* alleles were identified and characterised phenotypically (Jones and Schedl, 1995; Francis et al., 1995a; Francis et al., 1995b; Jones et al., 1996).

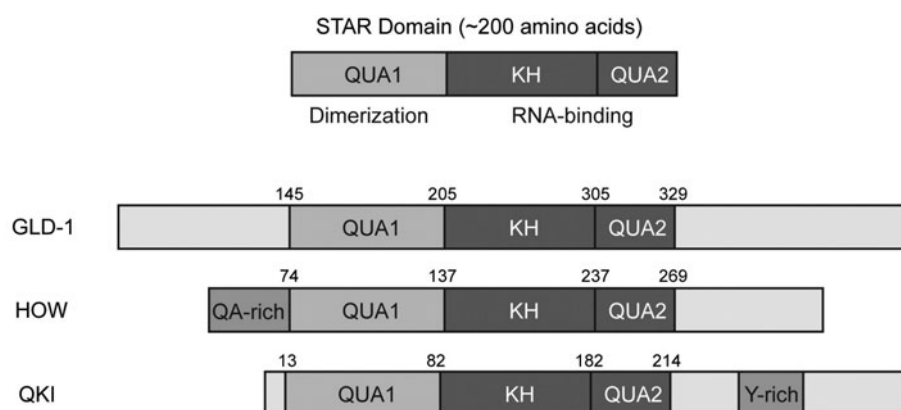


Figure 2.3.8. STAR protein family.

STAR proteins are characterised by a homology region composed of a central, single KH domain and flanking QUA1 and QUA2 domains. KH and QUA2 regions form together an RNA-interacting modus. QUA1 domain mediates dimerisation.

Figure adapted from Artzt and Wu (2010).

gld-1 null mutant hermaphrodites are sterile; germ cells enter meiosis apparently normally, but during early interphase they exit meiosis and divide mitotically, forming a tumor (Francis et al., 1995a). Interestingly, some cells in the tumorous population express protein markers and display morphology of neuronal or muscle cells (Biedermann et al., 2009; Ciosk et al., 2006). By this, tumorous germ line of *gld-1(0)* mutants resembles human teratoma, where the transdifferentiation of oogenic cells to somatic cell types is observed. Noteworthy, *gld-1(0)* males have no germline development defects, which indicates female-specific role of *gld-1* in meiosis (Francis et al., 1995a; Francis et al., 1995b). All these features make GLD-1 a widely studied translational regulator.

Phenotypes of *gld-1* loss-of-function (lf) mutants include germ cell arrest in early meiosis without tumor formation, or defects in oocyte development (Francis et al., 1995b; Francis et al., 1995a). In addition, *gld-1* was found to protect germ cells from apoptosis (Schumacher et al., 2005). Physiological

programmed cell death (PCD) affects 50-80% of germ cells in *C. elegans* (Fox et al., 2011; Gumienny et al., 1999). In a temperature sensitive allele *gld-1(op236)* maintained at the restrictive temperature, the apoptosis rate is increased (Schumacher et al., 2005). Furthermore, *gld-1* functions redundantly with *gld-2* and *gld-3* genes to promote entry into meiotic prophase. While meiotic entry is largely unaffected in *gld-1(0)*, *gld-2(0)* and *gld-3(0)* single mutants, in *gld-1(0) gld-2(0)* or *gld-1(0); gld-3(0)* double mutants no meiotic entry is observed and the tumor spans the whole germ line (Hansen and Schedl, 2006; Kimble and Crittenden, 2007).

All identified *gld-1* mutations with discernible phenotypes affect conserved residues in the STAR domain, underlining the importance of RNA-binding capacity for the GLD-1 function (Jones and Schedl, 1995). Recent high-throughput analyses of mRNAs co-immunoprecipitated with GLD-1 added hundreds of potential mRNA targets to a list of few that were characterised in closer detail (Jungkamp et al., 2011; Scheckel et al., 2012; Wright et al., 2011). For all mRNAs tested so far, GLD-1 acts as a translational repressor. Most of these mRNAs (e.g. *rme-2*, *gna-2*, *oma-1*, *oma-2*, *pal-1*, *tra-2*, *mes-3*) are expressed from early meiosis onwards, but their translation takes place only in growing oocytes, where GLD-1 is not detectable (Jan et al., 1999; Lee and Schedl, 2001; Lee and Schedl, 2004; Xu et al., 2001). Hence, GLD-1 and proteins encoded by mRNAs regulated by GLD-1 usually display mutually exclusive protein expression patterns. Some targets, however, such as *pal-1* and *glp-1*, remain translationally silent even after the reduction in GLD-1 levels (Marin and Evans, 2003; Mootz et al., 2004). This persisting translational repression is attributed to the activity of other translational repressors: MEX-3 protein for *pal-1* mRNA and PUF-5/-6/-7/-10 for *glp-1* mRNA (Lublin and Evans, 2007; Mootz et al., 2004). Thus, GLD-1 importance in regulating some mRNAs can be concealed by redundant activity of other RBPs.

The mechanism of GLD-1-mediated translational repression has not been clarified yet. To address this question, different groups performed polysome profiling experiments, which are based on fractionation of ribosomes in a sucrose gradient (Mootz et al., 2004; Scheckel et al., 2012). Heavier polysomal fractions contain mRNAs that are actively translated by multiple ribosomes or

translationally repressed at the elongation or termination stage. Lighter fractions contain monosomes and separate ribosomal subunits and mRNAs that are not translated or translationally inhibited at an initiation stage. Post-initiation repression has been suggested for the translational repression of *pal-1* and *mex-3* mRNAs, which co-sedimented with the ribosome fractions and were virtually absent from lighter fractions (Mootz et al., 2004). By contrast, a more recent study, in which polysome profiling was followed by a tiling array analysis, suggested that translational repression targets the initiation step (Scheckel et al., 2012). Two data points support this view. First, GLD-1 co-sedimented with the sub-polysomal fraction and was poorly abundant in heavier fractions. Second, most GLD-1 target mRNAs were enriched in sub-polysomal fractions. Together, translation initiation seems to be inefficient on GLD-1 bound mRNAs. Unfortunately, the two groups analysed the polysome profiles differently; whereas in the earlier study the monosome fraction was grouped together with polysomes, the later study grouped monosomes together with free ribosomal subunits. This concealed the consequences of assembling a single ribosome on regulated mRNA. Moreover, it remains possible that different mechanisms or translational repression operate on different mRNA targets (discussed in Lee and Schedl, 2010).

Regulation of poly(A) tail length may also be a part of GLD-1-mediated repressive mechanism. A reporter open reading frame fused to *tra-2* 3' UTR had a shorter poly(A) tail than the reporter whose *cis*-element bound by GLD-1 was deleted (Jan et al., 1997). Nonetheless, so far there was no report on an interaction between GLD-1 and any of *C. elegans* deadenylases, which could mediate shortening of the tail. Interestingly, an interaction between human QKI7 and a cytoplasmic poly(A) polymerase PAPD4/Gld2 has recently been reported (Yamagishi et al., 2016). QKI7 promotes elongation of the poly(A) tail when tethered to a reporter mRNA, and promotes translation of the reporter in cell culture. It remains to be shown whether QKI7 functions similarly *in vivo*, and whether any QKI7 homologs show analogous interactions. The finding is exciting because reports on protein-protein interactions with STAR family members are scarce. Moreover, until now, only CPEB proteins were known for their ability to recruit cytoPAPs to mRNAs. Unraveling molecular mechanisms of GLD-1-

mediated RNA regulation is desperately needed to improve our understanding of its biological functions.

2.4 Aim of Thesis

Gene expression in the *C. elegans* germ line is primarily regulated at the post-transcriptional level. In this respect, RNA-binding proteins (RBPs) emerged as essential factors of gene expression regulation to direct proper gametogenesis and safeguard animal fertility. Consequently, it is the presence or absence of certain RBPs that control the post-transcriptional fate of their cognate mRNA targets. Intriguingly, the abundance of numerous RBPs appears to be restricted at the protein level to defined stages of gametogenesis, arguing that developmental regulatory mechanisms exist to control RBP amounts. Currently, little is known about such post-translational regulation mechanisms of RBPs.

CPB-3 and GLD-1 are two evolutionarily conserved RBPs, which promote oogenesis. In the developing *C. elegans* germline tissue, both are expressed in early meiotic prophase I; however, as germ cells transit from the pachytene to the diplotene stage, their protein levels sharply decline. These drastic expression changes in meiotic prophase correlate – at least in the case of GLD-1 – with a clear translational activation of its mRNA targets and suggests that RBP-removal may be a prerequisite for efficient oogenesis.

The aim of this thesis is to elucidate the molecular mechanisms that are responsible for the developmentally induced elimination of CPB-3 and GLD-1 at the pachytene-to-diplotene transition of oocytes. Specifically, this thesis addresses the initial hypothesis that both RBPs are targeted for proteasomal degradation, which is the predominant mechanism for selective protein turnover in somatic cells. This thesis aims to elucidate the identity of the potentially involved ubiquitin ligases and unravels the developmental signaling cascade that initiates CPB-3 and GLD-1 turnover.

3. Results

3.1 CPB-3 expression is regulated by SCF^{SEL-10} complex and proteasome

3.1 Proteasome activity restricts CPB-3 expression

In order to test whether proteasome-mediated degradation shapes CPB-3 expression pattern, experiments were set up, in which the activity of the proteasome was inhibited, and CPB-3 expression was analysed by immunoblotting and immunofluorescent staining of extruded gonads. Initially, attempts were made to inhibit proteasome activity with the small molecule inhibitor, MG132, which is widely used in cell cultures and has also been administered to worms (Orsborn et al., 2007). However, previously observed stabilisation of GLH-2 (Orsborn et al., 2007) could not be recapitulated. On this basis, MG132 treatments were judged as inefficient, and a different approach to inhibit proteasomal activity was taken.

Proteasome activity was reduced by RNAi-mediated knock-down of proteasomal core subunits, which method was successfully used by several groups (Kahn et al., 2008, Kamath et al., 2003, Takahashi et al., 2002). To this end, several RNAi-feeding constructs were generated; however, the knock-down efficiency could not be evaluated at the protein level, as antibodies specific to targeted proteins (PAS-5, PBS-3 or PBS-6) did not exist. Therefore, RNAi efficiency of each gene was evaluated by comparing the induced phenotypes with those reported in the literature: embryonic lethality, larval lethality, slow growth, and morphological defects (Gönczy et al., 2000; Kamath et al., 2003; Sönnichsen et al., 2005). Reported phenotypes were observed in all three tested knock-downs (*pas-5*, *pbs-3* and *pbs-6*). *pbs-6* RNAi required shortest feeding times to induce observable changes and therefore was preferentially used in the following experiments.

3.1.1 Setting up RNAi feeding regimes to inhibit proteasome activity

To achieve RNAi-mediated knockdown in oogenic germ lines, mid-L4 worms were transferred onto RNAi feeding plates and kept at 20°C until

analysed. Initiating the knock-down as late as at L4 stage allowed body and germline structures to develop normally, whereas knock-downs at earlier developmental stages significantly affected somatic and germline morphology (data not shown).

Investigation of the proteasomal influence on CPB-3 expression pattern requires uninterrupted meiosis, as CPB-3 downregulation appears to be stage-specific. Hence, the duration of RNAi treatment had to be adjusted to obtain possibly strong reduction of proteasome activity while maintaining progression through meiosis. In order to find desired experimental conditions, a *pbs-6* RNAi time course experiment was done, in which manifestation of previously described phenotypes was analysed in parallel with monitoring meiotic progression.

After 24-30h of *pbs-6* RNAi, the mitotic region had a wild-type appearance and germ cells of all meiotic stages could be identified. However, in contrast to wild-type and control RNAi animals, the pachytene region in *pbs-6(RNAi)* animals was shortened, i.e. pachytene exit took place more distally than in control (mock RNAi) animals (Figure 3.1.1 A,B). Moreover, instead of being arranged in a single cell row, diplotene and diakinetik nuclei formed multiple rows (Figure 3.1.1 E,F). Additionally, membranous background staining of some antibodies visualised membrane-like structures between these diplotene and diakinetik nuclei, which is a likely sign of premature cellularisation (data not shown). Nonetheless, oocytes in the most proximal part of *pbs-6(RNAi)* gonads were arranged in a single row and appeared very similar to wild-type. These cells were probably formed prior to efficient *pbs-6* knock-down.

After 36-48h of *pbs-6* RNAi, changes at early stages of germ cell development could be observed. Compared to wild-type and control RNAi animals, the distal end of the germ line (mitotic region, MR) contained nuclei of different sizes (Figure 3.1.1 C,D). Occasionally, DAPI-stained foci that were reminiscent of fragmented chromatin were present. The number of these aberrant foci increased with the feeding time (data not shown), while the overall number of nuclei appeared to shrink. Moreover, crescent-shape nuclei of germ

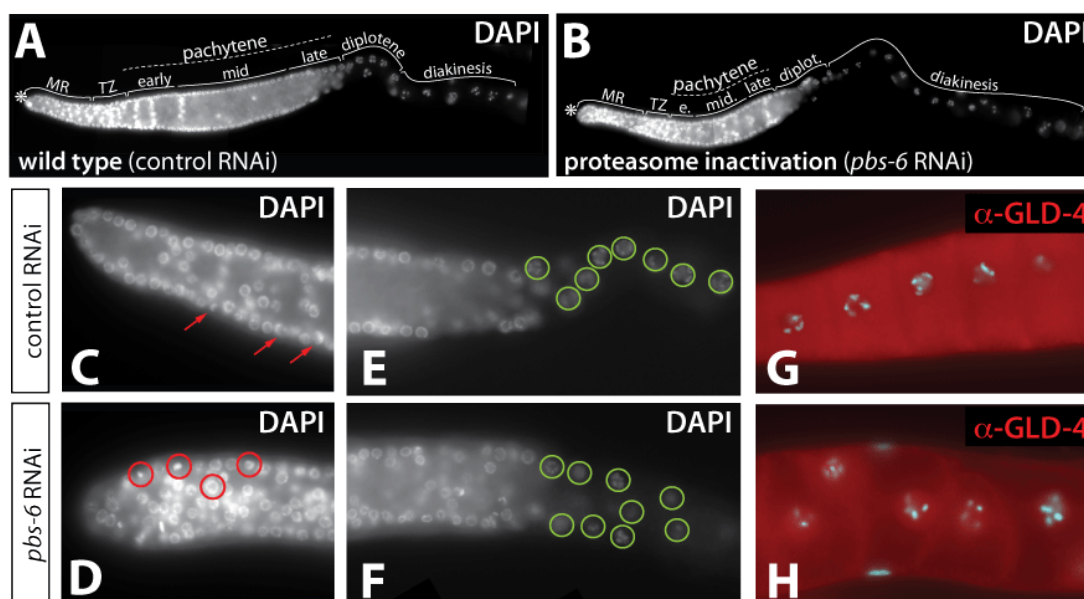


Figure 3.1.1 Proteasome inhibition induces phenotypic changes in various regions of the germ line.

(A,B) Mitotic region (MR), transition zone (TZ) and pachytene region shorten upon *pbs-6* RNAi. DAPI staining of extruded gonads. Asterisk indicates distal tip.

(C,D) Distal regions of gonads. Crescent-shape nuclei (arrows), a hallmark of meiotic entry, are rarely seen in *pbs-6* RNAi. Red circles, exemplary nuclei of different sizes.

(E,F) Different organisation of diplotene nuclei (green circles): single row in control gonads versus multiple rows in *pbs-6* RNAi.

(G,H) Control oocytes stain strongly and uniformly with anti-GLD-4 antibody (G), in contrast to weaker and mostly peripheral staining in *pbs-6*(RNAi) oocytes (H).

cells in the transition zone (TZ), which contains leptotene and zygotene stage cells, were very scarce (Figure 3.1.1 C,D). These two observations together suggest that mitotic divisions and meiotic entry are affected by the proteasome inhibition.

Any defects observed in the germ cells, in which proteasome activity was inhibited, may actually not result from reduced protein degradation at the point of phenotype occurrence but rather be a consequence of problems at earlier developmental stages, at which proteasome activity was already reduced. Thus, it was considered important to analyse an impact of *pbs-6* RNAi onto mitotic and early meiotic cells residing in the distal gonad. To this end, the size of the mitotic region (MR) was measured, to serve as an approximation of the germ cells proliferation capacity. MR size may be quantified as total number of germ cells occupying the distal end of the gonad until the beginning of the transition zone

(TZ). Distal border of the TZ is usually defined as the nuclear row, in which ~80% of cells have initiated meiosis. A simpler and faster approximation of MR size involves counting nuclear rows, rather than all the cells, until the TZ. A modified approximation method was applied in this study. The scarcity of crescent-shaped nuclei that indicate early meiotic cells hampered the determination of the border between the mitotic and early meiotic cells (i.e. MR-TZ border). Therefore, the length of combined mitotic region and transition zone (MR+TZ) was measured as a number of nuclear rows until first recognisable pachytene nuclei. The length of the pachytene region was measured in a similar manner.

pbs-6 RNAi reduced the length of MR+TZ region from 24.8 ± 5.9 nuclear rows (average \pm SD) in control animals, down to 19.9 ± 3.8 nuclear rows in *pbs-6* RNAi indicating that the inactivation of proteasomes influences mitotic divisions and meiotic entry. The observed aberrations likely result from impaired degradation of cell cycle regulators (Alberts, 2014). Pachytene nuclei did not display any obvious aberrations, but the pachytene zone was shortened upon proteasome inactivation (27.9 ± 3.4 nuclear rows in *pbs-6* RNAi; 42.1 ± 4.1 in control). Together with a shortened MR+TZ region, pachytene exit was visibly shifted towards the distal end of the germ line (Figure 3.1.1 A,B). As a consequence, *pbs-6(RNAi)* germ lines contained more diplotene- and diakinesis-like nuclei prior to the bend region than the corresponding control animals (Figure 3.1.1 A,B). Hence, proteasome inhibition by *pbs-6* RNAi changes the arrangement of the cells in the germ line. Distal regions in the gonad (MR, TZ and pachytene) shorten, pachytene exit takes place more distally from the bend region, and oocytes occupy not only the proximal gonad but also the bend region and a part of the distal gonad.

In addition to developmental defects, alterations in cellular arrangement were observed. The rachis in *pbs-6(RNAi)* gonads was not well defined; multiple pachytene nuclei were found in the cytoplasmic core, instead of forming a layer around the nuclei-free cytoplasmic core the distal gonadal arm, as it is observed in the wild type (data not shown). Diplotene and diakinesis nuclei were arranged in several rows, so that growing oocytes did not span the entire diameter of the gonad (Figure 3.1.1 E,F). This behaviour was more pronounced as feeding time

increased (data not shown). Additionally, changes in cellular appearance were observed. Inspection of the most proximal oocytes with Nomarski optics revealed regions of cytoplasm devoid of typical "roughness"; i.e. certain regions of oocytes looked 'smoother', less coarse, than the surrounding cytoplasm. Such heterogeneity of oocyte content in the most proximal oocytes was observed also in fixed and immunofluorescently stained germ lines. Proteins such as GLD-2, GLD-3 or GLD-4 gave a uniform, homogenous cytoplasmic staining pattern in control oocytes (Figure 3.1.1 G). By contrast, the staining signal is strong on the nuclear and cellular periphery, and weak in the remaining volume of *pbs-6*-depleted oocytes (Figure 3.1.1 H). These differences in cellular appearance were consistently observed upon proteasome inhibition by RNAi in all experiments but were not characterised further.

Importantly, the observed changes in the germ line had consequences for the experimental design that aimed at assessing the role of the proteasome in shaping the CPB-3 protein expression pattern. Specifically, a comparison of protein amounts between *pbs-6*-depleted and control germ lines, was not straightforward. First, the analysis of protein levels by immunoblotting was hampered by the fact that regions occupied by cells at particular meiotic stages had different sizes (Figure 3.1.1 A,B). Consequently, total levels of stage-specific proteins might change upon *pbs-6* RNAi but these changes would not necessarily result from the proteasome-mediated regulation of a particular protein. Instead, altered amounts of stage-specific proteins might reflect altered size of a particular zone. Secondly, the presence of multiple nuclei in the rachis, as well as an occurrence of 'void' spaces in the most proximal oocytes, caused uneven signal distribution in *pbs-6*-depleted gonads that were immunofluorescently stained for cytoplasmic proteins. This in turn hindered any fluorescence intensity-based comparisons of protein levels between *pbs-6(RNAi)* and wild-type germ lines. Third, due to the fact that MR, TZ, and the pachytene region shrink and shift distally upon proteasome inhibition, the anatomical hallmarks of the gonad could not serve as orientation points to approximate meiotic stage of germ cells. Therefore, the analysis of chromatin architecture, visualised by staining with DAPI, was always performed. In general, to avoid gross changes in the germ line, which would trouble interpretation of experiments, short RNAi

feeding times were used (24-36h, rarely 48h). On the other hand, shorter treatments result in weaker mRNA depletion, weaker inhibition of proteasome function, and less pronounced impact of the attempted proteasome inactivation on investigated processes.

3.1.2 Proteasome inhibition by RNAi leads to a partial stabilisation of CPB-3

To test whether CPB-3 expression is changed upon the reduction of proteasome activity, gonads of *pbs-6* RNAi-fed animals were extruded and analysed by indirect immunofluorescence (Figure 3.1.2). In control animals and similar to wild type, CPB-3 was abundant in early- and mid-pachytene, decreased in late pachytene, and dropped to background levels in diplotene and diakinetin cells (Figure 3.1.2 A, C, C'). In *pbs-6(RNAi)* germ lines, CPB-3 was also abundant in early and mid-pachytene, but the signal did not decrease as rapidly in late pachytene; instead, it was still above background levels around diplotene nuclei (Figure 3.1.2 B, D, D').

To quantify the stabilisation effect of *pbs-6* RNAi, the intensity of CPB-3 signal was measured 100 μ m distally and 100 μ m proximally from the pachytene exit (Figure 3.1.2 E). The transition point between pachytene and diplotene was determined by analysing nuclear morphology, visualised by DAPI staining. In control animals, CPB-3 signal decreased sharply before the pachytene-diplotene border, down to 20% of its peak intensity in the germ line (Figure 3.1.2 F). By contrast, germ lines of *pbs-6(RNAi)* animals showed CPB-3 signal reduction at the pachytene-diplotene border down to 80% of the maximum intensity. The signal kept decreasing toward the proximal end of gonad but not as sharply as in control animals. Thus, proteasomal activity is likely involved in shaping CPB-3 expression in late pachytene.

CPB-3 might be targeted for proteasomal degradation constitutively or only at a particular stage of germ cell development, e.g. in late pachytene. If CPB-3 degradation is constitutive, inhibition of proteasome is expected to lead to a noticeable increase in total amount of CPB-3. By contrast, if degradation occurs predominantly in late pachytene, inactivation of proteasome would increase CPB-3 levels predominantly in cells transiting from pachytene to diplotene. To

investigate these options, CPB-3 expression was analysed by immunofluorescence and immunoblotting.

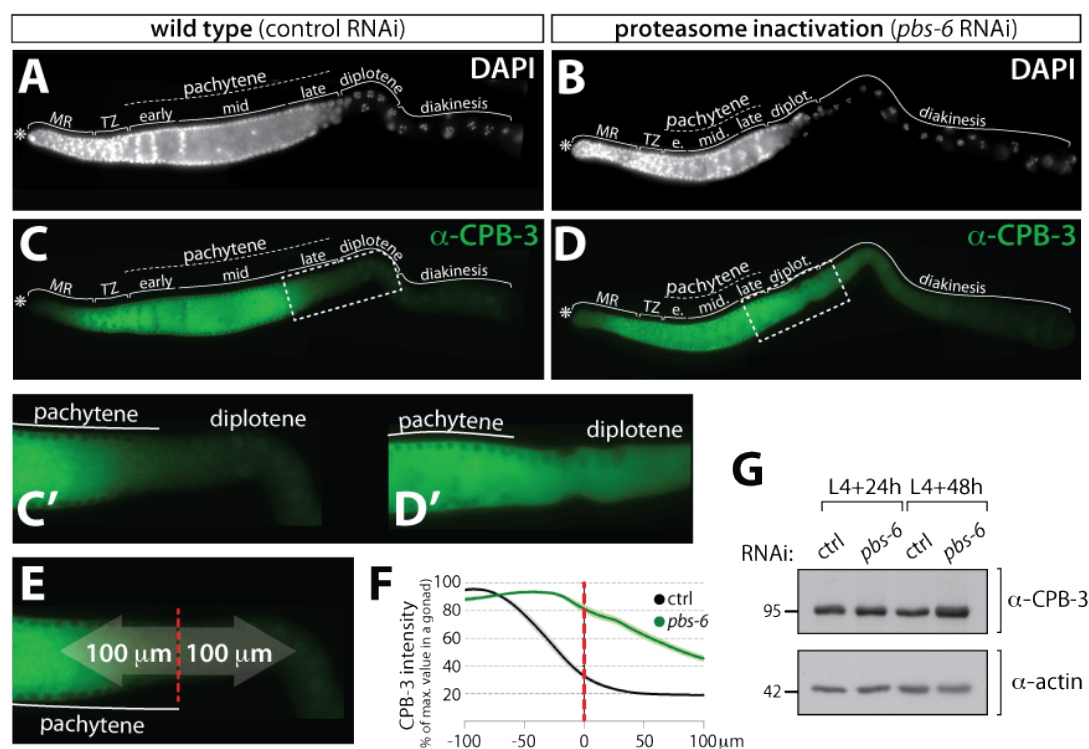


Figure 3.1.2 CPB-3 protein is partially stabilised upon the reduction of proteasome activity.

(A-D) Extruded gonads stained with anti-CPB-3 antibody. CPB-3 is detectable in diplotene and early diakinesis in *pbs-6*-depleted germ lines. Asterisk indicates the distal tip. Images A,B are identical to those in Figure 3.1.1. A,B.

(C',D') Close-up of C and D at the pachytene-diplotene border.

(E) Scheme of fluorescence intensity measurements. Dashed red line indicates the pachytene-diplotene border.

(F) Average intensity of CPB-3 signal around the pachytene-diplotene border (dashed red line at point 0); shadows represent SEM.

(G) Reduction of proteasome activity does not significantly affect total levels of CPB-3 in worms. Immunoblotting; 50 worms loaded in each lane. Molecular weight marker to the left.

Immunofluorescent stainings of extruded gonads showed comparable levels of CPB-3 in *pbs-6*-depleted and in control germ lines, arguing against the hypothesis of the constitutive turnover. Anti-CPB-3 immunoblotting of whole worm extracts showed minute changes in CPB-3 amounts upon *pbs-6* RNAi (Figure 3.1.2 G). Quantification of the signal intensity from four experiments did not reveal statistically significant changes (data not shown). Therefore,

proteasome-mediated degradation of CPB-3 most likely takes place only at a certain stage of meiosis, presumably in late pachytene.

The observation, that CPB-3 was stabilised only partially upon *pbs-6* RNAi, i.e. that CPB-3 was not detected in the proximal germ line, can be explained by several factors. First, *pbs-6* RNAi interferes with the production of a single proteasome subunit. Even if the knock-down is efficient, it does not affect already existing subunits (i.e. PBS-6 protein) or fully assembled proteasomes. Thus, residual proteasome activity might support a slow reduction of CPB-3 amounts. Moreover, proteasomes appear to be relatively stable. Although the half-lives of proteasomal subunits and assembled proteasomes in *C. elegans* are not known, the proteasome half-life in rat liver was determined to be 8.3 or 12-15 days (Cuervo et al., 1995; Tanaka and Ichihara, 1989). The life span of a rat is obviously much larger than the life span of *C. elegans* but even a several hour-long half-life of the proteasome in *C. elegans* would explain slow appearance of phenotypic changes in RNAi experiment. Fast inhibition of proteasome activity could be achieved by using a small-molecule proteasome inhibitor. Inhibition of proteasome by MG132, a molecule widely used in cell cultures, has been attempted several times without success. Nonetheless, partial stabilisation of CPB-3 was observed upon RNAi-mediated knock-downs of several proteasome subunits (*pbs-6*: figure 3.1.2; *pas-5*, *pbs-3*: data not shown), indicating that proteasomal activity is involved in reducing CPB-3 levels at pachytene exit.

3.2 SEL-10 is an F-box-WD40 protein that regulates CPB-3

Degradation of proteins in the proteasome requires their covalent modification by an attachment of a conserved polypeptide, ubiquitin. The modification is performed by a large and diverse class of proteins, which is referred to as ubiquitin ligases. The great number of ubiquitin ligases is encoded in eukaryotic genomes and provides specificity to the degradation process, as each ubiquitin ligase recognises only several target proteins. By contrast, proteasome acts rather non-specifically and is able to degrade virtually any ubiquitin-conjugated polypeptide. Unfortunately, the great number of ubiquitin ligases hampers identification of the one that is specific for the protein of

interest. This section describes experiments performed to identify a potential ubiquitin ligase for CPB-3.

3.2.1 CPB-3 interacts with SEL-10 in heterologous systems

In order to identify potential destabilising regulators of CPB-3, a yeast-two-hybrid (Y2H) screen was performed by Lisette Meerstein (Meerstein, 2009). One of the most frequently isolated clones encoded SEL-10, an F-box and WD40-domain protein and a homolog of Fbxw7, a well-characterised E3 component (Welcker and Clurman, 2008). Thus, SEL-10 might hypothetically mediate CPB-3 ubiquitination and destabilisation by serving as a substrate recognition subunit of a Cullin-RING E3 ubiquitin ligase. Noteworthy, SEL-10 had been previously described as a protein turnover factor in several biological settings (de la Cova and Greenwald, 2012; Ding et al., 2007; Hubbard et al., 1997; Jager et al., 2004; Peel et al., 2012) but never in the context of germ line development.

Several attempts were made to confirm that the interaction between CPB-3 and SEL-10 takes place *in vivo*. Co-immunoprecipitation of proteins from worm extracts was not possible due to the lack of SEL-10-specific antibodies. In pursuance of generating the antibodies, the N-terminal fragment of SEL-10 spanning amino acids 1-245 was expressed as a fusion protein with 6-histidine (6xHis) and glutathione S-transferase (GST) in bacteria, and purified. In total, 10 mice were injected with the fusion protein in adjuvant, which was done by the Antibody Facility at MPI-CBG (Dresden). Despite several boost injections, none of the tested sera contained antibodies detecting a band of expected size for SEL-10 (~65 kDa) that would be present in an extract of mixed stage wild-type but not *sel-10(0)* mutant worms. Thus, endogenous SEL-10 could not be detected.

Subsequently, generation of a transgenic line expressing tagged SEL-10 was essayed. A fosmid carrying *sel-10* gene fused with localisation and affinity purification (LAP) tag was introduced to worms by ballistic bombardment, which was performed by the TransgeneOmics Facility at MPI-CBG (Dresden). Judging by the rescue of the Unc phenotype, several lines of worms that stably inherited the fosmid were obtained. The worms were examined with the fluorescent microscope for the expression of GFP. Particular attention was paid to the cells, in which SEL-10 activity was previously reported, such as vulva precursor cells in L3/L4-stage worms (de la Cova and Greenwald, 2012), or a

zygote and a one-cell-stage embryo (Peel et al., 2012). Unfortunately, examined worms did not show any fluorescence signal above the level of animal autofluorescence (data not shown). Thus, generation of transgenic line was judged as unsuccessful. Due to the failure in raising antibodies and creating transgenic animals expressing tagged SEL-10, interaction between CPB-3 and SEL-10 has not been confirmed *in vivo*.

Co-immunoprecipitation from insect cells

To probe for a physical interaction between SEL-10 and CPB-3, the baculovirus expression system was used. The baculovirus system has several advantages: easy co-expression of proteins, high heterologous protein levels, and post-translational protein modifications (Kidd and Emery, 1993). Genes of interest are inserted into the genome of *Autographa californica* multicapsid nucleopolyhedrovirus (AcMNPV, family *Baculoviridae*). While posing a minimal risk for humans, the virus causes robust infections in insect cell lines, such as SF9 and SF+, which were derived from *Spodoptera frugiperda* ovaries. Moreover, a single insect cell can be infected by several viral particles, so protein co-expression can be easily achieved by infection with two viruses encoding different proteins (reviewed in Sokolenko et al., 2012).

In brief, genes of interest were cloned in pOEM vectors. All proteins were C-terminally tagged with 6xHis-tag, so the amounts of different proteins in an extract could be compared by probing an immunoblot with anti-5xHis antibodies. CPB-3 was N-terminally tagged with three tandem FLAG-tags (3xFLAG), SEL-10 - with maltose binding protein (MBP). Modified viruses were generated by the Protein Expression and Purification facility at MPI-CBG (Dresden), by recombining viral genome with pOEM constructs.

Prior to investigating the interactions of interest, the experimental setup was tested for its ability to recapitulate the previously reported binding of SEL-10 to SKR-1. This interaction was demonstrated in yeast (Killian et al., 2008) and in HEK273 cells (Yamanaka et al., 2002). SKR-1 recruits SEL-10 to the core of the E3 ubiquitin ligase complex by recognising F-box motif of SEL-10. Thus, SKR-1 was expected to bind full-length (FL) and the F-box-containing N-terminal fragment (Fb) of SEL-10, but not the C-terminal fragment, which contains the

substrate-binding WD40-repeats domain (WD) (Figure 3.2.1, top). To test these interactions, proteins were co-immunoprecipitated with anti-FLAG resin from co-infected SF+ cell extracts and analysed by immunoblotting. Full-length and F-box-containing fragment of SEL-10 were easily detectable in immunoprecipitated material, while WD40 domain-containing fragment was below detection levels (Figure 3.2.1, bottom). Therefore, the previously described interaction between SKR-1 and SEL-10 was recapitulated in the baculovirus expression system.

To test the interaction between SEL-10 and CPB-3, a similar experiment was performed. MBP-tagged SEL-10 fragments were co-expressed with FLAG-tagged CPB-3 and immunoprecipitated with anti-FLAG resin. Full length SEL-10 was enriched in CPB-3 immunoprecipitates (Figure 3.2.2). Importantly, no SEL-10 enrichment was observed in immunoprecipitates from cell extracts that did not contain FLAG-tagged protein, arguing, that SEL-10 did not bind non-specifically to the resin (Figure 3.2.2). Moreover, another *C. elegans* F-box-WD40 protein, MEC-15, was not enriched in CPB-3 immunoprecipitates (data not shown). Altogether, these results suggest, that CPB-3 binds SEL-10 in insect cells.

To find out whether SEL-10 recognises CPB-3 in a canonical way for Fbxw7 homologs, i.e. via the WD40 domain, co-immunoprecipitation of CPB-3 with F-box-containing (Fb) or WD40-containing (WD) fragments of SEL-10 was tested. WD fragment was enriched in immunoprecipitates (Figure 3.2.2), suggesting its involvement in CPB-3 binding. By contrast, Fb fragment was not enriched; although detectable in the immunoprecipitated material, its signal is reduced in comparison to the input. Hence, the interaction between Fb fragment and CPB-3 is weaker than the interaction between CPB-3 and full-length SEL-10 or WD fragment. Since Fb fragment was usually expressed at much higher levels than other SEL-10 constructs, it is also likely that the presence of Fb fragment in precipitated material arises from an inefficient washing of the resin after immunoprecipitation. Together, the co-immunoprecipitation experiments imply that SEL-10 can directly bind CPB-3 and that the WD40 domain mediates this binding.

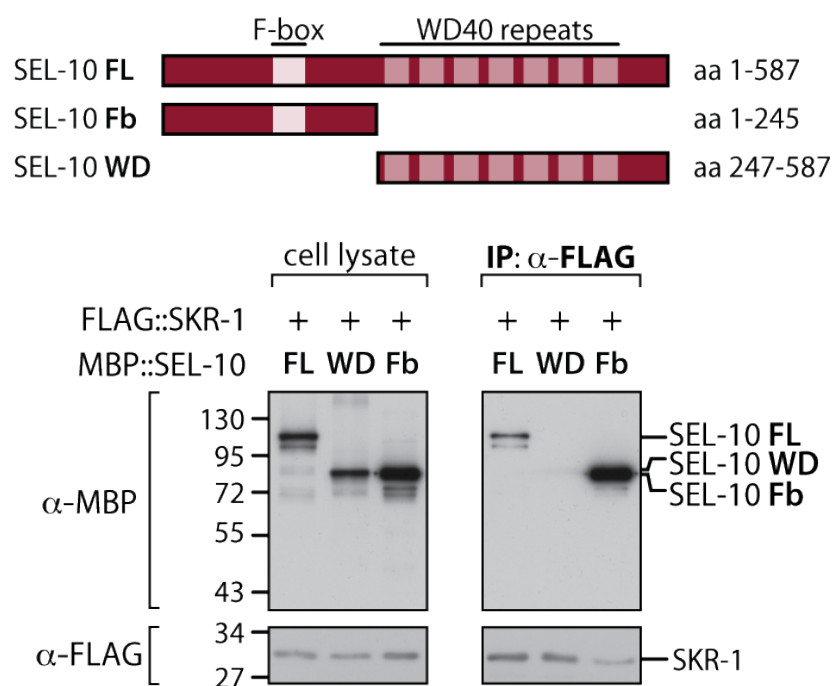


Figure 3.2.1 SEL-10 interacts with SKR-1 in insect SF+ cells.

(Top) Stick diagrams of SEL-10 fragments used in immunoprecipitation experiments. (Bottom) Immunodetection of FLAG::SKR-1-bound proteins. MBP-tagged full-length (FL) and F-box-containing fragment (Fb) of SEL-10 co-immunoprecipitate with FLAG::SKR-1. 1% of cell lysate and 20% of immunoprecipitated material were loaded.

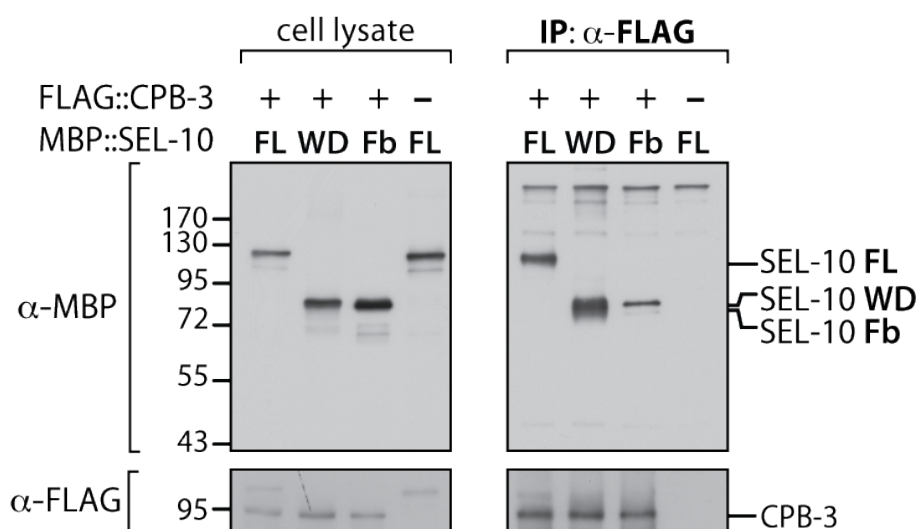


Figure 3.2.2 SEL-10 interacts with CPB-3 in insect SF+ cells.

MBP-tagged SEL-10 co-immunoprecipitates with FLAG-tagged CPB-3. MBP::SEL-10 does not visibly bind to anti-FLAG resin in the absence of FLAG::CPB-3. 1% of lysate and 20% of immunoprecipitated material were loaded.

3.2.2 CPB-3 is partially stabilised in *sel-10(0)* animals

If SEL-10 functions as an E3 ubiquitin ligase that targets CPB-3 for proteasomal degradation, then inactivation of *sel-10* should lead to the stabilisation of CPB-3 in meiosis. To test whether this is the case, germ lines of *sel-10(ok1632)* worms were extruded and analysed by indirect immunofluorescence. *sel-10(ok1632)* contains an 898 base pair deletion and 15 base pair insertion, which introduces a STOP codon after first 18 amino acids in the genomic locus of *sel-10*. Thus, *sel-10(ok1632)* likely represents a genetic null allele (Killian et al., 2008), and will be hereafter referred to as *sel-10(0)*.

The overall CPB-3 expression did not differ dramatically between wild-type and *sel-10(0)* germ lines. In both genotypes, CPB-3 levels gradually increased from proximal mitotic region towards pachytene region (data not shown), and the CPB-3 levels in the pachytene region were very similar. However, closer inspection of the late pachytene and early diplotene regions revealed elevated levels of CPB-3 in *sel-10(0)* mutant compared to wild type (Figure 3.2.3). The change in CPB-3 levels was quantified by measuring fluorescence intensity around the pachytene-diplotene transition border in multiple germ lines (n=7 for each genotype) (Figure 3.2.3, E). Although rather moderate, a difference in CPB-3 levels at pachytene-diplotene transition was repeatedly observed in more than 20 experiments. Moreover, RNAi-mediated knock-down of *sel-10* recapitulated anti-CPB-3 staining pattern observed in *sel-10(0)* germ lines (not shown). Together, these data suggest that the lack of *sel-10* activity partially stabilises CPB-3 amounts during meiosis.

Noteworthy, as cells progressed through the diplotene and diakinesis CPB-3 levels kept decreasing. Oocytes of both wild-type and *sel-10(0)* germ lines did not contain detectable CPB-3. This suggests, that additional factors may act to downregulate CPB-3 levels in oogenesis. The identities of these hypothetical factors were investigated by Britta Jedamzik (Jedamzik, 2009). Jedamzik searched translational regulators involved in shaping CPB-3 expression pattern. To this end, she analysed mutants or performed RNAi-mediated knock-downs of candidate genes (*gld-2/-3*, *fbf-1/-2*, *nos-3*, *mex-3*, *puf-5/-6/-7*, *oma-1/-2*). However, none of the tested gene deficiencies altered CPB-3 expression pattern, suggesting that the translational regulator was not among the candidates.

Alternatively, multiple factors may act together to repress CPB-3 in proximal germ line, and the simultaneous knock down of several genes is necessary to reveal their function.

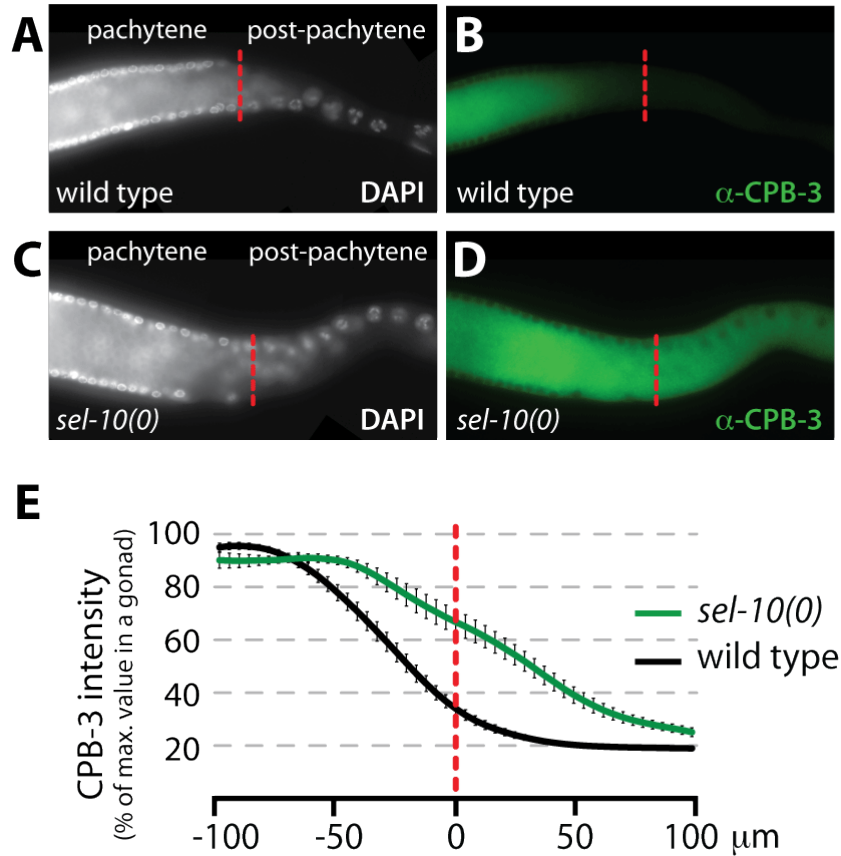


Figure 3.2.3 CPB-3 is partially stabilised in *sel-10(0)* mutant germ lines.

(Top) Anti-CPB-3 immunostaining of wild-type and *sel-10(ok1632)* mutant germ lines. Pachytene-diplotene (D-P) border was determined by analysing chromatin arrangement on z-stacks.

(Bottom) CPB-3 signal quantification around D-P border (vertical axis). Seven germ lines of each genotype were measured. Intensity is normalised to maximal average intensity in the germ lines of indicated genotype. Error bars show SEM.

3.2.3 Phosphorylated CPB-3 accumulates upon *cul-1* knock-down

Since homologs of SEL-10 function as substrate recognition subunits of SCF-type ubiquitin ligases (Welcker and Clurman, 2008), SEL-10 was expected to act in a complex with the *C. elegans* Cullin1 homolog, CUL-1, to destabilise CPB-3. To test if CUL-1 is involved in the regulation of CPB-3, *cul-1* activity was reduced by RNAi feeding. Accumulation of CPB-3 was analysed by immunofluorescent staining of extruded gonads and immunoblotting of worm extracts.

Gonads of *cul-1*-depleted worms stained with anti-CPB antibodies revealed a very similar expression pattern to control germ lines; no differences in CPB-3 levels were observed in the mitotic region (MR), transition zone (TZ) and early pachytene. However, CPB-3 levels were higher in late pachytene and diplotene germ cells of *cul-1(RNAi)* worms than in corresponding cells in controls (Figure 3.2.4). This partial stabilisation of CPB-3 during meiotic progression was quantified by measuring anti-CPB-3 signal intensities around the pachytene-diplotene border (Figure 3.2.4, bottom). The extent of CPB-3 stabilisation upon reduced *cul-1* activity is similar to the extended CPB-3 expression observed in *sel-10(0)* mutant germ lines (compare red and green line in figure 3.2.4). Thus, CUL-1 influences CPB-3 stability similarly to SEL-10.

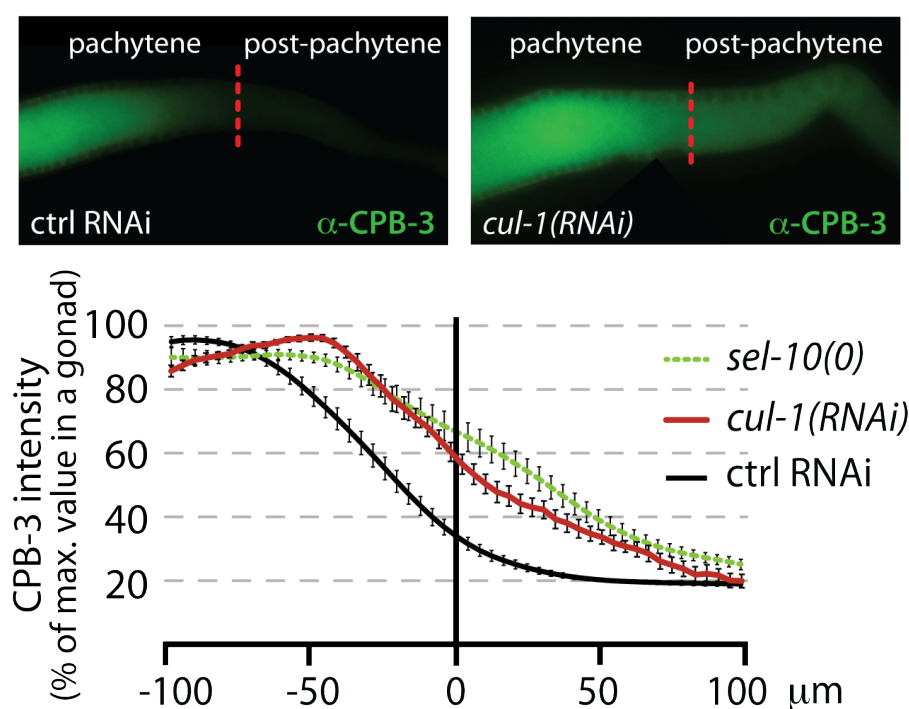


Figure 3.2.4 CPB-3 is partially stabilised upon *cul-1* RNAi.

(Top) Immunostainings of control and *cul-1*-depleted germ lines.

(Bottom) Quantification of signal intensity at the pachytene-diplotene border in germ lines immunofluorescently stained with anti-CPB-3 antibody. Numbers of germ lines in each group: *sel-10(0)* n=7; *cul-1(RNAi)* n=10; wild-type (ctrl RNAi) n=7. Intensity is expressed as percentage of maximal intensity in the germ line. Error bars show SEM.

CPB-3 accumulation in *cul-1*-depleted worms was verified by immunoblotting of worm extracts. Whereas CPB-3 migrates as a single band at 95 kDa in control animals (Figure 3.2.5: lane 1 and 5), additional, slower

migrating forms of CPB-3 accumulate upon *cul-1* RNAi (Figure 3.2.5: lane 2 and 6). These retarded forms resemble phosphorylated forms of CPB-3 in *sel-10(0)* mutant extracts, which will be discussed in detail in section 3.3.2. The phenotypic similarity of *sel-10* and *cul-1* inactivation suggests that both proteins may indeed act together in an SCF complex to destabilise modified CPB-3 forms in wild-type germ line.

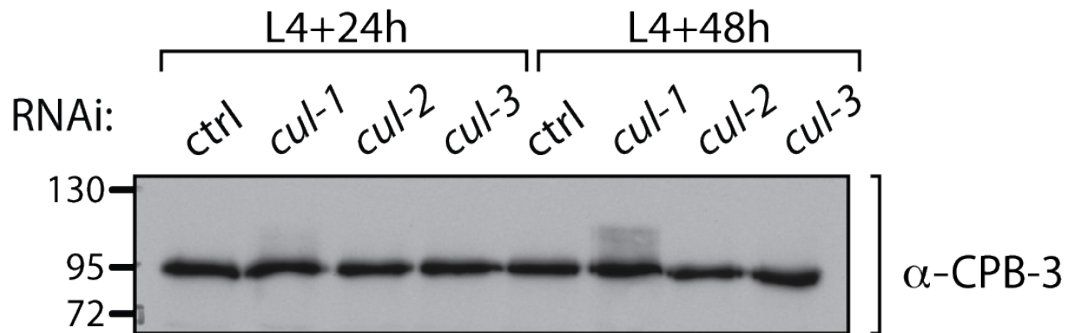


Figure 3.2.5 CUL-1 is involved in the regulation of CPB-3.

Modified CPB-3 protein accumulates upon *cul-1* RNAi but not *cul-2* or *cul-3* RNAi.

Representative immunoblotting of extracts of worms treated from L4 stage onwards with *cul-1*, -2, or -3 RNAi. 50 worms loaded in each lane.

3.2.4 An additional proteasome-dependent pathway regulates CPB-3 expression

Inactivation of *sel-10* or *cul-1* stabilises CPB-3 during meiosis only partially. Potentially, other ubiquitination pathways could operate redundantly with SCF^{SEL-10} complex to target CPB-3 for proteasomal degradation. To find out whether this is the case, proteasome activity was inhibited by RNAi-mediated depletion of proteasomal subunit, *pbs-6*, in *sel-10(0)* mutant worms. In parallel, RNAi feeding was performed in wild-type worms, where effects of this treatment were characterised previously (see section 3.1.2 and figure 3.1.2). Changes in CPB-3 expression were analysed by immunofluorescent staining of extruded gonads and immunoblotting of worm extracts (Figure 3.2.6 and data not shown).

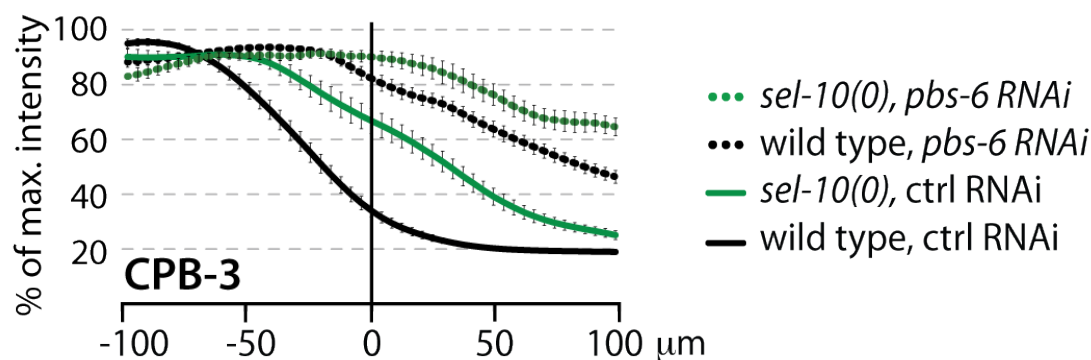


Figure 3.2.6 CPB-3 stabilisation at pachytene-diplotene transition in *sel-10(0)* mutant is enhanced by an inhibition of the proteasome.

Proteasome inhibition increases CPB-3 stability in *sel-10(0)* mutant germ lines.

Intensity of anti-CPB-3 signal in immunostained gonads represented as percentage of maximal signal intensity in a germ line (for details see Materials and Methods 5.18.2.). Point "0" on horizontal axis represents pachytene-diplotene border. For each curve, eight germ lines were quantified. Error bars represent SEM.

In wild-type mock-treated germ lines, CPB-3 levels were high in pachytene but rapidly decreased before the transition to diplotene, as observed previously. By contrast, upon *pbs-6* RNAi, CPB-3 was still detectable after pachytene-diplotene transition (pachytene exit, pEx) in wild-type germ lines, indicating reduced protein turnover and efficient *pbs-6* knock-down. As expected, CPB-3 was detectable after the pachytene-diplotene border in *sel-10(0)* germ lines. However, upon *pbs-6* RNAi, CPB-3 levels in post-pachytene cells increased further in this mutant background. Observed anti-CPB-3 fluorescence around the pachytene exit was measured, and the average signal intensities 100 μm distally and 100 μm proximally from pachytene-to diplotene border were plotted (Figure 3.2.6). While in control wild-type germ lines CPB-3 signal dropped to 30% of its maximal intensity at the pachytene exit, down to 20% shortly after, and then plateaued, *pbs-6* depletion increased CPB-3 levels at the pachytene exit to 80% of the maximal intensity, and the signal dropped to ~45% only 100 μm proximally from pEx. The increased signal can be interpreted as a stabilisation of CPB-3 protein upon proteasome inactivation. Signal intensities were correspondingly changed in *sel-10(0)* mutant. In control *sel-10(0)* germ lines, the anti-CPB-3 intensity at pEx was about 60% of the signal maximum in a germ line, i.e. around twice as high as in wild type germ lines at this point.

However, the signal decreased and reached 25% of the max value at the distance of 100 μm proximally from pEx, being there only 5% higher than in the wild type. By contrast, in *pbs-6*-depleted wild-type germ lines, the signal at this point was nearly two-fold higher, indicating that *sel-10* activity is less important than *pbs-6* activity to downregulate CPB-3.

Thus, proteasome inhibition seems to have stronger stabilisation effect on CPB-3 than the absence of *sel-10* activity. This suggests that other regulatory components beside SEL-10 may target CPB-3 to proteasomal degradation. Along these lines, *pbs-6* RNAi in *sel-10(0)* background resulted in an additional increase of CPB-3 levels at the pachytene exit and in diplotene cells (Figure 3.2.6 and data not shown). This increase in anti-CPB-3 signal is unlikely to reflect an increase in CPB-3 translation as proteasome inhibition usually triggers a global inhibition in protein synthesis (Wu et al., 2009; Yerlikaya et al., 2008). Thus, elevated CPB-3 levels in *sel-10(0)* mutant germ cells at the pachytene exit suggest that there is an additional, SEL-10-independent pathway to target CPB-3 for proteasomal degradation.

3.2.5 Additional pathways mediating CPB-3 degradation may be independent of Cullin-based ubiquitin ligases and APC/cyclosome

In an attempt to identify a molecular pathway that reduces CPB-3 levels in the absence of *sel-10*, a candidate-based RNAi screen was performed. Cullin-based ubiquitin ligases are the largest class of all ubiquitin ligases (Petroski and Deshaies, 2005; Sarikas et al., 2011; Skaar et al., 2013). Thus, RNAi feeding clones were generated to inactivate six cullin genes (*cul-1-6*) encoded in the *C. elegans* genome. RNAi feeding was performed in *sel-10(0)* mutant worms and the effects of knock-downs on CPB-3 expression were analysed by anti-CPB-3 immunostaining of extruded adult gonads. Experiments were performed at least three times for single knock-downs and at least two times for double knock-downs. In each experiment at least 10 germ lines were analysed.

Knock-downs of *cullins 1-4* were considered efficient, as they induced phenotypes described in the literature (Kipreos et al., 1996; Feng et al., 1999; Pintard et al., 2003; Zhong et al., 2003). However, no difference in CPB-3 expression pattern between control *sel-10(0)* animals and *cul-1*, *cul-2*, *cul-3* or

cul-4 knock-down conditions was observed, which suggests that *cullins 1-4* are probably not involved in the degradation of CPB-3 in *sel-10(0)* mutant germ lines. Since *cul-2* and *cul-3* play important roles in germ cell biology (reviewed in Bowerman and Kurz, 2006), the contribution of these genes to CPB-3 regulation was additionally analysed by immunoblotting of extracts from wild-type and *sel-10(0)* RNAi-treated worms. No significant changes in overall CPB-3 amounts were observed. (Figure 3.2.5: compare lanes 1 and 5 with 3,4 and 7,8; and data not shown). Thus, CUL-2, CUL-3, CUL-4 and the E3 ubiquitin ligase complexes that these cullins form are unlikely regulators of CPB-3 stability in the adult germ line.

RNAi feeding of the two remaining cullin genes in *C. elegans*, *cul-5* and *cul-6*, was also performed. However, the efficiency of the knockdown remains unclear as no obvious phenotypes were observed even after efficient knock-down of either gene (Nayak et al., 2002; Sasagawa et al., 2006). *cul-5* depleted wild-type worms have normal appearance and brood size. Due to the partially redundant function of *cul-5* with *cul-2* (Sasagawa et al., 2006), double RNAi feeding of *cul-5* and *cul-2* was performed. Neither single, nor double knock-downs affected CPB-3 expression pattern (data not shown), suggesting that *cul-5* is an unlikely regulator of CPB-3 stability. *cul-6* has not been characterised functionally. *cul-6* most likely originates from a gene duplication of *cul-1* (Nayak et al., 2002; Sarikas et al., 2011) and therefore might play redundant roles with *cul-1*. Hence, a double knockdown of *cul-1* and *cul-6* was performed, in addition to single knock-down of *cul-6*. In both, single and double knock-downs, CPB-3 expression pattern was indistinguishable from control germ lines (data not shown), suggesting that *cul-6* activity is unlikely to downregulate CPB-3. Together, none of the *C. elegans* cullin knock-downs affected CPB-3 expression pattern in *sel-10(0)* mutant worms.

APC/Cyclosome shares a structural similarity with cullin-based ubiquitin ligases and has a well-characterised role in regulating cell cycle progression (Bowerman and Kurz, 2006; Davis et al., 2002; Simpson-Lavy et al., 2010). Considering that APC/C promotes the metaphase-to-anaphase transition, its role in regulating CPB-3 in prophase, was rather unlikely. However, APC/C function in meiotic division is not as well characterised as in mitosis, and therefore the

possibility that it may function early in meiosis was not excluded. To test whether APC/C regulates CPB-3 stability, wild-type and *sel-10(0)* worms were subjected to RNAi-mediated knock-down of *apc-2*, a cullin-resembling subunit of APC/C complex. The knock-down of *apc-2* was considered efficient because it induced embryonic lethality, which is a phenotype reported in the literature (Rappleye et al., 2002; Furuta et al., 2000). CPB-3 expression pattern in the germ line tissues, examined by indirect immunofluorescence, looked identical in the *apc-2*-depleted and control gonads in three independent experiments (>30 germ lines analysed). Hence, APC/C most likely does not mediate destabilisation of CPB-3 in late pachytene.

In summary, seven genes that encode scaffold subunits for multiple E3 ubiquitin ligases were tested for their role in regulating CPB-3 stability during meiosis. One of these proteins, CUL-1, functions together with an F-box protein SEL-10 to downregulate CPB-3 at the pachytene-to-diplotene transition. However, CUL-1 does not seem to function outside a *sel-10*-containing complex to regulate CPB-3, as the *cul-1* depletion does not further increase CPB-3 stability in *sel-10(0)* mutant germ lines. None of the other candidate genes (*cul-2* to *-6* and *apc-2*) influenced the stability of CPB-3 in RNAi-feeding experiments in *sel-10(0)* mutant germ lines. Thus, a hypothetical additional regulator of CPB-3 stability in late pachytene remained unidentified.

3.3 CPB-3 is phosphorylated *in vivo*

3.3.1 Difficulties in detecting phosphorylated CPB-3

F-box proteins that act as ubiquitin ligases usually recognise their substrates in a phosphorylation-dependent manner (Skaar et al., 2013). Therefore, CPB-3 was expected to be a phosphoprotein, and as such, to migrate as multiple bands in an SDS-PAGE gel. However, probing immunoblots with several different anti-CPB-3 antibodies consistently led to a detection of a single band at 95 kDa (see below, e.g. figure 3.3.6, lane 6).

One possible reason of why no phosphorylated forms of CPB-3 were detected is that steady state levels of modified phospho-CPB-3 might be very

low. Increasing their prevalence would facilitate detection but requires knowing the identity of possible kinases or phosphatases of CPB-3. Unfortunately, no post-translational regulators of CPB-3 had been described in the literature. Another explanation of why phospho-CPB-3 cannot be readily detected is that such modifications may be rapidly removed or the modified protein is rapidly degraded during sample preparation. The worm extract used for immunoblotting was obtained by snap-freezing worms in liquid nitrogen, and adding pre-heated denaturing sample buffer to the frozen pellet; a procedure that leaves very little time for phosphatases or proteases to act. Hence, there is little room to speed-up or optimise sample preparation to prevent a potential loss of CPB-3 modifications. A third possibility is that phosphorylated CPB-3 is present in the extract but migrates too closely to its non-phosphorylated form to be visualised. If this was the case, an increase in the resolution power of standard SDS-PAGE gel should allow detection of modified CPB-3.

3.3.1.1 Optimisation of Phos-Tag SDS-PAGE

To increase the resolution power of an SDS-PAGE gel, a chemical compound that binds to phosphate residues and slows down the migration of phospho-proteins, known as Phos-Tag was added (Kinoshita et al., 2015; Kinoshita et al., 2006). However, the concentration of Phos-Tag and the running conditions must be empirically optimised for every protein to obtain greater separation between differently phosphorylated protein forms. The optimisation is usually easier for small proteins, as a higher percentage of acrylamide and shorter running times are used.

CPB-3 is 745 amino acids (aa) long, has a predicted mass of 85 kDa but migrates in standard SDS-PAGE as a 95 kDa band. CPB-3 is more than twice as big as a median *C. elegans* protein (344 aa, ca. 35 kDa) (Brocchieri and Karlin, 2005). Therefore, difficulties in establishing Phos-Tag conditions for full-length CPB-3 were expected and thus, short fragments of CPB-3 were used for initial rounds of optimisation. Three fragments of CPB-3 were expressed in yeast as proteins fused to a LexA domain: D1 (amino acids 425-745), D2 (aa 495-745) and D3 (aa 560-745). The advantage of using fusion proteins was that a very clean, commercially available anti-LexA antibody could be used for protein

detection on immunoblots. Protein extracts were prepared by TCA precipitation and resolved on SDS-PAGE gels with an addition of 5 μ M or 20 μ M of Phos-Tag, or on standard SDS-PAGE gels for comparison (Figure 3.3.1).

In standard SDS-PAGE, D1 and D3 migrated as single bands, while D2 showed a weak smear above a major distinct band (Figure 3.3.1 A). The presence of Phos-Tag in the SDS-PAGE resulted in the detection of multiple, upward-smearing bands in each lane (Figure 3.3.1 B). These additional bands above the major band may represent differently phosphorylated forms of CPB-3.

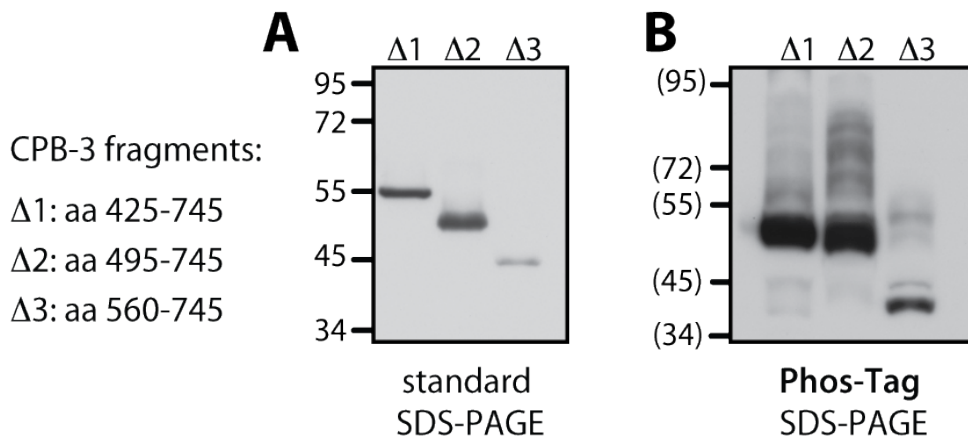


Figure 3.3.1 Phos-Tag gel resolves different forms of CPB-3 fragments.

anti-LexA immunoblots of CPB-3 fragments expressed in yeast, resolved with standard SDS-PAGE (A), and Phos-Tag SDS-PAGE (B).

Molecular masses in (B) are given in brackets due to potentially altered migration of marker bands in Phos-Tag gels.

To confirm that the additional bands represent phosphorylated CPB-3 and exclude a possibility that the bands represent partially degraded proteins or fragments bearing a post-translational modification (PTM) other than phosphate groups, protein extracts were dephosphorylated using lambda protein phosphatase (λ PP). λ PP was chosen because it has no preference towards serine (S), threonine (T) and tyrosine (Y) (Cohen and Cohen, 1989; Gordon, 1991). To confirm that removal of modified forms is specifically caused by its phosphatase activity, λ PP was inhibited in a control sample by the addition of orthovanadate

(Na_3VO_4), which acts as a competitive inhibitor (Gordon, 1991; Huyer et al., 1997). Orthovanadate mimics phosphate groups and binds to catalytic centers of phosphatases (Huyer et al., 1997). The extract containing D3 fragment was chosen for this assay, as the CPB-3 fragment D3 resolved to several distinct, sharp bands, in contrast to fragment D1 (Figure 3.3.1 B). Moreover, fragment D3 is the smallest of all three fragments, so it has fewer potential phosphorylation sites. Thus, D3 fragment may be a less challenging substrate for λPP ; partial λPP activity removing only a subset of phosphate groups would result little to no difference compared to the control.

In mock-treated yeast extracts, modified CPB-3 forms were stable on ice and at 30°C during the 30 min incubation time (Figure 3.3.2: lanes 1,2). In the sample to which λPP had been added, slower migrating bands disappeared and the intensity of the fastest band increased (Figure 3.3.2: lane 3), suggesting that phosphate groups had been taken off the protein, which speeded up their migration. Interestingly, a few slow-migrating bands are still detected in this lane, suggesting that the dephosphorylation reaction is inefficient or some residues are particularly resistant to λPP treatment. Alternatively, a post-translational modification different from phosphorylation can be hypothesised. Either way, the decrease in the amount of slow migrating bands in λPP -treated sample suggests that they represent phosphorylated CPB-3 fragments.

This interpretation is further strengthened by the observation that slower migrating forms of CPB-3 were preserved when a phosphatase inhibitor was present during λPP treatment. Although CPB-3 fragment D3 migrates differently in a Na_3VO_4 -containing than in a mock-treated sample (Figure 3.3.2: lane 4,5), altered migration is also observed when Na_3VO_4 is added to an extract containing no λPP (compare lanes 4 and 6). One caveat that needs to be kept in mind is that Na_3VO_4 structurally resembles phosphate group and it is conceivable that orthovanadate interferes with Phos-Tag molecules in the gel, locally changing migration conditions for proteins. Similar band pattern in the sample containing $\lambda\text{PP} + \text{Na}_3\text{VO}_4$, and the sample with Na_3VO_4 only, suggests that no changes to CPB-3 modifications occurred when the phosphatase and its inhibitor were present in the reaction. Thus, altered migration of CPB-3

fragments in the presence of Na_3VO_4 is independent of the presence of λPP and may be a consequence of chemical properties of Na_3VO_4 .

Altogether, this experiment suggests that yeast-expressed CPB-3 fragments are phosphorylated, likely by an evolutionarily conserved kinase. Additionally, it documents the establishment of technical basics for developing a protocol to analyse bigger proteins.

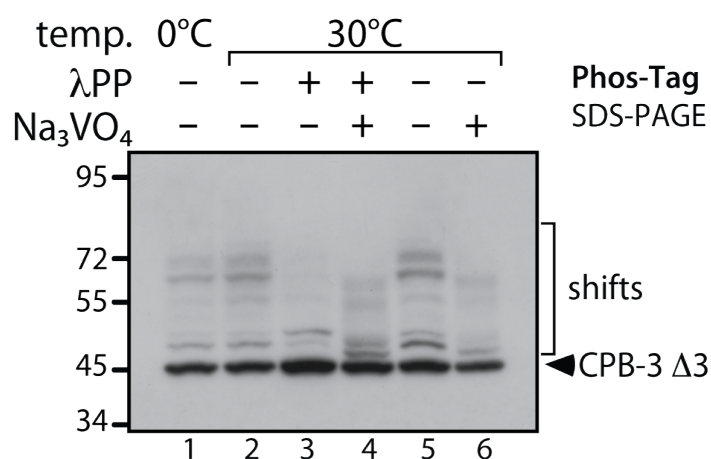


Figure 3.3.2 Additional bands represent phosphorylated forms of CPB-3.

anti-LexA immunoblot of CPB-3 $\Delta 3$ fragment expressed in yeast, incubated at indicated temperatures (temp.) and treated with lambda protein phosphatase (λPP). Sodium orthovanadate (Na_3VO_4) was used as a phosphatase inhibitor.

3.3.1.2 Phos-Tag SDS-PAGE optimisation for bigger fragments

Establishing Phos-Tag SDS-PAGE conditions for short CBP-3 fragments was followed by attempts to resolve the full-length protein. To this end, two proteins were expressed in yeast as LexA fusions: full-length CPB-3 (952 aa, predicted mass 106 kDa) and N-terminally truncated CPB-3, fragment D4 (802 aa, 89 kDa). For comparison, TCA-precipitated protein extracts were resolved in a Phos-Tag and standard SDS-PAGE gel. Immunoblot of the standard SDS-PAGE gel shows a single band of full-length CPB-3 and a doublet for D4 fragment (Figure 3.3.3). By contrast, in a Phos-Tag gel, multiple CPB-3 forms were detected, some of which formed distinct bands and some formed a smear. A simple interpretation of this behaviour is that full-length CPB-3 is modified at multiple sites, with some forms being more abundant and forming distinct bands than others, which may be less abundant and appear as a smear.

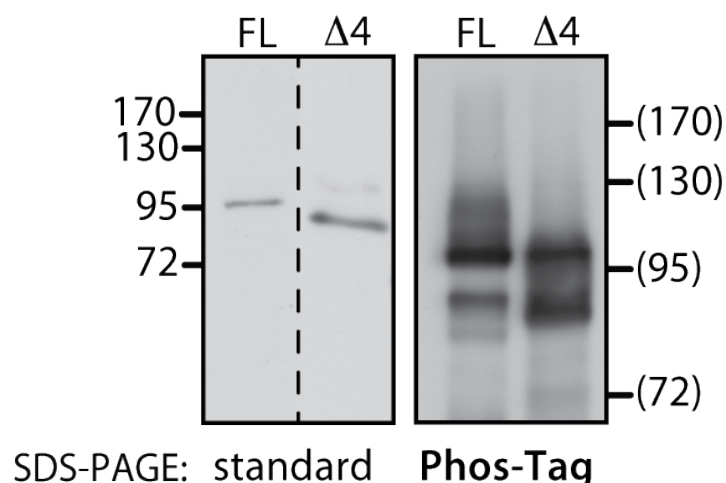


Figure 3.3.3 Phos-Tag gel increases resolution between differently modified forms of yeast-expressed CPB-3.

anti-LexA immunoblots of full-length (FL) CPB-3 and its fragment ($\Delta 4$) expressed in yeast resolved with standard and Phos-Tag SDS-PAGE.

Molecular masses for Phos-Tag blot are given in brackets due to potentially altered migration of marker bands in Phos-Tag gels.

3.3.2 CPB-3 is phosphorylated in wild-type worms

To test whether CPB-3 is phosphorylated in *C. elegans*, protein extracts from wild-type, *sel-10(0)* and *cpb-3(0)* mutant worms were prepared and resolved on a standard- and Phos-Tag SDS-PAGE gel (Figure 3.3.4). In the standard gel, CPB-3 migrates as single band at 95 kDa, which is 10 kDa bigger than protein mass calculated by Ape or ProtParam softwares from the CPB-3 amino acid sequence. Resolving worm extracts in a Phos-Tag gel reveals at minimum two additional distinct bands and a smear, which in light of previous experiments is indicative of additional, poorly resolved phospho-forms (Figure 3.3.4 A). Importantly, these bands are absent from the *cpb-3(0)* mutant extract, which argues that they are specific for CPB-3.

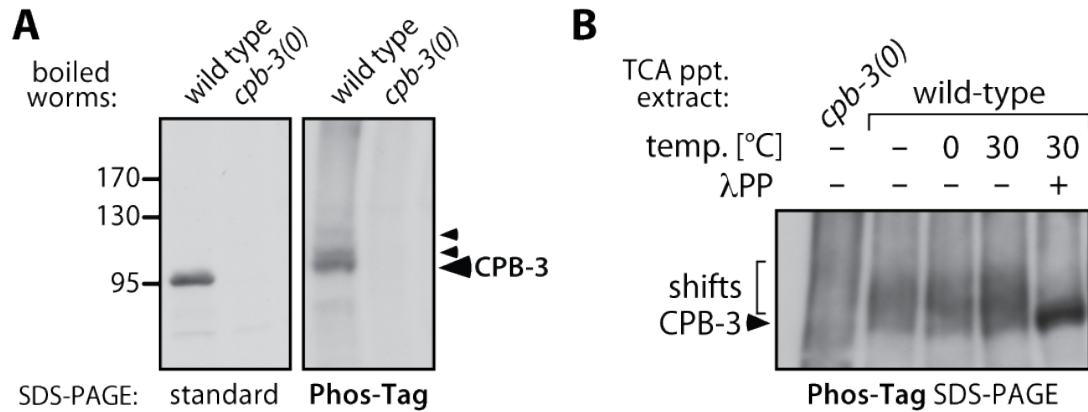


Figure 3.3.4 CPB-3 is phosphorylated in worms.

Mouse monoclonal anti-CPB-3 immunoblots of worm extracts.

(A) 50 worms boiled in SDS sample buffer were loaded in each lane.

(B) Phosphatase treatment of the TCA-precipitated worm extract. λPP: lambda protein phosphatase.

In order to confirm that the slower migrating forms represent phosphorylated CPB-3, a protein extract of wild-type worms was prepared and treated with lambda protein phosphatase (λPP). In contrast to previously observed distinct bands, CPB-3 appeared on the immunoblot as a smear (Figure 3.3.4 B). The different migratory behaviour may be a consequence of a different method used to generate the extract. The extracts in figure 3.3.4 A were prepared by boiling frozen worms in a sample buffer. This method could not be used for the λPP treatment as the components of the buffer would inactivate λPP. Instead, extracts were prepared by crushing snap-frozen worms, precipitating proteins with TCA and resuspending protein pellet in the λPP buffer. Importantly, in the extract treated with λPP the smear collapsed into a single, faster migrating band (Figure 3.3.4 B). This suggests that smearing behaviour of CPB-3 was caused by an unequal, retarded migration of differently modified phospho-CPB-3 forms. Moreover, λPP removed phosphate groups from CPB-3 and facilitated a homogenous migration through the gel matrix.

3.3.3 Phosphorylated CPB-3 accumulates in *sel-10(0)* animals

As an FbxW protein, SEL-10 is a likely component of an SCF ubiquitin ligase. Provided that SEL-10 functions similarly to its homolog Fbxw7, it is

expected to recognise a phosphorylated sequence motif (known as a phosphodegron) and to mediate turnover of phospho-CPB-3. Conversely, in the absence of SEL-10 activity, stabilisation of phosphorylated CPB-3 forms would be expected.

To test this hypothesis, protein extracts from wild-type and *sel-10(0)* adult worms were prepared by snap-freezing in liquid nitrogen and boiling in SDS-sample buffer prior to SDS-PAGE. Immunoblotting with anti-CPB-3 antibody shows that *sel-10(0)* extracts contain an additional fraction of CPB-3 forms that migrates slower than the predominant 95 kDa form present in both genotypes (Figure 3.3.5). These slower migrating bands are absent in *sel-10(0)* extracts and most likely represent post-translationally modified forms of CPB-3. The presence of several distinct, upshifting bands in *sel-10(0)* worm extracts suggests that CPB-3 carries several modifications.

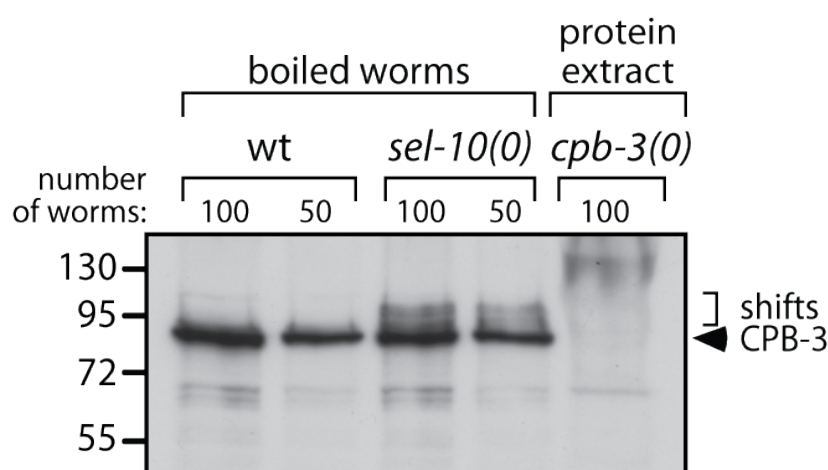


Figure 3.3.5 Modified CPB-3 accumulates in *sel-10(0)* animals.

anti-CPB-3 immunoblot of worm extracts of given genotype resolved by standard SDS-PAGE. Extracts were prepared by dissolving worms in SDS-sample buffer at 95°C (boiled worms) or by precipitating proteins of crushed worms with TCA (protein extract).

To test whether these additional bands represent phosphorylated CPB-3 forms, worm extracts were prepared by TCA protein precipitation and dephosphorylated with λ PP prior to SDS-PAGE and immunoblot analysis. In *sel-10(0)* extracts, modified forms of CPB-3 were present at similar levels when comparing the TCA-precipitated material with that of boiled worms, indicating that the majority of CPB-3 modifications are maintained upon TCA precipitation.

(Figure 3.3.6: lane 1 and 5). Prior experiments, in which proteins were extracted from crushed worms in a standard immunoprecipitation buffer, always resulted in losing modifications, even if high concentrations of phosphatase inhibitors were used (100 mM of NaF and 100 mM of β -glycerophosphate). By contrast, modified CPB-3 forms were stable in the extract kept at 4°C during 30 min incubation (Figure 3.3.6, lane 2); however, some instability was noticed when extracts were incubated at 30°C (Figure 3.3.6, lane 3). In the λ PP-treated sample, only the predominant 95 kDa band, is visible but slower migrating forms are strongly reduced. This indicates that slower migrating forms represent phosphorylated CPB-3.

Altogether, differently phosphorylated CPB-3 forms are present in wild-type worms but their detection requires increased resolving power of an SDS-PAGE gel. In the absence of *sel-10* activity, additional phosphorylated CPB-3 forms are stabilised and can be easily detected by standard SDS-PAGE.

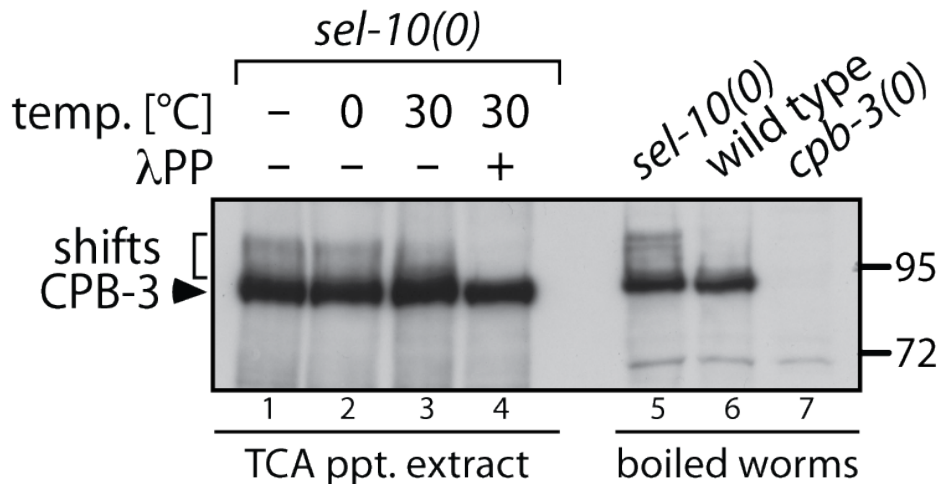


Figure 3.3.6 Phosphorylated CPB-3 accumulates in *sel-10(0)* animals.

anti-CPB-3 immunoblot of worm extracts resolved by standard SDS-PAGE. λ PP - lambda protein phosphatase. Extracts were prepared by precipitating proteins of crushed worms with TCA (TCA ppt. extract) or by dissolving worms in SDS-sample buffer at 95°C (boiled worms). 50 worms per lane loaded in lanes 5-7.

3.3.4 Bioinformatic analysis of CPB-3 sequence predicts phosphorylation sites and degrons

In order to identify potential factors and mechanisms that regulate CPB-3 stability, the amino acid sequence of CPB-3 was analysed with several bioinformatic tools for the presence of possible phosphorylation sites, protein binding motifs, and degradation motifs (degrons) (Figure 3.3.7). The employed software identifies potential functional motifs by finding similarities between sequences of annotated functional motifs deposited in the databases and the query protein.

CPB-3 has 163 phosphorylatable residues: 90 serines, 46 threonines and 27 tyrosines (Figure 3.3.7 B). NetPhos, a neural network-based prediction tool of general protein phosphorylation status, suggested modification of 82 residues: 57 serines, 17 threonines and eight tyrosines (Figure 3.3.7 C). The large number of modified residues suggested by NetPhos did not hint at any region of CPB-3 that could be particularly important for the regulation of its stability. The most recent version of the software, NetPhos3.1, which incorporates also a kinase-specific prediction tool (NetPhosK), assigned 12 kinases to the majority of candidate phosphosites. Four kinases, PKC, cdc2, cdk5, and p38MAPK were assigned most often, together potentially modifying 67 sites. Modification of CPB-3 by cyclin-dependent or MAP kinases would be consistent with the hypothesis that CPB-3 degradation is restricted to a certain meiotic stage, and that kinase activities couple nuclear events (meiotic progression) to cytoplasmic events (differentiation program). A thorough analysis of potential CPB-3 kinases was hindered by the fact that NetPhos database includes modifications made by only 17 kinases. Few homologs of these 17 kinases have been characterised in the *C. elegans* germ line. Therefore, motifs involved in the regulation of CPB-3 stability could not be identified by matching suggested phospho-sites to known kinase activities at the pachytene-to-diplotene transition in the worm germ line.

Further analysis was performed with ELM, a eukaryotic linear motif search tool, which scans the submitted protein sequence against the database of short linear motifs (SLiMs). To reduce the rate of false-positive calls, the software uses several filters based on contextual information including taxonomy, cellular compartment, evolutionary conservation and structural

features. In total, 344 instances of 62 different ELMs were identified in CPB-3 sequence. These numbers dropped to 241 and 47, respectively, after species- and globular domain filtering. 67 residues were identified as potential phosphosites for nine different kinase groups (CDK, CK1, CK2, GSK3, NEK2, PIKK, PKA, PLK, proline-dependent kinase).

Attempts to identify regulators of CPB-3 expression pattern, which are described in detail in section 3.2, suggested an important role of MAP kinase, MPK-1. MAPK are very promiscuous kinases with regard to the sequence they phosphorylate, as the minimal consensus is a proline that immediately follows modified serine or threonine (S or T). Thus, 19 proline-dependent kinase consensus sites were of particular interest (Figure 3.3.7 D). Specificity of MAPK kinases is determined by the site on the target protein to which they bind, a so-called "docking" site. Interestingly, three consensus docking sites were identified in CPB-3 (Figure 3.3.7 F). Due to the topography of MAP kinases, a phospho-acceptor site must be separated from the docking site by a minimal distance of ~9 amino acids (Fernandes et al., 2007). The phosphorylation usually occurs C-terminally from the docking site, within 10-100 amino acids (Garai et al., 2012; Zeke et al., 2015). Thus, two predicted docking sites and phosphoacceptor sets looked particularly likely to be functional: a docking site between amino acids 24-33, which is in optimal distance to S43 and T45, and a docking site between aa 87-94, which could allow phosphorylation of T106 or S108 (figure 3.3.7 D,F).

To see if the suggested MAPK phosphorylation sites could serve as motifs regulating CPB-3 stability, their location was compared with the location of degron motifs identified by ELM. The software searches for a consensus recognition site for the human homolog of SEL-10, Fbxw7. The sequence pattern is defined as [LIVMP].{0,2}(T)P..([ST]), where "[]" brackets indicate allowed amino acids, "." (dot) indicates any aa, "{}" brackets specify minimal and maximal number of repeats of a preceding feature, "()" parentheses indicate position of interest, which in this case is phosphorylated serine or threonine. Three sequences similar to the Fbxw7 consensus site have been identified in CPB-3 at positions 220-224, 641-645, and 694-698. Thus, none of the predicted degrons is located in a proximity to MAPK docking sites, suggesting that either MPK-1 acts

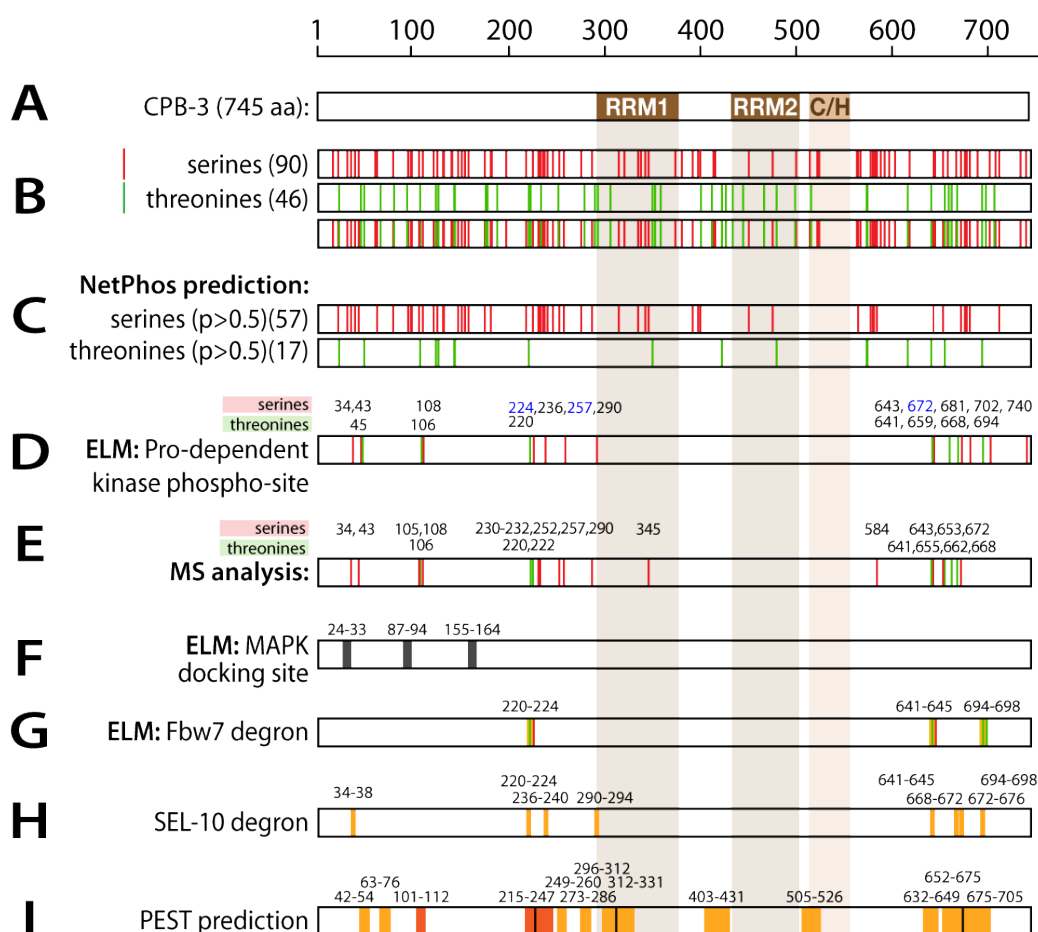


Figure 3.3.7 Potential regulatory sites in CPB-3.

Stick diagrams representing CPB-3 protein and results of sequence analyses. Red lines - serines, green lines - threonines.

(A) Conserved domains in CPEB proteins involved in RNA binding; RRM - RNA recognition motif, C/H - zinc fingers (C4 and C2H2 type)

(B) All serine and threonine residues present in CPB-3

(C) Serines and threonines predicted to be phosphorylated by NetPhos3.1; probability threshold = 0.5

(D) Serines and threonines predicted to be phosphorylated by proline dependent kinases (e.g MAPK or CDK) predicted by ELM. In blue: residues located in optimal context for cyclin dependent kinases (CDKs, recognition motif: ...([ST])P.[KR]).

(E) Results of mass spectrometry-based analysis of the phosphorylation of recombinant CPB-3 expressed in insect cells.

(F) Docking site for MAP kinases predicted by ELM defined as [KR]{0,2}[KR].[0,2][KR].[2,4][ILVM].[ILVF].

(G) Fbxw7/SEL-10 degrons predicted by ELM defined as [LIVMP].[0,2](T)P..([ST]).

(H) Sequences matching extended version of consensus sequence for SEL-10 binding defined as [ST]P..[ST] after de la Cova and Greenwald (2013).

on CPB-3 over the usual distance of 10-100 aa from the docking site, which has been reported for some proteins (Garai et al., 2012; Zeke et al., 2015), or these potential degrons are phosphorylated by a different kinase. Another possibility is that CPB-3 contains more degrons aside from those predicted by ELM.

Proteins whose stability is tightly regulated may contain multiple degrons, and their sequences may deviate from the consensus. Phosphorylation of majority of these degrons is then required to trigger protein degradation. A canonical example for such a regulatory mechanism is the budding yeast inhibitor of S-phase, Sic1p. Here, phosphorylation of at least six of its nine sub-optimal degrons is required to provide efficient recognition of Sic1p by the F-box protein Cdc4p. Four out of nine Sic1p degrons contain a suboptimal serine instead of the preferred threonine at the central position of the motif (Nash et al., 2001). Since a T/S alteration in the consensus for Fbxw7 is not supported by ELM definition of the motif, the sequence of CPB-3 was re-analysed to identify potential variations of the motif. To this end, CPB-3 was scanned for the presence of a sequence [ST]P.[ST], which largely resembles a consensus used in a bioinformatic screen for SEL-10 targets in *C. elegans* (de la Cova and Greenwald, 2012). Seven motifs corresponding to this definition were identified (Figure 3.3.7 H), including three found by ELM. The most N-terminally located putative SEL-10 degron (aa 34-38) adjoins one of the predicted MAPK docking sites (aa 24-33; Figure 3.3.7 F), not providing the minimal distance between the docking and phosphorylation site that is required for efficient phosphorylation by MAP kinases. Thus, MPK-1 is unlikely to generate a recognition site for SEL-10 at that location. Other potential SEL-10 recognition motifs cluster around Fbxw7 consensus sites identified by ELM (compare 3.3.7 H and F). Two SEL-10 degrons are located between the most terminal Fbxw7 consensus sequence and the first RNA recognition motif (RRM1), in proximity to the predicted MAPK docking site between aa 155-164. The other two potential SEL-10 degrons form a tandem located between the second and the third Fbxw7 consensus, in the C-terminal part of the protein (Figure 3.3.7 H). If CPB-3 regulation resembled that of Sic1p, requiring hyperphosphorylation of the protein and multiple phosphodegrons for efficient SEL-10 binding, all these sites could contribute to the regulation. Based on the data obtained from Cdc4p (Nash et al., 2001), exact Fbxw7/Cdc4

consensus sites would have a higher affinity to SEL-10 than the sites with S/T alterations. However, no studies of the affinity between SEL-10 and its substrates have been documented so far.

Interestingly, all identified degrons reside either within or in close proximity to PEST motifs. A PEST sequence is a stretch of a polypeptide chain that is rich in proline (P), glutamic acid (E), serine (S) and threonine (T), hence its name. The occurrence of such sequences has been found to correlate with short half-life of a protein (Rogers et al., 1986). A PEST prediction tool, ePESTfind, identified three regions that are likely to influence CPB-3 stability ('potential PESTs'). Additionally, it identified 11 'poor PESTs', whose influence on protein stability is less likely. The most N-terminal Fbxw7 degron identified by ELM resides in one of the 'potential PESTs', while the two others are located in less likely PESTs in the C-terminal end of the protein (Figure 3.3.7 I). Thus, different approaches of sequence analysis suggest that the region N-terminally neighbouring RRM1 (aa 215-294) and the C-terminal fragment behind the zinc-finger (aa 641-698) may function in a regulation of CPB-3 stability.

Altogether, bioinformatic analysis of CPB-3 sequence highlighted two regions that can be important for the regulation of CPB-3 stability. These regions contain phosphorylatable residues in a sequence context that makes them potential targets of kinases that are likely to be active in meiosis, such as MAPK or CDKs. Additionally, several potential phosphosites reside in an amino acid context resembling a degradation motif recognised by homologs of SEL-10. Moreover, three potential degrons are evolutionarily conserved in the *Caenorhabditis* genus (data not shown), which increases the probability that these motifs may indeed play a regulatory role in CPB-3 stability.

3.3.5 Identification of phosphorylated residues in CPB-3 by mass spectrometry

In order to find out which of 167 phosphorylatable residues in CPB-3 might be modified *in vivo*, mass spectrometry-based analysis of CPB-3 phosphorylation status was performed. Obtaining reliable results depends on submitting sufficient protein amount for the analysis. The aim was to identify peptides covering the entire protein sequence. Moreover, the phosphorylated forms have to be abundant, as rarely occurring modifications may be either not

detected or mistakenly classified as noise. Modified CPB-3 immunoprecipitated from worm extracts would be a preferred material for performing modification analysis. Unfortunately, phosphorylated forms of CPB-3, which are detectable in extracts of *sel-10(0)* mutant worms after immediate boiling, were highly unstable and could not be maintained in any tested immunoprecipitation buffer (data not shown). Therefore, CPB-3 was C-terminally tagged with six histidines (6xHis-tag), expressed in insect cells, and purified under denaturing conditions, which allowed maintaining modifications (Figure 3.3.8 A). Recombinant CPB-3 protein, as given in figure 3.3.8 B, was submitted to the analysis by the Mass Spectrometry facility at MPI-CBG (Dresden). The obtained results are summarised in figure 3.3.7 E.

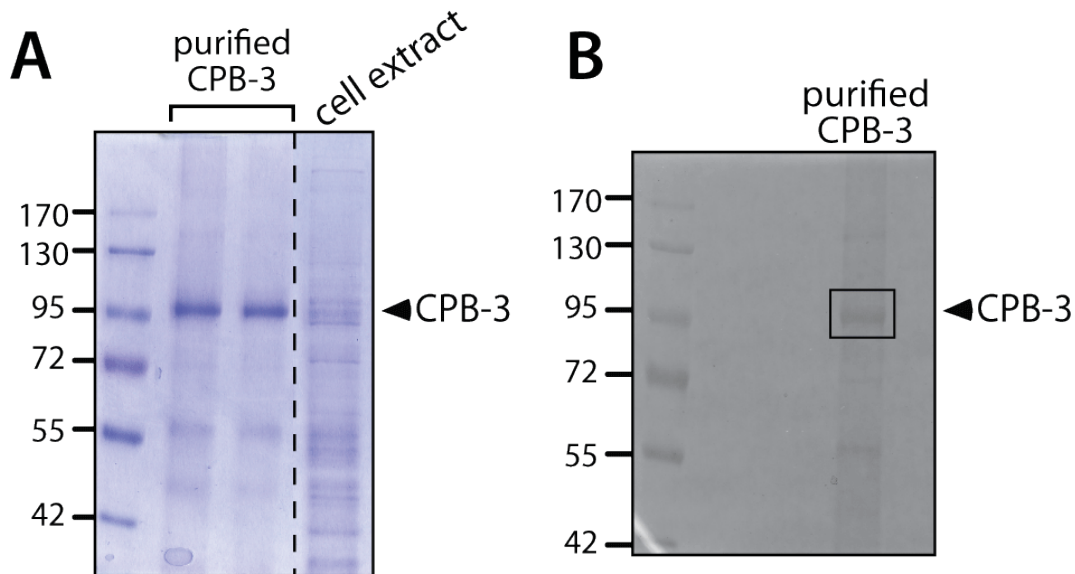


Figure 3.3.8 Purified recombinant CPB-3 for phosphorylation analysis by mass spectrometry.

Coomassie Brilliant Blue-stained gels showing recombinant 3xFLAG::CPB-3::6xHis protein expressed in insect cells.

(A) Cell extract and an eluate from CPB-3 purification in denaturing conditions. Modified CPB-3 forms are weakly visible above the major 95 kDa band in lanes loaded with eluate ("purified CPB-3"). Due to low expression levels of the recombinant CPB-3, it cannot be precisely indicated in the "cell extract" lane. Dashed line indicates region where some lanes were removed from the image for the clarity of the display.

(B) Image of the gel from which CPB-3 was excised for mass-spec analysis. Excised fragment is marked with a rectangle.

Results of analysis are presented in figure 3.3.9 E.

Peptides covering 71.5% of protein sequence were detected. Comparison of m/z values of detected peptides against the database of theoretical phosphorylated ions retrieved more than 16 potentially modified sites, including nine serines, three threonines, and four serine- and threonine-containing clusters, which could not be resolved to identify a single modified amino acid (Figure 3.3.7 E). Two identified residues (T220, T641) are located within predicted Fbxw7 degrons (Figure 3.3.7 G). The peptide covering the third predicted Fbxw7 phosphodegron was not detected. Four additional residues identified in mass-spec analysis (S34, S290, T668, S672) are located in the consensus for SEL-10/Fbxw7 phosphodegron. The identification of phosphorylations in these regions implies that these sites are not buried in the protein structure but are presumably accessible to other proteins. Thus, these sites could serve as regulatory regions. Moreover, seven phosphoserines and four phosphothreonines overlap with residues identified by ELM as consensus sites for proline-dependent kinases (Figure 3.3.7 D,E), suggesting that these sites are likely accessible to cyclin-dependent kinases and MAP kinases.

Since a great part of motifs in the ELM and NetPhos databases come from studies in mammalian cell cultures, identifying some of the predicted sites to be phosphorylated in insect cells suggests that conserved kinases may be involved in their modification. Thus, it is possible that identified serines and threonines are also modified in *C. elegans*. Their location in amino acid context of predicted SEL-10 consensus makes them likely to play a role in the regulation of CPB-3 turnover.

3.4 Kinase-mediated regulation of CPB-3 stability

Reduction in the CPB-3 protein levels during meiosis occurs shortly before the pachytene-to-diplotene transition and very likely requires a phosphorylation that generates a binding site for an SCF ubiquitin ligase. In order to identify a hypothetical kinase involved in CPB-3 regulation, RNAi-mediated knocked-down of several candidate genes was performed and followed by immunofluorescent staining of germ lines to test for changes in CPB-3

expression. At first, two kinases that regulate cell cycle progression were tested: cyclin-dependent kinase, CDK-1, and polo-like kinase, PLK-1. Noteworthy, CDK-1 and PLK-1 were shown to regulate CPEB stability in *Xenopus* oocytes (Setoyama et al., 2007). If the pathway that regulates CPB-3 stability is evolutionarily conserved, then stabilisation of CPB-3 should be observed upon CDK-1 or PLK-1 deficiency.

3.4.1 CDK-1 and PLK-1 are probably not involved in regulating CPB-3 stability

To investigate a presumed contribution of CDK-1 and PLK-1 to the regulation of CPB-3 expression in the germ line, RNAi feeding constructs against these genes were generated and the efficiency of gene knock-down was assessed by observing phenotypes previously reported in the literature (Boxem et al., 1999; Chase et al., 2000b). Immunofluorescently stained gonads of *cdk-1* or *plk-1*-depleted animals displayed similar CPB-3 expression pattern to germ lines of mock-treated worms (Figure 3.4.1). In particular, no difference was observed at pachytene-to-diplotene transition, where CPB-3 regulated turnover may occur. Moreover, overall CPB-3 levels in the pachytene region were similar among all samples. These observations suggest that *cdk-1* and *plk-1* are not major regulators of CPB-3 stability. Nonetheless, the fact that kinase activities were not well characterised in this experiment leaves the possibility that CDK-1 and PLK-1 do act on CPB-3, and their residual activity in RNAi experiment was sufficient to destabilise CPB-3. The efficiency of each kinase knock-down was assessed by morphological and physiological phenotypes, such as appearance of nuclear aberrations in the mitotic region (MR) of the gonad, or lethality among embryos. Embryos of animals treated with RNAi for 12 h failed to hatch, whereas nuclear aberrations in the MR were apparent later, after 24-36 h of feeding. Presented analysis of CPB-3 expression was performed after 24h of feeding; i.e. 12 h after first severely affected embryos were laid, and before proliferating germ cells displayed strong defects that could potentially affect meiosis. Nevertheless, even upon longer exposure to RNAi, a normal reduction of CPB-3 levels occurred normally (data not shown), stressing that CDK-1 and PLK-1 are not the very likely regulators of CPB-3 turnover.

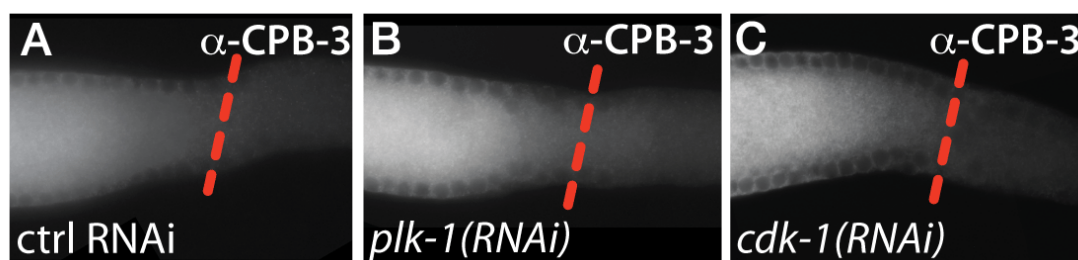


Figure 3.4.1 Activity of MPK-1, but not PLK-1 or CDK-1, regulates CPB-3 stability in late pachytene.

Representative immunostainings of extruded germ lines of wild-type worms treated with RNAi against indicated genes. RNAi feeding started at L4; worms were analysed 36 h later. Dashed red lines indicate the pachytene-to-diplotene border determined by the appearance of DAPI-stained chromatin (not shown).

C. elegans contains three genes encoding polo-like kinases, which could act redundantly regulating CPB-3 abundance. While a depletion of *plk-1* by RNAi leads to defects in nuclear envelope breakdown, meiotic chromosome segregation and cytokinesis, which result in embryonic arrest at one-cell stage (Chase et al., 2000b), large-scale RNAi studies did not uncover phenotypes for *plk-2* or *plk-3* depletion (Chase et al., 2000a; Rual et al., 2004). However, a more careful investigation into both gene functions revealed that *plk-2* has a partially redundant role with *plk-1* in establishing embryonic polarity (Nishi et al., 2008). Moreover, PLK-2 is required in meiotic cells for regulation of chromosome dynamics that leads to the attachment of meiotic chromosomes to the nuclear envelope (Nishi et al., 2008). By contrast, PLK-3 function is poorly characterised, as a slight delay in chromosome condensation at diakinesis is the only defect that has been reported (Harper et al., 2011). Thus, even though *plk-2* and *plk-3* are not essential genes, they are apparently active in meiosis and could regulate CPB-3 redundantly with PLK-1. To test this possibility, *plk-2* and *plk-3* were knocked-down by RNAi individually. In addition, a combined feeding against all three *plk* genes was performed (*plk-1/-2/-3* RNAi).

Consistent with previous reports, gross changes in the germ lines of *plk-2* or *plk-3* animals were not observed (data not shown). By contrast, a simultaneous knock-down of all three *plk* genes induced several defects in the germ line: oocytes were present in the distal gonad and aberrant misshapen oocytes occupied the proximal gonad (data not shown). Immunostaining of *plk-1*,

-2 and -3 tripple-depleted germ lines revealed that CPB-3 expression did not differ much from control germ lines (data not shown). A normal stepwise increase in CPB-3 intensity was observed in the distal end of the gonad. As cells entered meiosis, CPB-3 reached its maximum level, which was maintained until shortly before cells transited to diplotene and changed their arrangement in the gonad to form a single row of oocytes. Surprisingly, in the distal end, CPB-3 tended to form large foci of strong fluorescence (14/24 germ lines observed), which were not seen in controls (0/10 germ lines). Except for the foci formation, CPB-3 expression pattern upon RNAi-mediated knock-down of three *plk* genes did not differ from the control, suggesting that PLKs are likely not involved in regulating the reduction in CPB-3 levels in late pachytene.

3.4.2 MAP kinase MPK-1 influences CPB-3 stability

MPK-1 regulates multiple aspects of oogenesis, such as progression through pachytene, cellular organisation in the germ line and oocyte growth. Interestingly, activation of MPK-1 in the distal region of the gonad correlates with a decrease in CPB-3 levels, indicating potential functional interaction between the two proteins. Strong alleles of *mpk-1* cause pachytene arrest in germ cells (Church et al., 1995; Lackner and Kim, 1998), so they could not be used to test if CPB-3 stability increases when MPK-1 activity is reduced. Thus, *mpk-1* was knocked-down by RNAi feeding, which only partially reduced its function. Immunofluorescent stainings of extruded germ lines revealed a change in CPB-3 expression pattern upon *mpk-1* knock-down. While the CPB-3 expression pattern in the distal end remained apparently unaffected, CPB-3 signal intensity did not drop in late pachytene and remained high as cells transited to diplotene (Figure 3.4.2 A). This observation suggests that MPK-1 may regulate CPB-3 stability at pachytene-diplotene transition.

3.4.3 The MAP kinase MPK-1 regulates CPB-3 phosphorylation

Assuming that MPK-1 regulates CPB-3 stability, it is expected to affect CPB-3 phosphorylation status. It is technically challenging to detecting phosphorylated forms of CPB-3 in extracts from wild-type worms (described in section 3.3). Therefore, *mpk-1* RNAi feeding was performed in *sel-10(0)* mutant

worms, which contain increased amount of modified CPB-3. To test whether the amount of phosphorylated CPB-3 is reduced upon *mpk-1* depletion, worm extracts from RNAi-treated animals were analysed by SDS-PAGE followed by immunoblotting (Figure 3.4.2 B,C).

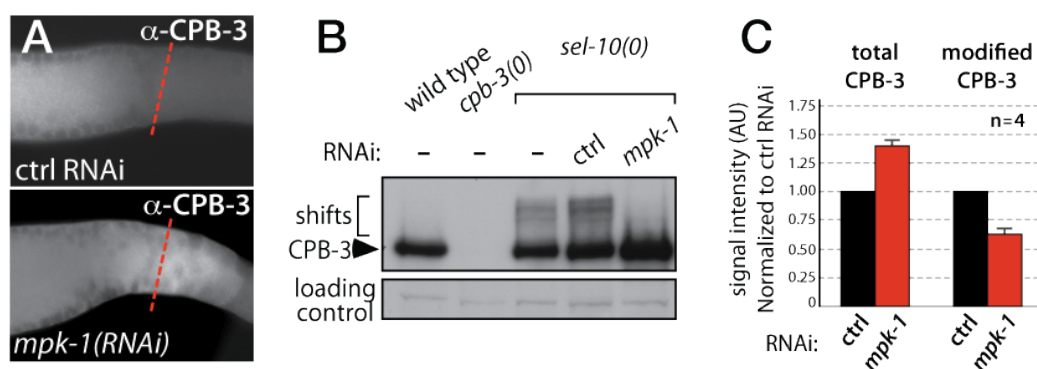


Figure 3.4.2 MPK-1 regulates CPB-3 expression pattern and phosphorylation status.

(A) Representative immunostaining images of extruded wild-type germ lines after RNAi-mediated depletion of *mpk-1*. Red dashed lines indicate pachytene-diplotene border determined by chromatin appearance (not shown).

(B) Immunoblotting of worm extracts of indicated genotypes upon indicated RNAi conditions; dashes indicate standard bacterial food (*E.coli* OP50). 50 worms at the age of L4+30 h were loaded per lane. Paramyosin is used as a loading control.

(C) Quantification of signal intensity on anti-CPB-3 probed immunoblots in four independent RNAi feeding experiments. 'Total CPB-3' includes the major 95 kDa band and slower migrating forms (shifts); 'modified CPB-3' includes shifts only. Average signal intensity values in control RNAi were set as 1. Error bars show SEM.

As observed previously, extract from wild-type worms contained a single prominent band at 95 kDa (Figure 3.4.2 B). By contrast extracts of *sel-10(0)* mutants contained the 95 kDa band and in addition many slower migrating, phosphorylated forms of CPB-3 (Figure 3.4.2 B). Neither the major band, nor the retarded forms were detected in the *cpb-3(0)* mutant, arguing that the detected signal is specific for CPB-3. Importantly, extracts of *mpk-1*-depleted *sel-10(0)* worms contained reduced amount of phosphorylated CPB-3, whereas the intensity of the major fastest-migrating band seemed to be higher than in the other samples (Figure 3.4.2 B).

The apparent changes in the migratory behaviour of CPB-3 upon *mpk-1* knock-down were quantified by measuring anti-CPB-3 signal intensity on immunoblots from four independent experiments. The intensity of the CPB-3

signal coming from the major band and the retarded forms (total CPB-3) increases upon *mpk-1* RNAi (Figure 3.4.2 C). This indicates an increase in total amount of CPB-3 protein in the germ line and suggests that CPB-3 is stabilised when MPK-1 activity is reduced. By contrast, the amount of phosphorylated CPB-3, measured as intensity of the signal above the major band, decreased upon *mpk-1* RNAi (Figure 3.4.2 C), suggesting that MPK-1 may regulate CPB-3 phosphorylation.

3.4.4 CPB-3 binds to MPK-1 in yeast

MPK-1 might bind and phosphorylate CPB-3 directly, or may modify activity of other kinases, and thus regulate CPB-3 phosphorylation indirectly. To test whether a direct interaction between CPB-3 and MPK-1 can occur, a yeast-two-hybrid (Y2H) assay was performed. CPB-3 was fused to the Gal4 activating domain (AD), MPK-1 was fused to the LexA DNA binding domain (DB). DB::SEL-10 fusion served as a positive control for the assay, as the interaction between CPB-3 and SEL-10 was identified in yeast and confirmed in co-immunoprecipitations from insect cells (section 3.2). Another FbxW protein, LIN-23, served as a likely negative control, as the analyses of *lin-23* loss-of-function mutation and RNAi-treated animals suggested that it does not influence CPB-3 regulation (data not shown). A physical interaction between DB/AD hybrid proteins in the Y2H system tethers the activating domain to the DB domain, reconstituting a functional transcription factor, and triggers synthesis of the reporter gene (here: β -galactosidase, β -gal). β -gal is detected by the ability of cells to convert its substrate X-gal into a blue product.

Expression of hybrid proteins was confirmed by immunoblotting of yeast extracts (data not shown). Yeast that co-expressed CPB-3 and SEL-10 turned blue in the assay, suggesting interaction of the hybrid proteins (Figure 3.4.3). By contrast, no blue colour was observed in cells co-expressing CPB-3 and LIN-23, demonstrating that CPB-3 does not induce reporter expression on its own or when co-expressed with a non-interacting hybrid. Importantly, cells that co-expressed CPB-3 and MPK-1 turned blue suggesting that MPK-1 binds CPB-3.

Altogether, the collected data indicate that the MAP kinase, MPK-1, regulates CPB-3 stability, whereas two regulators of cell cycle progression, CDK-1 and PLK-1, are unlikely to be involved in CPB-3 turnover in late pachytene.






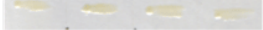
		DB fusion:	AD fusion:	% blue	n =
1		SEL-10ΔF	CPB-3	87	30
2		MPK-1	CPB-3	63	24
3		LIN-23	CPB-3	0	15
4		SEL-10ΔF	-	0	30
5		MPK-1	-	10	50
6		LIN-23	-	0	10

Figure 3.4.3 MPK-1 interacts with CPB-3 in yeast.

β -galactosidase activity on X-gal substrate in yeast co-expressing indicated fusion proteins. DB - DNA binding domain (bait), AD - activation domain (prey). Blue colonies indicate likely interaction between fusion proteins, white colonies - likely no interaction. n - number of tested colonies coming from at least two transformations. Expression of fusion proteins was verified by immunoblotting (not shown).

3.5 Phosphorylation of CPB-3 links its degradation to meiotic progression

CPB-stability may be regulated either constitutively, i.e. throughout meiosis, or only at a specific stage of meiosis. The expression pattern of CPB-3 suggests that its stability decreases at the end of pachytene. Moreover, a reduction in proteasome activity extends the expression of CPB-3 into two post-pachytene stages, diplotene and diakinesis, which is consistent with the expectation that in the absence of ubiquitin-mediated degradation, proteins persist longer during the course of meiosis. Importantly, a reduction in proteasome activity does not significantly affect total amounts of CPB-3, suggesting negligible regulation of CPB-3 by the ubiquitin-proteasome system (UPS) prior to late pachytene. Thus, turnover of CPB-3 is likely to be stage-specific.

3.5.1 Hyperphosphorylated CPB-3 does not accumulate in the pachytene-arrested mutant, *daz-1(0)*

If the degradation of CPB-3 exclusively happens at the pachytene-to-diplotene transition, an inhibition of degradation in pachytene-arrested germ line is expected to have no influence on CPB-3 levels. Furthermore, an accumulation of its phosphorylated forms should not be observed.

To test this hypothesis, *sel-10* activity was reduced by RNAi in *daz-1(e3)* null-mutant worms (henceforth referred to as *daz-1(0)*). In *daz-1(0)* hermaphrodites, spermatogenesis is unaffected but female-fated germ cells arrest in pachytene and do not progress to later meiotic stages (Karashima et al., 2000). Analysis of worm extracts by immunoblotting showed that *sel-10* RNAi in wild-type worms led to similar accumulation of phosphorylated CPB-3 as observed in *sel-10(0)* mutants (Figure 3.5.1: lanes 1,2,3), indicating efficient RNAi. However, *sel-10* RNAi did not induce accumulation of phosphorylated CPB-3 in *daz-1(0)* mutant animals (lanes 4,5), suggesting that *sel-10* does not regulate CPB-3 proteins prior to pachytene exit.

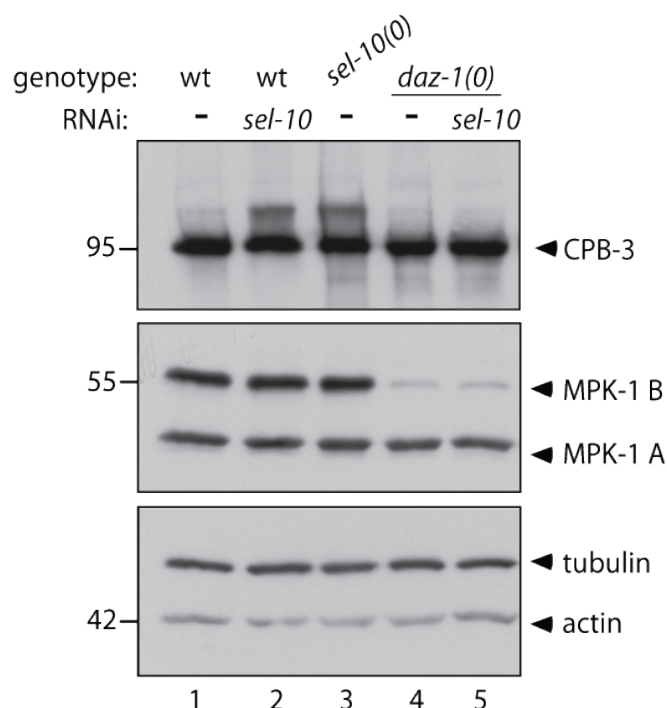


Figure 3.5.1 Modified CPB-3 does not accumulate in *daz-1(0)* mutants.

anti-CPB-3 and anti-MPK-1 immunoblots of worm extracts, 50 worms at L4+36h per lane. Two isoforms of MPK-1 are detected: smaller, predominantly somatic MPK-1A, and larger, germ line-specific MPK-1 B. Reduction of MPK-1 B signal in pachytene-arrested *daz-1(0)* mutants was consistently observed. Dashes indicate control RNAi. Size marker to the left. Tubulin and actin serve as loading controls.

3.5.2 The total amount and activity of MPK-1 are decreased in *daz-1(0)* mutant germ lines

The observation that phosphorylated forms of CPB-3 do not accumulate upon inactivation of *sel-10* in *daz-1(0)* mutant germ cells could be explained by the absence of upstream regulators, such as the CPB-3 regulatory kinase MPK-1. Previous results suggested that the mitogen-activated protein kinase, MPK-1, may play a role in regulating the abundance and phosphorylation status of CPB-3 (Figure 3.4.2). Therefore, both total amount and activity of MPK-1 were analysed in *daz-1(0)* mutant animals.

Immunoblotting of worm extracts showed that the levels of the somatic isoform of MPK-1, MPK-1A (45 kDa), are comparable between wild type and *daz-1(0)* mutants (Figure 3.5.1, compare lanes 1 with 4). By contrast, levels of the germ-line specific isoform MPK-1B (55 kDa), are reduced in *daz-1(0)* worms compared to wild type (Figure 3.5.1: lanes 1 and 4). However, *daz-1(0)* germ lines are smaller than wild-type ones (see Figure 3.5.2 A,B), so the total germline protein levels might be reduced.

To determine the levels of the active form of MPK-1, extruded gonads were stained with an antibody specific for activated MAPK (dpMPK-1), which is phosphorylated at two conserved residues. First, gonads from *mpk-1* RNAi depleted animals were compared to those from animals fed control RNAi to establish antibody specificity; a very weak dpMPK-1 signal was uniformly detected in gonads and corpses, which was barely above general slide background (data not shown). Next, wild-type germ lines were analysed to confirm that the staining procedure allows to recapitulate published observations (Lee et al., 2007a; Lee et al., 2007b) (Figure 3.5.2 A). As expected, the dpMPK-1 signal intensity varied according to the developmental stages of the germ cells, generating a distinct double-peak pattern across the gonad: distal proliferative germ cells and those in early meiosis – up to the stage of mid-pachytene – are barely stained; germ cells in late pachytene are moderately stained; those transiting to diplotene lose some signal intensity, whereas diakinetik germ cells regain stronger signals that reach maximum intensity in the most proximal part of the gonadal arm (Figure 3.5.2 A). Altogether, the staining

procedure allowed recapitulation of published results and could be used to investigate MPK-1 activity in various genetic backgrounds.

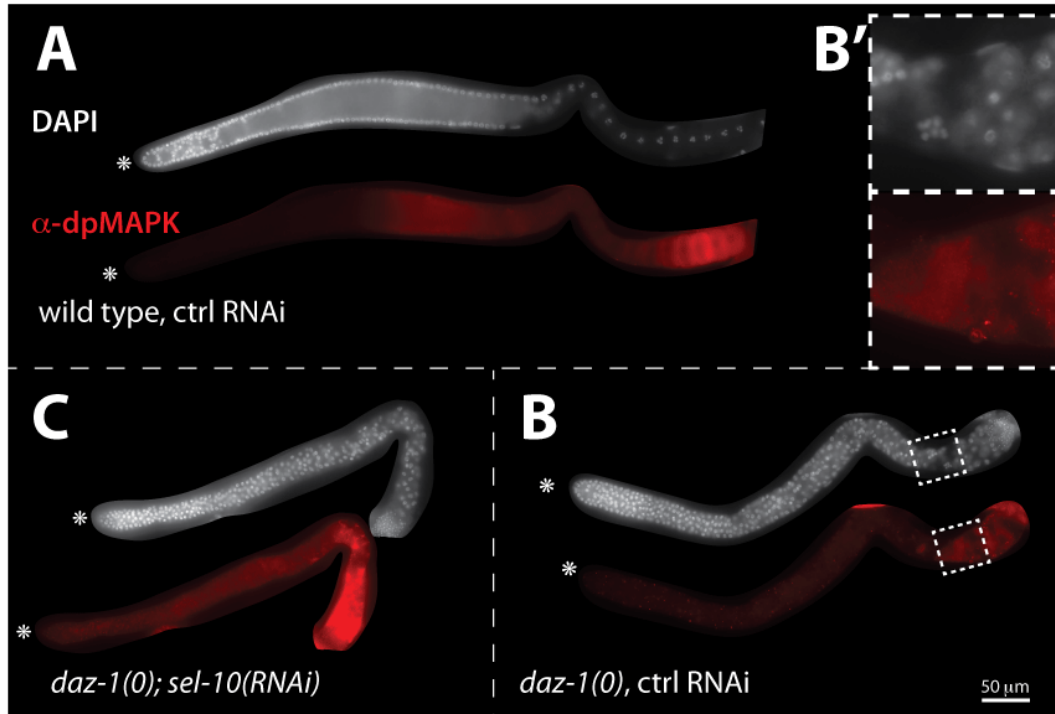


Figure 3.5.2 Levels of active MPK-1 are low in *daz-1(0)* germ lines but increase upon *sel-10* knock-down.

Extruded gonads of L4+36h animals fixed with method (18.2) and stained with DAPI (white) and anti-dpMAPK antibody (red). Asterisk indicate distal tip. Scale bar: 50 μ m.

(A) Localisation of active double phosphorylated (dp) MPK-1 in a wild-type germ line.

(B) dpMPK-1 signal is strongly reduced in *daz-1(0)* germ line.

(B') Cytoplasm around rare diakinetic nuclei in *daz-1(0)* germ lines show increased levels of MPK-1 activity.

(C) dpMPK-1 levels in *daz-1(0)* increase upon *sel-10* knock-down.

In *daz-1(0)* mutant germ lines, the mitotic region (MR) does not exhibit defects but the transition zone and pachytene region are extended and fill the gonad till its proximal end. Regions of diplotene and diakinesis are absent. In immunofluorescently stained germline tissue, anti-dpMPK-1 signal is close to background levels throughout distal gonad (Figure 3.5.2 B). In contrast to wild-type germ lines, there is no peak in MPK-1 activity before the bend region. Although the proximal *daz-1(0)* gonads stain very weakly with anti-dpMPK-1 antibodies, some signal above background levels is detectable. The signal in the proximal end of *daz-1(0)* gonads is much weaker than in the proximal end of

wild type gonads. Interestingly, in *daz-1(0)* germ lines, the cytoplasm around rarely occurring diakinetik-like nuclei has relatively high levels of dpMPK-1, corresponding roughly to signal intensities in the late pachytene region of a wild-type germ line (Figure 3.5.2 B'). This positive staining for dpMPK-1 confirms that MPK-1 protein is present in the germ line and may be activated in some conditions. Low signal intensity in *daz-1(0)* germ lines hints that MPK-1 activity is strongly reduced in comparison to wild-type germ lines and its distribution does not reflect wild-type distribution.

The observed low activity of MPK-1 in *daz-1(0)* germ lines could explain why phosphorylated CPB-3 does not accumulate in the germ line upon depletion of *sel-10*. Assuming that phosphorylation of CPB-3 by MPK-1 is necessary for CPB-3 binding to SEL-10 followed by CPB-3 turnover, the absence of SEL-10 should result in an accumulation of phosphorylated forms of CPB-3. However, the accumulation cannot occur if MPK-1 is inactive or shows very weak activity. Interestingly, anti-dpMPK-1 staining in *sel-10*-depleted *daz-1(0)* germ lines revealed very high activity of MPK-1 in the proximal gonad, where pachytene cells reside (Figure 3.5.2 C). Intensity of this signal was comparable to the intensity in proximal gonad of wild-type worms. Hence, MPK-1 activity in *daz-1(0); sel-10(RNAi)* germ lines is expected to be sufficient to phosphorylate CPB-3. The observation that phosphorylated forms of CPB-3 do not accumulate suggests that their occurrence may be linked to the pachytene-to-diplotene transition, which does not take place in *daz-1(0)* mutants.

3.5.3 Phosphorylated CPB-3 does not accumulate in early- and mid-pachytene

To investigate the timing of CPB-3 phosphorylation and destabilisation in an alternative way, the accumulation of phospho-CPB-3 in the *cpb-3(bt17)* mutant was examined. *cpb-3(bt17)* is a 1171 bp in-frame deletion that truncates the first RNA recognition motif (RRM), and eliminates the second RRM and the C-terminal ZZ-type zinc-binding domain (Hasegawa et al., 2006; Merkel et al., 2013). Although the resulting truncated protein, CPB-3bt17, is expressed at lower levels than wild type CPB-3 as indicated by immunoblotting analysis of worm extracts (Hasegawa et al., 2006), it has similar expression pattern to wild-type CPB-3, i.e. CPB-3bt17 protein levels are very low in the distal proliferative

region, start to increase in the proximal part of the mitotic region and increase to high levels in early meiotic cells. However, in contrast to wild-type CPB-3, CPB-3bt17 levels decrease shortly after pachytene onset, and fall down to background levels already in mid-pachytene (Figure 3.5.4; Eckmann Lab, unpublished). Thus, in contrast to wild-type CPB-3, truncated CPB-3(bt17) is not expressed in late pachytene.

If CPB-3 is constitutively regulated by SEL-10, i.e. throughout early meiosis, then *sel-10* knock-down should lead to a stabilisation of phosphorylated forms in *cpb-3(bt17)* worms. On the other hand, if SEL-10 regulates CPB-3 only at pachytene exit, or if phosphorylation of CPB-3 takes place only at pachytene exit, then *sel-10* knock-down in *cpb-3(bt17)* is expected not to result in any observable changes in CPB-3 modifications or expression pattern.

To test these two hypotheses, a *cpb-3(bt17); sel-10(ok1632)* double mutant was generated and analysed in collaboration with Christian Doreth. Using anti-CPB-3 antibodies, comparative immunoblottings revealed no noticeable difference; worm extracts of *cpb-3(bt17)* single and *cpb-3(bt17); sel-10(ok1632)* double mutants contained comparable amounts of CPB-3(bt17) (Figure 3.5.3). Moreover, an accumulation of modified CPB-3bt17 protein was not observed. This result suggests that phosphorylation and SEL-10-mediated regulation do not affect CPB-3 protein until mid-pachytene stage. This hypothesis was further supported by immunofluorescent stainings; while CPB-3 levels decrease in late pachytene of wild type, CPB-3(bt17) levels drop already in mid-pachytene (Figure 3.5.4). Similarly, CPB-3bt17 levels decrease in early-to-mid-pachytene of *cpb-3(bt17); sel-10(0)* double mutant germ cells (Figure 3.5.4 C), suggesting that *sel-10* does not act on CPB-3 at these stages.

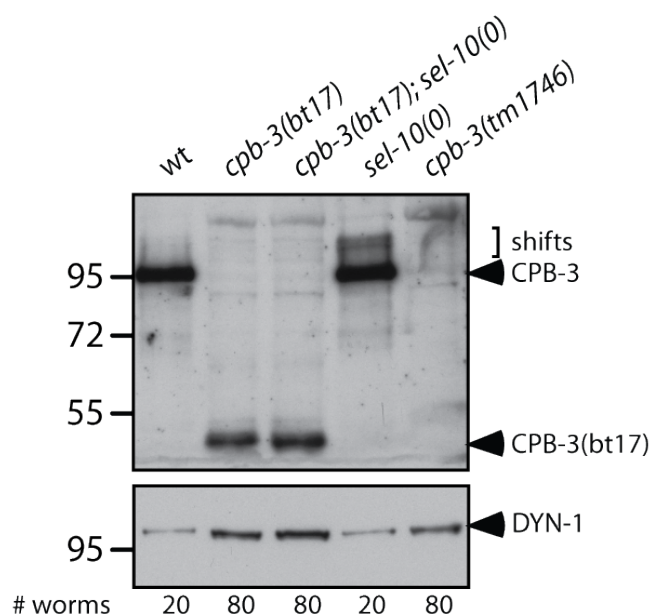


Figure 3.5.3 *sel-10*-depleted worms do not accumulate modified CPB-3bt17.

Immunoblotting of worm extracts; number of L4+36h worms per lane is indicated on the bottom. CPB-3bt17 is expressed at much lower levels than wild-type CPB-3. To obtain comparable signal intensity, more *cpb-3* mutant worms were loaded. *cpb-3(tm1746)* is a protein null mutation and serves as antibody specificity control. Dynamin (DYN-1) serves as loading control. Size marker to the left.

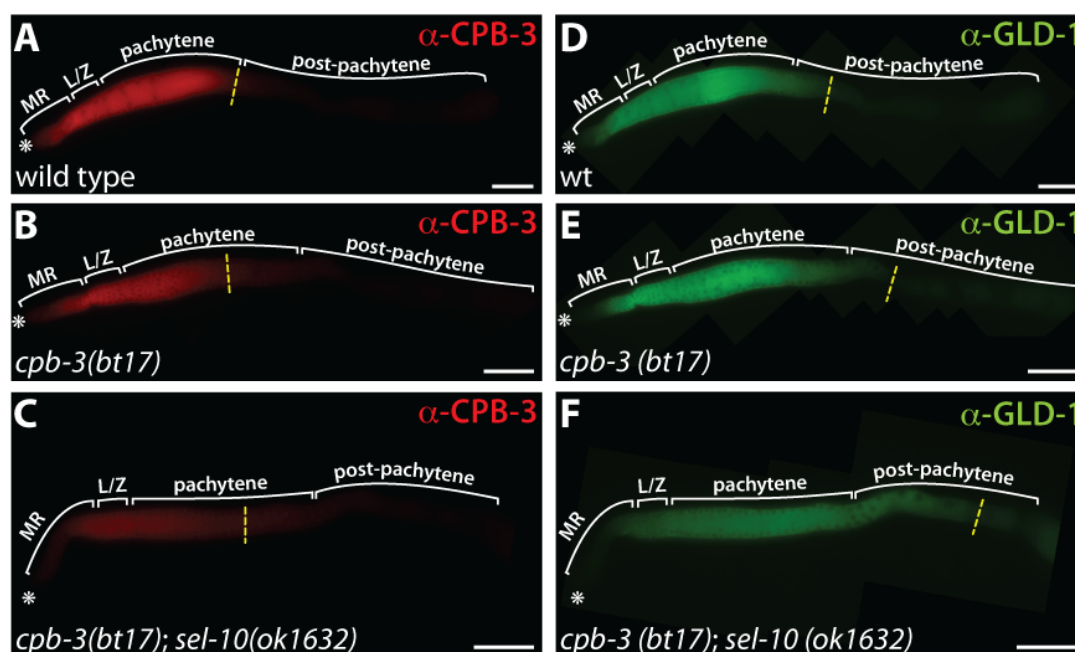


Figure 3.5.4 The absence of *sel-10* activity does not influence the expression of CPB-3bt17.

Immunostainings with monoclonal anti-CPB-3 antibody (A,B,C) or polyclonal anti-GLD-1 antibody (D,E,F) of gonads dissected from L4+24h adult worms. Asterisk - distal tip, MR - mitotic region, TZ - transition zone; yellow dashed line indicates place where signal drops to background levels (defined by signal intensity in *cpb-3(tm1746)* or *gld-1(q485)* germ lines, for CPB-3 and GLD-1 antibody, respectively). Scale bar: 50 μ m.

A translational repressor GLD-1 has a similar expression pattern to CPB-3, i.e. it is expressed in proximal part of mitotic region and in early meiotic cells occupying distal gonad. Close to bend region, around pachytene-to-diplotene transition, GLD-1 levels decrease and the protein is not detectable in growing oocytes in proximal gonad (Figure 3.5.4 D). Same expression pattern of GLD-1 is observed in *cpb-3(bt17)* mutants (Figure 3.5.4 E), which suggests that this mutation does not affect regulation of GLD-1 expression. In *sel-10(0)* mutants, GLD-1 expression pattern is extended, which suggests that GLD-1 and CPB-3 may be downregulated by the same molecular mechanism (this will be discussed in detail in sections 3.8-3.10). GLD-1 expression is also prolonged in *cpb-3(bt17); sel-10(ok1632)* germ lines (Figure 3.5.4 F), arguing that *cpb-3(bt17)* mutation does not affect activity of *sel-10*. Since lack of *sel-10* activity in *cpb-3(bt17); sel-10(0)* strain affects the expression of GLD-1 expressed in late pachytene, but not CPB-3(bt17) expressed till mid-pachytene, SEL-10 regulation of both investigated RNA-binding proteins appears to be restricted to the pachytene-diplotene transition.

3.6 CPB-3 influences the expression of its own regulators

3.6.1 SEL-10 expression is developmentally regulated

Despite the well-established role of *sel-10* in regulating different *C. elegans* proteins, the expression pattern of SEL-10 remains obscure. *sel-10* activity regulates LIN-45/MAPK signaling in vulva development (de la Cova and Greenwald, 2012), formation of synapses between vulva precursor cells and hermaphrodite specific motor neuron HSNL (Ding et al., 2007), and reduces ZYG-1/Plk4 levels in embryonic development (Peel et al., 2012). These studies suggest that SEL-10 protein is expressed in the vulva, nervous system and early embryo. However, SEL-10 protein has not been visualised in these studies by immunostaining or by expression of a tagged protein under control of endogenous regulatory elements. Dorfman et al. (2009) generated transgenic worms encoding GFP::SEL-10 fusion driven by endogenous elements but they

did not detect GFP signal in embryos younger than ~50-cell stage. This observation was explained by probable transgene silencing in the maternal germ line. The group reported GFP::SEL-10 fluorescence in head and tail neurons but did not perform a thorough expression analysis in other tissues. Thus, our knowledge of SEL-10 expression is incomplete and so far no germ line expression has been documented.

According to the Nematode Expression Pattern DataBase, NEXTDB, in which RNA *in situ* hybridisation images were deposited, *sel-10* mRNA is expressed in adult hermaphrodite gonad, suggesting that SEL-10 protein may also be present in germ cells. Protein expression in *C. elegans* female germline tissue is predominantly regulated at the translational level by mRNA 3' UTR sequence elements (Merritt et al., 2008). In order to test whether *sel-10* is translated during oogenesis, transgenic worms containing a translational *sel-10* 3' UTR reporter were generated. The reporter gene encoded a histone 2B protein that was N-terminally tagged with GFP (GFP::H2B) and was under the control of the *sel-10* 3' UTR. Expression of the reporter mRNA was driven by a ubiquitous germ cell-specific promoter ($P_{\text{mex-5}}$). This reporter construct was integrated into the genome as a single copy insertion (Frokjaer-Jensen et al., 2012). The expression of the reporter protein was analysed in anaesthetised one-day-old adult worms, using a fluorescent microscope (Figure 3.6.1).

sel-10 3' UTR reporter has a non-uniform expression pattern across the female gonad. In the distal part, comprising the mitotic region (MR), transition zone (TZ) and two-thirds of the pachytene region, GFP::H2B fluorescence was very weak (Figure 3.6.1 A,B). In late pachytene, fluorescence intensity sharply increased and reached its maximal level. The bend region and the proximal part of the gonad, which contain diplotene and diakinetik cells, displayed intermediate fluorescence levels. The observed expression pattern suggests two things. First, the sole presence of a fluorescent signal suggests that *sel-10* translation is permitted in the germ line and indicates that endogenous SEL-10 protein is expressed in germ cells. Second, the *sel-10* 3' UTR supports a complex expression pattern and suggests a potential posttranscriptional regulation of *sel-10*. This is particularly evident upon comparison with expression of the tubulin reporter, *tbb-2* (Figure 3.6.1 C). *tbb-2* is expressed uniformly across the germ line

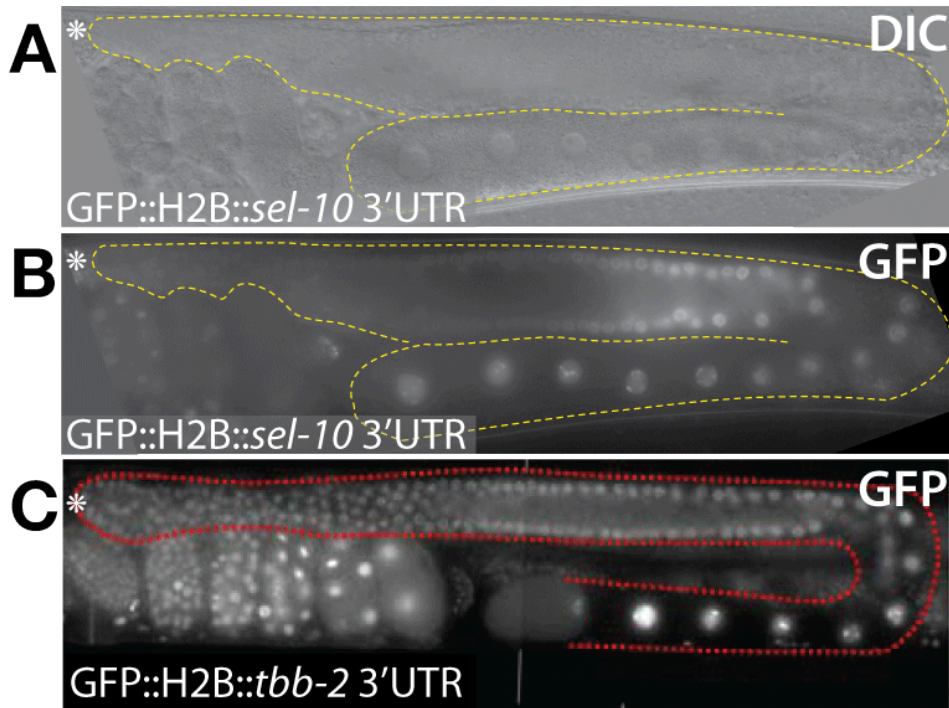


Figure 3.6.1 SEL-10 is likely translated before pachytene exit.

Photomicrograph of a single adult gonadal arm (outlined with dashed line) observed with Nomarski optics (A) or fluorescent microscope (B, C). Asterisk indicates distal tip. (A, B) Expression of *sel-10* 3' UTR reporter in adult germ line. Signal from the reporter ORF is barely detectable in the distal end but rapidly increases in late pachytene cells. (C) Expression of *tbb-2* 3' UTR reporter in adult germ line. *tbb-2* 3' UTR permits a uniform expression throughout the germ line. Panel adapted from (Merritt et al., 2008).

and is considered not to be translationally regulated (Merritt et al., 2008). Hence, *sel-10* mRNA may be subject to translational repression until late pachytene. By contrast, the steep increase in *sel-10* translational reporter levels before the bend is consistent with a translational up-regulation or de-repression of *sel-10* mRNA.

3.6.2 *cpb-3* activity promotes *sel-10* 3' UTR reporter translation in late pachytene

Several well-characterised translational regulators operate in the distal gonad (reviewed in Nousch and Eckmann, 2013) and could potentially repress *sel-10* mRNA. *sel-10* 3' UTR is ~710 nucleotides long, which also argues that it may contain regulatory elements. In order to find out which RBPs might be involved, *sel-10* 3' UTR sequence was scanned for the presence of candidate regulatory elements: FBF-binding elements (FBEs) (Crittenden et al., 2002;

Bernstein et al., 2005), GLD-1-binding motifs (GBMs) (Wright et al., 2011; Jungkamp et al., 2011), and cytoplasmic polyadenylation elements (CPE) (Fox et al., 1989; McGrew and Richter, 1990; Pique et al., 2008). Several potential regulatory elements were identified: two FBEs, one GBM and four CPEs (Figure 3.6.2).

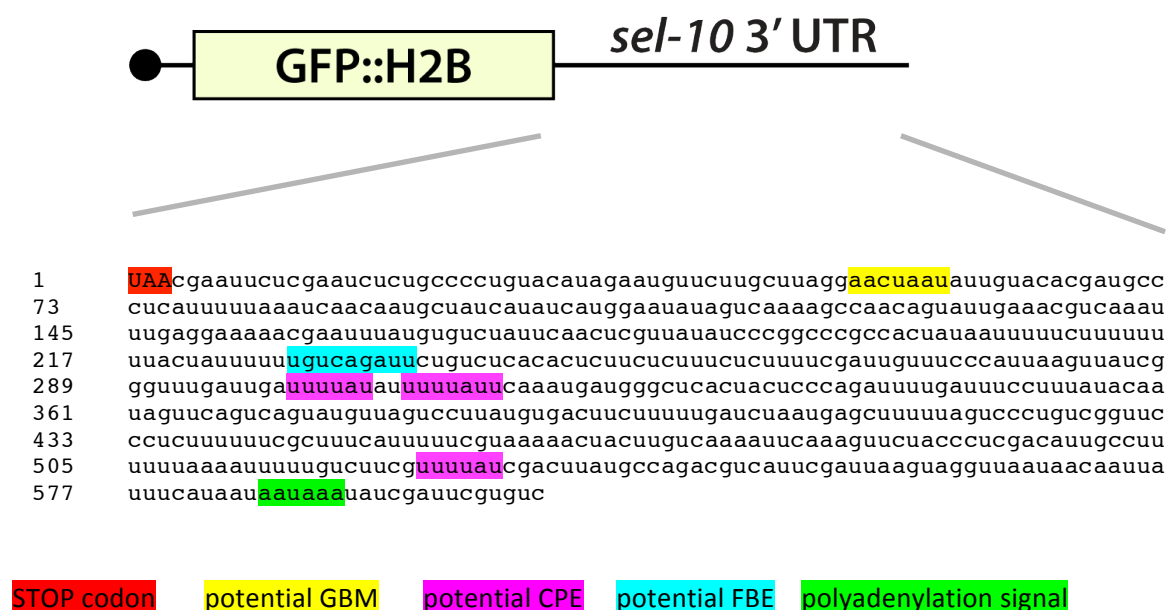


Figure 3.6.2 *sel-10* 3' UTR contains potential regulatory *cis*-elements.

Analysis of the *sel-10* 3' UTR (as deposited on WormBase, version WS255).

GBM - GLD-1-binding motif; CPE - cytoplasmic polyadenylation element; FBE - FBF-binding element

The presence of CPEs suggested, that CPB-3 might function as a translational regulator of *sel-10* mRNA. To test this hypothesis, CPB-3 was downregulated by RNAi feeding in the *sel-10* 3' UTR reporter strain and the changes in the fluorescence intensity in the nuclei were observed and quantified by measuring fluorescence intensity in nuclei in distal gonad. While the reporter expression did not change noticeably upon control RNAi feeding, depletion of *cpb-3* prevented the increase of the fluorescent signal before the bend region (Figure 3.6.3). This result suggests that CPB-3 is important for the translational activation of *sel-10* mRNA in late pachytene.

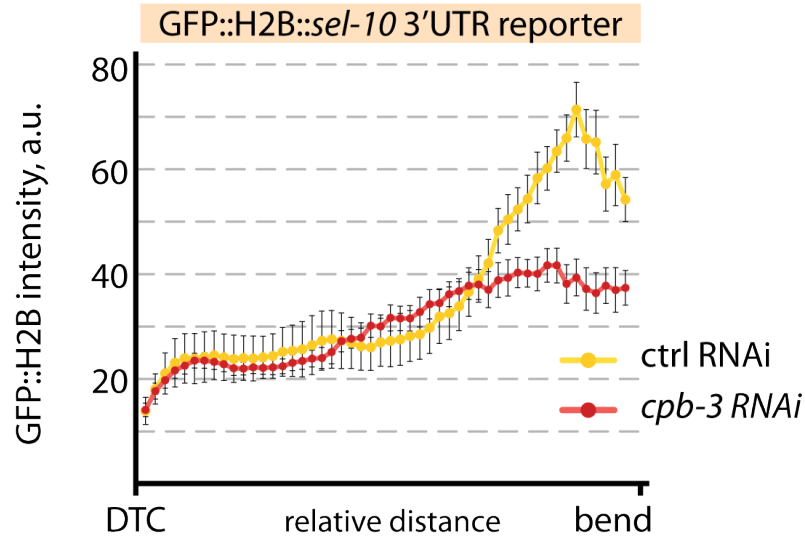


Figure 3.6.3 CPB-3 influences translation of *sel-10* 3' UTR reporter.

Quantification of the GFP::H2B fluorescence of *sel-10* 3' UTR translational reporter in control and *cpb-3*-depleted worms.

Average signal intensity (arbitrary units, a.u.) between distal tip cell (DTC) and gonadal turn (bend). Intensity values at this distance were binned and averaged, to obtain 50 evenly spaced data points regardless of germ line length. Eight control and ten *cpb-3(RNAi)* germ lines were measured. Error bars show SEM.

3.6.3 *cpb-3* activity promotes *mpk-1* 3' UTR reporter translation in pachytene

The possibility that *cpb-3* activity may affect translation of SEL-10, which destabilises CPB-3, raised the question whether *cpb-3* may also influence its other regulator, *mpk-1*. Analysis of *mpk-1* 3' UTR in search for candidate regulatory *cis*-elements, revealed the presence of two FBEs, two GBMs and at least two CPEs (Figure 3.6.4). The FBEs were characterised in detail by (Lee et al., 2007a) and shown to mediate partial translational repression of *mpk-1* in the mitotic region.

To test if CPB-3 is also involved in the translational regulation of *mpk-1*, the expression of *mpk-1* 3'UTR reporter was compared between *cpb-3*-depleted and control animals. An initial observation of the germ lines indicated lower levels of reporter expression upon *cpb-3* RNAi (Figure 3.6.5). Measurements of signal intensity revealed significant differences between the two groups. In control animals GFP::H2B intensity was low in the distal end but quickly rose and stayed high throughout two thirds of the distal gonad, and then began to drop (Figure 3.6.5). Reporter expression in *cpb-3* depleted animals was also very low in the distal end and increased proximally but plateaued at nearly half of the

3.II GLD-1 expression is regulated by the ubiquitin-proteasome system

In the course of these studies, another translational regulator, GLD-1, was found partially stabilised by an inhibition of the proteasome. Although GLD-1 and CPB-3 belong to two different protein families (STAR and CPEB, respectively) and do not share noticeable sequence similarity, their expression pattern in the germ line is nearly identical. This section extends the previous findings on CPB-3 to GLD-1 and addresses the mechanism that restricts GLD-1 expression to the distal gonad.

3.7 Regulated protein turnover of GLD-1

3.7.1 Reduced proteasome activity causes partial stabilisation of GLD-1

To test whether GLD-1 expression is regulated by proteasomal activity, an RNAi-mediated knock-down of the proteasome subunit-encoding *pbs-6*, was performed in wild-type worms and transgenic worms that express fluorescently tagged GLD-1. Changes in GLD-1 distribution in the germ line and in total GLD-1 amounts were analysed by microscopy and immunoblotting analysis, respectively.

To probe for changes in GLD-1 expression pattern upon the reduction of the proteasome activity, germ lines of *pbs-6*-depleted and control animals were extruded and immunofluorescently stained with anti-GLD-1 antibodies (Figure 3.7.1). In control animals, and similar to wild type, GLD-1 was barely detectable in the mitotic cells, which occupied the distal end of the gonad, but it accumulated as cells moved away from the distal tip and entered meiosis (Figure 3.7.1 A,B). GLD-1 protein expression peaked in the pachytene stage. As germ cells progressed from the pachytene to diplotene, which took place shortly before the bend region, GLD-1 levels gradually decreased. Protein levels were low in diplotene cells and not detectable in diakinetik cells. Upon *pbs-6* RNAi, overall anti-GLD-1 signal strength and distribution did not change noticeably in the distal gonad (Figure 3.7.1 D). By contrast, an increase in anti-GLD-1 signal was evident in the bend region, where diplotene and diakinetik cells reside (Figure 3.7.1 C,D). GLD-1 is normally barely detectable at these meiotic stages

(Figure 3.7.1 B). Similar observations were made using anti-GLD-1 antibody that was raised in a different species (data not shown). Thus, the signal detected in the bend region and proximal gonad in *pbs-6*-treated germ lines is most likely specific to GLD-1 and reflects increased GLD-1 levels. Thus, *pbs-6* RNAi extended the expression pattern of GLD-1, suggesting that the reduction of GLD-1 levels during diplotene in wild-type germ lines, may be regulated by the proteasome.

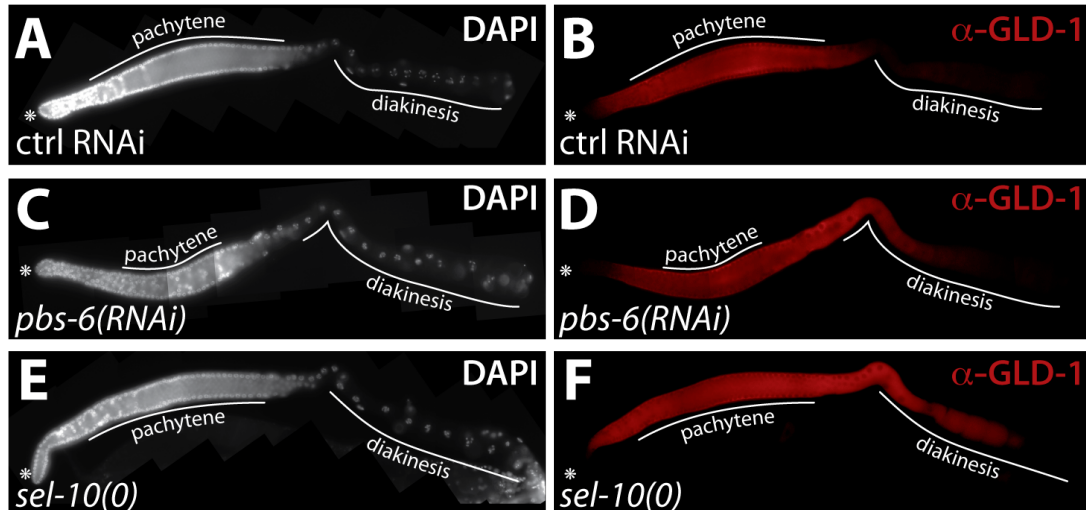


Figure 3.7.1 Upon reduction of the proteasome or *sel-10* activity, GLD-1 is partially stabilised in meiosis.

(A-F) Extruded germ lines of L4+24h hermaphrodites stained with DAPI (A,C,E) and anti-GLD-1 antibody (B,D,F).

In contrast to wild type worms (control RNAi), GLD-1 becomes easily detectable in diplotene and early diakinesis upon *pbs-6* RNAi (C,D) and in *sel-10(0)* mutant germ lines (E,F).

To exclude the possibility that the observed effect stems from an uneven fixation or permeabilisation of gonads, the expression of GLD-1 was examined *in vivo* in anaesthetised animals. To this end, *pbs-6* RNAi feeding was performed in transgenic worms (strain EV375) that express a GLD-1::GFP fusion protein under the control of the endogenous promoter and 3' UTR (Figure 3.7.2). The expression pattern of GLD-1::GFP fusion protein was very similar to the pattern of endogenous protein in the distal part of gonadal arms (compare figure 3.7.1 B and 3.7.2 A). In both cases a stepwise increase in distal end of the germ line (not shown), high expression levels in pachytene region, and a decrease before gonadal turn were observed. However, a partial proteasome inactivation

resulted in an increased persistence of GLD-1::GFP during meiosis; the fluorescent signal was detectable in gonadal turn and in several oocytes in the proximal gonad (Figure 3.7.2 D). This observation supports the hypothesis that proteasome activity shapes GLD-1 expression pattern, likely by restricting its abundance at the pachytene-to-diplotene transition (pachytene exit).

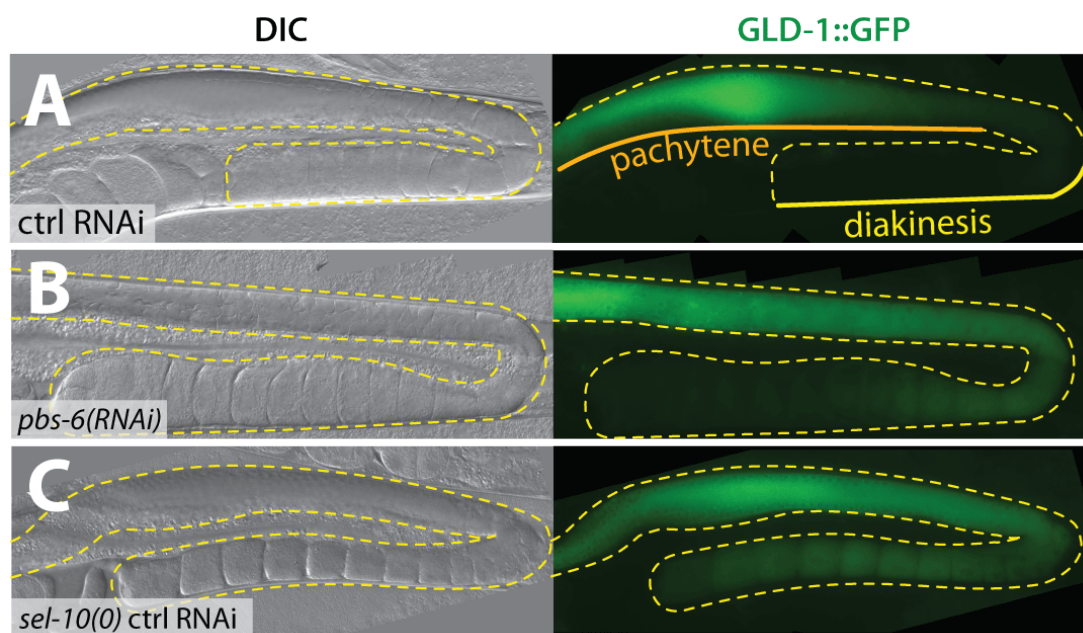


Figure 3.7.2 GLD-1::GFP is partially stabilised in meiosis upon reduced proteasome or *sel-10* activity.

(A-C) Transgenic L4+24 hermaphrodites expressing GLD-1::GFP (strain EV375), observed with Nomarski optics (left panel) and with fluorescent microscope. GFP signal is detectable in proximal gonad of *pbs-6*-depleted worms and in *sel-10(0)* mutant background (strain EV666). Nonetheless, GLD-1::GFP levels decrease during oogenesis.

To test the influence of proteasome inhibition onto the total levels of GLD-1, extracts of *pbs-6*-depleted worms were analysed by immunoblotting. This method allows easier comparison of approximated total amount of GLD-1 in the germ lines than immunohistochemistry. Immunoblots probed with anti-GLD-1 antibodies showed in control and *pbs-6*-depleted worm extracts a fuzzy band at around 55 kDa (Figure 3.7.3). Intensity of this band in both extracts was very similar, suggesting no gross changes in GLD-1 abundance. Quantification of signal intensity on immunoblots from four independent experiments revealed only a small difference that was statistically not significant (data not shown). The

insignificant accumulation of GLD-1 in *pbs-6* RNAi suggests that the proteasome plays a minor role in regulating total GLD-1 levels in the whole germ line. Taking the stage-specific increase in GLD-1 levels observed by immunocytochemistry into consideration, it seems possible that proteasome-mediated regulation of GLD-1 is restricted to certain meiotic stages.

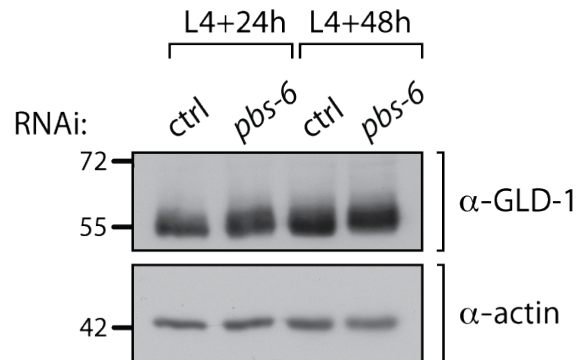


Figure 3.7.3 GLD-1 protein levels do not significantly change upon partial reduction of proteasome activity.

Representative immunoblotting of worm extracts treated with *pbs-6* RNAi from L4 stage. 50 worms were loaded per lane. Molecular weight marker to the left.

3.7.2 GLD-1 expression persists longer in oogenesis of *sel-10(0)* mutant worms

To address the question whether the F-box protein SEL-10 regulates GLD-1 expression pattern, as it does for CPB-3, germ lines of *sel-10(0)* worms were extruded, and immunofluorescently stained with anti-GLD-1 antibody (Figure 3.7.1). No differences in GLD-1 expression between the wild-type and *sel-10(0)* mutant worms were noticed in the distal end of the germ line and in the pachytene region (Figure 3.7.1 B,F). By contrast, GLD-1 levels were highly elevated in late pachytene, diplotene and diakinetik cells in *sel-10(0)* mutant germ lines in comparison to control (Figure 3.7.1 B,F). This suggests, that *sel-10* activity regulates GLD-1 expression pattern by restricting it to the pachytene stage.

The role of *sel-10* in regulating GLD-1 expression in the germ line was confirmed in three ways. First, *sel-10* activity was reduced by RNAi feeding in wild-type worms and GLD-1 expression was examined by immunofluorescent staining. A readily detectable anti-GLD-1 signal was observed in diplotene and

several diakinetetic cells, similarly to what was seen in *sel-10(0)* mutants, and in contrast to control germ lines (data not shown). Thus, prolonged GLD-1 expression in *sel-10(0)* can be attributed to reduced *sel-10* activity rather than to other, yet uncharacterised genetic lesions potentially present in the genome of *sel-10(0)* strain. As a second line of evidence for the role of *sel-10* in regulating GLD-1 abundance, the expression pattern of GLD-1::GFP was observed in living transgenic worms after RNAi-mediated *sel-10* depletion (data not shown). Third, the GLD-1::GFP-producing transgene (EV375) was crossed to the *sel-10(0)* mutant background (giving rise to strain EV666; Figure 3.7.2 C,D). Both ways of reducing *sel-10* activity, i.e. RNAi and the mutation, led to the same change in GLD-1::GFP expression. The fluorescent signal was detected in the bend region and the proximal gonad. No other changes in the GLD-1::GFP expression pattern were noticed. Altogether, all these observations suggest that *sel-10* activity restricts GLD-1 expression by reducing GLD-1 levels as cells transit from pachytene to diplotene.

3.7.3 *sel-10* activity regulates the abundance of GLD-1 on the protein level

At least two ways can be envisioned of how *sel-10* activity regulates GLD-1 expression. One possibility is that SEL-10 acts as a component of a ubiquitin ligase and mediates GLD-1 ubiquitination and degradation, similar to CPB-3 regulation. The other possibility is that SEL-10 regulates GLD-1 expression indirectly, e.g. by influencing the activity of *gld-1* translational regulators.

To distinguish between the two possibilities, GLD-1 was expressed under the control of a 3'UTR that is not translationally regulated, and GLD-1 expression pattern was analysed in the absence of *sel-10* activity. GLD-1 was C-terminally tagged with the localisation and affinity purification (LAP)-tag, which consists of the GFP and three tandem FLAG-tag repeats (Cheeseman and Desai, 2005). LAP tag allowed to observe protein expression *in vivo* and to circumvent the necessity of fixing tissues and using antibodies. Transgenic lines were generated with Mos-mediated single-copy insertion (Frokjaer-Jensen et al., 2012), to minimise differences in mRNA expression coming from differences in numbers of transgene copies or from an influence of integration sites. Two independent lines were obtained for each transgene and analysed in parallel.

3.7.3.1 GLD-1::LAP resembles endogenous GLD-1 expression

Prior to investigating the influence of *sel-10* activity on 3' UTR-independent GLD-1::LAP expression, the ability of the transgene to recapitulate the endogenous GLD-1 expression pattern was tested. To this end, the open reading frame *gld-1::lap* was fused to the endogenous *gld-1* 3' UTR. Transgenic lines EV661 and EV662 obtained by integration of this construct in the genome were analysed by fluorescent microscopy of living worms mounted on agar pads. GFP fluorescence of EV661 and EV662 was compared to the GFP fluorescence observed in GLD-1::GFP-expressing strain, EV375, which recapitulated in all aspects the GLD-1 distribution data obtained by staining with antibodies (see above, section 3.7.2).

The expression pattern of GLD-1::LAP in EV661 and EV662 gonads (Figure 3.7.4 A-F) was highly similar to the expression of GLD-1::GFP in EV375 (compare figure 3.7.4 A-F with G-L). Fluorescent signal was barely detectable in the distal-most part of the gonad (Figure 3.7.4 C,D). At the distance of several nuclear rows from the distal tip, the fluorescence gradually increased and the GLD-1::LAP signal levels in the rachis of the distal gonad were strong and predominantly cytoplasmic (Figure 3.7.4 A,B). Close to the gonadal turn, fluorescence signal weakened, and returned to background levels in the proximal arm. In all aspects, this expression pattern resembled GLD-1::GFP expression in EV375 (Figure 3.7.4 G-J). Also the subcellular distribution of GLD-1::LAP and GLD-1::GFP fusion proteins was similar: in addition to mainly cytoplasmic localisation, perinuclear GLD-1 foci were observed in both transgenic strains (Figure 3.7.4 F,L). Hence, the expression pattern of the GLD-1::LAP transgene recapitulates that of GLD-1::GFP and endogenous GLD-1 (Jones et al., 1996; Vought et al., 2005).

In order to test whether GLD-1::LAP fusion is regulated similarly to endogenous GLD-1 protein, the activity of *sel-10* was reduced by RNAi feeding in EV661 and EV662 strains. In *sel-10*-depleted but not in control animals, the LAP-tag signal was readily detectable in the bend region and in the proximal gonad (Figure 3.7.5 A-D). Thus, *sel-10* restricts GLD-1::LAP expression pattern, similarly to restricting endogenous GLD-1.

Together, these data suggest that the GLD-1::LAP fusion protein recapitulated all aspects of GLD-1 expression that were previously observed for the endogenous GLD-1 protein visualised with antibodies or for GLD-1::GFP transgene expression in strain EV375. Therefore, GLD-1::LAP was considered to be suitable for addressing the question whether *sel-10* acts on regulatory elements in GLD-1 protein or rather in *gld-1* mRNA sequence.

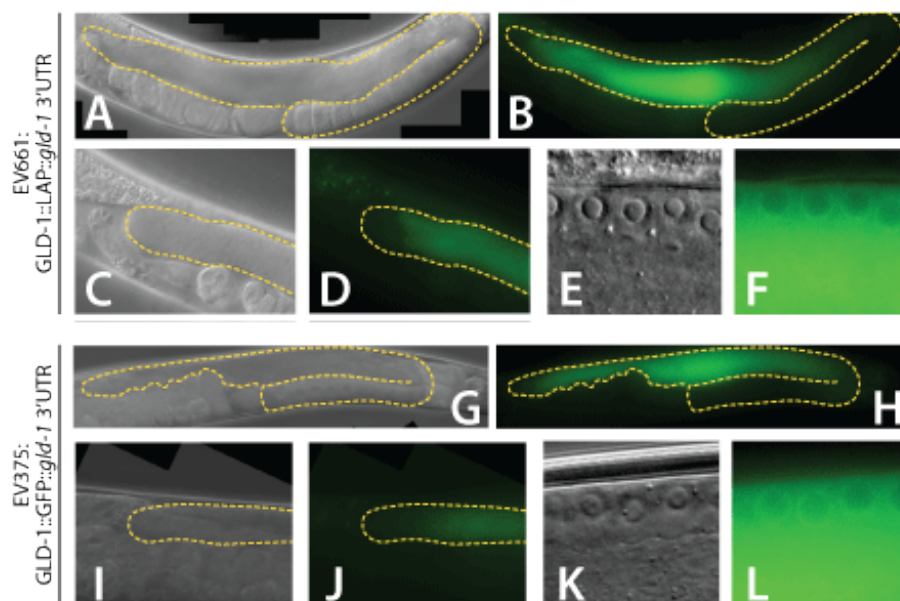


Figure 3.7.4 GLD-1::LAP and GLD-1::GFP fusions recapitulate endogenous GLD-1 protein expression.

Comparison of (A-F) GLD-1::LAP transgene expression in EV661 and (G-L) GLD-1::GFP in EV375. (A,C,E,G,I,K) DIC images and corresponding (B,D,F,H,J,L) GFP autofluorescence.

(A,B,G,H) Overview of entire germline tissue (dotted line).

(C,D,I,J) GLD-1::LAP expression is low in the distal end of the germ line.

(E,F and K,L) GLD-1 signal is predominantly cytoplasmic but some perinuclear accumulation is observed.

3.8.3.2 *sel-10*-dependent downregulation of GLD-1 is not mediated by *gld-1* 3' UTR

To address the question whether *sel-10* shapes GLD-1 expression pattern at the translational or the post-translational level, GLD-1::LAP was expressed under the control of the *tubulin-2* (*tbb-2*) 3' UTR in transgenic animals generated with MosSCI protocol. *tbb-2* 3' UTR is translationally active throughout the germ line (Merritt et al., 2008) and therefore, *tbb-2* 3' UTR was expected to provide a uniform expression pattern for GLD-1::LAP. Two independent lines were

obtained (EV733 and EV734) and GLD-1::LAP expression was analysed in living worms. Obtained data were identical for both transgenic lines; henceforth EV733 will serve as reference.

In contrast to endogenous GLD-1 expression, GLD-1::LAP in EV733 was readily detectable in the distal end of the gonad (data not shown). This observation is consistent with the notion, that *tbb-2* 3' UTR is not translationally repressed in the germ line. By contrast, *gld-1* 3'UTR is translationally repressed by FBF proteins in the mitotic region (Crittenden et al., 2002), which results in very low levels of endogenous and transgenic GLD-1 proteins expressed under the control of endogenous *gld-1* 3' UTR (e.g. Figure 3.7.4 D,J). In early meiotic cells of EV733, GLD-1::LAP was mainly cytoplasmic and rather uniformly distributed (data not shown). Pachytene cells of *tbb-2*-controlled EV733 had similar levels of GLD-1::LAP to pachytene cells of EV661 strain, expressing the GLD-1::LAP transgene under the control of the endogenous *gld-1* 3' UTR. Unexpectedly, GLD-1::LAP fluorescence in *tbb-2*-controlled EV733 germ lines weakened around the bend region (Figure 3.7.5 F). While the GFP signal was still detectable in the proximal gonad, it was at much lower levels than in the distal gonad, which suggests that the 3' UTR of *tbb-2* was either not able to permit translation throughout the germ line, or another layer of GLD-1 regulation is in place to prevent GLD-1 accumulation. The sudden reduction in GLD-1::LAP levels strongly resemble the reduction of endogenous GLD-1, and argues that GLD-1::LAP protein may be destabilised in proximity to the bend region.

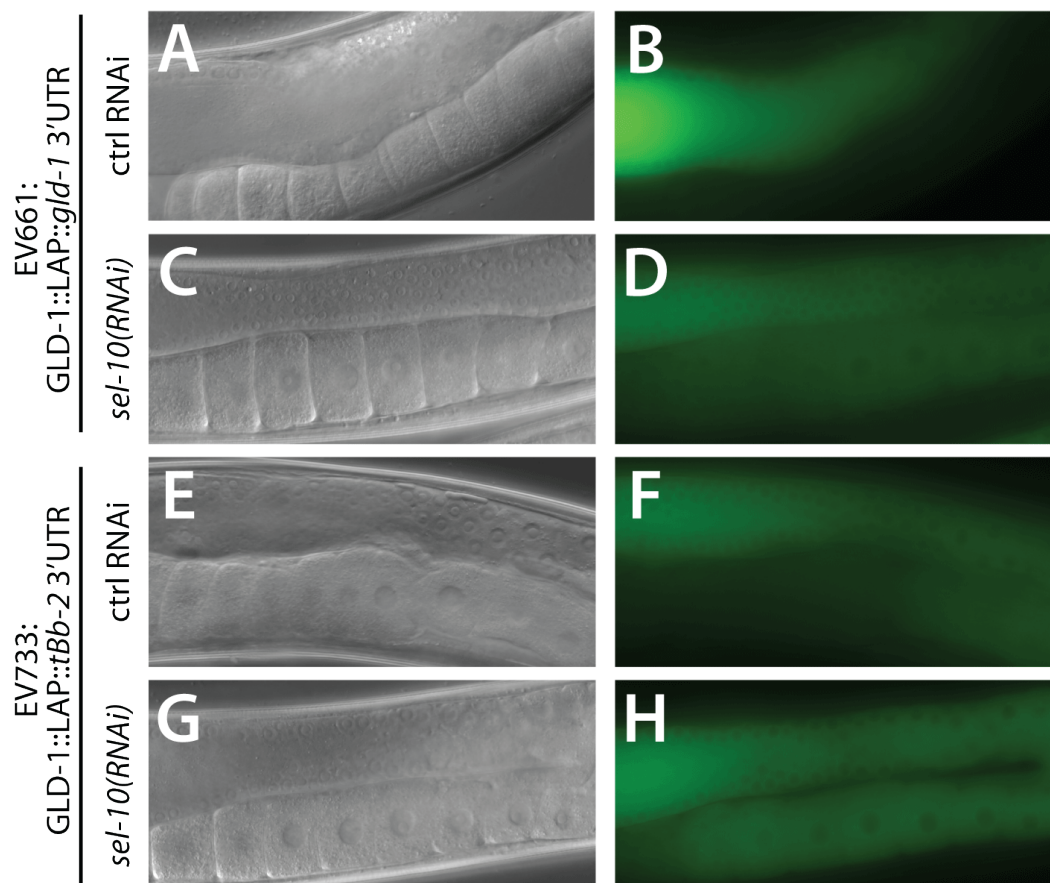


Figure 3.7.5 *sel-10* represses GLD-1::LAP expression in the proximal gonad at the protein level.

(A,C,E,G) DIC images and corresponding (B,D,F,H) GFP autofluorescence.

(A,B) In control conditions, GLD-1::LAP is not detectable in the oocytes of EV661.

(C,D) Upon *sel-10* knock-down, GLD-1::LAP is readily detectable.

(E-H) *tbb-2* 3'UTR-mediated GLD-1::LAP expression is weak in the oocytes of control animals (E,F) but increases upon *sel-10* RNAi (G,H).

3.7.3.3 GLD-1::LAP protein is a target of *sel-10* activity

In order to test whether the observed reduction in levels of the transgenic protein GLD-1::LAP is due to SEL-10 activity, an RNAi-mediated *sel-10* knock-down was performed in EV733 worms. To control for the knock-down efficiency, *sel-10* RNAi was performed in parallel in the EV661 strain, which expresses *gld-1::lap::gld-1 3' UTR* transgene. The expression of GLD-1::LAP was analysed by fluorescent microscopy in anaesthetised adult animals (Figure 3.7.5). To compare signal levels at different meiotic stages, fluorescence intensity was measured in several regions of the germ line as indicated in figure 3.7.6.

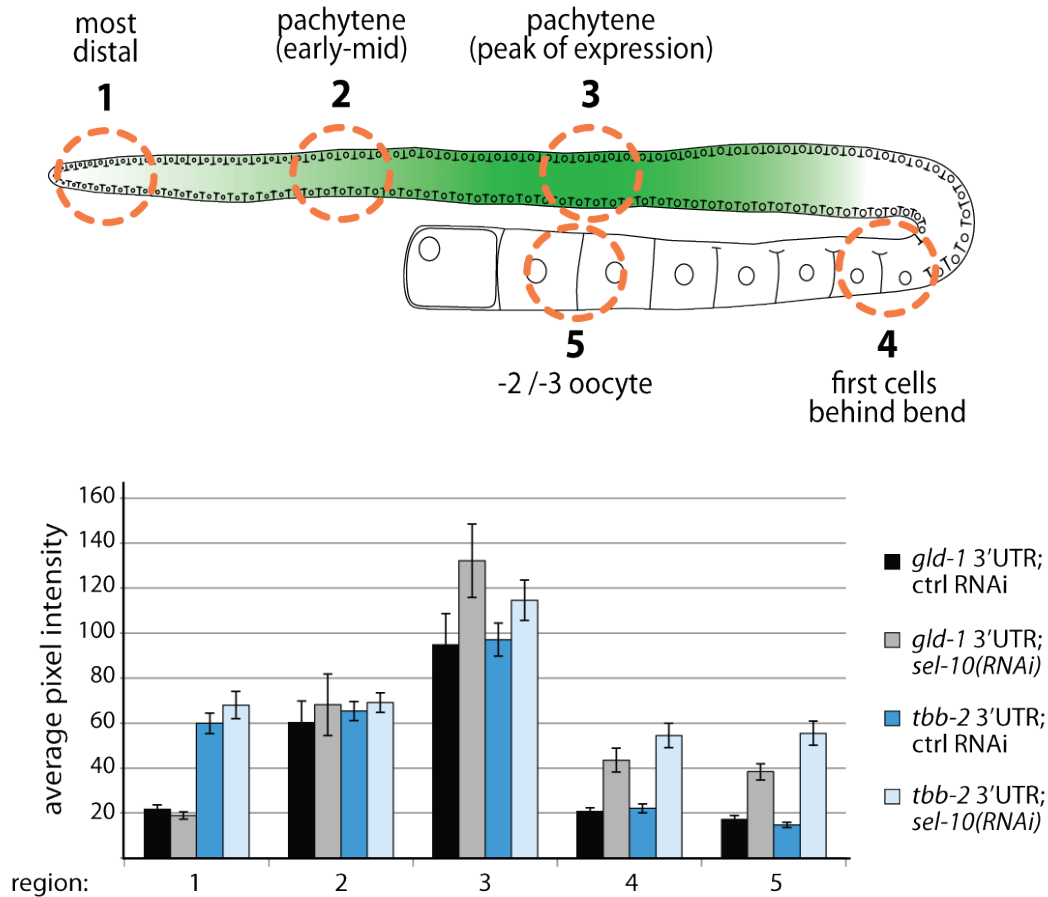


Figure 3.7.6 *sel-10* regulates GLD-1 levels in the proximal gonad independently of the translational regulation mediated by *gld-1* 3' UTR.

(Top) Schematic representation of an adult germ line. Dotted circles mark the regions where GFP intensity was measured.

(Bottom) Quantification of 10 germ lines per genotype in the indicated regions and given RNAi feeding conditions. Error bars represent standard deviation (SD).

Quantification of GFP fluorescence confirmed the observations that GLD-1::LAP levels in the mitotic region are higher when the expression of GLD-1::LAP is driven by *tbb-2* 3' UTR than *gld-1* 3' UTR (Figure 3.7.6: region 1). A reduction of *sel-10* activity causes only minor changes in the transgene expression in this region, irrespective of the 3' UTR regulating the transgene expression. In early-to-mid pachytene cells, GLD-1::LAP levels are similar in the two transgenic lines and do not change much upon *sel-10* RNAi (Figure 3.7.6: region 2). These observations suggest, that *sel-10* does not regulate GLD-1 levels in the distal end of the germ line. Around mid-to-late pachytene GLD-1::LAP levels reach their maximum levels in a germ line and peak intensity appears to be influenced by *sel-10* activity, as GLD-1::LAP signals increase upon *sel-10* RNAi in both strains

(Figure 3.7.6: region 3), suggesting that *sel-10* may act on GLD-1 already in late pachytene. Growing oocytes occupying proximal gonads of both transgenic strains have similar low levels of the fluorescent signal (Figure 3.7.6: regions 4 and 5).

Altogether, transgenic lines expressing tagged GLD-1 under the control of the endogenous *gld-1* or *tbb-2* 3' UTR supported previous observations that *gld-1* mRNA is a target of translational regulation in the distal gonad (Crittenden et al., 2002), as *tbb-2*-regulated transgene was de-repressed in the mitotic region and early-meiotic cells. Contrary to the expectations, GLD-1::LAP expression regulated by *tbb-2* 3' UTR did not result in uniform GLD-1::LAP protein levels in the germ line. Instead, transgenic protein levels were very low in the proximal gonad, suggesting existence of an additional protein-driven mechanism that regulates GLD-1::LAP amounts, likely by protein degradation. Moreover, *sel-10* depletion in GLD-1::LAP transgenic lines led to an increase in GLD-1::LAP signal in the proximal gonad, suggesting that SEL-10 acts on GLD-1::LAP protein to reduce GLD-1 levels in growing oocytes.

3.7.4 SEL-10 likely regulates GLD-1 in context of an SCF E3 ubiquitin ligase

SEL-10 protein most likely regulates GLD-1 expression as a subunit of an SCF^{SEL-10} E3 ubiquitin ligase complex. Thus, depletion of CUL-1, which forms the scaffold of the SCF complex, should affect GLD-1 in a similar way as the depletion of SEL-10. To test this hypothesis, RNAi-mediated knock down of *cul-1* was performed and GLD-1 expression was analysed in immunofluorescently stained extruded gonads and in immunoblotted worm extracts.

Analysis of extruded germ lines stained with an anti-GLD-1 antibody showed that GLD-1 levels were elevated in the bend region and proximal gonad of *cul-1*-depleted but not of control animals (data not shown), suggesting that CUL-1 negatively regulates GLD-1 stability during meiosis. Analysis of GLD-1 levels by immunoblotting with anti-GLD-1 antibody showed that *cul-1* depletion resulted in an accumulation of slower migrating forms of GLD-1 in worms (Figure 3.7.7). This accumulation is reminiscent of an increased amount of phosphorylated CPB-3 in *cul-1* depleted animals (Figure 3.3.8), suggesting that

phosphorylated GLD-1 may accumulate when SCF complexes are inactive. Noteworthy, neither accumulation of phosphorylated forms of GLD-1, nor partial stabilisation were observed upon *cul-2* or *cul-3* RNAi (Figure 3.7.7 and data not shown). This suggests, that CUL-1-based SCF complexes, and not CUL-2 or CUL-3-based E3 ubiquitin ligases, play a role in regulating GLD-1.

Together, these observations support the hypothesis that an SCF complex, consisting of the scaffold protein CUL-1 and the F-box protein SEL-10, negatively regulates GLD-1 stability in meiosis.

3.7.5 GLD-1 binds to SEL-10 in yeast

Assuming that SEL-10 functions as a substrate recognition subunit of an SCF complex to mediate GLD-1 ubiquitination, it should directly bind GLD-1. To test whether these two proteins interact with each other, a yeast-two-hybrid (Y2H) assay was performed. SEL-10 was fused to the DNA-binding domain (DB), and GLD-1 variants (the full-length protein and its fragments), were fused to the activation domain (AD). The interaction between co-expressed proteins was tested in a β -gal assay, which is based on the reconstitution of the transcription that promotes the expression of the enzymatic reporter protein, β -galactosidase.

In initial experiments, no interaction between SEL-10 and GLD-1 in the β -gal assay was detected, as all yeast colonies co-expressing SEL-10 and GLD-1 hybrids remained white (data not shown). Immunoblot analysis of the corresponding yeast extracts revealed that GLD-1 hybrid proteins were expressed very poorly, often below detection limit of the standard ECL substrate (data not shown). Thus, detecting an interaction between SEL-10 and GLD-1 might have been compromised by extremely low levels of GLD-1::AD hybrids. A potential reason for the low expression of GLD-1 fusions is that they may be recognised by SEL-10, ubiquitinated and degraded. Such assumption is consistent with previous reports that an ectopic expression of F-box proteins often reduces cellular levels of their targets.

In an attempt to increase the levels of GLD-1 hybrids, a deletion in the F-box domain of *sel-10* was made, which was supposed to render SEL-10 protein unable to associate with an E3 ubiquitin ligase complex. Importantly, the

deletion is expected not to affect SEL-10 ability to recognise its substrates. In line with these expectations, F-box-lacking SEL-10 variant (SEL-10 Δ F) did not bind its E3 adapter protein, SKR-1, but it maintained the ability to interact with the previously described target, CPB-3 (Figure 3.7.8). In the same β -gal assay, the reporter protein was detected in yeast cells co-expressing SEL-10 and GLD-1 (Figure 3.7.8). Colonies that expressed either SEL-10 or GLD-1 in the absence of the second hybrid protein remained white, arguing that reporter synthesis in SEL-10 and GLD-1 co-expressing colonies was triggered by an interaction between the hybrids, and was not due to other interactions, e.g. affinity to endogenous yeast transcriptional activators. SEL-10 interacted also with an N-terminal fragment of GLD-1 (amino acids 1-270), but not with three other GLD-1 fragments, which are N-terminal truncations (Figure 3.7.8).


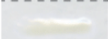






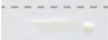
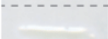
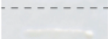

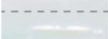

	DB fusion:	AD fusion:	blue colonies
	SEL-10 Δ F	CPB-3	39 / 45
	SEL-10 Δ F	–	0 / 45
	SEL-10 Δ F	SKR-1	1 / 45
	SEL-10 Δ F	GLD-1 full-length	40 / 45
	SEL-10 Δ F	GLD-1 aa 1-270	40 / 45
	SEL-10 Δ F	GLD-1 aa 84-341	15 / 45
	SEL-10 Δ F	GLD-1 aa 273-457	0 / 45
	SEL-10 Δ F	GLD-1 aa 283-463	0 / 45
	–	GLD-1 aa 1-270	0 / 45
	–	GLD-1 aa 84-341	0 / 45
	–	GLD-1 aa 273-457	0 / 45
	–	GLD-1 aa 283-463	0 / 45
	–	CPB-3	0 / 45
	–	SKR-1	0 / 45

Figure 3.7.8 SEL-10 binds N-terminal fragment of GLD-1 in yeast.

Yeast two-hybrid assay testing interaction between SEL-10 and GLD-1. SEL-10 variant with the deletion in F-box (SEL-10 Δ F) was fused to the DNA-binding domain (DB), other proteins, to the activation domain (AD). Dashes indicated empty vector (i.e. expression of DB or AD domain only). Black dashed line at the bottom of the image indicates the region where a fragment was deleted for the clarity of the display. The expression of fusion proteins was verified by immunoblotting (not shown). GLD-1 variants were very weakly expressed in all transformations performed.

Together, these observations suggest that SEL-10 may interact with GLD-1 directly, presumably by recognising a motif in the N-terminal part of GLD-1; this further strengthens the hypothesis that an SCF^{SEL-10} complex may regulate GLD-1 expression.

3.8 GLD-1 is phosphorylated *in vivo*

3.8.1 Modified GLD-1 accumulates in the absence of *sel-10* activity

F-box proteins recognise their targets by the phosphorylated linear motifs dubbed phosphodegrons (reviewed in Skaar et al., 2013). Thus, SEL-10 is expected to recognise a phosphorylated form of GLD-1. A loss of *sel-10* function may therefore result not only in the stabilisation of GLD-1 but also in an accumulation of its phosphorylated forms. To test whether this is the case, extracts from wild-type and *sel-10(0)* mutant worms were analysed by SDS-PAGE followed by immunoblotting with an anti-GLD-1 antibody.

In wild-type and *sel-10(0)* mutant extracts a fuzzy band at around 55 kDa was detected, which was composed of several closely migrating forms of GLD-1 (Figure 3.8.1). The intensity of the signal was similar in both extracts, which is consistent with a similar intensity of the anti-GLD-1 signal in immunofluorescently-stained distal gonads of wild-type and *sel-10(0)* worms (Figure 3.8.1 B,F). Importantly, in addition to the strong signal at 55 kDa, *sel-10(0)* extracts contained several bands of higher molecular mass (Figure 3.8.1, right). Similar retarded GLD-1 migration was observed in extracts of wild-type worms, in which *sel-10* activity was depleted by RNAi feeding (data not shown). By contrast, the slower migrating forms of GLD-1 were barely detectable in wild-type extracts. Thus, absence of *sel-10* activity leads to an accumulation of modified GLD-1.

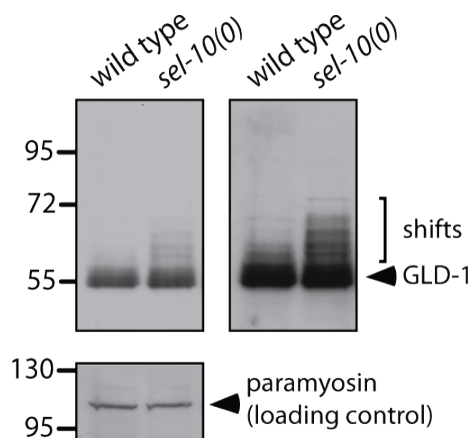


Figure 3.8.1 Modified GLD-1 accumulates in *sel-10(0)* animals.

Immunoblot of extracts of wild-type and *sel-10(0)* worms. Short exposure on the left, long exposure on the right. Lack of *sel-10* activity leads to the accumulation of modified forms of GLD-1. 50 adult hermaphrodites at L4+36h loaded per lane. Molecular weight marker to the left.

Together, these observations suggest that SEL-10 does not act to restrict the overall GLD-1 abundance in the germline tissue. Moreover, accumulation of retarded forms of GLD-1 resembles the accumulation of phosphorylated CPB-3 in *sel-10(0)* mutant worms (Figure 3.3.6) and is consistent with accumulation of phosphorylated protein destined for degradation in the absence of its ubiquitin ligase. Thus, GLD-1 is likely regulated by post-translational modifications, including phosphorylation.

3.8.2 Analysis of GLD-1 sequence predicts phosphorylation sites and degrons

In order to identify potential factors and mechanisms that regulate GLD-1 stability, the amino acid sequence of GLD-1 has been analysed with several bioinformatic tools for the presence of possible phosphorylation sites, protein binding motifs, and degradation motifs. The analysis of GLD-1 was performed in the same way as the analysis of CPB-3 (described in section 3.3.4) and therefore is described here in a brief form. Selected results of GLD-1 analysis are shown in figure 3.8.2.

GLD-1 has 112 phosphorylatable residues: 64 serines, 38 threonines and 10 tyrosines (Figure 3.9.2 B). NetPhos tool (Blom et al., 2004) suggested

modification of 44 residues: 34 serines, seven threonines and three tyrosines (Figure 3.8.2 C). Similarly to the results obtained for CPB-3, the number of suggested phosphosites was too large to perform functional studies by site-directed mutagenesis of indicated residues. Instead, additional analyses were performed.

Analysis with the eukaryotic linear motif search tool, ELM, identified in total 256 instances of 54 different eukaryotic linear motifs in the GLD-1 sequence. These numbers dropped to 183 and 42, respectively, after species- and globular domain filtering. 55 residues were identified as potential phosphosites for nine different kinase groups (CDK, CK1, CK2, GSK3, NEK2, PIKK, PKA, PLK, proline-dependent kinase).

MPK-1 activity in the germ line coincides with downregulation of GLD-1 and influences both phosphorylation status and expression pattern of CPB-3 (Figures 3.4.2 B,A). Therefore, a role of MPK-1 in regulating GLD-1 stability was hypothesised and phosphosites for proline-dependent kinases, to which MPK-1 belongs, were of particular interest. ELM identified 19 proline-dependent kinase consensus sites (Figure 3.8.2 D). The phosphorylatable residue followed by proline is a necessary but not sufficient prerequisite for a protein to be targeted by MAPK. Substrate recognition by MAPK requires a docking motif in a target protein. Two sites with consensus sequence of MAPK docking site were identified in GLD-1 (Figure 3.8.2 F). Interestingly, both are localised within functional domains of GLD-1. The more N-terminally located docking site (aa 155-162) resides in the Qua1 domain, which mediates GLD-1 dimerisation. The more C-terminal docking site (aa 313-322) resides in the Qua2 domain, which contributes to RNA binding. Such position may have interesting functional implications, as GLD-1 dimerisation or association with RNA could compete with kinase binding and phosphorylation. Importantly, there are a number of potential phosphoacceptor sites within a distance of 100 amino acids from each docking site (six and seven, for N- and C-terminal docking site, respectively), which is an optimal arrangement for efficient phosphorylation by MAPK (Garai et al., 2012; Zeke et al., 2015). Of note, proline-dependence is also a feature of cyclin-dependent kinases. Three identified candidate target sites for proline-dependent kinases (S22, S39 and T348) were previously shown to be modified

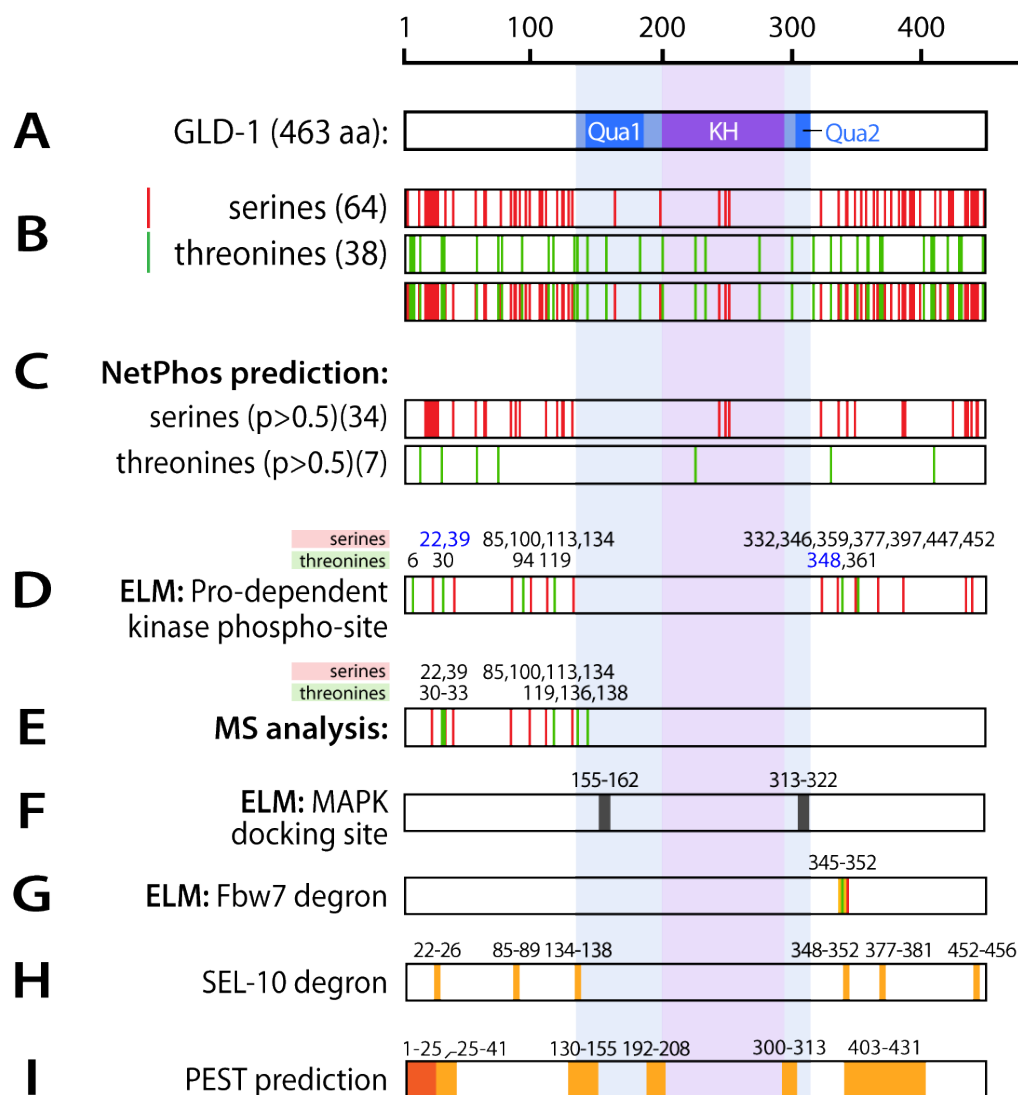


Figure 3.8.2 Predicted phosphorylation sites and regulatory motifs in the GLD-1 sequence.

Stick diagrams representing GLD-1 protein and results of sequence analyses. Red vertical lines - serines, green vertical lines - threonines.

(A) Conserved domains in STAR family proteins; Qua1,2 - quaking homology; KH - hnRNP K-homology.

(B) All serine and threonine residues present in GLD-1.

(C) Serines and threonines predicted to be phosphorylated by NetPhos3.1; probability threshold = 0.5.

(D) Serines and threonines predicted to be phosphorylated by proline-dependent kinases (e.g. MAPK or CDK) predicted by ELM. In blue: residues located in optimal context for cyclin dependent kinases (CDKs).

(E) Results of mass spectrometry-based analysis of the phosphorylation of recombinant GLD-1 expressed in insect cells.

(F) Docking site for MAP kinases predicted by ELM.

(G) Fbxw7/SEL-10 degrons predicted by ELM.

(H) Sequences matching extended version of consensus sequence for SEL-10 binding defined in de la Cova and Greenwald (2013), S/T-P-X-X-S/T.

(I) Destabilising PEST motifs predicted by ePESTfind. Yellow - poor PEST; orange - potential PEST.

by CDK-2 and influence GLD-1 phosphorylation status and stability in the distal end of the gonad (Jeong et al., 2011). The functionality of the 16 remaining predicted sites had not been experimentally addressed so far. Altogether, bioinformatic analysis supports potential involvement of MPK-1 in regulating GLD-1 and identifies a tractable, even if large, number of potential phosphoacceptors.

To see if the suggested MAPK phosphorylation sites could serve as motifs regulating GLD-1 stability, their location was compared with the location of predicted SEL-10/Fbxw7 degron motifs identified by ELM. Only one such sequence was found, spanning aa 345-352 (Figure 3.8.2 G). This potential degron is located 23 amino acids away from the C-terminal MAPK docking site and contains two residues that are potentially phosphorylated. The distance of the predicted degron from consensus MAPK docking site and its potential phosphorylation suggest that it may be a functional destabilising motif.

To investigate whether GLD-1 contains sub-optimal degrons that contain a serine instead of a preferred threonine in the central position of the motif, GLD-1 sequence was scanned for the sequence motif [ST]P..[ST]. Six motifs corresponding to this definition were identified (Figure 3.8.2 H), including the Fbxw7 (Fbw7) degron found by ELM. Two motifs were located within 100 aa distance from the N-terminal MAPK docking site, and two within 100 aa distance from C-terminal MAPK docking site. Thus, four Fbxw7 degron sequences, one optimal and three suboptimal, might be regulated by MAPK. Considering that instances of protein phosphorylation by MAPK kinases on residues located farther away than optimal 100 aa were also described (Garai et al., 2012; Zeke et al., 2015), the remaining two suboptimal Fbxw7 degrons, located at two termini (aa 22-26 and 452-456), may also be modified by MAPK. The most N-terminal suboptimal Fbxw7 degron (aa 22-26) and the optimal degron (aa 345-352) contain residues suggested to be phosphorylated by CDK-2 (S22 and T348) and regulate GLD-1 stability in the distal part of the gonad (Jeong et al., 2011). It would be interesting to find out if these residues and motifs regulate GLD-1 stability also around the gonadal bend region. It would be also interesting to reveal the identity of the ubiquitin ligase proposed to recognise these residues in

the distal end of the gonad. SEL-10 is unlikely to fulfill this function, as distal GLD-1 levels do not seem to increase in *sel-10(0)* mutants. Taking together, ELM analysis revealed several attractive candidate motifs that may regulate GLD-1 stability.

To further characterise the potential of particular GLD-1 regions to influence protein stability, GLD-1 amino acid sequence was analysed with ePESTFind (Rogers et al., 1986) to identify potential destabilising PEST motifs (Figure 3.8.2 I). The algorithm identified one region likely to influence GLD-1 stability ('potential PESTs'), which comprises 25 most N-terminal amino acids (Figure 3.8.2 I) and partially overlaps with predicted suboptimal Fbxw7 degron (Figure 3.8.2 H). Furthermore, five less likely destabilising regions ('poor PESTs') were identified, which altogether constitute around 18% of GLD-1 sequence (Figure 3.8.2 I). Two poor PESTs overlap with three predicted Fbxw7 degrons. Such overlaps are interesting sequence features, as functional degrons occasionally reside within or close to PEST sequences, contributing to an efficient binding of E3 ubiquitin ligases (Skaar et al., 2013).

Altogether, bioinformatic analysis of GLD-1 sequence highlighted several sequence elements that may be important for the regulation of GLD-1 stability. The most promising elements are phosphorylatable residues in a sequence context that makes them potential targets for kinases that are likely to be active in meiosis, such as MAPK or CDKs. Several potential phosphosites reside in an amino acid context resembling a degradation motif recognised by the SEL-10 homolog, Fbxw7. Moreover, some of these elements reside in a broader potentially destabilising amino acid context (PEST sequence). Thus, bioinformatic analysis highlighted numerous out of 112 phosphorylatable residues in GLD-1, which might be important for GLD-1 regulation.

3.8.3 Identification of phosphorylated residues in GLD-1 by mass spectrometry

In order to find out which of 112 phosphorylatable residues in GLD-1 might be modified *in vivo*, mass spectrometry-based analysis of GLD-1 phosphorylation status was performed. The approach was identical as used for CPB-3, described in section 3.3.5. Briefly, due to the instability of phosphorylated GLD-1 forms, the material for the Mass-Spec analysis could not be obtained from

worm extracts. Instead, recombinant GLD-1 was expressed in insect cells and purified under denaturing conditions, which allowed maintaining modifications (Figure 3.8.3 A). Recombinant GLD-1 protein, as given in figure 3.8.3 B, was submitted to the analysis by the Mass Spectrometry facility at MPI-CBG (Dresden). The obtained results are summarised in figure 3.8.2 E.

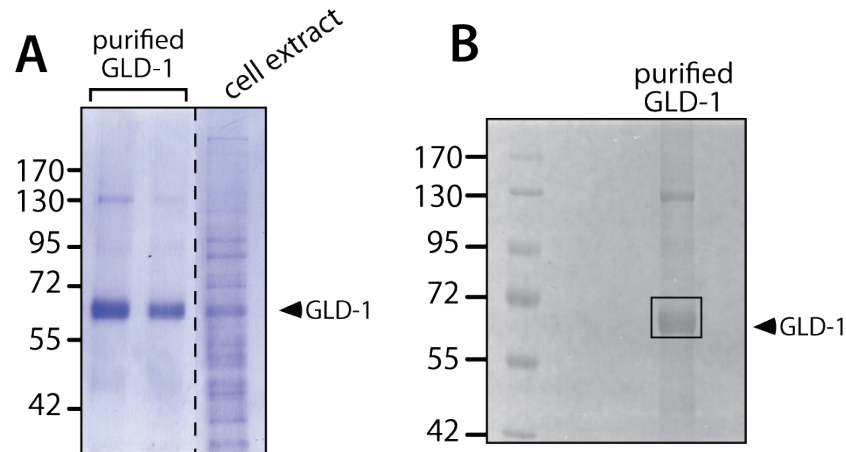


Figure 3.8.3 Purified recombinant GLD-1 for phosphorylation analysis by mass spectrometry.

Coomassie Blue-stained gels showing recombinant 3xFLAG::GLD-1::6xHis protein expressed in insect cells.

(A) An eluate from GLD-1 purification in denaturing conditions and cell extract from which GLD-1 was purified. Dashed line indicates region where some lanes were removed from the image for the clarity of the display.

(B) Image of the gel from which GLD-1 was excised for MS analysis. Excised fragment is marked with a rectangle.

Results of the analysis are presented in figure 3.9.2 E.

Peptides covering nearly 85% of protein sequence were detected. Comparison of m/z values of detected peptides against the database of theoretical phosphorylated ions retrieved at least 10 potentially modified sites, including six serines, three threonines, and one serine- and threonine-containing cluster that could not be resolved to identify a single modified amino acid (Figure 3.8.2 E). Surprisingly, no phosphopeptides were detected C-terminally from T146 despite relatively good sequence coverage of this region (~83%).

Seven identified phosphorylated residues (S22, S39, S85, S100, S113, S134, T119) overlap with ELM phospho-site predictions for proline-dependent kinases (Figure 3.8.2 D,E). Interestingly, S22 and S39 were previously suggested to be modified by CDK-2 (Jeong et al., 2011). Five identified residues (S22, S85,

S134, T136, and T138) are located within the three predicted N-terminal, suboptimal Fbxw7 degrons (Figure 3.8.2 G). Five others are not located in recognisable motifs but are followed by proline, suggesting that high activity of proline-depend kinases on GLD-1 protein in insect cells, and hypothetically, also in the worm.

3.9 GLD-1 is likely regulated by MAP kinase, a master regulator of oogenesis

3.9.1 The MAP kinase, MPK-1, regulates GLD-1 phosphorylation

MPK-1 regulates multiple aspects of oogenesis. As its activation spatially correlates with a decrease in GLD-1 levels in the germ line, it is possible that MPK-1 may be involved in the regulation of GLD-1 stability. If MPK-1 mediates GLD-1 phosphorylation then MPK-1 inactivation should reduce the accumulation of phosphorylated forms of GLD-1 in *sel-10(0)* mutants. To test whether this is the case, *mpk-1* was knocked-down by RNAi feeding in *sel-10(0)* mutant worms and worm extracts were analysed for the presence of modified GLD-1 by immunoblotting.

Slower migrating forms of GLD-1 were detected in extracts of *sel-10(0)* mutant, but not of wild-type worms (Figure 3.9.1 A). Similarly, the retarded forms were detected in extracts from the mock-treated *sel-10(0)* worms (RNAi against *gfp* gene). Thus, *sel-10* deficiency promotes accumulation of modified GLD-1. However, the slower migrating forms of GLD-1 were largely absent from the extracts of *mpk-1*-depleted *sel-10(0)* worms (Figure 3.9.1 A), suggesting that MPK-1 activity is necessary for the accumulation of phosphorylated GLD-1. Furthermore, intensity of the fastest-migrating forms of GLD-1 was higher upon *mpk-1* RNAi than in control RNAi feeding (Figure 3.9.1 A). This argues that the reduced detection of modified GLD-1 in *mpk-1*-depleted extracts does not result from overall reduction in GLD-1 signal but rather reflected reduced ratio of modified GLD-1.

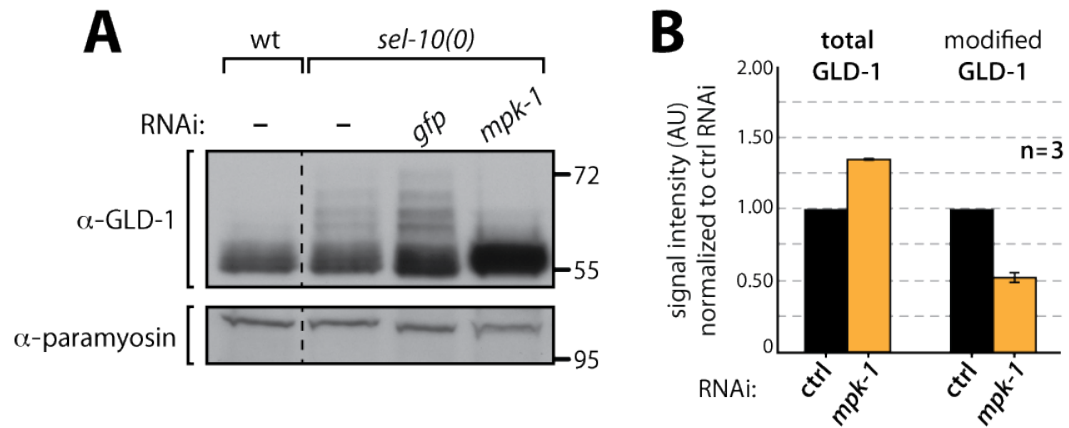


Figure 3.9.1 Accumulation of phosphorylated GLD-1 in *sel-10(0)* worms depends on MPK-1 activity.

(A) Immunoblot of *sel-10(0)* worms fed with standard food (-) or treated with control (*gfp*) or *mpk-1* RNAi. 50 adult hermaphrodites at L4+30 h were loaded per lane. Paramyosin serves as a loading control. Dashed vertical line marks the region where some lanes were removed from the blot for the clarity of the display.

(B) Quantification of the GLD-1 signal in control and *mpk-1*-depleted worm extracts in three independent experiments. 'Total GLD-1' includes 55 kDa band and slower migrating forms above. Measurements were done on shortly exposed films, to avoid saturation. 'Modified GLD-1' measurements included only shifts intensity and were done on longer exposed films, such as in (A). Average signal intensity values in control were set as 1. Error bars show SEM.

To confirm the changes in the relative amounts of modified and non-modified GLD-1 in *mpk-1*-depleted and mock-treated *sel-10(0)* extracts, intensity of the anti-GLD-1 signal on immunoblots was measured (Figure 3.9.1 B). The combined intensity of the GLD-1 signal coming from the major band and the retarded forms (total GLD-1) increased upon *mpk-1* RNAi (Figure 3.9.1 B). This indicates an increase in total amount of GLD-1 protein in the germ line and suggests a stabilisation of GLD-1 upon *mpk-1* reduction. By contrast, levels of phosphorylated GLD-1, measured as intensity of the signal above the most prominent band, decreased upon *mpk-1* RNAi, suggesting MPK-1-dependent phosphorylation of GLD-1.

Together, these observations suggest that MPK-1 activity regulates GLD-1 phosphorylation status and potentially may also influence its abundance.

3.9.2 GLD-1 binds to MPK-1 in yeast

To test whether MPK-1 can directly bind GLD-1, and thus function as its kinase, an interaction between the proteins was tested in the yeast-two-hybrid (Y2H) system using the β -galactosidase (β -gal) assay as readout. MPK-1 was fused to the DNA-binding domain (DB::MPK-1) and tested for an interaction with proteins fused to the activation domain (AD) (Figure 3.9.2).

To begin with, the ability of the Y2H system to recapitulate previously reported MPK-1 interaction was tested. To this end, DB::MPK-1 was co-expressed with a previously characterised substrate of MPK-1, NOS-3 (AD::NOS-3 fusion). Yeast co-expressing the two-hybrid proteins turned blue in the β -gal assay (Figure 3.9.2: lane 2), suggesting that the proteins had interacted with each other. Moreover, yeast co-expressing DB::MPK-1 and a truncated NOS-3::AD-fusion that lacked zinc-finger but contained the MAPK docking site (AD::NOS-3(-Zn)) also turned blue (Figure 3.9.2: lane 3), suggesting that an interaction took place. Thus, a previously observed physical interaction between MPK-1 and its substrate NOS-3 (Arur et al., 2011) was successfully recapitulated in the Y2H system, which suggests that this setup is suitable to probe for interactions of other MPK-1 candidate substrates.

Subsequently, an interaction between DB::MPK-1 and AD::GLD-1 was tested. Yeast co-expressing the two hybrids turned blue in the β -gal assay (Figure 3.9.2: lane 4). Thus, MPK-1 is likely to bind GLD-1. In order to find out which fragment of GLD-1 is important for this interaction, two fragments were tested: an N-terminal fragment, covering amino acids 1-270, and a C-terminal fragment, covering aa 273-457. The N-terminal fragment likely interacted with MPK-1, as all tested colonies turned strong blue in the β -gal assay. This interaction is consistent with the presence of a predicted docking site for MAP kinases between amino-acids 155-162 (Figure 3.8.2 F). Hence, MPK-1 is likely to bind to the N-terminal part of GLD-1. By contrast, the majority of tested yeast colonies that co-expressed MPK-1 and the C-terminal fragment of GLD-1 remained white. The C-terminal fragment of GLD-1 contains a predicted MAPK docking site at position aa 313-322 (Figure 3.8.2 F). However, the observation that MPK-1 and the C-terminal fragment of GLD-1 only sporadically gave weak


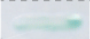














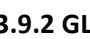
		DB fusion:	AD fusion:	% blue	n =
1		MPK-1	empty	9	35
2		MPK-1	NOS-3 full length	100	35
3		MPK-1	NOS-3 (-Zn)	90	30
4		MPK-1	GLD-1 full-length	75	20
5		MPK-1	GLD-1 aa 1-270	100	20
6		MPK-1	GLD-1 aa 273-457	10	20
7		MPK-1	CPB-3	60	20
8		MPK-1	GLD-1_17 mut	100	15
9		MPK-1	GLD-1_9 mut	93	15
10		empty	NOS-3 full length	0	25
11		empty	NOS-3 (-Zn)	0	25
12		empty	GLD-1 full length	0	20
13		empty	GLD-1 aa 1-270	0	20
14		empty	GLD-1 aa 273-457	0	20
15		empty	CPB-3	0	20
16		empty	GLD-1_17 mut	0	20
17		empty	GLD-1_9 mut	0	20

Figure 3.9.2 GLD-1 interacts with MPK-1 in yeast.

b-galactosidase assay of yeast co-expressing indicated hybrid proteins. DB - DNA-binding domain, AD - activation domain, aa - amino acids, n - number of tested colonies coming from three independent transformations. GLD-1_17 mut and GLD-1_9 mut are full-length GLD-1 proteins with selected serines and threonines substituted to alanines; explained in paragraph 3.10.2.

Yeast expressing GLD-1 mutants with 17 alanine substitutions (GLD-1_17 mut) grew very poorly, so they were streaked out as dots rather than lines.

blue colonies suggests that MPK-1 does not recognise this site efficiently or that the interaction of this GLD-1 fragment is in some way compromised in yeast.

In contrast to some other kinases, such as Polo-like kinases or glycogen synthase kinase-3 (GSK-3), MAPK binding to its substrates does not require any modification of the docking site. Thus, the interaction between MPK-1 and GLD-1 is expected to be insensitive to multiple alanine substitutions of phosphorylatable amino acids. In this respect, two GLD-1 mutant variants were tested: one carrying 17 serine and threonine substitutions (GLD-1_17 mut), the other carrying nine substitutions (GLD-1_9 mut). Majority of tested colonies that co-expressed MPK-1 together with either of these GLD-1 variants turned blue (Figure 3.9.2), suggesting that an interaction between the proteins took place.

Thus MPK-1 binding to GLD-1 is not sensitive to multiple mutations in the potential phosphorylation sites.

Altogether, data from the yeast two-hybrid system support the hypothesis that GLD-1 can directly interact with MPK-1 and suggest that the N-terminal part of GLD-1 may mediate this interaction. However, identification of functional docking motif(s) for MPK-1 requires additional experiments.

3.10 Prolonged GLD-1 expression in *sel-10(0)* mutant changes the expression pattern of GLD-1 mRNA targets modestly

GLD-1 binds and translationally represses various mRNAs during meiosis (Lee and Schedl, 2010 and references therein). Many GLD-1 targets, including *oma-2* and *rme-2*, encode proteins that are undetectable before the pachytene-to-diplotene transition but start accumulating in diplotene and become abundant in diakinetoc oocytes. An inhibition of GLD-1 binding to the 3' UTRs of target mRNAs results in the premature translation of these targets (Marin and Evans, 2003; Wright et al., 2011). Reduction of GLD-1 levels in diplotene and diakinetoc cells is thought to release GLD-1 target mRNAs from translational repression and promote protein synthesis. Along these lines, elevated levels of GLD-1 in diplotene and diakinesis are expected to interfere with translational activation of GLD-1 targets. To test if this is the case, protein expression of three GLD-1 targets, *oma-1*, *oma-2* and *rme-2* mRNAs, was examined in *sel-10(0)* mutant germ lines, which have higher than wild-type GLD-1 levels in post-pachytene cells.

First, potential changes in the expression of OMA-1 and OMA-2 proteins were investigated. OMA-1 and OMA-2, referred to collectively as OMA, are two highly similar proteins expressed in the cytoplasm of growing oocytes and essential for meiotic maturation (Detwiler et al., 2001). To test if prolonged GLD-1 expression affects accumulation of OMA proteins, germ lines of wild-type and *sel-10(0)* adult worms were extruded and stained with polyclonal anti-OMA antibody, which most likely recognises both, OMA-1 and OMA-2, proteins (Nousch et al., 2013). Germ lines were imaged and the intensity of the fluorescent signal was analysed.

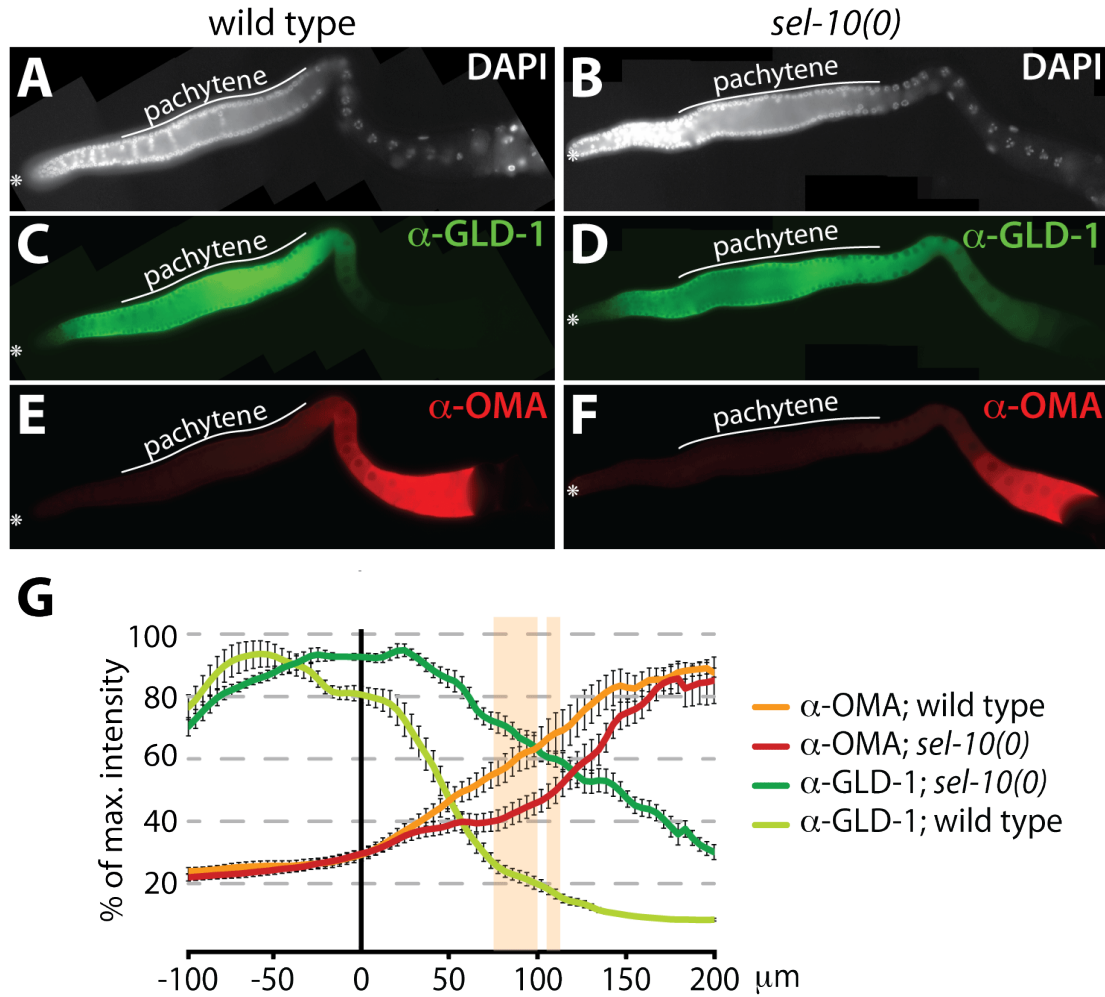


Figure 3.10.1 Accumulation of OMA proteins is slightly delayed upon the prolonged expression of GLD-1.

(A-F) DAPI staining and immunostaining of dissected gonads of wild-type (A,C,E) and *sel-10(0)* (B,D,F) hermaphrodites at L4+24h.

(G) Quantitation of the fluorescent signal in extruded gonads of wild type and *sel-10(0)* mutants stained with anti-GLD-1 and anti-OMA antibodies. Vertical axis represents pachytene-diplotene border, which was determined by analysing nuclear morphology on z-stacks. Eight wild-type and nine *sel-10(0)* germ lines were measured. Error bars show SEM. Shaded area indicates the region where intensity difference in OMA staining between the two genotypes is statistically significant.

Wild-type and *sel-10(0)* germ lines had no detectable OMA protein in their distal parts (Figure 3.10.1 E,F). OMA became detectable in late-pachytene cells and the signal increased proximally. This increase in OMA levels was analysed by plotting fluorescence intensity measured 100 μm distally and 200 μm proximally from the pachytene-to-diplotene border. In wild-type and *sel-10(0)* germ lines OMA levels started increasing at the same meiotic stage, in late-pachytene cells (Figure 3.10.1 G). Then, right after the pachytene exit, intensity curves split. OMA

intensity in *sel-10(0)* mutant germ line increased slower than in the wild type. The difference in the accumulation of OMA is modest but it was consistently observed in four experiments and the difference between average intensity values is statistically significant in a specific region (Figure 3.10.1 G, shaded area). Thus, the accumulation of OMA proteins seems to be slightly delayed in *sel-10(0)* mutant germ lines.

Next, protein expression of another GLD-1 target, *rme-2* mRNA, was analysed. *rme-2* (receptor-mediated endocytosis) encodes a cell surface receptor that mediates yolk uptake into the oocytes (Grant and Hirsh, 1999). In wild-type germ lines stained with anti-RME-2 antibody, the fluorescent signal is largely absent from the distal gonad; it becomes detectable shortly before the bend region, at the pachytene-to-diplotene transition, and accumulates toward the proximal end of the gonad (Figure 3.10.2). RME-2 is predominantly cytoplasmic in the bend region but accumulates in cell membranes as oocytes grow and cellularise. In contrast to both OMA proteins, whose levels gradually increase until the last oocyte, cytoplasmic RME-2 signal increases rapidly in the bend region and stays at similar levels in the cytoplasm of oocytes in the proximal gonad. In *sel-10(0)* mutant germ lines, RME-2 accumulates less rapidly than in wild-type germ lines (Figure 3.10.2). Although RME-2 protein in *sel-10(0)* germ lines is detectable at the pachytene-to-diplotene transition, RME-2 levels in the bend region and distal oocytes appear lower than in the wild type. By contrast, proximal oocytes of *sel-10(0)* worms are rather indistinguishable from the wild-type, as they have similar cytoplasmic levels and membranous enrichment of RME-2 (Figure 3.10.2). These observations suggest that *sel-10(0)* mutation weakly delays the accumulation of RME-2.

To quantify the observed effect, the intensities of the anti-RME-2 signal around the pachytene-to-diplotene transition in wild-type and *sel-10(0)* germ lines were measured. The averaged intensities showed a similar trend as initial observations suggested, i.e. RME-2 appeared to accumulate faster in wild-type than in *sel-10(0)* mutant germ lines (Figure 3.10.2 bottom: yellow vs. orange line). However, the differences between intensity values were not statistically significant. This can be partially attributed to the large spread of the intensity

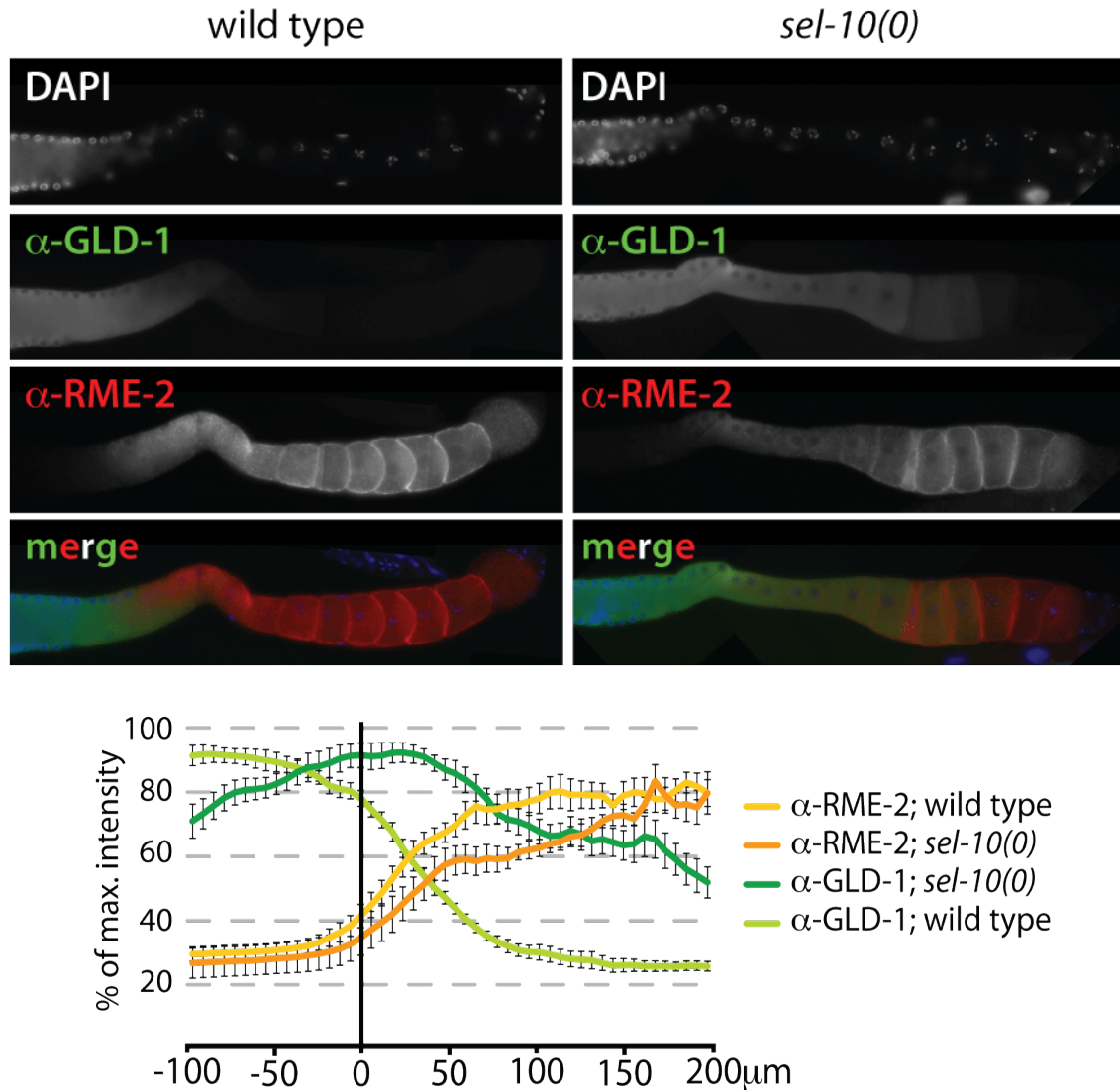


Figure 3.10.2 Accumulation of RME-2 protein is slightly delayed upon prolonged expression of GLD-1.

(Top) DAPI staining and immunostaining of dissected gonads of wild type (A,C,E) and *sel-10(0)* (B,D,F) hermaphrodites at L4+24h.

(Bottom) Measurements of the fluorescent signal in extruded gonads of wild type and *sel-10(0)* mutants stained with anti-GLD-1 and anti-RME-2 antibodies. Vertical axis represents pachytene-diplotene border, which was determined by analysing nuclear morphology on z-stacks. Nine wild-type and six *sel-10(0)* gonads were measured. Error bars show SEM.

values in the proximal gonad. Analyses of the changes in total RME-2 levels are complicated by protein re-localisation from the cytoplasm to the cell membrane and resulting uneven subcellular distribution of the signal. In presented analysis, the cytoplasmic and membranous signals were averaged. Possibly, a finer method of analysis, distinguishing between cellular locations, could give more

exact, significantly different results. For the moment, apparent delay of RME-2 accumulation in *sel-10(0)* germ lines (Figure 3.10.2) could not be confirmed by measurements of anti-RME-2 staining intensity.

Altogether, the available data suggest that accumulation of at least some of GLD-1 mRNA targets may be delayed in *sel-10(0)* mutant germ lines. Due to an apparent correlation between an increase in the levels of oogenic proteins, such as OMA, and a decrease in the levels of GLD-1, it is tempting to speculate that the delayed accumulation oogenic proteins in *sel-10(0)* germ lines is due to the prolonged translational repression mediated by ectopically expressed GLD-1.

3.11 GLD-1 expression in *sel-10(0)* mutant can be further stabilised by an inhibition of the proteasome

In wild-type germ lines, GLD-1 is abundant at the pachytene stage but not at later stages of meiosis. By contrast, in *sel-10(0)* mutant germ lines, GLD-1 is easily detectable by immunofluorescence at post-pachytene stages: in diplotene and diakinesis. Nonetheless, post-pachytene GLD-1 levels in *sel-10(0)* germ lines appear not so strong in comparison to the pachytene levels. To compare GLD-1 levels in distal and proximal gonad, fluorescence intensity was measured in germ lines of transgenic animals expressing GLD-1::GFP in *sel-10(0)* mutant background (strain EV666). Quantification of signal intensity revealed that the GFP signal in post-pachytene cells was at ~30% of an intensity measured in mid-to-late pachytene cells (data not shown), suggesting that there is a mechanism operating independently of *sel-10* to reduce GLD-1 levels after pachytene stage.

Furthermore, GLD-1 signal gradually decreases towards the proximal end of the germ line. GLD-1 intensity in the most proximal oocyte in the germ line ('-1 oocyte'), which is about to undergo meiotic maturation and ovulation, is usually noticeably lower than GLD-1 intensity in the neighbouring -2 oocyte, which is 'younger' and will mature ~23 min later (McCarter et al., 1999). This decrease in the signal intensity is visible in the strain EV666 (*gld-1::gfp; sel-10(0)*) (Figure 3.11.1 C) as well as in *sel-10(0)* mutant gonads stained with anti-GLD-1 antibody (Figure 3.7.1 F). Partial reduction in GLD-1 levels after the pachytene exit and further reduction in the -1 oocyte raise the possibility that there is a molecular

mechanism that acts independently of *sel-10* to destabilise GLD-1 in growing and maturing oocytes.

3.11.1 Extended GLD-1 expression can be further stabilised by an inhibition of the proteasome in the *sel-10(0)* mutant germ lines

To test whether a reduction of GLD-1 levels in proximal regions of the gonad of *sel-10(0)* mutants is due to proteasome activity, *pbs-6* was knocked-down in EV666 transgenic *sel-10(0)* mutant worms that express GFP::GLD-1, and the intensity of GFP fluorescence was observed in anaesthetised worms (Figure 3.11.1). Germ lines of mock-treated EV666 animals displayed strong GFP signal in the pachytene region and a decline in the signal strength in post-pachytene cells (Figure 3.11.1 C), paralleling GFP signals observed in animals fed with standard food. By contrast, germ lines of *pbs-6*-depleted animals had similar GFP levels in the pachytene region but they had less pronounced signal decline in the proximal region (Figure 3.11.1 D). This difference was not quantified, due to the fact that the distribution of the signal in a few most proximal oocytes was very uneven: perinuclear and cortical oocyte regions showed much higher fluorescence than the remaining cytoplasm (Figure 3.11.1 D). The cytoplasmic regions of particularly low GFP signal have also a distinct smooth appearance when observed with DIC; they were consistently observed upon knock-downs of proteasome subunits but not in control germ lines. Thus, such regions may represent cellular structures arising in response to the proteotoxic stress. Incorporation of GFP intensity values of these regions into the measurements of cytoplasmic GFP levels in the proximal germ line would lower the signal intensity values, which might lead to incorrect conclusions. Hence, an alternative approach to evaluate proteasomal degradation of GLD-1::GFP was required.

In order to measure stabilisation of GLD-1::GFP in *sel-10(0)* background upon *pbs-6* RNAi, levels of embryonic GFP signals were measured (Figure 3.11.2). It had been noticed that early embryos of *pbs-6*-depleted hermaphrodites had higher fluorescence levels than the embryos of mock-treated animals (Figure 3.11.2 A). Since GLD-1::GFP is expressed under the control of *gld-1* endogenous regulatory sequences, the fusion protein is expected to be absent from the very early embryo (until 4-cell stage) and re-appear

restricted to the P-lineage and its sister cells in later embryonic stages (Jones et al., 1996). Thus, GLD-1::GFP detected in *gld-1::gfp; sel-10(0); pbs-6(RNAi)* embryos likely represents protein carried over from the germ line. As the distribution of the signal was much more uniform in early embryos than in proximal oocytes, the former were used for signal intensity measurements. *pbs-6* was knocked-down by RNAi feeding in transgenic lines EV375 and EV666 and in genetically corresponding non-transgenic strains: wild-type and *sel-10(0)*. Non-transgenic lines served to set the background fluorescence levels and to control changes in autofluorescence upon RNAi.

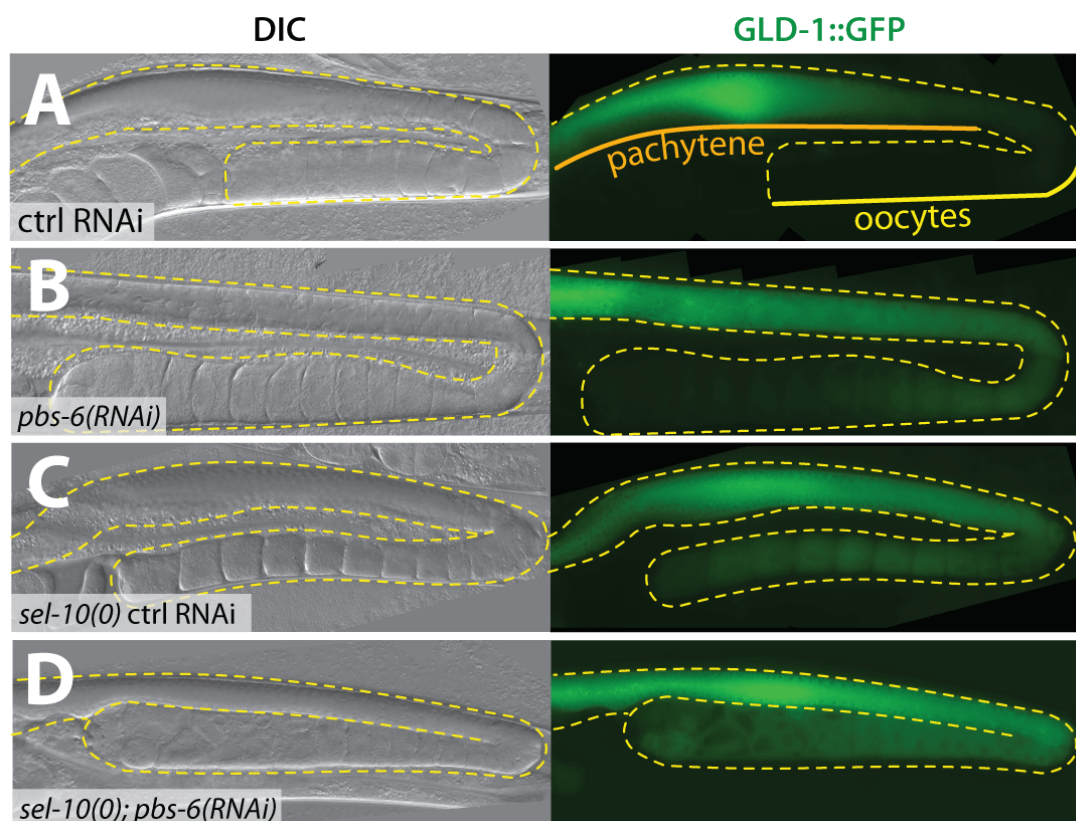


Figure 3.11.1 Expression of GLD-1::GFP in *sel-10(0)* background is increased upon proteasome inhibition.

DIC images (left) and corresponding GFP autofluorescence (right).

(A,B) *pbs-6* RNAi extends the expression pattern of GLD-1::GFP (strain EV375).

(C) In the absence of *sel-10(0)* activity, GLD-1::GFP is readily detectable in oocytes.

(D) Knock-down of *pbs-6* in EV666 (*gld-1::gfp; sel-10(0)*) worms increases GFP signal in the most proximal oocytes (to the left).

As shown in figure 3.11.2 B, autofluorescence in non-transgenic embryos was relatively low but tended to slightly increase upon *pbs-6* RNAi. Embryos of mock-treated EV375 worms, expressing GLD-1::GFP, had similarly low levels of fluorescence as non-transgenic embryos, suggesting that virtually no GLD-1::GFP is loaded to the embryos in otherwise wild-type genetic background. However, GFP fluorescence increased noticeably upon proteasome inhibition by RNAi. This is consistent with partial stabilisation of GLD-1::GFP observed in *pbs-6* RNAi-treated worms (see figure 3.11.1 A,B) and might result from an incomplete turnover of the fusion protein in the oocytes. Mock-treated embryos of EV666 worms (*gld-1::gfp; sel-10(0)*) had the highest levels of fluorescence intensity from all groups, which was expected, considering high GFP levels in oocytes of their mothers (Figure 3.11.1 C). The fluorescence intensity of EV666 embryos increased almost five-fold upon *pbs-6* knock-down (Figure 3.11.2 B). Thus, proteasome inhibition seems to additionally stabilise GLD-1::GFP that has been partially stabilised by *sel-10(0)* mutation.

Together, the observations suggest that GLD-1 protein amounts are reduced in oocytes and/or early embryos by proteasome activity. Hence, a destabilisation pathway independent of *sel-10* may act to degrade GLD-1 in the oocytes. Consequently, a second ubiquitin ligase might operate in addition to a SEL-10-containing complex to ubiquitinate GLD-1 and ensure its absence from early embryos.

3.11.2 A CUL-2-based ubiquitin ligase mediates GLD-1 degradation in late oogenesis

Since the proteasome activity seems to be involved in the removal of GLD-1 from growing oocytes in the proximal gonad (section 3.7.1), an attempt has been made to identify a hypothetical ubiquitin ligase that acts next to *sel-10* to mediate GLD-1 turnover. Three cullins in *C. elegans*, CUL-1, -2, and -3, are known to act in oocyte development and early embryogenesis (reviewed in Bowerman and Kurz, 2006; DeRenzo and Seydoux, 2004). CUL-1 acts in *C. elegans* as a negative regulator of the cell cycle commitment; the absence of maternal or zygotic *cul-1* activity results in hyperplasia and lethality in embryos or larvae, respectively (Kipreos et al., 2000). CUL-2 is involved in progression through the

second meiotic division of oocyte and in degradation of maternally-provided polarity proteins in early *C. elegans* embryos (DeRenzo et al., 2003; Feng et al., 1999). CUL-3 acts with the BTB protein, MEL-26, to degrade MEI-1, a katanin-like, microtubule severing protein, which is necessary for proper meiosis-to-mitosis transition, i.e. a proper orientation of microtubules and cytokinesis in early embryo (Pintard et al., 2003). Thus, CUL-1, CUL-2 and CUL-3 could potentially be components of an E3 that regulates GLD-1.

To test whether *cul-1*, *-2* or *-3* affect GLD-1::GFP in the proximal gonad, the activity of these genes was reduced by RNAi feeding in the *gld-1::gfp; sel-10(0)* strain (EV666). Consistent with published findings, all knock-downs led to embryonic lethality in the progeny of fed worms; thus, RNAi was considered efficient. Overall levels of GLD-1::GFP in the germ lines were similar in all feeding conditions (data not shown). Depletion of *cul-1* and *cul-3* had no effect on the GLD-1::GFP expression pattern. By contrast, depletion of *cul-2* resulted in higher levels of GLD-1::GFP in the -1 oocyte (data not shown). The increase in fluorescence intensity upon *cul-2* knock-down was particularly strongly pronounced in embryos. While *gld-1::gfp; sel-10(0)* control embryos had barely detectable GFP, *cul-2*-depleted embryos showed increased fluorescence (Figure 3.11.2 A).

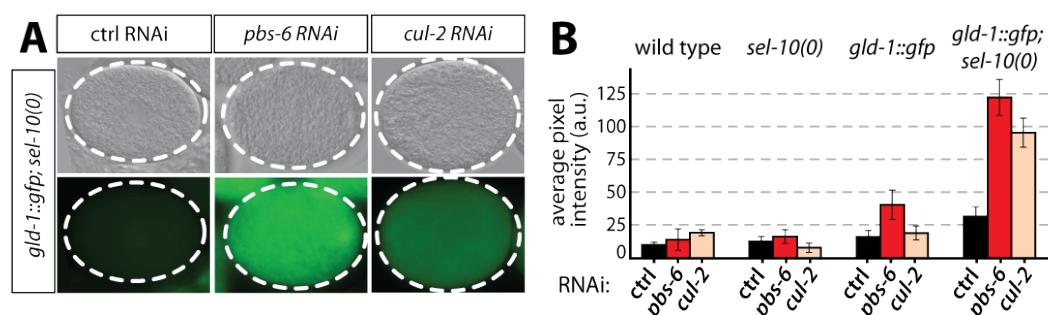


Figure 3.11.2 Proteasome-dependent mechanism independent of *sel-10* may destabilise GLD-1 in oocytes.

(A) Representative images of *gld-1::gfp; sel-10(0)* embryos upon mock, *pbs-6* or *cul-2* RNAi. DIC, top row; GFP fluorescence, bottom row.

(B) Quantification of GLD-1::GFP signal in embryos. Per bar, 20 one-cell-stage embryos were measured. Error bars show SEM.

The increase in signal intensity was quantified in *cul-2*-depleted one-cell embryos (see Materials and methods 18.3). To exclude the possibility that changes may arise from an increase in general autofluorescence, which could potentially be an off-target effect of RNAi feeding, the quantification was also done for embryos of non-transgenic strains: wild-type and *sel-10(0)* mutant. Autofluorescence in wild-type and *sel-10(0)* embryos did not change much upon *cul-2* RNAi (Figure 3.11.2 B), arguing that the fluorescence observed in transgenic lines is specific for GLD-1::GFP protein. Signal intensity in mock-treated embryos of *gld-1::gfp* (EV375) is similar to the signal intensity in non-transgenic embryos, suggesting that GLD-1::GFP is normally not deposited into embryos. Reduction of proteasomal activity in EV375 results in ~2.5-fold increase in GFP intensity but reduction of *cul-2* activity does not significantly change GFP fluorescence. Thus, inhibition of the proteasome stabilises GLD-1 that would be normally turned-over at the pachytene-to-diplotene transition. Depletion of the E3 ubiquitin ligase component *cul-2* does not induce comparable stabilisation.

Several reasons may account for GLD-1::GFP signal in the embryos. First, RNAi could have been inefficient. Secondly, *cul-2* may be not involved in the regulation of GLD-1. Thirdly, SEL-10 activity may be sufficient to reduce GLD-1 levels in the germ line, masking the role of *cul-2*. A weak efficiency of RNAi is rather unlikely, considering severe and highly penetrant embryonic defects that resemble those observed in *cul-2* mutant embryos (Feng et al., 1999). To distinguish between two other possibilities, *cul-2* RNAi was performed in the *sel-10(0)* mutant strain EV666 expressing GLD-1::GFP. Lack of *sel-10* activity results in increased embryonic GFP fluorescence in comparison to the GLD-1::GFP expressing wild-type strain EV375 (Figure 3.11.2 B). Depletion of *cul-2* increases GFP signal levels almost four-fold, so they nearly reach levels observed upon proteasome inhibition. This suggests that *cul-2* activity promotes removal of GLD-1::GFP from oocytes and/or early embryos. The observation that *cul-2* depletion did not stabilise GLD-1::GFP in EV375 strain suggests that CUL-2 acts later than SEL-10 in degradation of GLD-1. Destabilisation of GLD-1 by SEL-10 is sufficient to prevent GLD-1 presence in the embryos. However, in the absence of *sel-10*, activity of *cul-2* contributes to the reduction of GLD-1.

Taken together, these observations suggest that remaining GLD-1::GFP, which is expressed in the oocytes of *sel-10(0)* depleted worms, is destabilised in a proteasome-dependent manner before the formation of an egg. Presented results suggest that the activity of *cul-2* is required for this destabilisation. However, it remains unclear whether *cul-2* acts directly on GLD-1 and mediates its ubiquitination within CLR2/ECS complex, or it acts indirectly, e.g. by promoting degradation of a hypothetical factor that stabilises GLD-1::GFP in the proximal part of the gonad.

4. Discussion

Biological processes rely on regulatory proteins, which expression is often tightly controlled at the transcription level. However, some processes, such as gametogenesis and early embryogenesis, execute complex tasks, e.g. differentiation and patterning, despite periods of global transcriptional repression. This is possible because the regulation is shifted to the post-transcriptional levels and involves adjusting protein abundance by modulating translation and degradation, as well as controlling protein activity by post-translational modifications.

In order to unravel mechanisms of post-transcriptional gene expression control that operate during oogenesis, this work investigated restricted expression of two important translational regulators. Specifically, the thesis addressed involvement of the ubiquitin-proteasome system in reducing levels of two conserved RNA-binding proteins that promote oogenesis, and potential links between their degradation, meiotic progression and formation of oocytes.

4.1 Roles of the ubiquitin-proteasome system (UPS) in regulating RNA-binding proteins in the germ line

Gene expression during gametogenesis needs to be tightly controlled to couple nuclear division (meiosis) with a cell differentiation program, which leads to the formation of functional gametes. To achieve this goal, protein synthesis in germ cells is controlled by a spectrum of translational regulators. Restricted expression of these regulators limits their activity to certain meiotic stages (see figure 2.3.5). This thesis addressed mechanisms that shape the expression pattern of two distinct RNA binding proteins (RBPs), CPB-3 and GLD-1, during *C. elegans* oogenesis. Specifically, the involvement of the proteasome at the pachytene-to-diplotene transition in reducing CPB-3 and GLD-1 levels during meiotic prophase I, was investigated.

To date, the role of the proteasome in the *C. elegans* germ line was reported predominantly in three contexts: mitosis-meiosis balance in the mitotic

region of adult gonad (MacDonald et al., 2008; Gupta et al., 2015), in germ line blastomeres in an early embryo (deRenzo et al., 2003), and in sex-determination (Starostina et al., 2007). In these three biological situations, CUL-2-based ubiquitin ligases (Cullin2-RING ligases, CRL2) play most prominent roles.

In the mitotic region, CUL-2 associates with the leucine-rich repeat protein, LRR-1, to destabilise the cyclin-dependent kinase inhibitor, CKI-1, and to promote proliferative divisions (Merlet et al., 2010; Starostina et al., 2010). The same ubiquitin ligase complex, CRL2^{LRR-1}, destabilises the synaptonemal complex component, HTP-3, which is required for the progression through meiotic prophase (Burger et al., 2013). The balance between mitosis and meiosis is additionally regulated by RFP-1-mediated degradation of chromatin regulator MRG-1 (Gupta et al., 2015). Importantly, proteasome-mediated destabilisation was also suggested to regulate levels of GLD-1 in the mitotic region but in this case the ubiquitin ligase was not identified (Jeong et al., 2011). Hence, the ubiquitin-proteasome system (UPS) destabilises certain meiosis-promoting proteins and in this way modulates the proliferation-versus-differentiation (mitosis-versus-meiosis) decision, which is largely determined by GLP-1/Notch signaling and a network of translational regulators (GLD-1, GLD-2, GLD-3 and NOS-3) (Kimble and Crittenden, 2007).

Proteasomal degradation was also shown to play an important role in the oocyte-to-embryo (or meiosis-to-mitosis) transition and in embryonic germ line specification. Upon completion of meiosis, proteins that promoted the assembly of small acentriolar meiotic spindle must be degraded, to allow an assembly of a larger centriolar mitotic spindle. This essential function is fulfilled by a CUL-3-based ubiquitin ligase, which mediates degradation of the microtubule severing protein, MEI-1 (Pintard et al., 2003; Xu et al., 2003). Later on, mitotic divisions are promoted by CUL-1-based ubiquitin ligases that regulate levels of the functional counterpart of Polo-like kinase 4, ZYG-1, at mitotic spindles (Peel et al., 2012). As embryogenesis proceeds, the UPS plays an essential role in germ line specification. In this additional biological context, CUL-2-based complexes utilise the substrate recognition subunit, ZIF-1, to downregulate zinc-finger containing polarity determinants (MEX-1, -5, -6) and germ line determinants (POS-1, PIE-1) (DeRenzo et al., 2003; reviewed in DeRenzo and Seydoux, 2004).

Hence, a variety of ubiquitin ligases control the abundance of cell cycle regulators and cell fate determinants in early embryos.

CUL-2 has also a role in the sex determination pathway. It was shown to interact with the sex-determination pathway component, FEM-1, and mediate ubiquitination and degradation of the transcription factor, TRA-1/Gli (Starostina et al., 2007). Loss-of-function mutations in *fem-1* and partial loss of *cul-2* activity lead to feminisation of the germ line, which correlates with increased TRA-1 levels (Starostina et al., 2007). Moreover, the levels of FEM-1 are regulated by the F-box protein, SEL-10, which can bind and trigger ubiquitination of FEM-1 *in vitro*, most likely in the context of an SCF (Skp1, Cullin1, F-box) ubiquitin ligase (Jager et al., 2004). Furthermore, knock-down of two proteasome components, *rpn-10* and *ufd-2*, prevents hermaphrodite spermatogenesis (Shimada et al., 2006). Thus, proteasome-mediated degradation contributes to the sex determination, which is predominantly regulated at the transcriptional and translational levels.

In contrast to the aforementioned aspects of germ cell biology, proteasome-mediated degradation in *C. elegans* is far less characterised during progression through meiosis and gametogenesis. Some studies addressed regulators of meiotic divisions, some of which seem to be different between *C. elegans* and other model organisms. For instance, the anaphase-promoting complex/cyclosome (APC/C) is required for the metaphase-to-anaphase transition during meiosis I in *C. elegans* but dispensable for this transition in *Xenopus* (Boxem, 2006; Davis et al., 2002; Furuta et al., 2000; Peter et al., 2001; Taieb et al., 2001).

Particularly little is known about the requirement of proteasomal activity prior to meiotic division, i.e. during prophase I. Orsborn et al. (2007) suggested a role of the proteasome in regulating levels of GLH-1, a homolog of fly Vasa protein. Vasa is a DEAD-box RNA helicase required for the formation of the germ line (Breitwieser et al., 1996; Seervai and Wessel, 2013). In *C. elegans*, there are four Vasa orthologs, named GLH-1 to -4, which have largely redundant functions (Roussell and Bennett, 1993; Spike et al., 2008). Although GLH-1 is regulated by proteasomal activity (Orsborn et al., 2007), the identity of the ubiquitin ligase remains unknown. The majority of proteasome-dependent regulatory events in

the germ line, such as degradation of checkpoint kinases or cyclins, are inferred from findings in other systems, yet have not been demonstrated in *C. elegans*.

This work reveals a new aspect of the proteasome function during *C. elegans* gametogenesis. It shows that the ubiquitin-proteasome system (UPS) acts to restrict the expression patterns of RNA regulators and in this way limit their activity to early meiotic stages (Figure 4.1). CPB-3 and GLD-1, two conserved RBPs, are abundantly expressed in early meiosis until the pachytene-to-diplotene transition. This thesis shows that at this transition the proteasome activity reduces CPB-3 and GLD-1 levels. Furthermore, all presented data suggest that an SCF complex that utilises SEL-10 as a substrate recognition subunit regulates CPB-3 and GLD-1 stability, most likely by mediating ubiquitination of both RBPs (Figure 4.1). Downregulation of CPB-3 and GLD-1 coincides with an initiation of oocyte growth and cellular rearrangements in the gonad. Although it has never been proven, the reduction in CPB-3 and GLD-1 levels may be necessary for the onset of the oogenic gene expression program, which is expected to support the transition from small syncytial, early meiotic germ cells to large, fully cellularised, functional oocytes. Hypothetically, the low levels of CPB-3 and GLD-1 may also be important for early embryogenesis.

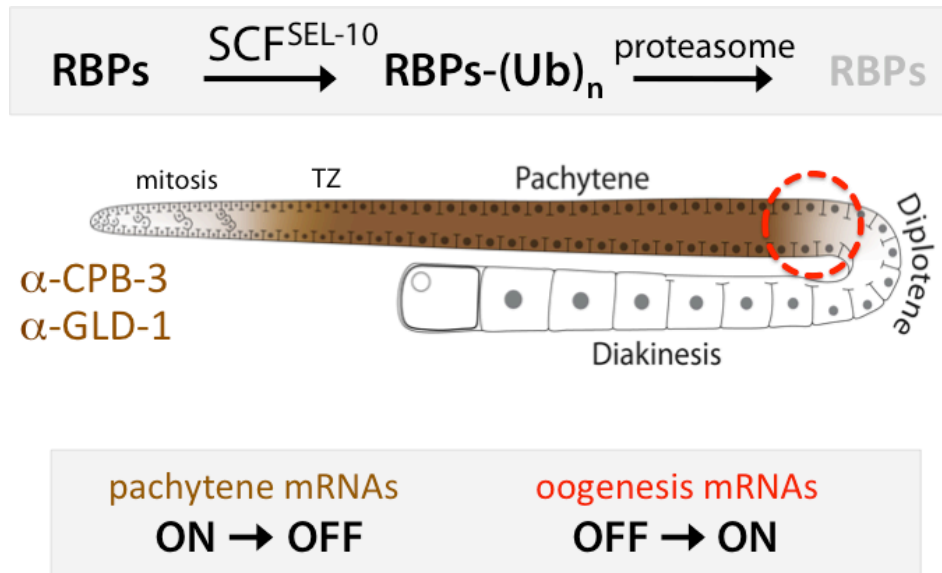


Figure 4.1. Degradation of RNA binding proteins (RBPs) may act to synchronise cell cycle progression with the oocyte differentiation program. In the distal part of the gonad, CPB-3 and GLD-1 regulate translation of mRNAs that contain binding motifs, CPE or GBM, respectively. Reduction in the CPB-3 and GLD-1 levels, which is observed at the pachytene-to-diplotene transition, sets mRNAs free for translation or regulation by other RBPs.

4.1.1 Degradation of CPB-3 and GLD-1 may support oogenic gene expression program

GLD-1 functions as a translational repressor and a reduction of its levels after the pachytene stage has been suggested to promote translational activation of GLD-1 mRNA targets (Jones et al., 1996). Many of these targets encode oocyte-specific proteins, such as the yolk receptor, RME-2, or RNA regulators, such as PUF-5 and PUF-6. Until now, a large number (>450) of GLD-1 mRNA targets were identified (Jungkamp et al., 2011; Scheckel et al., 2012; Wright et al., 2010) and many (>20) were functionally validated (Biedermann et al., 2010; Jan et al., 1999; Lee and Schedl, 2001; Lee and Schedl, 2004; Marin and Evans, 2003; Mootz et al., 2004; Schumacher et al., 2005; Xu et al., 2001). GLD-1 translationally represses its mRNA targets but the molecular mechanism of repression is not understood (discussed in Jungkamp et al., 2011; Scheckel et al., 2012). Except for FOG-2 (Clifford et al., 2000), no GLD-1 interacting proteins have been described so far.

In contrast to GLD-1, the molecular function and RNA regulatory potential of CPB-3 have not been demonstrated yet. However, certain assumptions can be made based on the role of its homologs in supporting oogenesis in flies, frogs and mice (reviewed in Ivshina et al., 2014). Importantly, degradation of CPEB1 in *Xenopus* is seen as an important trigger for the translational activation of certain mRNAs in oocytes (Mendez et al., 2002). The proteasome-mediated degradation of RBPs at the pachytene exit during *C. elegans* oogenesis might also serve to regulate gene expression during oogenesis.

Despite belonging to different protein families and potential differences in molecular functions, CPB-3 and GLD-1 have nearly identical expression pattern across the germline tissue. Both RBPs are barely detectable in the most distal mitotic cells but their expression increases toward the transition zone and stays at high levels throughout most of the pachytene region (Hasegawa et al., 2006; Jones et al., 1996; Figures 3.1.2 C and 3.7.1 B). CPB-3 levels decrease shortly before the pachytene-to-diplotene transition (pachytene exit) (Figure 3.1.2 F), whereas GLD-1 levels decrease at or shortly after this transition (Figure 3.10.2 bottom). Neither protein is detectable in diakinetic cells in the proximal gonad. This expression pattern suggests that CPB-3 and GLD-1 function is

required in early meiosis but is obsolete, if not detrimental, at the post-pachytene stages of meiosis.

The exit from pachytene is an important turning point in life of a female germ cell, as it determines whether a germ cell will become an oocyte, or will assume a 'nurse-cell' role and will undergo programmed cell death (PCD). Post-pachytene cells do not undergo PCD (Gumienny et al., 1999) but become transcriptionally silenced and grow in volume, supported by the material synthesised by pachytene-stage cells (Wolke et al., 2007). Thus, the gene expression program at the pachytene exit is likely to change significantly. RNA-binding proteins that are present prior to the pachytene exit but not afterwards are likely to provide such a regulatory switch. Removal of such early-meiotic RBPs would release their mRNA targets and allow a change in the translational outcome of their mRNA targets.

The mRNA targets of CPB-3 and GLD-1 are likely to be differently regulated during early gametogenesis and oocyte formation. Consistently with this assumption, protein products of many GLD-1 mRNA targets are sparse in pachytene-stage cells but accumulate in growing oocytes. Thus, regulation of CPB-3 and GLD-1 levels may be important for the fate of their mRNA targets. Although several studies addressed mechanisms regulating the synthesis and accumulation of CPB-3 and GLD-1 in mitotic and early meiotic cells (Hansen et al., 2004; Jeong et al., 2011; Jedamzik, 2009), downregulation of these proteins at pachytene exit has not been addressed.

4.1.2 Expression pattern of CPB-3 and GLD-1 is shaped by translational regulation and proteasomal degradation

Expression of CPB-3 and GLD-1 is likely to be regulated at the translational level, as this mode of regulation was observed for the majority of investigated mRNAs in adult hermaphrodite germ line (Merritt et al., 2008). The discrepancy between *cpb-3* and *gld-1* mRNA expression patterns, and the corresponding CPB-3 and GLD-1 protein expression patterns (Jedamzik, 2009; Jones et al. 1996) support this assumption. Furthermore, the expression patterns of *cpb-3* and *gld-1* 3' UTRs translational reporters largely recapitulate the cognate protein expression pattern (Merritt et al., 2008; Eckmann lab,

unpublished data). Specifically, both reporter proteins are barely detectable in the most distal cells, abundant in proximal mitotic and early meiotic cells until the diplotene stage. Furthermore, both translational reporters are weakly expressed in the proximal gonad, which suggests that elements in *cpb-3* and *gld-1* 3' UTRs mediate efficient translational repression in growing oocytes. However, RBPs that would mediate this repression have not been identified yet. Moreover, the translational repression of mRNAs does not explain the rapid decrease in levels of already synthesised proteins.

This thesis work addressed the hypothesis that CPB-3 and GLD-1 levels are regulated by the ubiquitin-proteasome system at the pachytene-to-diplotene transition. The hypothesis is supported by the observation that a reduction in proteasome activity due to a depletion of its subunits results in increased CPB-3 and GLD-1 levels in diplotene and diakinetik cells (Figures 3.1.2 D and 3.7.1 D). Interestingly, targeted degradation of CPB-3 and GLD-1 appears to be limited to late pachytene and post-pachytene cells, as an increase in the levels of both RBPs at earlier meiotic stages was not observed. Moreover, no gross changes in CPB-3 and GLD-1 levels were detected by immunoblotting of *pbs-6*-depleted worm extracts (Figure 3.1.2 G and 3.7.3), which further supports the idea that the degradation is restricted to a specific meiotic stage rather than takes place constitutively.

Thus, presented data suggest that CPB-3 and GLD-1 proteins are degraded by the proteasome at the pachytene-to-diplotene transition, whereas data obtained with translational reporters suggest that the synthesis of CPB-3 and GLD-1 proteins is reduced in post-pachytene cells. Since the two mechanisms, i.e. protein degradation and translational repression of mRNA, are not mutually exclusive, it is likely that the abundance of CPB-3 and GLD-1 is regulated at multiple levels to provide sharp decrease in the expression pattern of the two RBPs and efficiently eliminate their activity.

4.1.3 A conserved tumor suppressor, Fbxw7, regulates CPB-3 and GLD-1 stability

Presented work shows that the stability of CPB-3 and GLD-1 is regulated by a CUL-1-based ubiquitin ligase (SCF) that utilises SEL-10 as a substrate recognition subunit. *sel-10* is an ortholog of vertebrate *FBXW7*, a well-characterised, conserved tumor suppressor, which mediates the turnover of

several proliferation-promoting factors (including MYC, JUN, cyclin E and Notch)(reviewed in Skaar et al., 2013; Welcker and Clurman, 2008). *C. elegans* SEL-10 was shown previously to regulate levels of some proteins acting in vulva development: LIN-12/Notch, SEL-12/presenilin, LIN-45/RAF (de la Cova and Greenwald, 2012; Hubbard et al., 1997; Wu et al., 1998), in regulating ZYG-1/Plk4 levels in embryonic divisions (Peel et al., 2012), and uncharacterised targets during innervation of the vulva (Ding et al., 2007). Several transgenic strains had been generated in these and other (Dorfman et al., 2009) studies to confirm the expression of SEL-10 in investigated tissues. However, germ line expression of SEL-10 has never been reported so far, even though observations suggest a role of *sel-10* during spermatogenesis (Peel et al., 2012). In this thesis, germline SEL-10 expression was investigated by generating a transgenic line that expressed a reporter protein under the control of a permissive promoter and the *sel-10* 3' UTR. The expression of this reporter protein was detected in the adult germ line tissue (Figure 3.6.1 B), which together with the detection of *sel-10* mRNA in adult gonad (NEXTDB) indicates that SEL-10 protein is likely expressed during oogenesis. The levels of *sel-10* 3' UTR translational reporter peaked in late pachytene cells, coinciding with the decrease in CPB-3 and GLD-1 levels, and further supporting the hypothesis of SEL-10 involvement in the regulation of these two RBPs. Thus, presented results support a previously undocumented expression of SEL-10 in the germ line tissue. Moreover, they find a new role of an SCF^{SEL-10} complex in restricting germ line expression of RNA-binding proteins.

The degradation of CPEB proteins during oogenesis appears to be evolutionarily conserved, as it has been described in a variety of organisms, including frog, mouse, pig, cow, and slug (Lapasset et al., 2005; Thom et al., 2003; Uzbekova et al., 2008). However, it is not clear whether the molecular pathway destabilising CPEB is similar in these organisms as so far the molecular details of CPEB degradation have been elucidated only in frog (Setoyama et al., 2007). *Xenopus* CPEB1 is targeted to the proteasome by an SCF complex that utilises β -TrCP (aka FBXW1) as a substrate recognition subunit (Jin et al., 2004; Setoyama et al., 2007). The *C. elegans* protein most similar to β -TrCP is LIN-23 (Jin et al., 2004). In contrast to *sel-10*, whose loss of function does not induce any obvious

phenotype, *lin-23* is an essential gene, and the loss of *lin-23* activity results in somatic and germline defects that lead to sterility (Kipreos et al., 2000). Interestingly, instances were found where SEL-10/FBXW7 and LIN-23/ β -TrCP/FBXW1 act cooperatively to degrade a shared target, as has been described for the regulation of *C. elegans* ZYG-1/Plk4 levels during cell division (Peel et al., 2012) and for mammalian anti-apoptotic protein Mcl1 (Ren et al., 2013). Since LIN-23 is expressed in germ cells (Segref et al., 2010), it could participate in the destabilisation of CPB-3 and GLD-1. However, neither CPB-3 nor GLD-1 contains a consensus sequence for LIN-23/ β -TrCP binding, DSGXXS (including possible substitutions of serines by threonines or the phosphomimicking amino acids - aspartate and glutamate). Lack of the consensus sequence makes the binding between LIN-23 and the two RBPs rather unlikely. Nonetheless, the potential involvement of *lin-23* was tested in several experiments (data not shown). Protein-protein interactions between LIN-23 and CPB-3 or GLD-1 were not detected in the yeast two-hybrid system, suggesting that the proteins do not interact directly. Furthermore, *sel-10(0); lin-23(RNAi)* worms had similar germline expression pattern of CPB-3 and GLD-1 as *sel-10(0)* single mutants, suggesting that *lin-23* activity does not contribute to the regulation of CPB-3 and GLD-1. Altogether, obtained data suggest that *lin-23*/ β -TrCP is not involved in destabilising CPB-3 and GLD-1 in growing oocytes. Developmentally regulated degradation of STAR proteins remains poorly characterised; thus, a direct comparison of GLD-1 destabilisation with the regulation of its homologs in other systems cannot be made. At the same time, the presented findings are among the first reports of developmentally regulated degradation of STAR proteins. As far as the destabilisation of CPEB proteins is concerned, the literature and this thesis point at the prominent role of SCF complexes. SCFs regulate CPEBs in frogs and worms but different substrate recognition subunits (β -TrCP/LIN-23/Fbxw1 and SEL-10/Fbxw7, respectively) were assigned to fulfill this function.

4.1.4 Additional, yet unidentified E3 ubiquitin ligase may regulate CPB-3 and GLD-1 expression pattern

In *sel-10(0)* mutant germ lines, CPB-3 and GLD-1 are expressed at apparently normal levels in the pachytene region but at elevated levels in post-

pachytene germ cells. Despite a measurable increase in the amounts of the two RBPs in diplotene cells (Figures 3.1.2 D,F and 3.7.1 F), their levels gradually decrease in growing oocytes. Together, this suggests that the lack of *sel-10* activity stabilises CPB-3 and GLD-1 only partially, and that additional mechanism may exist to regulate CPB-3 and GLD-1 levels in the germ line. Neither RBP is detected in maturing oocytes and early embryos at the levels similar to those that CPB-3 and GLD-1 reach in the pachytene.

This additional level of regulation is likely to occur exclusively at the post-pachytene stages. LIN-23, another F-box-WD40 protein in *C. elegans* beside SEL-10, seems not to be a part of this mechanism (discussed in the previous paragraph). Nevertheless, the proposed additional mechanism is likely UPS-dependent, as a further increase of CPB-3 and GLD-1 levels in post-pachytene germ cells was observed upon proteasome inhibition in *sel-10(0)* mutant worms (Figures 3.2.6 and 3.11.2). This observation can be explained in at least two ways. First, an inhibition of the proteasome may regulate CPB-3 and GLD-1 indirectly, e.g. by promoting CPB-3 and GLD-1 protein synthesis. This could be accomplished if the proteasome inhibition stabilised translational activators of *cpb-3* and *gld-1* mRNAs. Alternatively, an inhibition of the proteasome in *sel-10(0)* germ cells may stabilise CPB-3 and GLD-1 proteins that are targeted to degradation by a hypothetical ubiquitin ligase that acts in addition to SEL-10. The latter hypothesis was addressed in this work by an RNAi-mediated depletion of several candidate ubiquitin ligases followed by an assessment of the RBPs stability. This approach failed to identify any additional stability regulators that would act around the pachytene-to-diplotene transition (data not shown) but revealed that *cul-2* activity contributes to the removal of GLD-1 from maturing oocytes and early embryos (Figure 3.11.2).

CUL-2 forms CRL2 (Cullin2-RING ligase) ubiquitin ligase complexes by recruiting ZIF-1 and ZYG-11 as substrate recognition subunits (SRSs) to degrade a variety of targets in an embryo (reviewed in Bowerman and Kurz, 2006; DeRenzo and Seydoux, 2004). The function of these complexes is essential for the embryonic development. At this moment it is unclear whether any of these SRSs interacts with GLD-1 and hence could indeed mediate GLD-1 ubiquitination. The probability that ZIF-1 regulates GLD-1 stability is rather low, as ZIF-1

recognises its known targets (POS-1, PIE-1, MEX-1,-5,-6) by a fragment of their zinc finger domain (DeRenzo et al., 2003) - a sequence that is absent from GLD-1. Furthermore, ZIF-1 is absent from oocytes and one-cell embryos, so it could not regulate GLD-1 stability at these developmental stages. The other SRS, ZYG-11, was shown to mediate degradation of cyclin B, CYB-3, during meiosis (Feng et al., 1999) and to regulate yet unidentified targets in polarity establishment (Liu et al., 2004; Sonnevile and Gönczy, 2004). Unfortunately, ZYG-11 degron has not been characterised, so it is difficult to predict the ability of ZYG-11 to bind GLD-1. Nevertheless, the meiotic function of ZYG-11 correlates well with the sudden decrease of GLD-1 observed in the maturing oocyte (Figure 3.7.2 C, 3.10.1 D and data not shown), making it a probable GLD-1 regulator. It remains to be discovered whether a CUL-2-based E3 ligase acts directly on GLD-1 and mediates its ubiquitination within a CLR2/ECS complex, or it acts indirectly, e.g. on hypothetical factors that stabilise GLD-1::GFP in the proximal gonad.

Altogether, despite the measurable stabilisation of CPB-3 and GLD-1 in *sel-10(0)* mutant germ lines, the importance of the downregulation of these proteins prior to embryogenesis cannot be inferred. The robust stabilisation of the two investigated RBPs in growing oocytes and early embryos has not been observed so far under any experimental conditions. Obtaining pachytene-like levels of CPB-3 and GLD-1 in early embryos is expected to reveal the importance of their removal prior to oocyte formation and early development of the worm. Currently, attempts are being made to achieve high oogenic and embryonic expression of CPB-3 and GLD-1 and to address this elusive question of the importance of stage-specific RBPs degradation.

4.2 Phosphorylation of RNA-binding proteins

4.2.1 Phosphorylation couples RBPs degradation to meiotic progression

Degradation of proteins during various biological processes is often synchronised with other molecular events by phosphorylation. This is the case for cell cycle regulators, such as cyclins and cyclin-dependent kinase inhibitors (CKIs), and signal transduction pathway components, such as Ras/LIN-45

(reviewed in Skaar et al., 2013; Zheng et al., 2016b). Many F-box proteins serve as ubiquitin ligase components in such regulatory pathways as they are sensitive to the phosphorylation status of their targets.

Regulation of CPB-3 and GLD-1 by SEL-10 most likely involves phosphorylation of these RBPs. An accumulation of modified forms of CPB-3 and GLD-1 is observed in *sel-10(0)* mutant worms but not observed in wild-type animals (Figures 3.3.5 and 3.8.1). Modified forms are indeed phosphorylated, as they are sensitive to phosphatase treatment (Figure 3.3.6). These observations suggest that phosphorylation of CPB-3 and GLD-1 occurs in germ cells but modified forms of RBPs are unstable and targeted to degradation by SEL-10. Furthermore, data suggest that phosphorylation and degradation may be stage-specific. Low amounts of modified CPB-3 and GLD-1 detected in *sel-10(0)* mutants extracts correlate well with only partial stabilisation of these two proteins visualised by immunofluorescent stainings of extruded *sel-10(0)* mutant gonads (Figures 3.2.3 and 3.7.1 F). This correlation suggests that the phosphorylation may be restricted to late pachytene and post-pachytene cells, and may not occur at earlier meiotic stages. A further support for the stage-specific regulation of the two investigated RBPs comes from analysing pachytene-arrested *daz-1(0)* mutant. Modified CPB-3 and GLD-1 do not accumulate in the germ lines of *daz-1(0)* animals (Figure 3.5.3 and data not shown), in which germ cells arrest at early- to mid-pachytene stage of meiosis (Karashima et al., 2000; Maruyama et al., 2005).

Hence, the phosphorylation of CPB-3 and GLD-1 might be restricted to mid to late pachytene and serve to couple the turnover of these proteins with meiotic progression. Altogether, collected data indicate that the abundance of RNA regulators during gametogenesis might be coupled by phosphorylation to meiotic progression.

4.2.2 MPK-1/MAPK regulates phosphorylation of CPB-3 and GLD-1

Mitogen-activated protein kinases are universal signal transduction molecules in eukaryotes. MAPKs regulate a variety of cellular processes, such as proliferation, differentiation, and cell cycle progression, in response to stress or external stimuli (reviewed in Cargnello and Roux, 2011; Plotnikov et al., 2011).

In the past few years, *C. elegans* MAP kinase MPK-1 emerged as a master regulator of cellular events during oogenesis, influencing at least seven biological processes, such as cellular organisation within the gonad, meiotic progression, apoptosis, differentiation and growth of oocytes, maturation, and ovulation (Arur et al., 2009). Despite being rather uniformly expressed throughout the gonad, MPK-1 displays a dynamic pattern of activity, with one peak in mid-to-late pachytene and another one in a few most proximal diakinetically oocytes (Lee et al., 2007b; Lee et al., 2007a). The first surge in MPK-1 activity promotes transition from mid to late pachytene, whereas the second is required for oocyte maturation (Lee et al., 2007b). Also the reduction of MPK-1 activity in diplotene cells plays an important role, allowing disassembly of synaptonemal complexes (Nadarajan et al., 2016) and diakinetically arrest of oocytes (Hajnal and Berset, 2002). The timing of MPK-1 activation in mid-pachytene correlates well with the decrease in CPB-3 and GLD-1 levels, making MPK-1 an attractive candidate for a regulator of CPB-3 and GLD-1 stability.

Four observations suggest that MPK-1 indeed regulates CPB-3 and GLD-1. First, depletion of MPK-1 prevents accumulation of phosphorylated CPB-3 and GLD-1 in *sel-10(0)* mutants (Figures 3.4.2 B,C and 3.9.1), arguing that MPK-1 activity regulates phosphorylation status of the two RBPs *in vivo*. Secondly, MPK-1 interacts with CPB-3 and GLD-1 in the yeast two-hybrid system (Figures 3.4.3 and 3.9.2), suggesting it may regulate these proteins directly. Thirdly, CPB-3 and GLD-1 amino acid sequences contain potential docking and phosphoacceptor sites for MAP kinases (Figures 3.3.7 D,F and 3.8.2 D,F). Last but not least, depletion of MPK-1 partially stabilises GLD-1 and CPB-3 in the germ line (Figure 3.4.2 A and data not shown). Altogether, MPK-1 emerges as a likely regulator of CPB-3 and GLD-1 stability.

Mammalian homologs of MPK-1, ERK-1/2, phosphorylate over 200 proteins in various subcellular localisations (Plotnikov et al., 2011). Among the targets identified to date are transcription factors, cell cycle regulators, signaling proteins (receptors and adaptors in signaling pathways), kinases and phosphatases, apoptotic regulators, cytoskeletal proteins, and various other proteins. The spectrum of *C. elegans* MPK-1 targets identified *in silico* is similarly broad (Arur et al., 2009). However, the set of validated *C. elegans* MAPK targets

was strongly enriched for RNA-regulating proteins (14 out of 37 candidate MPK-1 targets). This includes six RNA helicases (MTR-4, DDX-19, RHA-2, CGH-1, HEL-1, F56D2.6), five components of the translation machinery (MRPS-5, MRS-1, RPS-8, IRS-1, EIF-3.D), the RNA-binding protein ROP-1, the dsRNA-specific nuclease DCR-1, and RNase III DRSH-1. The high number of RNA regulators identified as MPK-1 targets is consistent with a predominantly post-transcriptional mode of gene expression regulation in the germ line.

CPB-3 and GLD-1 were not identified by Arur et al. (2009) as high-probability MPK-1 targets. By contrast, the analyses presented in this thesis argue that both proteins contain potential MAP kinase docking sites and potential phosphoacceptor sites (Figures 3.3.7 D,F and 3.8.2 D,F). The discrepancy between these results most likely stems from the stringent filtering conditions used by the authors (Arur et al., 2009). The authors imposed a requirement that a target protein contains a minimum of two docking sites, at least one of which is conserved between *C. elegans* and *H. sapiens*. Moreover, the consensus sequence used in this thesis, defined by Eukaryotic Linear Motif (ELM) database ([KR]{0,2}[KR].{0,2}[KR].{2,4}[ILVM].[ILVF]) is broader than consensus sequences used by Arur et al. (2009). Thus, three docking sites in CPB-3 and two in GLD-1 were identified in this work (Figures 3.3.7 F and 3.8.2 F), whereas only one docking site in each protein may be identified with several consensus sequences used by Arur et al. (2009). Furthermore, with an exception for the predicted docking site in GLD-1 (aa 313-322) that resides within the QUA2 domain, other predicted docking sites are not conserved between nematode and human protein sequences. Since regulatory pathways for CPB-3 and GLD-1, and their human orthologs, CPEB1 and QKI, might have diverged, the binding motifs for kinases and phosphoacceptor sites may also differ between species. It will be important to test if predicted docking sites identified in CPB-3 and GLD-1 are functional. If they are, it will be possible to test the biological importance of the interaction between MAPK and the two RBPs. According to the model presented in this thesis, MPK-1 phosphorylates CPB-3 and GLD-1 generating binding sites for SEL-10. If this is true, disruption of MPK-1 binding is expected to prevent it from phosphorylating CPB-3 and GLD-1, which would

impair creating phosphodegrons. As a result, RBPs would become "invisible" for SCF^{SEL-10} ubiquitin ligase and remain stable.

4.2.3 Functional implications of RBPs phosphorylation

An important step forward in our understanding of RBP-based regulatory networks is to comprehend the real impact of CPB-3 and GLD-1 regulation onto the oogenic gene expression program. In other words, it would be valuable to learn whether these two RBPs must be removed from growing oocytes, and what happens if they persist in an oocyte until fertilisation. The way towards this understanding is complicated by the possibility that the degradation of the investigated RBPs, which is likely coupled to their phosphorylation, might regulate RBPs activity irrespective of affecting protein stability. Regulation of RBPs activity (and not stability) by phosphorylation has been described before. CPEB1 phosphorylation on serine S174, originally proposed to be mediated by Aurora kinase (Andresson and Ruderman, 1998; Mendez et al., 2000; Roghi et al., 1998) switches CPEB from a translational repressor to an activator. Importantly, this phosphorylation event is not essential for protein turnover. Destabilisation of CPEB1 is triggered later by hyperphosphorylation, which is mediated by cyclin-dependent kinase, Cdc2, and Polo-like kinase, Plk1, (Setoyama et al., 2007). The phosphorylation-dependent control of the activity of a translational regulator has also been described in the *C. elegans* germ line. The translational repressor NOS-3, a homolog of *Drosophila* Nanos, is uniformly expressed in oogenic germ cells at all stages of their development. However, NOS-3 apparently functions as a translational repressor only in the distal region of the gonad to promote sexual fate determination and meiosis. By contrast, in the proximal region of the gonad, NOS-3 is inactive, due to its phosphorylation by MPK-1, which occurs at late pachytene. This inactivation is important for oocyte growth (Arur et al., 2011). Thus, MPK-1 activity provides a switch in an activity of at least one translational regulator in the *C. elegans* germ line. It is easy to imagine that MPK-1 mediates phosphorylation of CPB-3 and GLD-1 in late pachytene and that this phosphorylation may affect their RNA-regulatory activity.

An opposite mode of regulating RBP activity by phosphorylation involves affecting both activity and stability. A *C. elegans* zinc-finger protein, OMA-1, is regulated in this way. A phosphorylation of threonine T239 by the dual-specificity tyrosine-regulated kinase (DYRK), MBK-2, abolishes OMA-1 function as a translational repressor of *zif-1* mRNA and destabilises OMA-1 protein (Güven-Ozkan et al., 2008; Güven-Ozkan et al., 2010). It will be essential to identify which residues of CPB-3 and GLD-1 are phosphorylated *in vivo*, and whether these modifications affect only protein stability or have additional functions as well.

Characterisation of the influence of CPB-3 and GLD-1 phosphorylation on their activity will require additional experimental work. Although a number of RBPs was found phosphorylated, there are no general rules on how phosphorylation affects RBP function. Post-translational modifications of RBPs may exert their effect in two main ways: by changing the affinity of an RBP to its target RNA or by affecting interactions between a modified RBP and other RNP protein components.

The former mode of regulation was identified in various organisms and found to result in an increase or decrease in RBP binding to RNA, depending on the protein. For instance, phosphorylation of nuclear STAR proteins, SLM-1 and SLM-2/T-STAR, reduced their affinity to synthetic RNA *in vitro* (Haegebarth et al., 2004). Similarly, phosphorylation of Rnc1, a *Schizosaccharomyces pombe* RNA-binding protein that shares some homology with GLD-1, reduces its binding to its cognate mRNA target, Pmp1 (Sugiura et al., 2003). By contrast, phosphorylation of stem-loop binding proteins (SLBPs) increases their binding strength to the stem-loop structures of histone mRNAs up to 30-fold (Zhang et al., 2012). An impact of phosphorylation on the RBP affinity to RNA cannot be easily predicted; just like phosphorylation of a kinase may have either activating or inhibitory effect, depending on the modified protein and targeted residues.

The second mode of modulating RBPs activity is changing their affinity to other proteins serving as RNA regulators, and this mode is thought to be prevalent (Thapar, 2015). Two previously discussed proteins, worm OMA-1 and vertebrate CPEB1, can again serve as examples. Phosphorylation of OMA-1 by MBK-2/DYRK does not observably change OMA-1 association with its target, *zif-*

1 mRNA, but it decreases OMA-1 binding to the eIF4E-binding protein, SKN-2 (Guven-Ozkan et al., 2008; Guven-Ozkan et al., 2010). Thus, it was proposed that the dissociation of SKN-2 from an RNP, rather than the dissociation of OMA-1 from mRNA, relieves the translational repression of *zif-1*. Similarly, CPEB protein forms a complex with cytoplasmic poly(A) polymerase Gld2 and deadenylase PARN in vertebrate oocytes and neurons (reviewed in Ivshina et al., 2014; Weill et al., 2012). Phosphorylation of CPEB decreases its affinity to PARN, resulting in a dissociation of the deadenylase from the complex. At the same time, phosphorylation increases CPEB affinity to the polyadenylation-promoting cleavage and polyadenylation specificity factor (CPSF). Hence, phosphorylation induces changes in the composition of a CPEB-containing mRNP and switches its activity towards the polyadenylation-promoting.

Altogether, phosphorylation affects multiple aspects of RBPs, including modifying their activity and stability. The common theme is that phosphorylation results in remodeling of messenger ribonucleoprotein (mRNP) complexes. This remodeling in turn, influences mRNA stability or translatability and leads to changes in translational output, cell proteome and, thus, in cell physiology.

4.2.4 CPB-3 and GLD-1 orthologs are regulated by phosphorylation.

Distinct phosphorylations may regulate different aspects of CPB-3 and GLD-1 activity. Multiple modified forms of CPB-3 and GLD-1 observed in *sel-10* mutant extracts analysed by immunoblots (Figures 3.3.5 and 3.8.1), or in wild-type extracts resolved on Phos-Tag gels (Figure 3.3.4), suggest that CPB-3 and GLD-1 are phosphorylated at multiple sites. Potentially, RNA-binding, protein binding and stability of these RBPs could be regulated separately.

CPEB protein phosphorylations and their functions

CPB-3 phosphorylation has not been addressed in the literature to date, so its potential consequences could be only inferred from data available for its orthologs in flies or vertebrates. Although some trends in regulatory mechanisms are clearly visible, relatively poor conservation of phosphorylation

sites identified so far prevents from making predictions regarding CPB-3 regulation by kinases.

The fly ortholog, Orb, is heavily phosphorylated, and its hyperphosphorylation was attributed to casein kinase 2 (CK2) activity. Hyperphosphorylated Orb is found in complexes with the cytoplasmic poly(A) polymerase Wispy, whereas hypophosphorylated Orb is found in complexes with the translational repressor, Bruno (Wong et al., 2011). Thus, similarly as in *Xenopus* CPEB1, phosphorylation provides a switch between Orb activity as a translational repressor and translational activator (Kim and Richter, 2006; Wong et al., 2012). Unfortunately, the exact phosphosites that regulate Orb affinity to Bruno or Wispy have not been identified so far. Nonetheless, post-translational modifications of *Drosophila* Orb support the view that the phosphorylation status is an important regulator of CPEB activity.

Xenopus CPEB1 phosphorylation is relatively well characterised (Setoyama et al., 2007; Kim and Richter 2006). In contrast to CPB-3, which is downregulated at pachytene exit, *Xenopus* CPEB1 is degraded later, just about meiotic maturation. Thus, signaling pathways and ubiquitin ligases involved in degradation of CPEB in these two systems may differ.

Similarly to nematode CPB-3, mouse CPEB1 activity is required early in meiosis, as CPEB1 null oocytes do not develop beyond the pachytene stage (Tay and Richter, 2001). The early meiotic activity of mouse CPEB1 is required for the synthesis of synaptonemal complex proteins and is likely triggered by phosphorylation of threonine T171 by Aurora A kinase. Later on, CPEB1 is dephosphorylated in late pachytene, which renders it inactive until meiotic maturation (Tay et al., 2003). This example shows that CPEB phosphorylation may act as a reversible on-off switch and may not influence protein stability.

Altogether, CPEB activity and stability is regulated by phosphorylation in all studied organisms. Unfortunately, the low sequence conservation around identified phosphorylated residues in CPEB proteins hampers predicting functional phosphosites in CPB-3. Bioinformatic tools used in this work suggest multiple sites serving as potential phosphoacceptors (Figure 3.3.7 and data not shown) and a variety of potential kinases involved in CPB-3 modification. Revealing regulatory mechanisms of CPB-3 will require systematic mutagenesis

of potential phosphosites. In addition, to unravel potential functions of CPB-3 phosphorylation, CPB-3 interactions with its mRNA targets and other RNA regulatory proteins must be characterised in detail.

STAR proteins phosphorylation and their functions

STAR protein family members are also regulated by phosphorylation. The two common features of STAR proteins are the presence of the STAR domain, and the presence of post-translationally modified motifs that mediate different protein-protein interactions. To date, GLD-1 stands out as an exception in regard to the latter feature, as in contrast to other STAR proteins it lacks the hallmarks of motifs involved in signaling (Sette, 2010; Vernet and Artzt, 1997). Nonetheless, a large number of phosphorylatable residues and detected phosphorylated forms of GLD-1 (Jeong et al., 2011; this thesis, figure 3.8.2) indicate a large capacity for GLD-1 regulation by post-translational modifications.

Two mammalian STAR proteins, Sam68 and T-STAR/SLM-2, have well-established roles in gametogenesis and could potentially hint at the regulation of GLD-1. T-STAR/SLM-2 expression is largely restricted to mouse testes, whereas Sam68 is expressed in many tissues and therefore its regulation is better characterised, even if not all the aspects of the regulation may be relevant for Sam68 role in gametogenesis (reviewed in Frisone et al., 2015). Post-translational modifications of Sam68 involve phosphorylation of tyrosines, serines, and threonines, as well as methylation of arginines, and acetylation and SUMOylation of lysines (reviewed in Sette, 2010).

A number of tyrosine kinases phosphorylate Sam68, including several Src-family kinases (SFKs) or Breast Tumor Kinase, BRK (Derry et al., 2000; Andreotti et al., 1997; Guinamard et al., 1977). SFK- and BRK-mediated phosphorylation decreases the affinity of Sam68 for RNA, and consequently affects splicing (Frisone et al., 2015). Consistently with a wide range of tyrosine kinases regulating Sam68, its C-terminal domain contains multiple tyrosine residues that are conserved also in closely related T-STAR/SLM-2 and SLM-1 (Ehrmann and Elliott, 2010). However, this domain is not conserved in GLD-1 (Ryder and Massi, 2010). Out of ten tyrosine residues present in GLD-1, three

tyrosines were predicted by NetPhos, and none by ELM, to serve as phosphoacceptors (data not shown). Mass-spectrometry-based analysis of GLD-1 phosphorylation also failed to detect tyrosine modifications. Thus, this thesis fails to reveal tyrosine-based regulation of GLD-1, although the analyses were not thorough enough to exclude such a possibility.

Sam68 is also regulated by phosphorylation of serine and threonine residues and, interestingly, these phosphorylations are linked to the cell cycle (Resnick et al., 1997). Threonine phosphorylation was detected only in mitotic cells, while serine phosphorylation was detected in mitotic and interphase cells. Threonine phosphorylation is mediated by Cdc2/CDK1 (Resnick et al., 1997), whereas serine phosphorylation was suggested to be mediated by extracellular signal-regulated kinases 1 and 2 (ERK1/2), members of MAPK protein family (Sette, 2010; Matter et al., 2002). ERK1/2-mediated phosphorylation was found to regulate splicing (Matter et al., 2002). Furthermore, Cdc2/CDK1 and ERK-1/2 were found to phosphorylate Sam68 during male meiosis (Paronetto et al., 2006). ERK1/2 activity correlated with cytoplasmic localisation of Sam68, promoted Sam68 association with polyribosomes and seemed to positively influence transcript and protein levels of several spermatogenesis regulators (Spag16, Nedd1, and Spdya). Together, published data indicate that serine/threonine phosphorylations mediated by cyclin-dependent kinase and ERK1/2 activity regulate mammalian Sam68 functions but do not address Sam68 stability.

ERK kinase regulates also *Drosophila* STAR protein Held-Out Wings (HOW) in embryonic muscles and heart cardioblasts (Nir et al., 2012). Phosphorylation facilitates HOW dimerisation and potentiates its ability to bind RNA. Muscle-specific knock-down of the *Drosophila* ERK, *rolled*, increased levels of titin protein, Sallimus (SLS), whose mRNA is translationally repressed by HOW. In this aspect, the lack of ERK phenocopied a loss of HOW function, underscoring the importance of the phosphorylation for HOW activity. The two identified phosphorylation sites, threonines T59 and T64, are located N-terminally from the STAR domain and are poorly conserved outside *Drosophila* genus. By contrast, the docking sites for MAPK kinases reside within the STAR domain and are much better conserved: out of four identified docking sites, two

are conserved in *C. elegans*, and two others in mammalian quaking (QKI) and Sam68.

Lack of the amino acid sequence conservation around phosphorylated sites identified in HOW precludes predicting phosphoacceptor sites in GLD-1. However, regulation of *Drosophila* HOW and mouse Sam68 by MAP kinases and the evolutionary conservation of MAPK docking sites suggest that *C. elegans* GLD-1 may also be regulated by MAPK. This work identified MPK-1/ERK as a protein interacting with GLD-1 (Figure 3.9.2) and influencing its phosphorylation status (Figure 3.9.1). Thus, regulation by MAP kinases seems to be a shared feature of STAR proteins.

Whether MAPK-mediated regulation of STAR proteins is evolutionarily conserved or evolved independently in different organisms is difficult to tell. The conservation of MAPK docking sites within STAR domains suggests that an interaction between STAR proteins and MAP kinases might have appeared early in evolution and remained functional due to the STAR domain sequence conservation. However, this hypothesis is somewhat difficult to reconcile with different effects of MAPK-mediated phosphorylation on different STAR proteins. ERK1/2 activity promotes translation of Sam68 mRNA targets in mouse but increases translational repression of HOW mRNA targets in *Drosophila* (Paronetto et al., 2006; Nir et al., 2012). Moreover, phosphorylation slightly decreases Sam68 but increases HOW affinity to RNA (Paronetto et al., 2006; Nir et al., 2012). Different effect of phosphorylation on RNA regulation might suggest that regulation of STAR proteins by phosphorylation evolved independently in different contexts. The presence of docking site-like motifs in the STAR domain and low selectivity of MAP kinases toward phosphorylation site could facilitate the recurring emergence of MAPK-mediated regulation of STARs.

Similarly to Sam68, GLD-1 is regulated by a cyclin-dependent kinase. CDK-2/Cdk2-cyclin E complex phosphorylates GLD-1 in germ cells in the mitotic region of *C. elegans* gonad. This phosphorylation negatively regulates GLD-1 protein levels, presumably acting as a signal for the proteasome-mediated degradation (Jeong et al., 2011). Three residues were suggested as potential phosphoacceptor sites: serines S22 and S39 located N-terminally-, and threonine T348, located C-terminally from the STAR domain. Alanine substitutions of these

residues decreased the phosphorylation status of GLD-1 and increased GLD-1 protein levels in the mitotic region of the germ line, supporting the view that these sites regulate GLD-1 stability (Jeong et al., 2011). In this thesis, the two serines, S22 and S39, were found phosphorylated in the mass spectrometry-based analysis of recombinant GLD-1 (Figure 3.8.2), suggesting that they might have been recognised by CDK-2 homolog in insect cells. For the moment it remains unknown, whether GLD-1 is phosphorylated by CDKs also during meiosis. Importantly, CDKs and MAPKs are promiscuous kinases regarding the phosphoacceptor site in target proteins as the minimal consensus for both families consists of phosphorylatable residue followed by proline (S/T-P). Thus, hypothetically, S22 and S39 could serve as destabilising residues in mitotic and meiotic cells, being phosphorylated by CDK-2 and MPK-1, respectively.

Altogether, this thesis contributes data that reveal that CPB-3 and GLD-1 are phosphorylated by MAP kinase. Whereas regulation by MAPK was reported for members of CPEB and STAR protein families, its influence on the stability of modified proteins has not been directly addressed. Noteworthy, it is still unclear, whether CPB-3 and GLD-1 modification by MPK-1 is necessary or sufficient to trigger their degradation. Further studies will be required to address this issue and the potential effect of phosphorylation onto translation of RBPs mRNA targets.

4.3 Consequences of the prolonged expression of CPB-3 and GLD-1 on oogenesis

An interesting question that is posed by restricted expression patterns of CPB-3 and GLD-1 is whether there is an absolute need to remove these two RBPs from growing oocytes and early embryos? In other words: would the expression of CPB-3 and GLD-1 be detrimental for oogenesis and/or embryogenesis as it could interfere with the post-transcriptional regulation of gene expression program at these developmental stages?

In an attempt to address this question, the expression of GLD-1 mRNA targets, *rme-2*, *oma-1* and *oma-2* (Lee and Schedl, 2001; Lee and Schedl, 2004), was investigated in *sel-10(0)* mutant worms, which contain noticeable GLD-1 levels in the oocytes (Figure 3.10.1 D). Despite a trend for a delayed accumulation of RME-2, OMA-1, and OMA-2 in *sel-10(0)* mutants in comparison

to wild-type gonads, the difference in accumulation dynamics was small, and in case of RME-2 not statistically significant (Figures 3.10.1 and 3.10.2).

The lack of statistical significance of the difference between anti-RME-2 intensities in the wild-type and mutant background may be due to a suboptimal approach for data analysis, which ignored subcellular distribution of the signal. RME-2 is synthesised from late pachytene/early diplotene onwards and initially the immunofluorescent signal is uniformly distributed in germ cells cytoplasm. However, as oocytes grow, the redistribution of RME-2 to cell membranes occurs and is manifested by a strong increase in membranous immunofluorescence intensity, whereas the cytoplasmic signal remains rather constant (Figure 3.10.2). In the presented analysis, the signal intensity was averaged along the measurement line. A better-suited analysis, separating cytoplasmic and membranous signal of RME-2, might bring in more insight into the regulation of RME-2 accumulation.

The small but statistically significant difference in OMA proteins accumulation in wild-type and *sel-10(0)* mutant germ lines (Figure 3.10.1 G) suggests that prolonged expression of GLD-1 may indeed interfere with the translation of its mRNAs targets. The modest effect observed is in fact an interesting aspect, as it poses a question of how GLD-1 presence in the oocytes affects translational activation of its targets.

In one scenario, the ratio between GLD-1 molecules and the GLD-1 binding motifs (GBMs) in its target mRNAs would be a key determinant of the strength of translational repression. An analogous mechanism was proposed to govern CPEB-mediated regulation (Mendez et al., 2002). CPEB degradation at meiotic maturation diminishes the pool of CPEB molecules that can interact with CPE-containing mRNAs. As a result, some mRNAs are no longer bound by CPEB, and other RBPs start playing a predominant role in their regulation. If GLD-1 operates in a similar manner, then it is the number of GLD-1 molecules that has to match the number of GBM-containing mRNAs to provide efficient translational repression. This simple mechanism might be in place. The levels of GLD-1 in the oocytes of *sel-10(0)* mutants are low in comparison the levels in the pachytene cells (Figure 3.10.1 C,D). A fluorescence intensity-based approximation suggests around three-fold difference (data not shown). Thus, there may be not enough

GLD-1 molecules in *sel-10(0)* mutant oocytes to occupy all GBMs, and, as a consequence, some of GLD-1-regulated mRNAs are translationally activated and their protein products accumulate; with only slightly reduced kinetics than in the wild-type worms.

In an alternative scenario, (hyper)phosphorylation would have an effect on mRNA binding or translational repressor activity of GLD-1. Collected data suggest that MPK-1 mediates GLD-1 phosphorylation in late pachytene (Figure 3.9.1). Since the presence of GLD-1 in *sel-10(0)* mutant oocytes (Figure 3.10.1 D) is accompanied by an accumulation of phosphorylated GLD-1 in *sel-10(0)* worm extracts (Figure 3.8.1), it is possible that the oocytes contain predominantly phosphorylated GLD-1. If phospho-GLD-1 was unable to repress translation, the protein products of its mRNA targets would accumulate in the oocytes. The difference in the dynamics of OMA or RME-2 accumulation between *sel-10(0)* mutant and wild-type germ lines is rather small (Figures 3.10.1 G and 3.10.2), suggesting that GLD-1 in *sel-10(0)* oocytes is not acting efficiently as a translational repressor. The fact that differences in OMA or RME-2 accumulation were detected, small as they are, could be explained by a pool of fully active GLD-1 molecules present in the oocytes. This active, likely non-phosphorylated, GLD-1 could exist due to the inefficient phosphorylation of GLD-1 in late pachytene or result from the dephosphorylation in the oocytes.

To reveal which scenario is closer to the actual mechanism, several experiments can be done. First, the expression of GLD-1 in the oocytes at the levels comparable to those observed in the pachytene could tell how important is the total amount of GLD-1 in the cells (or the ratio between GLD-1 and its mRNA targets). Such ectopic expression may be achieved by increasing translation of *gld-1* mRNA in the oocytes, e.g. by fusing GLD-1 open reading frame to a 3' UTR of an oocyte-enriched protein (e.g. PUF-6). The caveat of this approach is that levels of ectopically expressed GLD-1 may be still low due to the proteasome-mediated degradation. However, if ectopic GLD-1 expression will be sufficient to increase oocyte GLD-1 levels above the levels observed in *sel-10(0)* mutant, and simultaneously a stronger delay in OMA protein accumulation will be observed, the 'GLD-1 to GBM ratio' hypothesis will be supported. To directly address the role of phosphorylation, mutagenesis approach could be used to modify kinase-

binding sites or phosphoacceptor sites. Introduced mutations could affect GLD-1 activity, stability or both, potentially providing interesting insight into how GLD-1 is regulated and how it affects gene expression in the oocytes.

4.4 CPB-3 and GLD-1 may regulate translation of their own degradation machinery

Sequence analyses of *mpk-1* and *sel-10* mRNA revealed the presence of several cytoplasmic polyadenylation elements (CPEs) and GLD-1-binding motifs (GBMs) in their 3' UTRs (Figures 3.6.2 and 3.6.4). Additionally, very preliminary data from the analysis of 3' UTR translational reporters suggests that CPB-3 might be involved in regulating *mpk-1* and *sel-10* translation. The two translational reporters have very different expression patterns (compare yellow lines in figures 3.6.3 and 3.6.5), which complicate the analysis of how their translation can be regulated by the same protein. Hence, they will be discussed separately.

Regulation of *sel-10* translation by CPB-3

sel-10 3' UTR reporter is very weakly expressed in distal germline tissue until the late pachytene region, where its expression suddenly surges (Figures 3.6.1 B and 3.6.3). The rapid increase in the reporter protein intensity apparently coincides with a sharp decrease in CPB-3 levels. Interestingly, the rapid increase in the reporter signal is not observed in *cpb-3(0)* mutant gonads or upon *cpb-3* RNAi. Together with the presence of CPEs in *sel-10* mRNA, this observation suggests that CPB-3 may regulate *sel-10* translation. This would imply a spatio-temporal co-existence of counteracting components: CPB-3 protein promoting *sel-10* mRNA translation and SEL-10 protein promoting CPB-3 degradation. Such regulatory loop is possible if one takes into consideration the time frame that germ cells in late pachytene have, i.e. that it takes around one hour to progress from one nuclear row to the next one (Morgan et al., 2010). Thus, mid-to-late pachytene cells could keep accumulating SEL-10 for a few hours. High levels of SEL-10 protein would eventually lead to complete removal of its translational activator. This model would hold true if SEL-10 was synthesised more efficiently than CPB-3.

An alternative explanation for the observed dependency of *sel-10* translational reporter on *cpb-3* activity involves indirect regulation of *sel-10* translation by CPB-3. For instance, translation of *sel-10* might require activity of yet-unidentified translational activator or might depend on removal of a yet-unidentified translational repressor. The levels of these hypothetical regulators could be changed in *cpb-3*-deficient germ lines, affecting synthesis of SEL-10 protein. This explanation does not exclude the possibility that CPB-3 directly binds *sel-10* mRNA. Hypothetical regulatory factor(s) could be recruited to *sel-10* mRNA by CPB-3.

Another possibility is that the observed reduction in *sel-10* 3' UTR reporter levels in late pachytene results from meiotic defects occurring in *cpb-3*-depleted animals. *cpb-3(0)* mutants show reduced fertility and reduced egg production (Hasegawa et al., 2006). It is possible that cells present just before bend region in *cpb-3*-depleted animals are in reality not as advanced in meiosis as cells at the same gonadal location in controls. Molecular markers that characterise more precisely meiotic stage of the cells in question could be used to clarify this issue.

Regulation of *mpk-1* translation by CPB-3

Similarly to what was observed for the *sel-10* reporter, *cpb-3* deficiency leads to the lower intensity of the *mpk-1* translational reporter (Figure 3.6.5). *cpb-3* depletion affected *mpk-1* reporter levels early in pachytene, whereas the effect on *sel-10* is observed in late pachytene. This different timing of translational onset of potential CPB-3 targets is reminiscent of waves of CPEB-dependent translational activation in *Xenopus* oocytes (Igea and Mendez, 2010). These waves were attributed to different positioning of potential CPEs in relation to the polyadenylation signal (PAS). Such positional code was proposed to determine the timing of translational activation of CPEB targets, cyclin mRNAs (Piqué et al., 2008). The conservation of this mechanism is certainly an exciting issue to investigate. Nonetheless, the direct interaction between CPB-3 and suggested mRNA targets, *sel-10* and *mpk-1*, has to be confirmed first.

Regulation of *sel-10* and *mpk-1* translation by GLD-1

The possibility of GLD-1-mediated translational regulation of *mpk-1* and *sel-10* mRNAs has not been experimentally addressed so far. *mpk-1* and *sel-10* mRNAs were poorly enriched in the genome-wide studies of GLD-1 targets (Jungkamp et al., 2011; Wright et al., 2010). However, both mRNAs contain predicted GLD-1 binding motifs (GBMs, (Wright et al., 2010); Figures 3.6.2 and 3.6.4), raising the possibility that GLD-1 binds directly to these mRNAs. MPK-1 protein and *mpk-1* translational reporter are rather uniformly expressed in the germ line (Lee et al., 2007b; Lee et al., 2007a; Figure 3.6.5 and data not shown); thus, GLD-1 mediated repression of *mpk-1* mRNA would be expected to be weak.

Interestingly, Rnc1, a *Schizosaccharomyces pombe* RNA-binding protein that shares some homology with GLD-1, was identified as a regulator of MAPK signaling. Rnc1 acts as an indirect repressor of yeast MAP kinase, Pmk1, by stabilising the transcript of MAPK phosphatase, Pmp1, which inactivates Pmk1/MAPK (Sugiura et al., 2003). Thus, Rnc1 negatively regulates MAPK signaling and an analogous function could be fulfilled by GLD-1-mediated translational repression of *mpk-1*. Interestingly, the RNA-binding activity of Rnc1 protein is regulated by MAPK-mediated phosphorylation. Phosphorylated Rnc1 strongly binds mRNA, which increases stability of Pmp1 transcript and increases Pmp1 protein levels. High Pmp1 levels inactivate Pmk1/MAPK. Thus, MAPK signaling pathway contains an intrinsic off-switch, mediated by RNA-binding proteins (Sugiura et al., 2003; reviewed in Sugiura et al., 2011).

Data presented in this thesis suggest that phosphorylation of GLD-1 (and the following degradation) serve to inhibit GLD-1 activity, which would promote *mpk-1* translation, creating a positive, rather than a negative feedback loop. Furthermore, MPK-1 activating kinase, *lin-45*, is likely to be translationally regulated by GLD-1, as its mRNA associates with GLD-1 (Lee and Schedl, 2004; Scheckel et al., 2012; Wright et al., 2010). Importantly, GLD-1-mediated *lin-45* repression was reported to contribute to meiotic prophase progression and prevention of return to mitotic proliferation (Lee and Schedl, 2010). Thus, GLD-1 might translationally repress at least two components of MAPK pathway (*lin-45* and *mpk-1*). If phosphorylation of GLD-1 were inactivating GLD-1 repressive activity, then GLD-1 phosphorylation would be followed by a translational activation of both mRNAs, and an accumulation of LIN-45 and MPK-1 proteins.

This reasoning is consistent with an observed MPK-1 expression pattern, which is characterised by lower levels in the distal gonad and higher levels in the proximal gonad (Lee et al., 2007b; Lee et al., 2007a). The expression pattern of LIN-45 in the germ line has not been characterised yet, so the hypothesis remains to be tested. A *lin-45* 3' UTR translational reporter could give an insight into this issue. If *mpk-1* and *lin-45* are translationally regulated by GLD-1 and their protein products control GLD-1 activity, then a cross-talk between MAPK signaling and GLD-1/KH-domain protein exists in *C. elegans*, as it does in fission yeast.

GLD-1 could also control synthesis of its stability regulator, SEL-10. The *sel-10* translational reporter has a complex expression pattern, characterised by the low levels in the distal gonad, a peak of expression shortly before the bend and mid-to-high levels in the proximal gonad (Figure 3.6.1 B). Low reporter levels observed in the distal gonadal end and in the pachytene region could result from GLD-1-mediated repression of *sel-10* mRNA. Consistently with this hypothesis, the 3' UTR of *sel-10* contains a medium-strength GBM and *sel-10* mRNA was detected among RNAs co-immunoprecipitated with GLD-1 protein (Wright et al., 2010). Whether the predicted GBM is indeed recognised by GLD-1 and whether it contributes to generating SEL-10 expression pattern remains to be tested.

In summary, this thesis presents data that show that the expression of the two evolutionarily conserved RNA-binding proteins is restricted by the combined activity of a MAP kinase and the proteasome. This work identifies also a conserved tumor suppressor SEL-10/Fbxw7 as a ubiquitin ligase that destabilises the two investigated RBPs (Figure 4.2). Proposed mechanism suggests that the gene expression during oogenesis is controlled by restricted abundance of RNA regulators. Degradation of two RBPs, CPB-3 and GLD-1, at the transition from the pachytene to diplotene stage may serve to switch off genes required at early meiotic stages, and switch on genes required for the oocyte formation and embryogenesis.

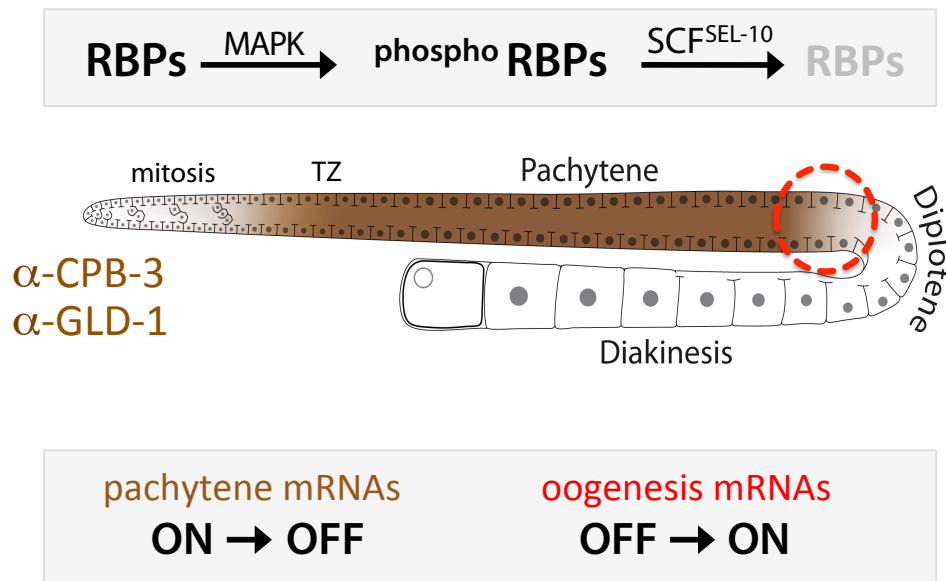


Figure 4.2. Proposed mechanism and function of the regulated RBP turnover.

Degradation of CPB-3 and GLD-1 is likely mediated by their phosphorylation by a MAP kinase, MPK-1, and subsequent ubiquitination by an SCF ubiquitin ligase complex that utilises an F-box protein SEL-10/Fbxw7 as its substrate recognition subunit. Degradation of the two RBPs may act to synchronise cell cycle progression (i.e. meiosis) with an oogenic differentiation program by switching the translational activity of target mRNAs.

5. Materials and Methods

5.1 Media and solutions

LB medium: 10 g/l tryptone, 5 g/l yeast extract, 10 g/l NaCl, adjusted to pH 7.2 and autoclaved.

SOC medium: 20 g/l bacto-tryptone, 5 g/l yeast extract, 20 mM glucose, 0.5 g/l NaCl, 2.5 ml/l KCl (1 M), adjusted to pH 7 and autoclaved. Before use, 5 ml/l MgCl_2 (2 M) and 5 ml/l Mg_2SO_4 (2 M) were added.

YPD: 20 g/l bacto-peptone, 5 g/l yeast extract, 20 g/l glucose, 0.05 g/l adenine

Yeast drop-out media: (Qbiogene) were supplemented with adenine 0.1 g/l; SD-Trp was used for CPB-3::LexA expression, SD-Trp-Leu double drop-out was used for yeast-two-hybrid assay

PBS: 137 mM NaCl, 2.7 mM KCl, 10 mM Na_2HPO_4 , 2 mM KH_2PO_4

PBST: PBS + 0.05% Tween-20

PBSBT: PBS + 0.5% BSA + 0.02% Tween-20

M9: 7 g/l $\text{Na}_2\text{HPO}_4 \cdot 7\text{H}_2\text{O}$, 3 g/l KH_2PO_4 , 0.5 g/l NaCl and 1 g/l NH_4Cl . The solution was sterilised by autoclaving.

TBE: 17.8 mM Tris (10.8 g/l), 17.8 mM boric acid (5.5 g/l), 0.4 mM EDTA (0.586 g/l)

10x DNA loading dye: 0.25 % bromophenol blue, 0.25 % xylene cyanol, 50% glycerol

SDS-PAGE buffer: 3.02 g/l Tris base, 14.2 g/l glycine, 1 g/l SDS

Blotting buffer: 3.082 g/l Tris base and 14.412 g/l glycine

2x SDS sample buffer: 100 mM Tris-HCl pH 6.8, 20% glycerol, 4% SDS, 0.04% bromophenol blue, 5% β -mercaptoethanol.

High-Urea (HU)-sample buffer: 200 mM Tris-HCl [pH 6.5], 8 M urea, 5% SDS, 0.02% bromophenol blue, and 5% β -mercaptoethanol

Stripping solution: 0.5% SDS, 2% acetic acid

Buffer A+ (after Lai et al, 2011): 50 mM Tris-HCl [pH 8.9], 1 mM MnCl_2 , EDTA-free cOmplete protease inhibitor cocktail, 100 mM NaCl

Buffer B70: 50 mM HEPES-KOH pH 7.4, 70 mM KAc, 1mM NaF, 20mM β -glycerolphosphate, 5mM magnesium acetate ($\text{Mg}(\text{CH}_3\text{COO})_2$), 0.1% Triton X-100 and 10% glycerol. All components were dissolved in water and autoclaved. Subsequently, sterile filtered 1 M HEPES-KOH was added. Given phosphatase inhibitors concentrations are the minimal that were used.

Buffer SF: 50 mM HEPES pH 7.4 (KOH), 100 mM KCl, 8.7% glycerol, 0.1% Tween-20 and 2 mM EDTA. The buffer was prepared as 2x, sterile filtered and stored at room temperature. Just before use, protease inhibitors listed in 2.1 and phosphatase inhibitors were added.

Urea Binding Buffer: 8 M urea, 300 mM NaCl, 50 mM NaH_2PO_4 , 20 mM imidazole, pH 7.5 (NaOH)

Washing buffer: 50 mM HEPES pH 7.3, 100 mM NaCl, 0.01% SDS, 0.1 mM EGTA, 20 mM imidazole, 1 $\mu\text{l}/\text{ml}$ leupeptin, 1 $\mu\text{l}/\text{ml}$ pepstatin, 100 $\mu\text{g}/\text{ml}$ Pefabloc, 2 mM benzamidine, 1 mM PMSF

Coomassie Brilliant Blue: 1 g Coomassie Brilliant Blue R: 250 ml methanol, 50 ml acetic acid, 200 ml water

Destaining solution: 45 ml methanol, 2 ml acetic acid, 45 ml water

5.2 Inhibitors and blocking reagents.

5.2.1 Protease inhibitors

Leupeptin (Serva: 51867.02): 1 mg/ml stock in ddH₂O, final concentration 1 µg/ml. Pepstatin A (Serva: 52682.02): 1 mg/ml stock in ethanol, final concentration 1 µg/ml.

Pefabloc (Serva: 31682.01): 100 mg/ml stock in ddH₂O, final concentration 0.1 mg/ml.

Benzamidine (Serva: Benzamidine.HCl Hydrate, 14525.01) MW = 156.6 g/mol: 1 M stock in ddH₂O, final concentration 2mM.

PMSF (Roche: 1 359 061) MW 174.2 g/mol: 100 mM stock in ethanol, final concentration 1 mM.

cOmplete Protease Inhibitors Cocktail: one tablet dissolved in 2 ml ddH₂O to reach a 25x stock. (with EDTA: Roche, 11697498001; EDTA-free: Roche, 11 873 580 001), final concentration 1x.

E64 (BIOMOL, PI105) MW 357.5 g/mol: 1 mM stock solution in ddH₂O, final concentration 1 µM.

5.2.2 Phosphatase Inhibitors

Sodium fluoride (NaF, Sigma, S 7920): 0.5 M stock in ddH₂O, final concentration 1-100 mM.

Sodium orthovanadate (Sigma: Na₃VO₄, S6508): A 200 mM solution was activated (depolymerised) according to Gordon, 1991, and stored at -20°C; final concentration 10-50 mM.

β-glycerolphosphate (Glycerol 2-phosphate hydrate disodium salt: Sigma, G6251): 0.5 M stock in ddH₂O, final concentration 16-100 mM.

Stacking gel mix: 213.5 ml ddH₂O, 25 ml 40% Acrylamide/Bis (37.5:1), 31.5 ml 1M Tris pH 6.8 and 2.5 ml 10% SDS; stored at 4°C.

5.3 Other chemicals and reagents

anti-FLAG M2 Affinity Gel (Sigma)

Bovine serum albumin, fraction V (Roth)

CloneJET PCR Cloning Kit (ThermoFisher Scientific)

DAPI (4',6-diamidino-2-phenylindole) (Serva)

ECL solution (GE Healthcare)

HRP-juice (PJK GmbH)

Levamisole (50 mM stock solution)

Phos-Tag™ Acrylamide AAL-107 (Nard Institute/Wako Pure Chemicals)

Protino Ni-IDA resin (MACHERY-NAGEL)

Sodium dodecyl sulphate (SDS), natrium salt (Serva)

TritonX-100 (Serva)

Tween-20 (Serva)

Vectashield mounting solution (Vector Laboratories)

5.4 Cells

Escherichia coli OP50: uracil auxotroph, standard feeding bacteria for nematode propagation

E. coli HTT115 (RNAi feeding): F⁻, mcrA, mcrB, IN (rrnD-rrnE)¹, λ⁻, rnc14::Tn10 (DE3 lysogen: lacUV5 promoter -T7 polymerase) (IPTG-inducible T7 polymerase) (RNase III minus). The Tn10 transposon interrupting the rnc14 gene carries a tetracycline resistance gene.

DH5α (cloning): F⁻ *endA1 glnV44 thi-1 recA1 relA1 gyrA96 deoR nupG purB20* ϕ80dlacZΔM15 Δ(*lacZYA-argF*)U169, hsdR17(*r_K⁻m_K⁺*), λ⁻

XL1 Blue (cloning): *endA1 gyrA96(nal^R) thi-1 recA1 relA1 lac glnV44 F'[::Tn10 proAB⁺ lacI^q Δ(lacZ)M15] hsdR17(r_K⁻ m_K⁺)*

Saccharomyces cerevisiae strain L40: *MATa his3Δ200 trp1-901 leu2-3112 ade2 LYS::(4lexAop-HIS3) URA3::(8lexAop-LacZ)GAL4*

Spodoptera frugiperda cells "expressSF+" (Protein Sciences)

5.5 Primers

general	gene	CE number	sequence (5' - 3')	FOR/rev	inner/outer
Genotyping primers					
	MosSCI	3376	CCAGCTTTCTTGTACAAAGTGG	FORWARD	outer
	MosSCI	4314	ataattcactggccgtctgtttaca	FORWARD	inner
	MosSCI	2640	cgtgttctccattcttcac	reverse	outer
	MosSCI	2634	ATCGGGAGGCGAACCTAACTG	reverse	inner
	<i>sel-10</i>	2225	CAGTGACCATCGAACACCTG	FORWARD	outer
	<i>sel-10</i>	2226	ATCAAGTGAACAAACGTGCG	FORWARD	inner
	<i>sel-10</i>	3412	ATGGAACCAAGCCATAGC	reverse	outer
	<i>sel-10</i>	3387	AGATCCAGTCACCAAGAC	reverse	inner
	<i>sel-10</i>	3386	TGGATTCTCTGAAGCAGAC	reverse	inner
Gateway constructs					
	<i>sel-10 3'UTR</i>	4877	ggggacagctttctgtacaagaaggGATGCTGTATACCCTTAACG	FORWARD	na
	<i>sel-10 3'UTR</i>	5243	ggggacaactttgtataataaagttGCAAGTTGCCAGTCAGTTGTG	reverse	na
	<i>mpk-1 3'UTR</i>	3656	GGGGACAGCTTTCTTGTACAAAGTGGGGAATAATGGAGGGCAGAAATCCTG	FORWARD	na
	<i>mpk-1 3'UTR</i>	3657	GGGACAACTTTGTATAATAAAGTTGgtcactgaaattgagccctcc	reverse	na
	<i>gld-1::LAP</i>	4647	gaagtgcataccaatcaggaccATGCCGTCGTGCACCACTC	FORWARD	na
	<i>gld-1::LAP</i>	4648	ggtcctgattggtatgcacttcGAAAGAGGTGTTGTTGACTGAAGAAGC	reverse	na
	LAP	4300	GAAGTGCATACCAATCAGGACC	FORWARD	na
	LAP-att	4461	ggggaccactttgtacaagaagggtTCACTTGTCTGTCATCCTTGTAG	reverse	na
Baculovirus					
	<i>cpb-3</i>	976	CAGGATCCATGAACCTGAATGACCGAGTG	FORWARD	na
	<i>cpb-3</i>	3811	ttttctgcacTGGCCGTAATTGGGAGAG	reverse	na
	<i>sel-10</i>	3801	ttttggatccATGTGGCCACGAAATGATGTACAC	FORWARD	na
	<i>sel-10</i>	3802	ttttctcgagGGGTATACAGCATCAAAGTCGAG	reverse	na
	<i>sel-10 WD</i>	3803	ttttggatcctTGGGGTCGACAGTGCTAC	FORWARD	na
	<i>sel-10 Nt</i>	3804	ttttctcgagAATTGGATTGCGATTCCAGTTCTTTTC	reverse	na
	<i>mec-15</i>	3807	tttttagatctATGACAAATGCTCAACCAACGG	FORWARD	na
	<i>mec-15</i>	3808	ttttctcgagTTTTCTTGATCCGGAGCCGATG	reverse	na
	<i>skr-1</i>	3812	ttttggatccATGGCTGATCAAAAGAAAGTATCC	FORWARD	na
	<i>skr-1</i>	3813	ttttctcgagTCCTCGCACCAGGCATTTC	reverse	na
	<i>gld-1</i>	3104	ttttggatccATGCCGTCGTGCACCACTCCAA	FORWARD	na
	<i>gld-1</i>	3105	ttttctcgAGAAAGAGGTGTTGTTGACTGAAG	reverse	na
RNAi clones					
	<i>pas-5</i>	3660	ATGTTCTCACTCGCAGC	FORWARD	na
	<i>pas-5</i>	3661	GATGTGATAAATGTATCGAGCTC	reverse	na
	<i>pbs-3</i>	3662	CGATTATGAGCTACACTGGTGG	FORWARD	na
	<i>pbs-3</i>	3663	CGAGCCTTGATAGTTGAGACG	reverse	na
	<i>pbs-5</i>	3664	ATGTGGGGCGAGACATTCTG	FORWARD	na
	<i>pbs-5</i>	3665	TCACTCGACTGGGTGTAGG	reverse	na
	<i>pbs-6</i>	3666	ACAAGCTTCACTGGAATCACG	FORWARD	na
	<i>pbs-6</i>	3667	ATCTCACGAAGTGGCAGG	reverse	na
	<i>cul-2</i>	4481	GTGGAATTTGACAAAGTATGGGTG	FORWARD	outer
	<i>cul-2</i>	4482	GTCATTTTGATCGGTTTCGCTG	reverse	outer
	<i>cul-2</i>	4486	cgatgaattcgagctccaccgGTGGAATTTGACAAAGTATGGGTG	FORWARD	inner
	<i>cul-2</i>	4487	cctcgaggtcgacggtatcgGTCATTTTGATCGGTTTCGCTG	reverse	inner
	<i>cul-3</i>	4483	GGGAACTTTGAAGCGTGCC	FORWARD	outer
	<i>cul-3</i>	4485	ATCGCGAGCCAAATATTCTCG	reverse	outer
	<i>cul-3</i>	4488	cgatgaattcgagctccaccgGGGAACTTTGAAGCGTGCC	FORWARD	inner
	<i>cul-3</i>	4490	cctcgaggtcgacggtatcgATCGCGAGCCAAATATTCTCG	reverse	inner
	<i>cul-4</i>	4627	ATGACATCTGGAGCACCACCG	FORWARD	outer
	<i>cul-4</i>	4628	tggatgcacatgttaggtgaagag	reverse	outer
	<i>cul-4</i>	4629	cgatgaattcgagctccaccgACAGCCAGCACCGTTGAAGG	FORWARD	inner
	<i>cul-4</i>	4630	CCTCGAGGTGACGGTATCGgggcaaacgagatgagaagagacc	reverse	inner
	<i>cul-5</i>	4631	GACGAAGAATGGAGCAAAGCCG	FORWARD	outer
	<i>cul-5</i>	4632	ccacatgtttgaaaagagaacgc	reverse	outer
	<i>cul-5</i>	4633	cgatgaattcgagctccaccgCAGAAATCAGTAACCTCCGGCTGC	FORWARD	inner
	<i>cul-5</i>	4634	CCTCGAGGTGACGGTATCGgaccataccaatcgaagatgc	reverse	inner
	<i>cul-6</i>	4635	AAGCAGTGTGGGGAAACATTGC	FORWARD	outer
	<i>cul-6</i>	4636	CTGATCGACGTATGTACAACCTGCT	reverse	outer
	<i>cul-6</i>	4637	cgatgaattcgagctccaccgTGACACAACAACACTTGCC	FORWARD	inner
	<i>cul-6</i>	4638	cctcgaggtcgacggtatcgTAATGAGCAATGTGTGGGTGAGAC	reverse	inner

Table 1. List of primers used in this work.

5.6 Antibodies

5.6.1 Antibodies for immunoblotting

Primary antibodies:

protein	origin	name	dilution	reference
a-CPB-3*	mouse	mo875-A11-1	1:1000	Eckmann laboratory
a-CPB-3	rabbit	rb296 - a.p.	1:3000	Eckmann laboratory
a-CPB-3	rabbit	rb32332 - a.p.**	1:3000	Eckmann laboratory
a-ERK-1/2	rabbit	K-23	1:5000	Santa Cruz, Cat. #: sc-94
a-actin	mouse	Clone C4	1:50.000	MP Biomedicals, Inc., Product #: 69100
a-tubulin	mouse	Clone B-5-1-2	1:100.000	Sigma-Aldrich, Cat. #T5168
a-dynamin	mouse	DYN1	1:1000	Developmental Studies Hybridoma Bank
a-LexA	mouse	2-12	1:1500	Santa Cruz, Cat. #: sc-7544
a-FLAG	mouse	Clone M2	1:10.000	Sigma-Aldrich, Cat. #F3165
a-MBP	mouse		1:2000	NEB, Cat. #: 8030S
a-GLD-1	rabbit		1:3000	Kimble Laboratory (Suh et al., 2006)
a-5xHis	mouse	Penta-His Antibody	1:1000	Qiagen, Cat. #: 34660
a-GLD-2	mouse	ms554: A52-1, A4-4, A4-2	1:1000	Eckmann laboratory
a-OMA-1/2	guinea pig	SAC38	1:500	Eckmann laboratory
a-GLH-1/2	guinea pig	SAC47	1:500	Eckmann laboratory
a-RME-2	rabbit		1:500	Grant Laboratory (Grant and Hirsh, 1999)
a-paramyosin	mouse	MH16	1:250	Developmental Studies Hybridoma Bank

Table 2. Primary antibodies used for immunoblotting.

* monoclonal anti-CPB-3 was used for all immunoblots shown in this thesis.

** prior to use, the antibody was additionally purified by incubation with powdered *cpb-3(0)* mutant worms. This acetone powder was prepared according to Cold Spring Harb Protoc; 2009, doi:10.1101/pdb.rec11891.

Secondary antibodies:

HRP-conjugated anti-mouse, anti-rabbit or anti-guinea pig antibodies (Jackson ImmunoResearch) were used at dilutions between 1:20,000 and 1:40,000.

5.6.2 Antibodies for immunostaining

Primary antibodies:

protein	species	name	dilution	reference
a-CPB-3	mouse	mo875-A11-1**	1:100	Eckmann laboratory
a-CPB-3	rabbit	rb296 - a.p.**	1:300	Eckmann laboratory
a-CPB-3	rabbit	rb32332 - a.p.**	1:300	Eckmann laboratory
a-GLD-1	rabbit		1:300	Kimble Laboratory (Suh et al. 2006)
a-GLH-1/2	guinea pig	SAC47	1:200	Eckmann laboratory
a-OMA-1/2	guinea pig	SAC38	1:200	Eckmann laboratory
a-dpMAPK	mouse	anti-MAP kinase, activated	1:100	Sigma-Aldrich, Product #: M8159
a-RME-2	rabbit		1:200	Grant Laboratory (Grant and Hirsh, 1999)
a-PUF-6	rat	PUF-6-rat1	1:200	Eckmann laboratory
a-GLD-2	mouse	ms554: A52-1, A4-4, A4-2	1:1000	Eckmann laboratory

Table 3. Primary antibodies used for immunostaining.

** prior to use, the antibody was additionally purified by incubation with powdered *cpb-3(0)* mutant worms. This acetone powder was prepared according to Cold Spring Harb Protoc; 2009, doi:10.1101/pdb.rec11891.

Cy5-, Cy3- or FITC-conjugated AffiniPure donkey anti-rabbit, -mouse or -guinea pig IgG antibodies (Jackson ImmunoResearch Laboratories) were used as secondary antibodies at a concentration of 0.75 µg/ml, which corresponds to a 1:1000 dilution of a 0.75 mg/ml stock solution

5.7 Strains

Strain number	Genotype
EV32	cpb-3(tm1746) I
YM19	cpb-3(bt17) I
RB1432	sel-10(ok1632) V
EV267	him-8(e1489) IV; sel-10(ok1632) V
EV375	ozIs5[unc-119 (ed3); GLD-1::GFP] I; unc-119 (+) III
EV666	ozIs5[unc-119 (ed3); GLD-1::GFP] I; unc-119 (+) III; sel-10(ok1632) V
TX189	unc-119(ed3) III; tels1[pRL475(P(oma-1)oma-1::GFP; + pDPMM016(unc-119+)]
EV554	unc-119(ed3) III; tels1[pRL475(P(oma-1)oma-1::GFP; + pDPMM016(unc-119+)], sel-10(ok1632) V
EV414	cpb-3(tm1746); efEx14[cpb-3::LAP + Cbr-unc-119(+)]
EV503	cpb-3(tm1746); efEx14[cpb-3::LAP + Cbr-unc-119(+)]; sel-10(ok1632) V
EG6699	ttTi5605 II; unc-119(ed3) III; oxEx1578 [eft-3p::GFP + Cbr-unc-119]
EV763	efIs124[Cbr-unc-119(+)+ Pmex-5::GFP::H2B::sel-10 3'UTR] II
EV759	efIs123[Cbr-unc-119(+)+ Pmex-5::GFP::H2B::mpk-1 3'UTR] II
EV764	cpb-3(tm1746) I; efIs123[Cbr-unc-119(+)+ Pmex-5::GFP::H2B::mpk-1 3'UTR] II
SA25	daz-1(tj3)/mln1[dpy-10(e128) mIs14] II
EV661, 662	efIs81[Cbr-unc-119(+)+ Pmex-5:gld-1::LAP::gld-1 3'UTR] II; unc-119(ed3) III
EV733, 734	efIs113[Cbr-unc-119(+)+ Pmex-5:gld-1::LAP::tbb-2 3'UTR] II; unc-119(ed3) III

Table 4. *C. elegans* strains used in this work

Strain RB1432 was provided by the *C. elegans* Gene Knockout Project at OMRF, www.celeganskoconsortium.omrf.org

5.8 Worm maintenance, crosses and genotyping

C. elegans strains were handled and crossed according to standard procedures (Brenner, 1974). Worms were grown at 20°C on NGM plates seeded with *E. coli* OP50 bacteria and used for experiments, if not otherwise stated, at an age of 24 h past mid-L4. Bristol N2 served as the wild type strain.

Strain EV414 was generated by bombarding unc-119 animals with the WRM0619cA04 fosmid containing LAP-tagged *cpb-3* locus and *C. briggsae* *unc-119* (*cbunc-119*). Non-unc, rescued animals were established as a strain (EV398) and crossed into *cpb-3(tm1746)* mutant background. This work was done by Nick Jourjine.

Strains EV661, EV662, EV733, EV734, EV759 and EV763 were generated using MosSCI protocol (Frokjaer-Jensen et al., 2012). Briefly, Unc animals of EG6699 strain were injected (see table 5.5 for injection mix), singled and kept at

25°C for a week, until the plates were starved. Then, plates were placed for 2 h in 32°C incubator, to induce expression of the injected plasmid-encoded, toxic gene *peel-1*, which kills worms that contain the extrachromosomal array. After 4 h recovery at 25°C, plates were screened for animals with Unc phenotype rescue. These were singled and their progeny was analysed for GFP expression. Integration in MosSCI locus on LGII was confirmed by nested PCR with two primer combinations, CE3376+CE2640 and CE4314+CE2634 (see table 5.1)

Plasmid	Description	Final concentration
pCFJ601	Peft-3::transposase	50 ng/μl
	Transgene in targeting vector	10 – 50 ng/μl
pMA122	Phsp::peel-1	10 ng/μl
pGH8	Prab-3::mCherry (Pan-neuronal)	10 ng/μl
pCFJ90	Pmyo-2::mCherry (pharynx muscle)	2.5 ng/μl
pCFJ104	Pmyo-3::mCherry (body muscle)	5 ng/μl

Table 5. Injection mix for generating transgenic animals with MosSCI.

Genotype of worms in particular locus was confirmed with nested PCR on DNA obtained by freeze-thaw lysis of worms followed by proteinase K (PK)-treatment (0.2 U/μl PK in 8 μl ProteinaseK buffer), 75 min at 60°C. 0.8 μl of the sample was used as template for the first PCR. For the second PCR reaction, 0.5 μl of the first PCR reaction was used as a template. After the second PCR, 10 μl of the second PCR were analysed by agarose gel electrophoresis.

Identical PCR reaction conditions were used for all genotypes, as the primers were designed accordingly.

Genotyping PCR setup:

reagent	volume
H2O	14,75
primer FOR (10 uM)	1
primer reverse (10 uM)	1
10x PCR buffer	2
10 mM dNTPs	0,4
Taq/Pfu polymerase	0,05
template	0,8

Reaction conditions:

	temp [C]	time
1	95	4 min
2	95	50 s
3	56	45 s
4	72	2 min
5	go to step 2, 34 times	
6	72	7 min
7	20	20 s
8	end	

5.9 Large-scale worm culture.

To generate large amounts of worms for primarily biochemical experiments, NGM plates of 10 cm or 14.5 cm in diameter (Greiner) were used. OP50 bacteria for spotting large plates were grown in a fermenter, frozen in LB medium with an addition of 5% glycerol, and stored in -20°C until needed. 0.16 g and 0.32 g of OP50 were spotted on 10 cm and 14.5 cm plates, respectively. Worm population was propagated from small plates to large plates exactly as described in (Jedamzik and Eckmann, 2009; Jedamzik, 2009):

"Day 1: Three to four starved clean N2 hermaphrodite plates (without bacterial or fungal contaminants) were washed off with 3 to 4 ml M9 buffer into 1.5 ml tubes. Worms were pelleted by centrifugation at 400 x g for 1 min. After washing 3 times with 1 ml M9 the worms were placed on ice for 5 min to settle them to the ground of the tube. All supernatant was removed and the worms were resuspended in 1.2 ml M9. 100 µl worm suspension were placed on each of 12 10-cm NGM plates with 1 ml OP50 under a laminar flow hood. The plates were kept for three days at 20°C.

Day 4: The worms were fed by adding 1 ml OP50 to each plate under a laminar flow hood and kept over night at 20°C.

Day 5: The worms were washed off the 10-cm plates with two times 10 ml M9 per 6 plates into 15 ml Falcon tubes. Worms were pelleted by centrifugation at 600 x g for 2 min. After washing three times with M9 the worms were resuspended in 60 ml OP50 solution. The worms in OP50 were distributed on 30 14.5-cm NGM agar/agarose plates with OP50, 2 ml suspension per plate under a laminar flow hood. Worms were grown two more days at 20°C until most of them reached at least the L4 larval stage without running out of food.

Day 7: Worms were washed off the plates with two times 20 ml M9 per 5 plates into 15 ml Falcon tubes. Worms were pelleted by centrifugation at 600 x g for 2 min, always kept on ice and washed three times with M9 and 2 times in Buffer B70 (including all protease, phosphatase and RNase inhibitors). During the washing procedure the worms were pooled into two 15 ml Falcon tubes. Each worm pellet, typically 2.5 to 4.5 ml, was re-suspended in an equal volume Buffer B70 (incl. inhibitors) and dripped into liquid N2. The frozen worm pearls were stored at -80°C."

For preparation of worm lysate for phosphatase assay (sections 14.2.2 and 16.2), A+ buffer was used instead of B70.

5.10 RNAi feeding

RNAi experiments were performed in a similar manner to the published feeding RNAi procedures (Kamath and Ahringer, 2003).

5.10.1 Generation of RNAi feeding constructs

Constructs for the knock-down of proteasome subunits were generated by amplification of *pas-5*, *pbs-3*, *pbs-5* and *pbs-6* from cDNA with primers listed in table 5.1. PCR products were cloned in pJet2.1 vector (Thermo Fisher Scientific) and subcloned in pL4440 by restriction digest and ligation. Constructs were verified by restriction digest and sequencing.

Constructs targeting all six cullin-encoding genes in *C. elegans* were generated by overlap extension PCR using cDNA as a template. No products for *cul-2* and *cul-3* were obtained with 25 cycles of amplification on cDNA. Thus, for these and subsequently generated *cul-4*, *cul-5* and *cul-6* constructs, genes were amplified with a nested PCR. 1 µl of a PCR reaction with outer primer set served as a template for the second PCR. Only primers in the second round of PCR contained overhangs complementary to the pL4440 backbone.

Constructs were verified by sequencing and transformed into *E. coli* HT114 strain.

Fragment amplification PCR set-up:

template DNA	5-10 ng
5xHF Buffer	10 ul
dNTPs (10 mM)	2 ul
primer FOR (10 uM)	2.5 ul
primer rev (10 uM)	2.5 ul
Polymerase	1 U
ddH2O	up to 50 ul

	temp [C]	time
1	98	2 min
2	98	15 s
3	58	15 s
4	72	25 s/ kb
5	go to step 2, 19 times	
6	72	7 min
7	20	20 s
8	end	

Fragment fusion PCR set-up:

DNA fragments	100-200 ng of each
5xHF Buffer	10 ul
dNTPs (10 mM)	2 ul
Polymerase	1 U
ddH ₂ O	up to 50 ul

	temp [C]	time
1	98	3 min
2	98	20 s
3	72	20 s
4	temp. gradient -0.1 C/s to 55 C	
5	55	20 s
6	72	45 s/kb
7	go to step 2, 29 times	
8	72	10 min
9	20	20 s
10	end	

5.10.2 Preparation of RNAi plates and feeding procedures

HT115 containing plasmids of interests were stored as glycerol stocks at -80°C. To obtain single colonies, bacteria were streaked out on LB plates supplemented with ampicillin 100 µg/ml and tetracyclin 25 µg/ml. A single colony was used to set up a pre-culture in 1 ml of LB+Ampicillin (100 µg/ml), which was shaken at 37°C for 3-5 h. Then, bacteria were harvested at 9000 rcf for 1 min, washed twice with LB, and transferred to a flask containing 20 ml of LB plus 100 µg/ml Ampicillin. The cultures were shaken overnight at 37°C. On the next day, cultures were collected in 50 ml Falcon tubes, spun down at 3800 rcf for 6 min, washed with 20 ml LB, pelleted again and re-suspended in 2 ml of LB+Ampicillin. To induce production of dsRNA, IPTG was added to cultures, to the final concentration of 1 mM. Between 100 and 200 µl of bacteria suspension were spotted on 6 cm plates containing NGM-agar supplemented with 1 mM IPTG and 25 µM Carbenicillin.

sel-10 and *cpb-3* RNAi feeding started from L1 stage. Several adult hermaphrodites were placed on a RNAi feeding plate for a few hours to lay eggs. Adult worms were removed and worms developed for next 2 days. Then, stage of worms was examined. If worms at different larval stages were present on a plate, mid-L4 worms were transferred to a new feeding plate.

Knock-down of proteasome subunits was initially performed by feeding from L1 stage onwards. However, each of the four constructs, targeting *pas-5*, *pbs-3*, *pbs-5* or *pbs-6*, induced developmental defects and sterility. Thus, for investigating the function of proteasome in oogenesis and potential regulation of CPB-3 and GLD-1 expression, RNA feeding was performed from L4 stage.

mpk-1 RNAi feeding was started at early L4 stage and carried out at 25°C. Worms were analysed 36h later.

RNAi knock down with constructs targeting *cullin 1-6* was initially performed from L1 stage onwards. The induced phenotypes of *cul-1*, *cul-2*, *cul-3* and *cul-4* knock downs, recapitulated previously reported ones in the literature for RNAi of these genes or for null mutations (Kipreos 1999, 2001 etc). Therefore, RNAi was considered efficient. *cul-1* and *cul-2* RNAi resulted in underproliferated germ line; thus, the influence of these genes onto CPB-3 and GLD-1 expression was assessed by feeding from the L4 stage onward, so that the germ line could first develop in full until oogenic stage. *cul-5* and *cul-6* RNAi or null mutants do not display easily observable phenotypes. Therefore, efficiency of knock-downs of these two genes was not verified. Nonetheless, RNAi feeding of both constructs did not lead to any observable changes in CPB-3 expression pattern. *cul-5* was reported to act in parallel with *cul-2* (Sasagawa et al., 2007) and *cul-6* might act redundantly with *cul-1*, to which it is closely related (Nayak et al., 2002). Thus, double feedings: *cul-2/cul-5* and *cul-1/cul-6* were performed. Neither of them altered CPB-3 expression pattern.

5.11 Immunocytochemistry.

For the majority of stainings a standard protocol was used (11.1). Protocol 11.2 was used for stainings with anti-dpMAPK antibody and for fixation of transgenic GFP.

5.11.1 Standard fixation protocol.

To extrude germ lines, ~20 worms were placed in a 10 µl drop of cutting solution (M9+0.1 mM levamisole) and quickly dissected with a syringe needle (25G 1" – Nr.18, 0.5 x 25mm) under a stereo microscope. 20 µl of fixing solution (2% paraformaldehyde in PBS+0.02% Tween20) was added and the worms were transferred to a 200 µl tube containing 150 µl fixing solution. The samples were fixed while rotating on a wheel for 10 minutes at room temperature. Then the fixing solution was replaced by 150 µl permeabilisation solution (0.2% Triton-X in PBS) and sample was rotated for next 10 min. Next, permeabilisation solution was removed, dissected worms washed three times with PBSBT and

blocked with PBSBT for 30 min. Blocking solution was replaced with 15 μ l mix of primary antibodies diluted in PBSBT and the samples were incubated overnight at 4°C on a rotating wheel. On the next day, the samples were washed three times with 100 μ l PBSBT and incubated with secondary antibodies diluted in 20 μ l PBSBT for 2 hours in the dark at room temperature. Samples were washed once with PBSBT, incubated with DAPI solution (100 ng/ml in PBSBT) for 20 min and washed two more times with PBSBT. The liquid was aspirated, 6 μ l of Vectashield (Vector Laboratories) liquid mounting medium were added and dissected worms were transferred onto a coverslip and mounted on a glass slide.

5.11.2 Fixation for anti-dpMAPK staining and GFP visualisation

Worms were placed in an 8 μ l drop of cutting solution (M9+0.1 mM levamisole) and dissected with a syringe needle. Special care was taken that cutting did not take longer than 3 min. Worms were transferred to a tube containing fixing solution II (4% paraformaldehyde in PBS+0.02% Tween20). After 45 min, fixing solution was removed and the worms were post-fixed in 150 μ l of 100% methanol at -20°C for 5 min. Samples were washed two times with PBSBT, blocked with PBSBT for 30 min at room temperature and incubated with anti-dpMAPK antibody in PBSBT or immediately stained with DAPI, along the procedure described in 10.1.

5.12 Gel electrophoresis

5.12.1 Standard SDS-PAGE

For analyses of protein extracts, SDS-polyacrylamide gels were prepared using the BioRad PROTEAN-minigel system according to the protocols in (Sambrook and Russell, 2006).

	6%	7%	8%	9%	10%	12%
H ₂ O	2,27	2,15	2,00	1,88	1,75	1,50
1M Tris, pH8	1,88	1,88	1,88	1,88	1,88	1,88
40% AA solut	0,75	0,88	1,00	1,13	1,25	1,50
10% SDS	50	50	50	50	50	50
TEMED	40	40	40	40	40	40
10% APS	10	10	10	10	10	10

Table 6. Composition of SDS-PAGE gels with different percentage of acrylamide.

The gels were poured immediately after the addition of APS and covered with isopropanol. Once gels had solidified, the isopropanol was removed and 4% stacking gel, prepared by mixing 5.45 ml stacking gel mix with 15 μ l TEMED and 40 μ l APS (10%) was poured on top. The gels were run in 1x SDS-PAGE running buffer for 1 hour at constant 25 mA/gel and maximum 200 V.

5.12.2 Phos-Tag SDS-PAGE

Phos-tag SDS-polyacrylamide gels were prepared according to the manufacturer's instructions. As recommended, various concentrations of Phos-Tag in a gel were tested. For the resolution of CPB-3 fragments expressed in yeast, Phos-Tag concentrations of 20 μ M, 50 μ M and 100 μ M were tried. 20 μ M gave best results, consistently with manufacturer's recommendations to decrease Phos-Tag amount for complex samples, such as cell lysates. Thus, 20 μ M Phos-Tag gels were used for the analysis of small CPB-3 fragments. For analyses of full length CPB-3 expressed in yeast or from worm lysate, Phos-Tag concentrations of 2.5 μ M, 10 μ M, 20 μ M, 50 μ M and 100 μ M were tested. Again, lower concentrations (2.5 μ M - 20 μ M) gave better resolution. Attempts to further increase the signal strength and the resolution of differently modified CPB-3 forms in worm extracts were made. Different sample preparation methods were tested (with HU buffer or high-SDS sample buffer) and heating samples at 65°C instead of 95°C. However, none of these attempts could improve results presented in this thesis.

Phos-Tag gels were prepared using the BioRad PROTEAN-minigel system and the following reagents:

- for CPB-3 fragments (10% gel, 20 μ M Phos-Tag, 40 μ M MnCl₂)
- for full length CPB-3 (7% gel, 5 μ M Phos-Tag, 10 μ M MnCl₂)

Stacking gel was the same as for the standard SDS-PAGE. Gels were run in 1x SDS-PAGE running buffer for 4 -7 hours at constant 5-10 mA/gel and maximum 200 V.

5.13 Western blotting

5.13.1 Western blotting of standard SDS-PAGE gels

For the immuno-detection of proteins resolved by SDS-PAGE, proteins were immobilised on a nitrocellulose (NC) membrane by Western blotting using the BioRad Mini Trans-Blot Cell. The nitrocellulose membrane (Millipore, BA 85) was soaked in ddH₂O and then in 1x blotting buffer together with Whatman 3MM filter papers (Whatman, 3030917). The polyacrylamide gel overlaid with the membrane was sandwiched between two filter papers and the two fiber pads, and assembled into a blotting sandwich. This was placed into a blotting cassette and blotted for two hours at constant 400 mA and maximum 180 mA, in a coldroom or on ice.

5.13.2 Western blotting of Phos-Tag gels

According to the manufacturer, the removal of the manganese ions from a Phos-tag gel before electroblotting is necessary (Kinoshita et al., 2006). Therefore, the gel was washed in 75 ml of transfer buffer with an addition of 1 mM EDTA two times for 10 min. Afterwards, two washes with transfer buffer without EDTA were performed. The gel was assembled in a blotting sandwich as described above. Proteins were blotted for 3h hours at constant 400 mA and maximum 180 mA, on ice in a coldroom.

Nitrocellulose and PVDF membranes were used for blotting to test whether one material performs better than the other. However, no significant difference between the two sorts was observed with respect to CPB-3 detection. Additionally, an attempt was made to increase CPB-3 transfer efficiency by using blotting buffer containing 20% methanol. It is possible that more phosphorylated CPB-3 forms were resolved in the gel than were detected by immunoblotting. If the transfer efficiency was low, a fraction of CPB-3 could have been retained in a gel, and as a result, scarce forms of phosphorylated CPB-3 could have remained undetected. However, the addition of methanol to the blotting buffer did not increase CPB-3 signal detected on immunoblots.

5.13.3 Immunodetection of a Western blot

After transfer, a membrane was blocked in 5% low-fat milk in PBST for 10 min. Subsequently, the membrane was placed in a tightly-sealed plastic bag with antibodies diluted in 0.5% milk in PBST. An overnight incubation at 4°C or 3 h incubation at room temperature was followed by washing the membrane three

times for at least 10 min with PBST in a plastic dish. After 1-1.5 h incubation with secondary antibodies diluted in 0.5% milk in PBST, the membrane was washed again three times with PBST. A chemiluminescent signal was generated using the ECL Western Blotting Detection Reagents (GE Healthcare, RPN 2106) and detected by exposition to an X-ray film. In case of very weak signals, HRP-Juice (PJK GmbH) substrate was used.

5.13.4 Re-probing nitrocellulose membranes

The membrane was washed in PBST for 5 min. Then it was placed in a 50 ml Falcon tube filled with 2% acetic acid and 0.5% SDS solution and incubated at 55°C for 30 min. Afterwards, the membrane was quickly rinsed in distilled water, incubated three times 10 min with distilled water on a shaking platform, and three times washed with PBST for a minimum of 15 min in total. For re-probing, the membrane was again blocked in 5% milk in PBST and incubated with a primary antibody as described in 13.3.

5.14 Protein extracts

5.14.1 Yeast protein extracts

5.14.1.1 Yeast transformation

Transformations were performed according to Gietz & Woods, 2002.

A single colony of the L40 reporter strain was grown overnight at 30°C in 20 ml YPD media. On the next day, the culture was diluted to 5×10^6 cells/ml in 50 ml YPD (enough for 10 transformations). If more than 10 transformation were done, additional 50 ml cultures were set up. Yeast was grown at 30°C until the $OD_{600}=0.7$, harvested (3000 rcf, 5min), and washed with 25 ml water. The entire yeast pellet was re-suspended in 0.1 M lithium acetate (LiAc) and transferred to a 1.5 ml tube. Cells were spun down at 15,000 rcf for 15 s, supernatant was discarded, and cells were re-suspended in 400 μ l 0.1 M LiAc. Per transformation reaction, 50 μ l of cell suspension was distributed into individual tubes. Each cell fraction was harvested; its supernatant discarded, and 326 μ l of a premade transformation mix was added to each cell pellet. The transformation mix contained 240 μ l of 50% PEG, 36 μ l of 1M LiAc, and 50 μ l of 2

mg/ml salmon sperm DNA (Roche) per reaction. Salmon sperm DNA was boiled for 5 min and quickly chilled on ice, before its addition to the transformation mix. Subsequently, 250-500 ng of DNA in 34 μ l water were added on top of the transformation mix. The tubes were racked vigorously, vortexed, and incubated at 30°C for 25 min. The transformation was induced by heat shock, by shifting the tubes to 42°C. After 25 min the yeast cells were harvested for 15 s at 4000 rcf, gently re-suspended in 1 ml water and a fraction of 100 - 200 μ l was plated on respective drop-out medium plates; SD-Leu for transformation with pACT plasmids, SD-Trp for transformation with pLex plasmid, and double drop-out for double transformation. Plates were kept at 30°C for three days before further experiments.

5.14.1.2 Yeast protein extraction by precipitation with TCA.

This protocol is based on (Lai et al., 2011). Yeast was grown overnight in 20 ml drop-out medium at 30°C. Three OD units of yeast cells were harvested (3000 rcf, 5 min), re-suspended in 1 ml of water, transferred to a 1.5 ml microfuge tube, and pelleted at ~15.000 rcf for 1 min. After discarding the supernatant, the cells were re-suspended in 1 ml of ice-cold water and addition of 150 μ l of freshly prepared solution D (1.85 M NaOH, 7.5% β -mercaptoethanol) were added. After 15 min incubation on ice, 150 μ l of 55% trichloroacetic acid (TCA) were added. Cells were incubated for next 10 min on ice and then centrifuged at 10.000 rcf for 10 min at 4°C. Supernatant was aspirated with a fine-drawn glass Pasteur pipette with the aim to remove as much liquid as possible. Pellet was re-suspended in 200 μ l of 2xSDS-sample buffer and 100 μ l of 1M Tris Base (pH not adjusted) for an SDS-PAGE gel sample, or in 250 μ l of buffer A+ for a phosphatase assay.

5.14.2 Worm protein extracts

5.14.2.1 Boiled animal extracts

For most analyses of worm proteins by immunoblotting, worm extracts were prepared by boiling whole animals in 2xSDS-sample buffer. To this end, worms were hand picked into 0.5 ml M9+0.05% Tween-20, spun down at 600 rcf for 30 s, washed with 0.5 ml M9+0.05% Tween20, and spun down again. The majority of the supernatant was discarded and the remaining buffer was

aspirated to a minimum of 10 μ l after placing the samples for a few seconds on ice water, to make the worms settle on the bottom of the tube. Each sample was snap-frozen in LN₂ and processed further or stored at -20°C for up to two weeks. To each tube, 15 μ l of pre-heated 2xSDS sample buffer were added, samples were boiled for 5 min, sonicated in 80°C water bath for 20 min, boiled again for 5 min, and centrifuged at 15.000 rcf for 1 min to generate a pellet of non-dissolvable material.

Per sample, 40 or 50 worms were collected for a Mini-Protean gel with 10-well comb; 30 worms for a 15-well gel.

5.14.2.2 Worm protein extract for phosphatase assay

As standard worm lysate preparations used in immunoprecipitation experiments did not allow for a maintenance of modified CPB-3 forms, even if 100 mM NaF, 100 mM β -glycerophosphate and 5 mM Na₃VO₄ were added, worm protein extracts for phosphatase assays, were prepared by TCA precipitation.

To this end, worms were grown in large amounts and frozen as pearls (see description in section 5.9). Pearls were ground to a powder using a bead mill (Mixer Mill MM301, Retsch) with a 1.5 cm stainless steel ball. Before use, the equipment used for grinding pearls and handling worm powder had been pre-cooled in liquid nitrogen (LN₂) before use and the grinding procedure was performed in a cold room. Using pre-cooled metal funnel and spatula, worm powder was transferred from the mill to cooled 2 ml tubes, which were immediately placed in LN₂. Desired amount of worm powder, measured with fine balance, was placed in a 1.5 ml tube, and rest was stored at -80°C for future experiments. 1 ml of 7% TCA was added to 40 mg of worm powder. The tube was briefly vortexed and then spun down at 5000 rcf, 4°C, for 10 min. While the supernatant was discarded, the pellet was re-suspended by sonication in 250 μ l of buffer A+, supplemented with protease inhibitors and 4 μ l of 2 M Tris base. The pH of the samples was between 7 and 8.

5.14.3 SF+ insect cell extract.

A baculovirus expression system was employed for protein expression in insect cells. A modified Bac-to-Bac system was used with the assistance of the Protein Expression and Purification (PEP) walk-in facility at MPI-CBG.

SF+ cells were grown in suspension in SF-900 medium (GIBCO) containing penicillin and streptomycin, at 27°C, shaking at 100 rpm. Cell maintenance was done by PEP facility. For infections, cell cultures at a density of 1 million cells/ml were used.

5.14.3.1 Generating clones and baculoviruses

Coding sequences of genes to be expressed in insect cells were cloned in pOEM vector, a derivative of pOET (Oxford Expression Technologies). Two versions of a vector with C-terminal hexa-histidine (6xHis) tag were used, pOEM-M and pOEM-F. The former contains a N-terminal maltose binding protein (MBP) tag, the latter - three repeats of a FLAG epitope (3xFLAG). Coding sequences were amplified from cDNA (*skr-1*) or existing constructs (others) with primers introducing restriction sites (table 5.1). Amplicons were digested with appropriate restriction enzymes and ligated into the multiple cloning site (MCS) of pre-digested pOEM vectors. All constructs were verified by restriction digest and sequencing.

Obtained plasmids were used to generate baculoviruses. The initial step of co-transfection into SF9 insect cells together with a defective baculovirus genome was performed by the PEP facility, MPI-CBG (Dresden). A successful recombination event generates a fully functional genome that supports the production of new viral particles, which bud from cultured cells and can be collected with a supernatant as P1 virus. P1 was used to infect next batch of cells, which led to an increase in the virus titer. Supernatant containing the second generation of the virus (P2) was used for another round of infection/amplification, which gave rise to P3 virus. At the same time, a fraction of P2 was mixed with glycerol and frozen for the long-term storage at -80°C. P3 virus was also aliquoted and frozen until needed.

5.14.3.2 Test expression analysis of recombinant proteins in insect cells

Each new virus was tested for the peak of protein expression in a time-course experiment. For this, 40 ml of SF+ cells were infected with 40 µl of P3 virus and grown for 5 days. At the day of infection, T=0 (or 'day 0') sample was taken. 0.5 ml samples were collected on 5 consecutive days in 1.5 ml microfuge tubes, spun down at 300 rcf for 5 min at 4°C, and snap-frozen in LN₂ after the removal of the supernatant, or processed further. Cell pellets were quickly re-suspended in 100 µl of ice-cold PBS. After the addition of 100 µl of 2xSDS sample buffer, samples were boiled for 5 min and cooled down to room temperature. To digest remaining nucleic acids, samples were incubated with 1 unit of Benzonase (Merck Millipore) at 37°C for 15 min. Prior to gel loading, samples were boiled again for 5 min and spun down. . Proteins separated by electrophoresis were detected by immunoblotting, with anti-FLAG, anti-MBP or anti-5xHis antibodies. Usually, expression of fusion proteins peaked at the second or third day post infection.

5.14.3.3 Double infections for protein interaction studies

To express two proteins of interest in SF+ cells, 30 ml of the culture were placed in 250 ml sterile Erlenmeyer flasks and infected with 30 µl of two different P3 viruses encoding proteins of interest. Cells were grown for 2 or 3 days, then collected in 50 ml Falcon tubes and spun down at 300 rcf for 10 min. Supernatant was discarded, cells re-suspended in 3 ml of SF buffer containing protease inhibitors, aliquoted in 1.5 ml tubes and frozen in LN₂.

5.15 Protein co-immunoprecipitation (Co-IP) experiments (at 4°C)

5.15.1 Resin preparation

50 µl of 50% anti-FLAG resin (Sigma) was used per reaction. The resin was prepared by three washes with SF buffer. Tubes were rotated for 1 h at room temperature or overnight at 4°C. Then, beads were washed twice with SF buffer and used for IP.

5.15.2 Co-IP from insect cell extracts

500 µl of SF buffer supplemented with protease and phosphatase inhibitors were added to 500 µl frozen aliquots of SF+ cells. Tubes were rotated

on a wheel for 5 min and then spun down at 16000 rcf, 4°C, for 10 min. Supernatant was transferred to new tubes. 200 µl of an extract were added to a 500 µl microfuge tube containing pre-washed resin. Immunoprecipitation was done for 1 h on a rotating wheel. Then, the extract was discarded and beads were washed thrice with 400 µl SF buffer. To elute precipitated proteins, beads were boiled in 40 µl of SDS-sample buffer. Usually, 8 µl of eluate, corresponding to 1/5 of total precipitated material, was loaded on a gel.

Input samples were prepared by mixing 30 µl of each extract with 30 µl of 2xSDS-sample buffer and boiling for 5 min.

5.16 Phosphatase assays

5.16.1 Dephosphorylation of yeast extracts

Lambda protein phosphatase (λPP, New England Biolabs) was used to dephosphorylate yeast proteins extracted by the TCA precipitation method. Protein pellet from 6 OD600 units (corresponding to roughly 6×10^7 yeast cells) was re-suspended in 250 µl of buffer A+ and 4 µl of 2 M Tris-Base were added to adjust the pH to 7.5. Per sample, 25 µl of the extract and 1000 units (2.5 µl) of λPP were used. For λPP, one unit is defined as the amount of enzyme that hydrolyses 1 nmol of p-Nitrophenyl Phosphate (50 mM) (NEB #P0757) in 1 minute at 30°C in a total reaction volume of 50 µl. To inhibit the λPP, sodium orthovanadate (Na_3VO_4) was added to the final concentration of 50 µM. The λPP storage buffer (50 mM HEPES, 100 mM NaCl, 2 mM DTT, 0.01% Brij 35, 0.1 mM EGTA, 0.1 mM MnCl_2 , 50% Glycerol, pH 7.5 @ 25°C) was added to one of the control samples to exclude an influence of its components on the protein migration in the Phos-Tag gel. Samples were incubated for 30 min at 30 C and then precipitated by addition of 100% TCA to a final concentration of 7%. Samples were spun down at 3000 rcf for 10 min, supernatant was aspirated using fine-drawn glass Pasteur pipette, and the pellet was re-suspended in 20 µl of High Urea (HU) sample buffer. 1 µl of 1 M Tris pH 8.8 was added to each sample, to increase the pH. Samples were shaken at 65°C for 10 min, then spun down at 3000 rcf for 5 min, and loaded on a Phos-Tag gel.

5.16.2 Dephosphorylation of worm extracts

25 µl of the worm extract prepared as in 14.2.2. were treated with 1000 U of λPP (NEB). 2.5 µl of λPP storage buffer (50 mM HEPES, 100 mM NaCl, 2 mM DTT, 0.01% Brij 35, 0.1 mM EGTA, 0.1 mM MnCl₂, 50% Glycerol, pH 7.5 @ 25°C) were added to the mock-treated sample. Samples were incubated at 30°C for 30 min, and then the reaction was stopped and proteins precipitated by an addition of 100% TCA to the final concentration of 7%. Samples were spun down at 3000 rcf for 10 min, supernatant was aspirated using fine-drawn glass Pasteur pipette, and the pellet was re-suspended in 20 µl of High Urea (HU) sample buffer. 2 µl of 1 M Tris pH 8.8 were added to each sample, to increase the pH. Samples were shaken at 65°C for 10 min, then spun down at 3000 rcf for 5 min, and loaded on a gel.

5.17 Purification of recombinant proteins from insect cells for mass spectrometry analysis

All solutions used in purification steps, electrophoresis and staining of the SDS-PAGE gel were prepared freshly, with an aim to prevent any contamination, particularly with keratin. All solutions were sterile filtered with 0.22 µm disc filters (Corning). To this aim, lab coat and gloves were worn at all steps of the procedure described below. Gloves were frequently washed with water or 70% EtOH.

To a frozen aliquot of SF+ cells in SF buffer (0.5 ml), 0.5 ml of 14% TCA was added. Tubes were vortexed and rotated at 4°C for 5 min. 200 µl aliquot was taken, spun down at 5000 rcf for 5 min at 4°C. Supernatant was removed and 1 ml of the Urea Binding Buffer was added. The tube was vortexed and spun down at 10,000 rcf for 2 min. This served as an "input" sample. Remaining 800 µl of cell extract were transferred to a microfuge tube containing Ni-IDA resin, that has been beforehand washed 2 times in the Urea Binding Buffer. The sample was rotated for 10 min at room temperature and afterwards beads were washed once with 1 ml of Urea Binding Buffer. Subsequently, three washes were performed to gradually decrease urea concentration. 0.5 ml of urea buffer was removed, 0.5 ml of washing buffer was added, and the sample was rotated for 5 min. This sequence was repeated two more times. In the end, beads were quickly

washed with washing buffer and the protein was eluted with 40 μ l of 2xSDS sample buffer without β -mercaptoethanol (β -ME), by incubation at 95°C for 5 min. Sample buffer was transferred to a new tube and elution repeated with sample buffer containing β -ME. Most of the protein was eluted in the first step. 8 μ l of the sample were loaded onto an SDS-PAGE gel.

After electrophoresis, the gel was stained with Coomassie Brilliant Blue solution in a 14.5 cm Petri dish, with gentle agitation on a shaking platform at room temperature for 2h. Subsequently, the gel was de-stained in the de-staining solution for 1 h, washed briefly with water, placed in a plastic sleeve, scanned and delivered to Mass Spectrometry facility at MPI-CBG.

5.18 Analysis of fluorescent images

Images were taken on a Zeiss Imager M1 with a 63X/1.4NA objective, equipped with an AxioCam MRm (Zeiss). Identical exposure conditions were used for all samples in each dataset. Images were pre-processed with AxioVision (Zeiss). Fluorescence intensity was measured using FIJI/ImageJ software (www.fiji.sc) and analysed in Excel (Microsoft). Student's two-tailed t-test was used to test statistical significance.

5.18.1 Measurements of the signal intensity along the gonadal length

For the analyses of protein expression pattern in a germ line, images in the focal plane of the rachis were collected and stitched. A 70 points-wide segmented line, which corresponds roughly to the width of two nuclei, was drawn from the distal tip to the proximal end of a germ line. In addition, fluorescence intensity of a glass slide was measured and the average background intensity was subtracted from all values. Intensity values from each gonad were binned into 500 groups and averaged. This treatment gave 500 evenly spaced intensity values irrespective of germ line length. Average values were then calculated for all gonads belonging to the same genotype. Error bars in figures show standard error of the mean (SEM).

5.18.2 Measuring signal intensity at the pachytene exit

Z-stack images were collected for the analysis of signal intensity in germ cells at the pachytene exit. Images in the focal plane of the rachis were stitched, and the segmented line tool was used to extract intensity values from the distal tip to the proximal end of the germ line. In each germ line, the intensity values were divided by the maximal intensity in the germ line and thus represented as percentage of the maximal intensity. To determine the location of the pachytene-diplothe (P-D) border, the gross chromatin morphology of germ cell nuclei was analysed across several focal planes. Measurements covering the distance 100 μm distally and 100 μm proximally from the (P-D) border were extracted and averaged.

5.18.3 Measuring signal intensity in early embryos

Images in focal plane of a nucleus were collected. A square $\sim 150 \mu\text{m}^2$ was used to measure intensity. For each embryo, 5 values were collected and averaged. Background intensity was measured in a similar way and subtracted from embryo intensity. For each genotype, 20 embryos were measured in this way and averaged.

5.18.4 Measuring signal intensity in defined regions

GFP intensity was measured in the regions indicated in figure 3.8.6 using a square $\sim 150 \mu\text{m}^2$. Three measurements were taken for each region in each germ line. Per genotype, 10 germ lines were measured. Obtained 30 values per region of interest were averaged. Background fluorescence was determined by measuring signal intensity of the area of the slide at some distance from mounted worms, averaging obtained values and subtracting the average value from averages calculated for distinct regions of the germ line.

5.19 Bioinformatic tools

ELM - The Eukaryotic Linear Motif resource for Functional Sites in Proteins:

<http://elm.eu.org/> (Dinkel et al., 2016)

NetPhos 3.1 Server:

<http://www.cbs.dtu.dk/services/NetPhos/> (Blom et al., 2004)

ePESTfind - algorithm for identification of PEST motifs in proteins:

<http://emboss.bioinformatics.nl/cgi-bin/emboss/epestfind> (Rogers et al., 1986)

Ape - freeware for DNA *in silico* editing:

<http://biologylabs.utah.edu/jorgensen/wayned/ape/>

ProtParam - online protein analysis tool:

<http://web.expasy.org/protparam/>

References

- Afroz, T., Skrisovska, L., Belloc, E., Guillén-Boixet, J., Mendez, R. and Allain, F. H. T. (2014). A fly trap mechanism provides sequence-specific RNA recognition by CPEB proteins. *Genes Dev.* **28**, 1498–1514.
- Aitken, C. E. and Lorsch, J. R. (2012). A mechanistic overview of translation initiation in eukaryotes. *Nature Publishing Group* **19**, 568–576.
- Alberts, B., Johnson, A., Lewis, J., Morgan, D., Raff, M., Roberts, K. and Walter, P. (2014). *Molecular Biology of the Cell, Sixth Edition*. Garland Science.
- Alberts, B., Johnson, A., Lewis, J., Raff, M., Roberts, K. and Walter, P. (2008). *Molecular Biology of the Cell*. Garland Science.
- Andreotti, A. H., Bunnell, S. C., Feng, S., Berg, L. J. and Schreiber, S. L. (1997). Regulatory intramolecular association in a tyrosine kinase of the Tec family. *Nature* **385**, 93–97.
- Andresson, T. and Ruderman, J. V. (1998). The kinase Eg2 is a component of the *Xenopus* oocyte progesterone-activated signaling pathway. *The EMBO Journal* **17**, 5627–5637.
- Artzt, K. and Wu, J. I. (2010). STAR TREK An Introduction to STAR Family Proteins and Review of Quaking (QKI). *Adv. Exp. Med. Biol.* **693**, 1–24.
- Arur, S., Ohmachi, M., Berkseth, M., Nayak, S., Hansen, D., Zarkower, D. and Schedl, T. (2011). MPK-1 ERK Controls Membrane Organization in *C. elegans* Oogenesis via a Sex-Determination Module. *Developmental Cell* **20**, 677–688.
- Arur, S., Ohmachi, M., Nayak, S., Hayes, M., Miranda, A., Hay, A., Golden, A. and Schedl, T. (2009). Multiple ERK substrates execute single biological processes in *Caenorhabditis elegans* germ-line development. *Proc. Natl. Acad. Sci. U.S.A.* **106**, 4776–4781.
- Austin, J. and Kimble, J. (1987). glp-1 is required in the germ line for regulation of the decision between mitosis and meiosis in *C. elegans*. *Cell* **51**, 589–599.
- Barnard, D. C., Ryan, K., Manley, J. L. and Richter, J. D. (2004). Symplekin and xGLD-2 are required for CPEB-mediated cytoplasmic polyadenylation. *Cell* **119**, 641–651.
- Bell, G. (1982). *The Masterpiece of Nature*. London, Croom Helm.
- Belloc, E. and Mendez, R. (2008). A deadenylation negative feedback mechanism governs meiotic metaphase arrest. *Nature* **452**, 1017–1021.
- Belloc, E., Piqué, M. and Mendez, R. (2008). Sequential waves of polyadenylation and deadenylation define a translation circuit that drives meiotic progression. *Biochem. Soc. Trans.* **36**, 665–670.
- Benoit, P., Papin, C., Kwak, J. E., Wickens, M. and Simonelig, M. (2008). PAP- and GLD-2-type poly(A) polymerases are required sequentially in cytoplasmic polyadenylation and oogenesis in *Drosophila*. *Development* **135**, 1969–1979.
- Berndsen, C. E. and Wolberger, C. (2014). New insights into ubiquitin E3 ligase mechanism. *Nature Publishing Group* **21**, 301–307.

- Bernstein, D., Hook, B., Hajarnavis, A., Opperman, L. and Wickens, M.** (2005). Binding specificity and mRNA targets of a *C. elegans* PUF protein, FBF-1. *RNA* **11**, 447–458.
- Berry, L. W., Westlund, B. and Schedl, T.** (1997). Germ-line tumor formation caused by activation of glp-1, a *Caenorhabditis elegans* member of the Notch family of receptors. *Development* **124**, 925–936.
- Biedermann, B., Hotz, H.-R. and Ciosk, R.** (2010). The Quaking family of RNA-binding proteins: coordinators of the cell cycle and differentiation. *Cell Cycle* **9**, 1929–1933.
- Biedermann, B., Wright, J., Senften, M., Kalchauer, I., Sarathy, G., Lee, M.-H. and Ciosk, R.** (2009). Translational Repression of Cyclin E Prevents Precocious Mitosis and Embryonic Gene Activation during *C. elegans* Meiosis. *Developmental Cell* **17**, 355–364.
- Blom, N., Sicheritz-Pontén, T., Gupta, R., Gammeltoft, S. and Brunak, S.** (2004). Prediction of post-translational glycosylation and phosphorylation of proteins from the amino acid sequence. *PROTEOMICS* **4**, 1633–1649.
- Bosu, D. R. and Kipreos, E. T.** (2008). Cullin-RING ubiquitin ligases: global regulation and activation cycles. *Cell Div* **3**, 7–13.
- Bowerman, B. and Kurz, T.** (2006). Degrade to create: developmental requirements for ubiquitin-mediated proteolysis during early *C. elegans* embryogenesis. *Development* **133**, 773–784.
- Boxem, M.** (2006). Cell Division. *Cell Div* **1**, 6–12.
- Boxem, M., Srinivasan, D. G. and van den Heuvel, S.** (1999). The *Caenorhabditis elegans* gene ncc-1 encodes a cdc2-related kinase required for M phase in meiotic and mitotic cell divisions, but not for S phase. *Development* **126**, 2227–2239.
- Breitwieser, W., Markussen, F. H., Horstmann, H. and Ephrussi, A.** (1996). Oskar protein interaction with Vasa represents an essential step in polar granule assembly. *Genes Dev.* **10**, 2179–2188.
- Brenner, S.** (1974). The genetics of *Caenorhabditis elegans*. *Genetics*.
- Brocchieri, L. and Karlin, S.** (2005). Protein length in eukaryotic and prokaryotic proteomes. *Nucleic Acids Res* **33**, 3390–3400.
- Brummer, A., Kishore, S., Subasic, D., Hengartner, M. and Zavolan, M.** (2013). Modeling the binding specificity of the RNA-binding protein GLD-1 suggests a function of coding region-located sites in translational repression. *RNA* **19**, 1317–1326.
- Burger, J., Merlet, J., Tavernier, N., Richaudeau, B., Arnold, A., Ciosk, R., Bowerman, B. and Pintard, L.** (2013). CRL2LRR-1 E3-Ligase Regulates Proliferation and Progression through Meiosis in the *Caenorhabditis elegans* Germline. *PLoS Genetics* **9**, e1003375–13.
- Cardozo, T. and Pagano, M.** (2004). The SCF ubiquitin ligase: insights into a molecular machine. *Nat. Rev. Mol. Cell Biol.* **5**, 739–751.
- Cargnello, M. and Roux, P. P.** (2011). Activation and Function of the MAPKs and Their Substrates, the MAPK-Activated Protein Kinases. *Microbiology and Molecular Biology Reviews* **75**, 50–83.
- Carmel, A. B., Wu, J., Lehmann-Blount, K. A. and Williamson, J. R.** (2010). High-affinity consensus binding of target RNAs by the STAR/GSG proteins GLD-1, STAR-2 and Quaking. *BMC Mol Biol* **11**, 48–13.

- Chang, J. S., Tan, L. H. and Schedl, P.** (1999). The *Drosophila* CPEB homolog, Orb, is required for Oskar protein expression in oocytes. *Developmental Biology* **215**, 91–106.
- Chang, J. S., Tan, L. H., Wolf, M. R. and Schedl, P.** (2001). Functioning of the *Drosophila* orb gene in gurken mRNA localization and translation. *Development* **128**, 3169–3177.
- Charlesworth, A., Wilczynska, A., Thampi, P., Cox, L. L. and MacNicol, A. M.** (2006). Musashi regulates the temporal order of mRNA translation during *Xenopus* oocyte maturation. *The EMBO Journal* **25**, 2792–2801.
- Charlesworth, B.** (2006). The evolutionary biology of sex. *Curr. Biol.* R693–R695.
- Chase, D., Golden, A., Heidecker, G. and Ferris, D. K.** (2000a). *Caenorhabditis elegans* contains a third polo-like kinase gene. *DNA Sequence*.
- Chase, D., Serafinas, C., Ashcroft, N., Kosinski, M., Longo, D., Ferris, D. K. and Golden, A.** (2000b). The Polo-like kinase PLK-1 is required for nuclear envelope breakdown and the completion of meiosis in *Caenorhabditis elegans*. *genesis* **26**, 26–41.
- Cheeseman, I. M. and Desai, A.** (2005). A combined approach for the localization and tandem affinity purification of protein complexes from metazoans. *Sci. STKE* **2005**, pl1–pl1.
- Chen, P. J., Singal, A., Kimble, J. and Ellis, R. E.** (2000). A novel member of the tob family of proteins controls sexual fate in *Caenorhabditis elegans* germ cells. *Developmental Biology* **217**, 77–90.
- Chen, S., Wu, J., Lu, Y., Ma, Y.-B., Lee, B.-H., Yu, Z., Ouyang, Q., Finley, D. J., Kirschner, M. W. and Mao, Y.** (2016). Structural basis for dynamic regulation of the human 26S proteasome. *Proc. Natl. Acad. Sci. U.S.A.* **113**, 12991–12996.
- Cho, P. F., Poulin, F., Cho-Park, Y. A., Cho-Park, I. B., Chicoine, J. D., Lasko, P. and Sonenberg, N.** (2005). A New Paradigm for Translational Control: Inhibition via 5′-3′ mRNA Tethering by Bicoid and the eIF4E Cognate 4EHP. *Cell* **121**, 411–423.
- Christerson, L. B. and Mckearin, D. M.** (1994). Orb Is Required for Anteroposterior and Dorsoventral Patterning During *Drosophila* Oogenesis. *Genes Dev.* **8**, 614–628.
- Church, D. L., Guan, K. L. and Lambie, E. J.** (1995). Three genes of the MAP kinase cascade, mek-2, mpk-1/sur-1 and let-60 ras, are required for meiotic cell cycle progression in *Caenorhabditis elegans*. *Development* **121**, 2525–2535.
- Ciosk, R., DePalma, M. and Priess, J. R.** (2006). Translational regulators maintain totipotency in the *Caenorhabditis elegans* germline. *Science* **311**, 851–853.
- Clemens, M. J.** (2001). Initiation factor eIF2 alpha phosphorylation in stress responses and apoptosis. *Prog. Mol. Subcell. Biol.* **27**, 57–89.
- Clifford, R., Lee, M. H., Nayak, S., Ohmachi, M., Giorgini, F. and Schedl, T.** (2000). FOG-2, a novel F-box containing protein, associates with the GLD-1 RNA binding protein and directs male sex determination in the *C. elegans* hermaphrodite germline. *Development* **127**, 5265–5276.
- Coghlan, A.** (2005). Nematode genome evolution. *WormBook* 1–15.
- Cohen, P. and Cohen, P.** (1989). Discovery of a Protein Phosphatase-Activity Encoded in the Genome of Bacteriophage-Lambda - Probable Identity with Open Reading Frame 221. *Biochem. J.* **260**, 931–934.
- Corsi, A. K., Wightman, B. and Chalfie, M.** (2015). A Transparent window into biology: A primer

- on *Caenorhabditis elegans*. *WormBook* 1–31.
- Costa-Mattioli, M., Sossin, W. S., Klann, E. and Sonenberg, N.** (2009). Translational Control of Long-Lasting Synaptic Plasticity and Memory. *Neuron* **61**, 10–26.
- Cragle, C. and MacNicol, A. M.** (2014). Musashi Protein-directed Translational Activation of Target mRNAs Is Mediated by the Poly(A) Polymerase, Germ Line Development Defective-2. *Journal of Biological Chemistry* **289**, 14239–14251.
- Crittenden, S. L., Bernstein, D. S., Bachorik, J. L., Thompson, B. E., Gallegos, M., Petcherski, A. G., Moulder, G., Barstead, R., Wickens, M. and Kimble, J.** (2002). A conserved RNA-binding protein controls germline stem cells in *Caenorhabditis elegans*. *Nature* **417**, 660–663.
- Crittenden, S. L., Leonhard, K. A., Byrd, D. T. and Kimble, J.** (2006). Cellular analyses of the mitotic region in the *Caenorhabditis elegans* adult germ line. *Mol. Biol. Cell* **17**, 3051–3061.
- Crittenden, S. L., Troemel, E. R., Evans, T. C. and Kimble, J.** (1994). GLP-1 is localized to the mitotic region of the *C. elegans* germ line. *Development* **120**, 2901–2911.
- Cuervo, A. M., Palmer, A., Rivett, A. J. and Knecht, E.** (1995). Degradation of Proteasomes by Lysosomes in Rat Liver. *Eur J Biochem* **227**, 792–800.
- Curran, J. A. and Weiss, B.** (2016). What Is the Impact of mRNA 5' TL Heterogeneity on Translational Start Site Selection and the Mammalian Cellular Phenotype? *Front Genet* **7**, 251–13.
- Darnell, J. C., Van Driesche, S. J., Zhang, C., Hung, K. Y. S., Mele, A., Fraser, C. E., Stone, E. F., Chen, C., Fak, J. J., Chi, S. W., et al.** (2011). FMRP Stalls Ribosomal Translocation on mRNAs Linked to Synaptic Function and Autism. *Cell* **146**, 247–261.
- Davis, E. S., Wille, L., Chestnut, B. A., Sadler, P. L., Shakes, D. C. and Golden, A.** (2002). Multiple subunits of the *Caenorhabditis elegans* anaphase-promoting complex are required for chromosome segregation during meiosis I. *Genetics* **160**, 805–813.
- Davuluri, R. V., Suzuki, Y., Sugano, S., Plass, C. and Huang, T. H. M.** (2008). The functional consequences of alternative promoter use in mammalian genomes. *Trends in Genetics* **24**, 167–177.
- de la Cova, C. and Greenwald, I.** (2012). SEL-10/Fbw7-dependent negative feedback regulation of LIN-45/Braf signaling in *C. elegans* via a conserved phosphodegron. *Genes Dev.* **26**, 2524–2535.
- DeRenzo, C. and Seydoux, G.** (2004). A clean start: degradation of maternal proteins at the oocyte-to-embryo transition. *Trends in Cell Biology* **14**, 420–426.
- DeRenzo, C., Reese, K. J. and Seydoux, G.** (2003). Exclusion of germ plasm proteins from somatic lineages by cullin-dependent degradation. *Nature* **424**, 685–689.
- Dernburg, A. F., McDonald, K., Moulder, G., Barstead, R., Dresser, M. and Villeneuve, A. M.** (1998). Meiotic recombination in *C. elegans* initiates by a conserved mechanism and is dispensable for homologous chromosome synapsis. *Cell* **94**, 387–398.
- Derry, J. J., Richard, S., Carvajal, H. V., Ye, X., Vasioukhin, V., Cochrane, A. W., Chen, T. P. and Tyner, A. L.** (2000). Sik (BRK) phosphorylates Sam68 in the nucleus and negatively regulates its RNA binding ability. *Molecular and Cellular Biology* **20**, 6114–6126.
- Detwiler, M. R., Reuben, M., Li, X., Rogers, E. and Lin, R.** (2001). Two zinc finger proteins, OMA-1 and OMA-2, are redundantly required for oocyte maturation in *C. elegans*.

- Developmental Cell* **1**, 187–199.
- Dickinson, D. J. and Goldstein, B.** (2016). CRISPR-Based Methods for *Caenorhabditis elegans* Genome Engineering. *Genetics* **202**, 885–901.
- Ding, M., Chao, D., Wang, G. and Shen, K.** (2007). Spatial Regulation of an E3 Ubiquitin Ligase Directs Selective Synapse Elimination. **317**, 947–951.
- Dinkel, H., Van Roey, K., Michael, S., Kumar, M., Uyar, B., Altenberg, B., Milchevskaya, V., Schneider, M., Kühn, H., Behrendt, A., et al.** (2016). ELM 2016--data update and new functionality of the eukaryotic linear motif resource. *Nucleic Acids Res* **44**, D294–300.
- Dorfman, M., Gomes, J. E., O'Rourke, S. and Bowerman, B.** (2009). Using RNA Interference to Identify Specific Modifiers of a Temperature-Sensitive, Embryonic-Lethal Mutation in the *Caenorhabditis elegans* Ubiquitin-Like Nedd8 Protein Modification Pathway E1-Activating Gene *rfl-1*. *Genetics* **182**, 1035–1049.
- Dowling, R. J., Topisirovic, I., Alain, T., Bidinosti, M., Fonesca, B. D., Petroulakis, E., Wang, X., Larsson, O., Selvaraj, A., Liu, Y., et al.** (2010). mTORC1-Mediated Cell Proliferation, But Not Cell Growth, Controlled by the 4E-BPs. *Science* **328**, 1172–1176.
- Eckmann, C. R., Crittenden, S. L., Suh, N. and Kimble, J.** (2004). GLD-3 and control of the mitosis/meiosis decision in the germline of *Caenorhabditis elegans*. *Genetics* **168**, 147–160.
- Eckmann, C. R., Kraemer, B., Wickens, M. and Kimble, J.** (2002). GLD-3, a Bicaudal-C homolog that inhibits FBF to control germline sex determination in *C. elegans*. *Developmental Cell* **3**, 697–710.
- Eckmann, C. R., Rammelt, C. and Wahle, E.** (2011). Control of poly(A) tail length. *Wiley Interdisciplinary Reviews: RNA* **2**, 348–361.
- Ehrmann, I. and Elliott, D. J.** (2010). Expression and Functions of the Star Proteins Sam68 and t-star in Mammalian Spermatogenesis. In *Germ Cell Development in C. elegans* (ed. Schedl, T., pp. 67–81. Boston, MA: Springer US.
- Eichhorn, S. W., Subtelny, A. O., Kronja, I., Kwasnieski, J. C., Orr-Weaver, T. L. and Bartel, D. P.** (2016). mRNA poly(A)-tail changes specified by deadenylation broadly reshape translation in *Drosophila* oocytes and early embryos. *Elife* **5**.
- Eletr, Z. M. and Wilkinson, K. D.** (2014). Regulation of proteolysis by human deubiquitinating enzymes. *BBA - Molecular Cell Research* **1843**, 114–128.
- Elkon, R., Ugalde, A. P. and Agami, R.** (2013). Alternative cleavage and polyadenylation: extent, regulation and function. *Nature Reviews Genetics* **14**, 496–506.
- Ellis, R. and Schedl, T.** (2007). Sex determination in the germ line. *WormBook*, ed. The *C. elegans* Research Community, doi/10.1895/wormbook.1.82.2.
- Ellis, R. E.** (2008). Sex determination in the *Caenorhabditis elegans* germ line. *Current Topics in Developmental Biology*.
- Ellis, R. E. and Stanfield, G. M.** (2014). The regulation of spermatogenesis and sperm function in nematodes. *Seminars in Cell & Developmental Biology* **29**, 17–30.
- Fang, S. and Weissman, A. M.** (2004). A field guide to ubiquitylation. *Cell. Mol. Life Sci.* **61**, 1546–1561.
- Fang, S. Y., Jensen, J. P., Ludwig, R. L., Vousden, K. H. and Weissman, A. M.** (2000). Mdm2 is a RING finger-dependent ubiquitin protein ligase for itself and p53. *Journal of Biological*

- Chemistry* **275**, 8945–8951.
- Feng, H., Zhong, W., Punkosdy, G., Gu, S., Zhou, L., Seabolt, E. K. and Kipreos, E. T.** (1999). CUL-2 is required for the G1-to-S-phase transition and mitotic chromosome condensation in *Caenorhabditis elegans*. *Nat Cell Biol* **1**, 486–492.
- Fernandes, N., Bailey, D. E., VanVranken, D. L. and Allbritton, N. L.** (2007). Use of Docking Peptides to Design Modular Substrates with High Efficiency for Mitogen-Activated Protein Kinase Extracellular Signal-Regulated Kinase. *ACS Chem. Biol.* **2**, 665–673.
- Finley, D.** (2009). Recognition and Processing of Ubiquitin-Protein Conjugates by the Proteasome. *Annu. Rev. Biochem.* **78**, 477–513.
- Finley, D., Chen, X. and Walters, K. J.** (2016). Gates, Channels, and Switches: Elements of the Proteasome Machine. *Trends in Biochemical Sciences* **41**, 77–93.
- Fox, P. M., Vought, V. E., Hanazawa, M., Lee, M. H., Maine, E. M. and Schedl, T.** (2011). Cyclin E and CDK-2 regulate proliferative cell fate and cell cycle progression in the *C. elegans* germline. *Development* **138**, 2223–2234.
- Fox, C. A., Sheets, M. D. and Wickens, M. P.** (1989). Poly(A) addition during maturation of frog oocytes: distinct nuclear and cytoplasmic activities and regulation by the sequence UUUUUUAU. *Genes Dev.* **3**, 2151–2162.
- Francis, R., Barton, M. K., Kimble, J. and Schedl, T.** (1995a). gld-1, a tumor suppressor gene required for oocyte development in *Caenorhabditis elegans*. *Genetics* **139**, 579–606.
- Francis, R., Maine, E. and Schedl, T.** (1995b). Analysis of the multiple roles of gld-1 in germline development: interactions with the sex determination cascade and the glp-1 signaling pathway. *Genetics* **139**, 607–630.
- Frisone, P., Pradella, D., Di Matteo, A., Belloni, E., Ghigna, C. and Paronetto, M. P.** (2015). SAM68: Signal Transduction and RNA Metabolism in Human Cancer. *BioMed Research International* **2015**, 1–14.
- Frokjaer-Jensen, C., Davis, M. W., Ailion, M. and Jorgensen, E. M.** (2012). Improved Mos1-mediated transgenesis in *C. elegans*. *Nat Meth* **9**, 117–118.
- Furuta, T., Tuck, S., Kirchner, J., Koch, B., Auty, R., Kitagawa, R., Rose, A. M. and Greenstein, D.** (2000). EMB-30: an APC4 homologue required for metaphase-to-anaphase transitions during meiosis and mitosis in *Caenorhabditis elegans*. *Mol. Biol. Cell* **11**, 1401–1419.
- Fuster, J. J., Gonzalez, J. M., Edo, M. D., Viana, R., Boya, P., Cervera, J., Verges, M., Rivera, J. and Andres, V.** (2010). Tumor suppressor p27Kip1 undergoes endolysosomal degradation through its interaction with sorting nexin 6. *The FASEB Journal* **24**, 2998–3009.
- Galan, J. M. and Peter, M.** (1999). Ubiquitin-dependent degradation of multiple F-box proteins by an autocatalytic mechanism. *Proceedings of the National Academy of Sciences* **96**, 9124–9129.
- Galarneau, A. and Richard, S.** (2009). The STAR RNA binding proteins GLD-1, QKI, SAM68 and SLM-2 bind bipartite RNA motifs. *BMC Mol Biol* **10**, 47–12.
- Garai, A., Zeke, A., Gogl, G., Toero, I., Foerdos, F., Blankenburg, H., Barkai, T., Varga, J., Alexa, A., Emig, D., et al.** (2012). Specificity of Linear Motifs That Bind to a Common Mitogen-Activated Protein Kinase Docking Groove. *Sci Signal* **5**, –ra74.
- Garneau, N. L., Wilusz, J. and Wilusz, C. J.** (2007). The highways and byways of mRNA decay. *Nat. Rev. Mol. Cell Biol.* **8**, 113–126.

- Gebauer, F. and Hentze, M. W.** (2004). Molecular mechanisms of translational control. *Nat. Rev. Mol. Cell Biol.* **5**, 827–835.
- Gietz, R. D. and Woods, R. A.** (2002). Transformation of yeast by lithium acetate/single-stranded carrier DNA/polyethylene glycol method. *Meth. Enzymol.* **350**, 87–96.
- Gilbert, S. F.** (2006). *Developmental Biology*. Sunderland, MA: Sinauer Associates, Inc.
- Goodwin, E. B., Hofstra, K., Hurney, C. A., Mango, S. and Kimble, J.** (1997). A genetic pathway for regulation of tra-2 translation. *Development* **124**, 749–758.
- Gordon, J. A.** (1991). Use of vanadate as protein-phosphotyrosine phosphatase inhibitor. In *Protein Phosphorylation Part B: Analysis of Protein Phosphorylation, Protein Kinase Inhibitors, and Protein Phosphatases*, pp. 477–482. Elsevier.
- Gorla, L., Cantù, M., Miccichè, F., Patelli, C., Mondellini, P., Pierotti, M. A. and Bongarzone, I.** (2006). RET oncoproteins induce tyrosine phosphorylation changes of proteins involved in RNA metabolism. *Cellular Signalling* **18**, 2272–2282.
- Gönczy, P., Echeverri, C., Oegema, K. and Coulson, A.** (2000). Functional genomic analysis of cell division in *C. elegans* using RNAi of genes on chromosome III. *Nature* **408**, 331–336.
- Grant, B. and Hirsh, D.** (1999). Receptor-mediated endocytosis in the *Caenorhabditis elegans* oocyte. *Mol. Biol. Cell* **10**, 4311–4326.
- Greenstein, D., Hird, S., Plasterk, R., Andachi, Y., Kohara, Y., Wang, B., Finney, M. and Ruvkun, G.** (1994). Targeted Mutations in the *Caenorhabditis elegans* Pou Homeo Box Gene Ceh-18 Cause Defects in Oocyte Cell-Cycle Arrest, Gonad Migration, and Epidermal Differentiation. *Genes Dev.* **8**, 1935–1948.
- Guinamard, R., Fougereau, M. and Seckinger, P.** (1997). The SH3 Domain of Bruton's Tyrosine Kinase Interacts with Vav, Sam68 and EWS. *Scandinavian Journal of Immunology* **45**, 587–595.
- Gumienny, T. L., Lambie, E., Hartwig, E., Horvitz, H. R. and Hengartner, M. O.** (1999). Genetic control of programmed cell death in the *Caenorhabditis elegans* hermaphrodite germline. *Development* **126**, 1011–1022.
- Gupta, P., Leahul, L., Wang, X., Wang, C., Bakos, B., Jasper, K. and Hansen, D.** (2015). Proteasome regulation of the chromodomain protein MRG-1 controls the balance between proliferative fate and differentiation in the *C. elegans* germ line. *Development* **142**, 291–302.
- Güven-Ozkan, T., Nishi, Y., Robertson, S. M. and Lin, R.** (2008). Global transcriptional repression in *C. elegans* germline precursors by regulated sequestration of TAF-4. *Cell* **135**, 149–160.
- Güven-Ozkan, T., Robertson, S. M., Nishi, Y. and Lin, R.** (2010). zif-1 translational repression defines a second, mutually exclusive OMA function in germline transcriptional repression. *Development* **137**, 3373–3382.
- Haegebarth, A., Heap, D., Bie, W., Derry, J. J., Richard, S. and Tyner, A. L.** (2004). The nuclear tyrosine kinase BRK/Sik phosphorylates and inhibits the RNA-binding activities of the Sam68-like mammalian proteins SLM-1 and SLM-2. *Journal of Biological Chemistry* **279**, 54398–54404.
- Hajnal, A. and Berset, T.** (2002). The *C. elegans* MAPK phosphatase LIP-1 is required for the G(2)/M meiotic arrest of developing oocytes. *The EMBO Journal* **21**, 4317–4326.
- Hansen, D. and Schedl, T.** (2006). The regulatory network controlling the proliferation–meiotic

- entry decision in the *Caenorhabditis elegans* germ line. *Current Topics in Developmental Biology*.
- Hansen, D. and Schedl, T.** (2012). Stem Cell Proliferation Versus Meiotic Fate Decision in *Caenorhabditis elegans*. In *Germ Cell Development in C. elegans*. Ed. Schedl, T., pp. 71–99. New York, NY: Springer New York.
- Hansen, D., Wilson-Berry, L., Dang, T. and Schedl, T.** (2004). Control of the proliferation versus meiotic development decision in the *C. elegans* germline through regulation of GLD-1 protein accumulation. *Development* **131**, 93–104.
- Harper, N. C., Rillo, R., Jover-Gil, S., Assaf, Z. J., Bhalla, N. and Dernburg, A. F.** (2011). Pairing centers recruit a Polo-like kinase to orchestrate meiotic chromosome dynamics in *C. elegans*. *Developmental Cell* **21**, 934–947.
- Hasegawa, E., Karashima, T., Sumiyoshi, E. and Yamamoto, M.** (2006). *C. elegans* CPB-3 interacts with DAZ-1 and functions in multiple steps of germline development. *Developmental Biology* **295**, 689–699.
- Haupt, Y., Maya, R., Kazaz, A. and Oren, M.** (1997). Mdm2 promotes the rapid degradation of p53. *Nature* **387**, 296–299.
- Hay, N. and Sonenberg, N.** (2004). Upstream and downstream of mTOR. *Genes Dev.* **18**, 1926–1945.
- Heinrich, S. U. and Lindquist, S.** (2011). Protein-only mechanism induces self-perpetuating changes in the activity of neuronal *Aplysia* cytoplasmic polyadenylation element binding protein (CPEB). *Proc. Natl. Acad. Sci. U.S.A.* **108**, 2999–3004.
- Henderson, S. T., Gao, D., Lambie, E. J. and Kimble, J.** (1994). lag-2 may encode a signaling ligand for the GLP-1 and LIN-12 receptors of *C. elegans*. *Development* **120**, 2913–2924.
- Hillers, K. J., Jantsch, V., Martinez-Perez, E. and Yanowitz, J. L.** (2015). Meiosis. *WormBook*, Ed. The *C. elegans* Research Community
- Hinnebusch, A. G., Ivanov, I. P. and Sonenberg, N.** (2016). Translational control by 5'-untranslated regions of eukaryotic mRNAs. *Science* **352**, 1413–1416.
- Hirsh, D., Oppenheim, D. and Klass, M.** (1976). Development of the reproductive system of *Caenorhabditis elegans*. *Developmental Biology*.
- Hodgkin, J., Horvitz, H. R. and Brenner, S.** (1979). Nondisjunction Mutants of the Nematode *Caenorhabditis elegans*. *Genetics* **91**, 67–94.
- Huang, X., Luan, B., Wu, J. and Shi, Y.** (2016). An atomic structure of the human 26S proteasome. *Nature Publishing Group* **23**, 778–785.
- Hubbard, E. J. and Greenstein, D.** (2005). Introduction to the germ line (September 1, 2005), *WormBook*, Ed. The *C. elegans* Research Community
- Hubbard, E. J., Wu, G., Kitajewski, J. and Greenwald, I.** (1997). *sel-10*, a negative regulator of lin-12 activity in *Caenorhabditis elegans*, encodes a member of the CDC4 family of proteins. *Genes Dev.* **11**, 3182–3193.
- Hubert, A. and Anderson, P.** (2009). The *C. elegans* sex determination gene *laf-1* encodes a putative DEAD-box RNA helicase. *Developmental Biology* **330**, 358–367.
- Hunter, T.** (2007). The Age of Crosstalk: Phosphorylation, Ubiquitination, and Beyond. *Molecular Cell* **28**, 730–738.

- Huyer, G., Liu, S., Kelly, J., Moffat, J., Payette, P., Kennedy, B., Tsaprailis, G., Gresser, M. J. and Ramachandran, C.** (1997). Mechanism of inhibition of protein-tyrosine phosphatases by vanadate and pervanadate. *Journal of Biological Chemistry* **272**, 843–851.
- Igea, A. and Mendez, R.** (2010). Meiosis requires a translational positive loop where CPEB1 ensues its replacement by CPEB4. *The EMBO Journal* **29**, 2182–2193.
- Ignatochkina, A. V., Takagi, Y., Liu, Y., Nagata, K. and Ho, C. K.** (2015). The messenger RNA decapping and recapping pathway in *Trypanosoma*. *Proceedings of the National Academy of Sciences* **112**, 6967–6972.
- Igreja, C. and Izaurralde, E.** (2011). CUP promotes deadenylation and inhibits decapping of mRNA targets. *Genes Dev.* **25**, 1955–1967.
- Ikematsu, N., Yoshida, Y., Kawamura-Tsuzuku, J., Ohsugi, M., Onda, M., Hirai, M., Fujimoto, J. and Yamamoto, T.** (1999). Tob2, a novel anti-proliferative Tob/BTG1 family member, associates with a component of the CCR4 transcriptional regulatory complex capable of binding cyclin-dependent kinases. *Oncogene* **18**, 7432–7441.
- Ivshina, M., Lasko, P. and Richter, J. D.** (2014). Cytoplasmic Polyadenylation Element Binding Proteins in Development, Health, and Disease. *Annu. Rev. Cell Dev. Biol.* **30**, 393–415.
- Jackson, P. K., Eldridge, A. G., Freed, E., Furstenthal, L., Hsu, J. Y., Kaiser, B. K. and Reimann, J.** (2000). The lore of the RINGs: substrate recognition and catalysis by ubiquitin ligases. *Trends in Cell Biology* **10**, 429–439.
- Jackson, R. J., Hellen, C. U. T. and Pestova, T. V.** (2010). The mechanism of eukaryotic translation initiation and principles of its regulation. *Nat. Rev. Mol. Cell Biol.* **11**, 113–127.
- Jäger, S., Schwartz, H. T., Horvitz, H. R. and Conradt, B.** (2004). The *Caenorhabditis elegans* F-box protein SEL-10 promotes female development and may target FEM-1 and FEM-3 for degradation by the proteasome. *Proceedings of the National Academy of Sciences* **101**, 12549–12554.
- Jalkanen, A. L., Coleman, S. J. and Wilusz, J.** (2014). Determinants and implications of mRNA poly(A) tail size – Does this protein make my tail look big? *Seminars in Cell & Developmental Biology* **34**, 24–32.
- Jan, E., Motzny, C. K., Graves, L. E. and Goodwin, E. B.** (1999). The STAR protein, GLD-1, is a translational regulator of sexual identity in *Caenorhabditis elegans*. *The EMBO Journal* **18**, 258–269.
- Jan, E., Yoon, J. W., Walterhouse, D., Iannaccone, P. and Goodwin, E. B.** (1997). Conservation of the *C.elegans* tra-2 3'UTR translational control. *The EMBO Journal* **16**, 6301–6313.
- Jaramillo-Lambert, A., Ellefson, M., Villeneuve, A. M. and Engebrecht, J.** (2007). Differential timing of S phases, X chromosome replication, and meiotic prophase in the *C. elegans* germ line. *Developmental Biology* **308**, 206–221.
- Jedamzik, B.** (2009). mRNA targets of GLD-3 in *Caenorhabditis elegans*. PhD. Thesis at the Faculty of Science, Technical University Dresden
- Jedamzik, B. and Eckmann, C. R.** (2009). Analysis of in vivo protein complexes by coimmunoprecipitation from *Caenorhabditis elegans*. *Cold Spring Harbor Protocols*.
- Jeong, J., Verheyden, J. M. and Kimble, J.** (2011). Cyclin E and Cdk2 Control GLD-1, the Mitosis/Meiosis Decision, and Germline Stem Cells in *Caenorhabditis elegans*. *PLoS Genetics* **7**, e1001348–14.

- Jeske, M., Moritz, B., Anders, A. and Wahle, E.** (2010). Smaug assembles an ATP-dependent stable complex repressing nanos mRNA translation at multiple levels. *The EMBO Journal* **30**, 90–103.
- Jin, J., Cardozo, T., Lovering, R. C., Elledge, S. J., Pagano, M. and Harper, J. W.** (2004). Systematic analysis and nomenclature of mammalian F-box proteins. *Genes Dev.* **18**, 2573–2580.
- Jones, A. R. and Schedl, T.** (1995). Mutations in *gld-1*, a female germ cell-specific tumor suppressor gene in *Caenorhabditis elegans*, affect a conserved domain also found in Src-associated protein Sam68. *Genes Dev.* **9**, 1491–1504.
- Jones, A. R., Francis, R. and Schedl, T.** (1996). GLD-1, a cytoplasmic protein essential for oocyte differentiation, shows stage- and sex-specific expression during *Caenorhabditis elegans* germline development. *Developmental Biology* **180**, 165–183.
- Jungkamp, A.-C., Stoeckius, M., Mecnas, D., Grün, D., Mastrobuoni, G., Kempa, S. and Rajewsky, N.** (2011). In Vivo and Transcriptome-wide Identification of RNA Binding Protein Target Sites. *Molecular Cell* **44**, 828–840.
- Kadyk, L. C. and Kimble, J.** (1998). Genetic regulation of entry into meiosis in *Caenorhabditis elegans*. *Development* **125**, 1803–1813.
- Kadyrova, L. Y., Habara, Y., Lee, T. H. and Wharton, R. P.** (2007). Translational control of maternal Cyclin B mRNA by Nanos in the *Drosophila* germline. *Development* **134**, 1519–1527.
- Kahn, N. W., Rea, S. L., Moyle, S., Kell, A. and Johnson, T. E.** (2008). Proteasomal dysfunction activates the transcription factor SKN-1 and produces a selective oxidative-stress response in *Caenorhabditis elegans*. *Biochem. J.* **409**, 205–213.
- Kamath, R. S. and Ahringer, J.** (2003). Genome-wide RNAi screening in *Caenorhabditis elegans*. *Methods* **30**, 313–321.
- Kamath, R. S., Fraser, A. G., Dong, Y., Poulin, G. and Durbin, R.** (2003). Systematic functional analysis of the *Caenorhabditis elegans* genome using RNAi. *Nature* **421**, 231–237.
- Karashima, T., Sugimoto, A. and Yamamoto, M.** (2000). *Caenorhabditis elegans* homologue of the human azoospermia factor DAZ is required for oogenesis but not for spermatogenesis. *Development* **127**, 1069–1079.
- Kaul, G., Pattan, G. and Rafeequi, T.** (2011). Eukaryotic elongation factor-2 (eEF2): its regulation and peptide chain elongation. *Cell Biochemistry and Function* **29**, 227–234.
- Kaushik, S. and Cuervo, A. M.** (2012). Chaperone-mediated autophagy: a unique way to enter the lysosome world. *Trends in Cell Biology* **22**, 407–417.
- Khan, M. R., Li, L., Pérez-Sánchez, C., Saraf, A., Florens, L., Slaughter, B. D., Unruh, J. R. and Si, K.** (2015). Amyloidogenic Oligomerization Transforms *Drosophila* Orb2 from a Translation Repressor to an Activator. *Cell* **163**, 1468–1483.
- Kidd, I. M. and Emery, V. C.** (1993). The use of baculoviruses as expression vectors. *Applied Biochemistry and Biotechnology* **42**, 137–159.
- Killian, D. J. and Hubbard, E. J. A.** (2005). *Caenorhabditis elegans* germline patterning requires coordinated development of the somatic gonadal sheath and the germ line. *Developmental Biology* **279**, 322–335.
- Killian, D. J., Harvey, E., Johnson, P., Otori, M., Mitani, S. and Xue, D.** (2008). SKR-1, a homolog

- of Skp1 and a member of the SCFSEL-10 complex, regulates sex-determination and LIN-12/Notch signaling in *C. elegans*. *Developmental Biology* **322**, 322–331.
- Kim, J. H. and Richter, J. D.** (2006). Opposing polymerase-deadenylase activities regulate cytoplasmic polyadenylation. *Molecular Cell* **24**, 173–183.
- Kim, J. H. and Richter, J. D.** (2007). RINGO/cdk1 and CPEB mediate poly(A) tail stabilization and translational regulation by ePAB. *Genes Dev.* **21**, 2571–2579.
- Kim, S., Spike, C. and Greenstein, D.** (2012). Control of Oocyte Growth and Meiotic Maturation in *Caenorhabditis elegans*. In *Germ Cell Development in C. elegans* (ed. Schedl, T., pp. 277–320. New York, NY: Springer New York.
- Kimble, J. and Crittenden, S. L.** (2007). Controls of germline stem cells, entry into meiosis, and the sperm/oocyte decision in *Caenorhabditis elegans*. *Annu. Rev. Cell Dev. Biol.* **23**, 405–433.
- Kimble, J. and Hirsh, D.** (1979). The postembryonic cell lineages of the hermaphrodite and male gonads in *Caenorhabditis elegans*. *Developmental Biology* **70**, 396–417.
- Kimble, J. and Ward, S. A.** (1988). Germ-line Development and Fertilization. In *The Nematode Caenorhabditis elegans* (ed. Wood, W. B., Cold Spring Harbor Laboratory Press.
- Kimble, J. E. and White, J. G.** (1981). On the Control of Germ-Cell Development in *Caenorhabditis elegans*. *Developmental Biology* **81**, 208–219.
- Kinoshita, E., Kinoshita-Kikuta, E. and Koike, T.** (2015). Advances in Phos-tag-based methodologies for separation and detection of the phosphoproteome. *BBA - Proteins and Proteomics* **1854**, 601–608.
- Kinoshita, E., Kinoshita-Kikuta, E., Takiyama, K. and Koike, T.** (2006). Phosphate-binding tag, a new tool to visualize phosphorylated proteins. *Molecular & Cellular Proteomics* **5**, 749–757.
- Kipreos, E. T., Lander, L. E., Wing, J. P., He, W. W. and Hedgecock, E. M.** (1996). *cul-1* is required for cell cycle exit in *C. elegans* and identifies a novel gene family. *Cell* **85**, 829–839.
- Kipreos, E. T. and Pagano, M.** (2000). The F-box protein family. *Genome Biol* **1**.
- Kipreos, E. T., Gohel, S. P. and Hedgecock, E. M.** (2000). The *C. elegans* F-box/WD-repeat protein LIN-23 functions to limit cell division during development. *Development* **127**, 5071–5082.
- Kisselev, A. F., Akopian, T. N. and Goldberg, A. L.** (1998). Range of sizes of peptide products generated during degradation of different proteins by archaeal proteasomes. *Journal of Biological Chemistry* **273**, 1982–1989.
- Klass, M., Wolf, N. and Hirsh, D.** (1976). Development of Male Reproductive-System and Sexual Transformation in Nematode *Caenorhabditis elegans*. *Developmental Biology* **52**, 1–18.
- Kojima, S., Sher-Chen, E. L. and Green, C. B.** (2012). Circadian control of mRNA polyadenylation dynamics regulates rhythmic protein expression. *Genes Dev.* **26**, 2724–2736.
- Komander, D.** (2009). The emerging complexity of protein ubiquitination. *Biochem. Soc. Trans.* **37**, 937–953.
- Komander, D. and Rape, M.** (2012). The Ubiquitin Code. *Annu. Rev. Biochem.* **81**, 203–229.
- Komander, D., Clague, M. J. and Urbé, S.** (2009). Breaking the chains: structure and function of the deubiquitinases. *Nat. Rev. Mol. Cell Biol.* **10**, 550–563.

- Kondrashov, A. S.** (1993). Classification of hypotheses on the advantage of amphimixis. *J. Hered.* **84**, 372–387.
- Kong, J. and Lasko, P.** (2012). Translational control in cellular and developmental processes. *Nat Rev Genet* **13**, 383–394.
- Kraemer, B., Crittenden, S., Gallegos, M., Moulder, G., Barstead, R., Kimble, J. and Wickens, M.** (1999). NANOS-3 and FBF proteins physically interact to control the sperm-oocyte switch in *Caenorhabditis elegans*. *Curr. Biol.* **9**, 1009–1018.
- Kuersten, S. and Goodwin, E. B.** (2003). The power of the 3' UTR: translational control and development. *4*, 626–637.
- Krüttner, S., Stepien, B., Noordermeer, J. N., Mommaas, M. A., Mechtler, K., Dickson, B. J. and Keleman, K.** (2012). *Drosophila* CPEB Orb2A Mediates Memory Independent of Its RNA-Binding Domain. *Neuron* **76**, 383–395.
- Kupinski, A.** (2008). The Ste20 kinase GCK-3 is essential for *C. elegans* development and regulates centrosome maturation during meiosis. PhD. Thesis at the Faculty of Science, Technical University Dresden
- Kuwabara, P. E.** (2003). The multifaceted *C. elegans* major sperm protein: an ephrin signaling antagonist in oocyte maturation. *Genes Dev.* **17**, 155–161.
- Lackner, M. R. and Kim, S. K.** (1998). Genetic analysis of the *Caenorhabditis elegans* MAP kinase gene mpk-1. *Genetics* **150**, 103–117.
- Lai, Y. J., Lin, F. M., Chuang, M. J., Shen, H. J. and Wang, T. F.** (2011). Genetic Requirements and Meiotic Function of Phosphorylation of the Yeast Axial Element Protein Red1. *Molecular and Cellular Biology* **31**, 912–923.
- Lamont, L. B., Crittenden, S. L., Bernstein, D., Wickens, M. and Kimble, J.** (2004). FBF-1 and FBF-2 Regulate the Size of the Mitotic Region in the *C. elegans* Germline. *Developmental Cell* **7**, 697–707.
- Lantz, V., Chang, J. S., Horabin, J. I., Bopp, D. and Schedl, P.** (1994). The *Drosophila* orb RNA-binding protein is required for the formation of the egg chamber and establishment of polarity. *Genes Dev.* **8**, 598–613.
- Lapasset, L., Pradet-Balade, B., Lozano, J.-C., Peaucellier, G. and Picard, A.** (2005). Nuclear envelope breakdown may deliver an inhibitor of protein phosphatase 1 which triggers cyclin B translation in starfish oocytes. *Developmental Biology* **285**, 200–210.
- Lee, M. H. and Schedl, T.** (2001). Identification of in vivo mRNA targets of GLD-1, a maxi-KH motif containing protein required for *C. elegans* germ cell development. *Genes Dev.* **15**, 2408–2420.
- Lee, M.-H. and Schedl, T.** (2004). Translation repression by GLD-1 protects its mRNA targets from nonsense-mediated mRNA decay in *C. elegans*. *Genes Dev.* **18**, 1047–1059.
- Lee, M.-H. and Schedl, T.** (2010). *C. elegans* STAR proteins, GLD-1 and ASD-2, regulate specific RNA targets to control development. *Adv. Exp. Med. Biol.* **693**, 106–122.
- Lee, M.-H., Hook, B., Pan, G., Kershner, A. M., Merritt, C., Seydoux, G., Thomson, J. A., Wickens, M. and Kimble, J.** (2007a). Conserved regulation of MAP kinase expression by PUF RNA-binding proteins. *PLoS Genetics* **3**, e233.
- Lee, M.-H., Ohmachi, M., Arur, S., Nayak, S., Francis, R., Church, D., Lambie, E. and Schedl, T.** (2007b). Multiple functions and dynamic activation of MPK-1 extracellular signal-regulated

- kinase signaling in *Caenorhabditis elegans* germline development. *Genetics* **177**, 2039–2062.
- Lints, R. and Hall, D. H.** *WormAtlas*. <http://www.wormatlas.org>
- Liu, J., Vasudevan, S. and Kipreos, E. T.** (2004). CUL-2 and ZYG-11 promote meiotic anaphase II and the proper placement of the anterior-posterior axis in *C. elegans*. *Development* **131**, 3513–3525.
- Lopez, A. L., III, Chen, J., Joo, H.-J., Drake, M., Shidate, M., Kseib, C. and Arur, S.** (2013). DAF-2 and ERK Couple Nutrient Availability to Meiotic Progression during *Caenorhabditis elegans* Oogenesis. *Developmental Cell* **27**, 227–240.
- Lu, Y., Lee, B.-H., King, R. W., Finley, D. and Kirschner, M. W.** (2015). Substrate degradation by the proteasome: a single-molecule kinetic analysis. *Science* **348**, 1250834.
- Lublin, A. L. and Evans, T. C.** (2007). The RNA-binding proteins PUF-5, PUF-6, and PUF-7 reveal multiple systems for maternal mRNA regulation during *C. elegans* oogenesis. *Developmental Biology* **303**, 635–649.
- Lui, D. Y. and Colaiácovo, M. P.** (2012). Meiotic Development in *Caenorhabditis elegans*. In *Germ Cell Development in C. elegans* (ed. Schedl, T., pp. 133–170. New York, NY: Springer New York.
- Luitjens, C., Gallegos, M., Kraemer, B., Kimble, J. and Wickens, M.** (2000). CPEB proteins control two key steps in spermatogenesis in *C. elegans*. *Genes Dev.* **14**, 2596–2609.
- Lukong, K. E., Larocque, D., Tyner, A. L. and Richard, S.** (2005). Tyrosine Phosphorylation of Sam68 by Breast Tumor Kinase Regulates Intranuclear Localization and Cell Cycle Progression. *Journal of Biological Chemistry* **280**, 38639–38647.
- MacDonald, L. D., Knox, A. and Hansen, D.** (2008). Proteasomal Regulation of the Proliferation vs. Meiotic Entry Decision in the *Caenorhabditis elegans* Germ Line. *Genetics* **180**, 905–920.
- Majumdar, A., Cesario, W. C., White-Grindley, E., Jiang, H., Ren, F., Khan, M. R., Li, L., Choi, E. M.-L., Kannan, K., Guo, F., et al.** (2012). Critical Role of Amyloid-like Oligomers of *Drosophila* Orb2 in the Persistence of Memory. *Cell* **148**, 515–529.
- Marin, V. A. and Evans, T. C.** (2003). Translational repression of a *C. elegans* Notch mRNA by the STAR/KH domain protein GLD-1. *Development* **130**, 2623–2632.
- Maruyama, R., Endo, S., Sugimoto, A. and Yamamoto, M.** (2005). *Caenorhabditis elegans* DAZ-1 is expressed in proliferating germ cells and directs proper nuclear organization and cytoplasmic core formation during oogenesis. *Developmental Biology* **277**, 142–154.
- Mathews, M. B. and Sonenberg, N.** (2007). Origins and principles of translational control. In *Translational Control in Biology and Medicine*. Cold Spring Harbor Monograph Archive, **48**
- Matter, N., Herrlich, P. and König, H.** (2002). Signal-dependent regulation of splicing via phosphorylation of Sam68. *Nature* **420**, 691–695.
- Mauxion, F., Chen, C.-Y. A., Séraphin, B. and Shyu, A.-B.** (2009). BTG/TOB factors impact deadenylases. *Trends in Biochemical Sciences* **34**, 640–647.
- McCarter, J., Bartlett, B., Dang, T. and Schedl, T.** (1997). Soma-germ cell interactions in *Caenorhabditis elegans*: Multiple events of hermaphrodite germline development require the somatic sheath tend spermathecal lineages. *Developmental Biology* **181**, 121–143.
- McCarter, J., Bartlett, B., Dang, T. and Schedl, T.** (1999). On the control of oocyte meiotic maturation and ovulation in *Caenorhabditis elegans*. *Developmental Biology* **205**, 111–128.

- McGovern, M., Voutev, R., Maciejowski, J., Corsi, A. K. and Hubbard, E. J. A.** (2009). A “latent niche” mechanism for tumor initiation. *Proc. Natl. Acad. Sci. U.S.A.* **106**, 11617–11622.
- McGrew, L. L. and Richter, J. D.** (1990). Translational Control by Cytoplasmic Polyadenylation During *Xenopus* Oocyte Maturation - Characterization of *Cis* and *Trans* Elements and Regulation by Cyclin/Mpf. *The EMBO Journal* **9**, 3743–3751.
- Meerstein, L.** (2009). Polyadenylation mechanisms in *Caenorhabditis elegans*: Measuring the poly(A) tail length of *in vivo* mRNAs and screening for protein interactors of the presumed poly(A) tail regulator CPB-3. B.Sc. Thesis at Technical University Dresden
- Mendez, R., Barnard, D. and Richter, J. D.** (2002). Differential mRNA translation and meiotic progression require Cdc2-mediated CPEB destruction. *The EMBO Journal* **21**, 1833–1844.
- Mendez, R., Hake, L. E., Andresson, T., Littlepage, L. E., Ruderman, J. V. and Richter, J. D.** (2000). Phosphorylation of CPE binding factor by Eg2 regulates translation of c-mos mRNA. *Nature* **404**, 302–307.
- Merkel, D. J., Wells, S. B., Hilburn, B. C., Elazzouzi, F., Pérez-Alvarado, G. C. and Lee, B. M.** (2013). The C-Terminal Region of Cytoplasmic Polyadenylation Element Binding Protein Is a ZZ Domain with Potential for Protein–Protein Interactions. *Journal of Molecular Biology* **425**, 2015–2026.
- Merlet, J., Burger, J., Tavernier, N., Richaudeau, B., Gomes, J. E. and Pintard, L.** (2010). The CRL2LRR-1 ubiquitin ligase regulates cell cycle progression during *C. elegans* development. *Development* **137**, 3857–3866.
- Merritt, C., Rasoloson, D., Ko, D. and Seydoux, G.** (2008). 3′ UTRs Are the Primary Regulators of Gene Expression in the *C. elegans* Germline. *Current Biology* **18**, 1476–1482.
- Mootz, D., Ho, D. M. and Hunter, C. P.** (2004). The STAR/Maxi-KH domain protein GLD-1 mediates a developmental switch in the translational control of *C. elegans* PAL-1. *Development* **131**, 3263–3272.
- Morgan, D. E., Crittenden, S. L. and Kimble, J.** (2010). The *C. elegans* adult male germline: Stem cells and sexual dimorphism. *Developmental Biology* **346**, 204–214.
- Moussian, B. and Roth, S.** (2005). Dorsoventral Axis Formation in the Drosophila Embryo—Shaping and Transducing a Morphogen Gradient. *Current Biology* **15**, R887–R899.
- Mukherjee, C., Patil, D. P., Kennedy, B. A., Bakthavachalu, B., Bundschuh, R. and Schoenberg, D. R.** (2012). Identification of Cytoplasmic Capping Targets Reveals a Role for Cap Homeostasis in Translation and mRNA Stability. *CellReports* **2**, 674–684.
- Nadarajan, S., Mohideen, F., Tzur, Y. B., Ferrandiz, N., Crawley, O., Montoya, A., Faull, P., Snijders, A. P., Cutillas, P. R., Jambhekar, A., et al.** (2016). The MAP kinase pathway coordinates crossover designation with disassembly of synaptonemal complex proteins during meiosis. *Elife* **5**, e12039.
- Nakamura, A., Sato, K. and Hanyu-Nakamura, K.** (2004). *Drosophila* cup is an eIF4E binding protein that associates with Bruno and regulates oskar mRNA translation in oogenesis. *Developmental Cell* **6**, 69–78.
- Nakanishi, T., Kumagai, S., Kimura, M., Watanabe, H., Sakurai, T., Kimura, M., Kashiwabara, S.-I. and Baba, T.** (2007). Disruption of mouse poly(A) polymerase mGLD-2 does not alter polyadenylation status in oocytes and somatic cells. *Biochemical and Biophysical Research Communications* **364**, 14–19.
- Nakayama, K. I. and Nakayama, K.** (2006). Ubiquitin ligases: cell-cycle control and cancer. *Nat*

- Rev Cancer* **6**, 369–381.
- Nash, P., Tang, X., Orlicky, S., Chen, Q., Gertler, F. B., Mendenhall, M. D., Sicheri, F., Pawson, T. and Tyers, M.** (2001). Multisite phosphorylation of a CDK inhibitor sets a threshold for the onset of DNA replication. *Nature* **414**, 514–521.
- Nayak, S., Santiago, F. E., Jin, H., Lin, D., Schedl, T. and Kipreos, E. T.** (2002). The *Caenorhabditis elegans* Skp1-related gene family: Diverse functions in cell proliferation, morphogenesis, and meiosis. *Curr. Biol.* **12**, 277–287.
- Nelson, M. R., Leidal, A. M. and Smibert, C. A.** (2004). *Drosophila* Cup is an eIF4E-binding protein that functions in Smaug-mediated translational repression. *The EMBO Journal* **23**, 150–159.
- Nir, R., Grossman, R., Paroush, Z. and Volk, T.** (2012). Phosphorylation of the *Drosophila melanogaster* RNA-Binding Protein HOW by MAPK/ERK Enhances Its Dimerization and Activity. *PLoS Genetics* **8**, e1002632–15.
- Nishi, Y., Rogers, E., Robertson, S. M. and Lin, R.** (2008). Polo kinases regulate *C. elegans* embryonic polarity via binding to DYRK2-primed MEX-5 and MEX-6. *Development* **135**, 687–697.
- Noble, D. C., Aoki, S. T., Ortiz, M. A., Kim, K. W., Verheyden, J. M. and Kimble, J.** (2016). Genomic Analyses of Sperm Fate Regulator Targets Reveal a Common Set of Oogenic mRNAs in *Caenorhabditis elegans*. *Genetics* **202**, 221–234.
- Norvell, A., Wong, J., Randolph, K. and Thompson, L.** (2015). Wispy and Orb cooperate in the cytoplasmic polyadenylation of localized gurken mRNA. *Dev. Dyn.* **244**, 1276–1285.
- Nousch, M. and Eckmann, C. R.** (2013). Translational control in the *Caenorhabditis elegans* germ line. *Adv. Exp. Med. Biol.* **757**, 205–247.
- Nousch, M., Techritz, N., Hampel, D., Millonigg, S. and Eckmann, C. R.** (2013). The Ccr4-Not deadenylase complex constitutes the main poly(A) removal activity in *C. elegans*. *J Cell Sci* **126**, 4274–4285.
- Ohno, G., Hagiwara, M. and Kuroyanagi, H.** (2008). STAR family RNA-binding protein ASD-2 regulates developmental switching of mutually exclusive alternative splicing *in vivo*. *Genes Dev.* **22**, 360–374.
- Orsborn, A. M., Li, W., McEwen, T. J., Mizuno, T., Kuzmin, E., Matsumoto, K. and Bennett, K. L.** (2007). GLH-1, the *C. elegans* P granule protein, is controlled by the JNK KGB-1 and by the COP9 subunit CSN-5. *Development* **134**, 3383–3392.
- Ou, C.-Y., Lin, Y.-F., Chen, Y.-J. and Chien, C.-T.** (2002). Distinct protein degradation mechanisms mediated by Cul1 and Cul3 controlling Ci stability in *Drosophila* eye development. *Genes Dev.* **16**, 2403–2414.
- Parker, G. A., Baker, R. R. and Smith, V. G.** (1972). The origin and evolution of gamete dimorphism and the male-female phenomenon. *Journal of Theoretical Biology* **36**, 529–553.
- Paronetto, M. P., Farini, D., Sammarco, I., Maturo, G., Vespasiani, G., Geremia, R., Rossi, P. and Sette, C.** (2004). Expression of a Truncated Form of the c-Kit Tyrosine Kinase Receptor and Activation of Src Kinase in Human Prostatic Cancer. *The American Journal of Pathology* **164**, 1243–1251.
- Paronetto, M. P., Messina, V., Barchi, M., Geremia, R., Richard, S. and Sette, C.** (2011). Sam68 marks the transcriptionally active stages of spermatogenesis and modulates alternative splicing in male germ cells. *Nucleic Acids Res* **39**, 4961–4974.

- Paronetto, M. P., Zalfa, F., Botti, F., Geremia, R., Bagni, C. and Sette, C.** (2006). The nuclear RNA-binding protein Sam68 translocates to the cytoplasm and associates with the polysomes in mouse spermatocytes. *Mol. Biol. Cell* **17**, 14–24.
- Pazdernik, N. and Schedl, T.** (2012). Introduction to Germ Cell Development in *Caenorhabditis elegans*. In *Germ Cell Development in C. elegans*. Ed. Schedl, T., pp. 1–16. New York, NY: Springer New York.
- Peel, N., Dougherty, M., Goeres, J., Liu, Y. and O'Connell, K. F.** (2012). The *C. elegans* F-box proteins LIN-23 and SEL-10 antagonize centrosome duplication by regulating ZYG-1 levels. *J Cell Sci* **125**, 3535–3544.
- Pereira, S. F. F., Gonzalez, R. L. and Dworkin, J.** (2015). Protein synthesis during cellular quiescence is inhibited by phosphorylation of a translational elongation factor. *Proc. Natl. Acad. Sci. U.S.A.* **112**, E3274–81.
- Peter, M., Castro, A., Lorca, T., Le Peuch, C., Magnaghi-Jaulin, L., Dorée, M. and Labbé, J. C.** (2001). The APC is dispensable for first meiotic anaphase in *Xenopus* oocytes. *Nat Cell Biol* **3**, 83–87.
- Peters, J. M., Tedeschi, A. and Schmitz, J.** (2008). The cohesin complex and its roles in chromosome biology. *Genes Dev.* **22**, 3089–3114.
- Petroski, M. D. and Deshaies, R. J.** (2005). Function and regulation of cullin–RING ubiquitin ligases. *Nat. Rev. Mol. Cell Biol.* **6**, 9–20.
- Pérez-Sala, D., Boya, P., Ramos, I., Herrera, M. and Stamatakis, K.** (2009). The C-Terminal Sequence of RhoB Directs Protein Degradation through an Endo-Lysosomal Pathway. *PLoS ONE* **4**, e8117–15.
- Pintard, L., Willis, J. H., Willems, A., Johnson, J.-L. F., Srayko, M., Kurz, T., Glaser, S., Mains, P. E., Tyers, M., Bowerman, B., et al.** (2003). The BTB protein MEL-26 is a substrate-specific adaptor of the CUL-3 ubiquitin-ligase. *Nature* **425**, 311–316.
- Piqué, M., López, J. M., Foissac, S., Guigó, R. and Mendez, R.** (2008). A Combinatorial Code for CPE-Mediated Translational Control. *Cell* **132**, 434–448.
- Plotnikov, A., Zehorai, E., Procaccia, S. and Seger, R.** (2011). The MAPK cascades: Signaling components, nuclear roles and mechanisms of nuclear translocation. *Biochimica et Biophysica Acta (BBA) - Molecular Cell Research* **1813**, 1619–1633.
- Puoti, A. and Kimble, J.** (1999). The *Caenorhabditis elegans* sex determination gene mog-1 encodes a member of the DEAH-box protein family. *Molecular and Cellular Biology* **19**, 2189–2197.
- Radford, H. E., Meijer, H. A. and de Moor, C. H.** (2008). Translational control by cytoplasmic polyadenylation in *Xenopus* oocytes. *Biochimica et Biophysica Acta (BBA) - Gene Regulatory Mechanisms* **1779**, 217–229.
- Raught, B. and Gingras, A. C.** (2007). Signaling to Translation Initiation. In *Translational Control in Biology and Medicine. Cold Spring Harbor Monograph Archive*, **48**
- Ren, H., Koo, J., Guan, B., Yue, P., Deng, X., Chen, M., Khuri, F. R. and Sun, S.-Y.** (2013). The E3 ubiquitin ligases β -TrCP and FBXW7 cooperatively mediates GSK3-dependent Mcl-1 degradation induced by the Akt inhibitor API-1, resulting in apoptosis. *Mol. Cancer* **12**, 146.
- Resnick, R. J., Taylor, S. J., Lin, Q. and Shalloway, D.** (1997). Phosphorylation of the Src substrate Sam68 by Cdc2 during mitosis. *Oncogene* **15**, 1247–1253.

- Richter, J. D.** (2007). CPEB: a life in translation. *Trends in Biochemical Sciences* **32**, 279–285.
- Rogers, S., Wells, R. and Rechsteiner, M.** (1986). Amino acid sequences common to rapidly degraded proteins: the PEST hypothesis. *Science* **234**, 364–368.
- Roghi, C., Giet, R., Uzbekov, R., Morin, N., Chartrain, I., Le Guellec, R., Couturier, A., Dorée, M., Philippe, M. and Prigent, C.** (1998). The *Xenopus* protein kinase pEg2 associates with the centrosome in a cell cycle-dependent manner, binds to the spindle microtubules and is involved in bipolar mitotic spindle assembly. *J Cell Sci* **111** (Pt 5), 557–572.
- Rose, K. L., Winfrey, V. P., Hoffman, L. H., Hall, D. H., Furuta, T. and Greenstein, D.** (1997). The POU gene *ceh-18* promotes gonadal sheath cell differentiation and function required for meiotic maturation and ovulation in *Caenorhabditis elegans*. *Developmental Biology* **192**, 59–77.
- Rouget, C., Papin, C., Boureux, A., Meunier, A.-C., Franco, B., Robine, N., Lai, E. C., Pelisson, A. and Simonelig, M.** (2010). Maternal mRNA deadenylation and decay by the piRNA pathway in the early *Drosophila* embryo. *Nature* **467**, 1128–1132.
- Roussell, D. L. and Bennett, K. L.** (1993). *glh-1*, a germ-line putative RNA helicase from *Caenorhabditis*, has four zinc fingers. *Proceedings of the National Academy of Sciences* **90**, 9300–9304.
- Rual, J. F., Ceron, J., Koreth, J., Hao, T., Nicot, A. S., Hirozane-Kishikawa, T., Vandenhaute, J., Orkin, S. H., Hill, D. E., van den Heuvel, S., et al.** (2004). Toward improving *Caenorhabditis elegans* phenome mapping with an ORFeome-based RNAi library. *Genome Research* **14**, 2162–2168.
- Ryazanov, A. G. and Davydova, E. K.** (1989). Mechanism of elongation factor 2 (EF-2) inactivation upon phosphorylation. Phosphorylated EF-2 is unable to catalyze translocation. *FEBS Letters* **251**, 187–190.
- Ryder, S. P. and Massi, F.** (2010). Insights Into the Structural Basis of Rna Recognition by Star Domain Proteins. *Adv. Exp. Med. Biol.* **693**, 37–53.
- Salinas, L. S., Maldonado, E., Macías-Silva, M., Blackwell, T. K. and Navarro, R. E.** (2007). The DEAD box RNA helicase VBH-1 is required for germ cell function in *C. elegans*. *genesis* **45**, 533–546.
- Salz, H. K. and Erickson, J. W.** (2010). Sex determination in *Drosophila*: The view from the top. *Fly (Austin)* **4**, 60–70.
- Sambrook, J. and Russell, D. W.** (2006a). Agarose gel electrophoresis. *CSH Protoc* **2006**, pdb.prot4020.
- Sambrook, J. and Russell, D. W.** (2006b). SDS-Polyacrylamide Gel Electrophoresis of Proteins. *CSH Protoc* **2006**, pdb.prot4540–pdb.prot4540.
- Sanges, C., Scheuermann, C., Zahedi, R. P., Sickmann, A., Lamberti, A., Migliaccio, N., Baljuls, A., Marra, M., Zappavigna, S., Rapp, U., et al.** (2012). Raf kinases mediate the phosphorylation of eukaryotic translation elongation factor 1A and regulate its stability in eukaryotic cells. *Cell Death & Disease* **3**, e276.
- Saric, T., Graef, C. I. and Goldberg, A. L.** (2004). Pathway for degradation of peptides generated by proteasomes: a key role for thimet oligopeptidase and other metallopeptidases. *Journal of Biological Chemistry* **279**, 46723–46732.
- Sarikas, A., Hartmann, T. and Pan, Z.-Q.** (2011). The cullin protein family. *Genome Biol* **12**, 220.

- Sasagawa, Y., Sato, S., Ogura, T. and Higashitani, A.** (2006). *C. elegans* RBX-2-CUL-5- and RBX-1-CUL-2-based complexes are redundant for oogenesis and activation of the MAP kinase MPK-1. *FEBS Letters* **581**, 145–150.
- Scheckel, C., Gaidatzis, D., Wright, J. E. and Ciosk, R.** (2012). Genome-Wide Analysis of GLD-1-Mediated mRNA Regulation Suggests a Role in mRNA Storage. *PLoS Genetics* **8**, e1002742–12.
- Schedl, T. and Kimble, J.** (1988). *fog-2*, a germ-line-specific sex determination gene required for hermaphrodite spermatogenesis in *Caenorhabditis elegans*. *Genetics* **119**, 43–61.
- Schmid, M., Kuchler, B. and Eckmann, C. R.** (2009). Two conserved regulatory cytoplasmic poly(A) polymerases, GLD-4 and GLD-2, regulate meiotic progression in *C. elegans*. *Genes Dev.* **23**, 824–836.
- Schumacher, B., Hanazawa, M., Lee, M.-H., Nayak, S., Volkmann, K., Hofmann, R., Hengartner, M., Schedl, T. and Gartner, A.** (2005). Translational Repression of *C. elegans* p53 by GLD-1 Regulates DNA Damage-Induced Apoptosis. *Cell* **120**, 357–368.
- Schwarzstein, M., Wignall, S. M. and Villeneuve, A. M.** (2010). Coordinating cohesion, co-orientation, and congression during meiosis: lessons from holocentric chromosomes. *Genes Dev.* **24**, 219–228.
- Schweitzer, A., Aufderheide, A., Rudack, T., Beck, F., Pfeifer, G., Plitzko, J. M., Sakata, E., Schulten, K., Förster, F. and Baumeister, W.** (2016). Structure of the human 26S proteasome at a resolution of 3.9 Å. *Proc. Natl. Acad. Sci. U.S.A.* **113**, 7816–7821.
- Seervai, R. N. H. and Wessel, G. M.** (2013). Lessons for inductive germline determination. *Mol. Reprod. Dev.* **80**, 590–609.
- Seet, B. T., Dikic, I., Zhou, M.-M. and Pawson, T.** (2006). Reading protein modifications with interaction domains. *Nat. Rev. Mol. Cell Biol.* **7**, 473–483.
- Segref, A., Cabello, J., Clucas, C., Schnabel, R. and Johnstone, I. L.** (2010). Fate specification and tissue-specific cell cycle control of the *Caenorhabditis elegans* intestine. *Mol. Biol. Cell* **21**, 725–738.
- Setoyama, D., Yamashita, M. and Sagata, N.** (2007). Mechanism of degradation of CPEB during *Xenopus* oocyte maturation. *Proceedings of the National Academy of Sciences* **104**, 18001–18006.
- Sette, C.** (2010). Post-translational Regulation of STAR Proteins and Effects on Their Biological Functions. In *Germ Cell Development in C. elegans*. Ed. Schedl, T., pp. 54–66. Boston, MA: Springer US.
- Seydoux, G., Schedl, T. and Greenwald, I.** (1990). Cell-cell interactions prevent a potential inductive interaction between soma and germline in *C. elegans*. *Cell* **61**, 939–951.
- Shabek, N., Herman-Bachinsky, Y., Buchsbaum, S., Lewinson, O., Haj-Yahya, M., Hejjaoui, M., Lashuel, H. A., Sommer, T., Brik, A. and Ciechanover, A.** (2012). The Size of the Proteasomal Substrate Determines Whether Its Degradation Will Be Mediated by Mono- or Polyubiquitylation. *Molecular Cell* **48**, 87–97.
- Shimada, M., Kanematsu, K., Tanaka, K., Yokosawa, H. and Kawahara, H.** (2006). Proteasomal ubiquitin receptor RPN-10 controls sex determination in *Caenorhabditis elegans*. *Mol. Biol. Cell* **17**, 5356–5371.
- Simpson-Lavy, K. J., Oren, Y. S., Feine, O., Sajman, J., Listovsky, T. and Brandeis, M.** (2010). Fifteen years of APC/cyclosome: a short and impressive biography. *Biochem. Soc. Trans.* **38**,

78–82.

- Singh, G., Pratt, G., Yeo, G. W. and Moore, M. J.** (2015). The Clothes Make the mRNA: Past and Present Trends in mRNP Fashion. *Annu. Rev. Biochem.* **84**, 325–354.
- Skaar, J. R., Pagan, J. K. and Pagano, M.** (2013). Mechanisms and function of substrate recruitment by F-box proteins. *Nat. Rev. Mol. Cell Biol.* **14**, 369–381.
- Smorag, L., Xu, X., Engel, W. and Pantakani, D. V. K.** (2014). The roles of DAZL in RNA biology and development. *Wiley Interdisciplinary Reviews: RNA* **5**, 527–535.
- Sokolenko, S., George, S., Wagner, A., Tuladhar, A., Andrich, J. M. S. and Aucoin, M. G.** (2012). Co-expression vs. co-infection using baculovirus expression vectors in insect cell culture: Benefits and drawbacks. *Biotechnology Advances* **30**, 766–781.
- Sonneville, R. and Gönczy, P.** (2004). Zyg-11 and cul-2 regulate progression through meiosis II and polarity establishment in *C. elegans*. *Development* **131**, 3527–3543.
- Sönnichsen, B., Koski, L. B., Walsh, A. and Marschall, P.** (2005). Full-genome RNAi profiling of early embryogenesis in *Caenorhabditis elegans*. *Nature* **434**, 462–469.
- Spike, C., Meyer, N., Racen, E., Orsborn, A., Kirchner, J., Kuznicki, K., Yee, C., Bennett, K. and Strome, S.** (2008). Genetic Analysis of the *Caenorhabditis elegans* GLH Family of P-Granule Proteins. **178**, 1973–1987.
- Spitz, F. and Furlong, E. E. M.** (2012). Transcription factors: from enhancer binding to developmental control. *Nature Reviews Genetics* **13**, 613–626.
- Spratt, D. E., Walden, H. and Shaw, G. S.** (2014). RBR E3 ubiquitin ligases: new structures, new insights, new questions. *Biochem. J.* **458**, 421–437.
- Srayko, M., O'Toole, E. T., Hyman, A. A. and Müller-Reichert, T.** (2006). Katanin Disrupts the Microtubule Lattice and Increases Polymer Number in *C. elegans* Meiosis. *Current Biology* **16**, 1944–1949.
- Starostina, N. G., Lim, J.-M., Schvarzstein, M., Wells, L., Spence, A. M. and Kipreos, E. T.** (2007). A CUL-2 Ubiquitin Ligase Containing Three FEM Proteins Degrades TRA-1 to Regulate *C. elegans* Sex Determination. *Developmental Cell* **13**, 127–139.
- Starostina, N. G., Simpliciano, J. M., McGuirk, M. A. and Kipreos, E. T.** (2010). CRL2LRR-1 Targets a CDK Inhibitor for Cell Cycle Control in *C. elegans* and Actin-Based Motility Regulation in Human Cells. *Developmental Cell* **19**, 753–764.
- Stetina, Von, J. R. and Orr-Weaver, T. L.** (2011). Developmental Control of Oocyte Maturation and Egg Activation in Metazoan Models. *Cold Spring Harbor Perspectives in Biology* **3**, a005553–a005553.
- Subtelny, A. O., Eichhorn, S. W., Chen, G. R., Sive, H. and Bartel, D. P.** (2014). Poly(A)-tail profiling reveals an embryonic switch in translational control. *Nature* **508**, 66–71.
- Sugiura, R., Kita, A., Shimizu, Y., Shuntoh, H., Sio, S. and Kuno, T.** (2003). Feedback regulation of MAPK signalling by an RNA-binding protein. *Nature* **424**, 961–965.
- Sugiura, R., Satoh, R., Ishiwata, S., Umeda, N. and Kita, A.** (2011). Role of RNA-Binding Proteins in MAPK Signal Transduction Pathway. *J Signal Transduct* **2011**, 109746.
- Suh, N., Jedamzik, B., Eckmann, C. R., Wickens, M. and Kimble, J.** (2006). The GLD-2 poly(A) polymerase activates gld-1 mRNA in the *Caenorhabditis elegans* germ line. *Proceedings of the National Academy of Sciences* **103**, 15108–15112.

- Sulston, J. E. and Horvitz, H. R.** (1977). Post-embryonic cell lineages of the nematode, *Caenorhabditis elegans*. *Developmental Biology* **56**, 110–156.
- Sundaram, M. V.** (2013). Canonical RTK-Ras-ERK signaling and related alternative pathways. *WormBook* 1–38.
- Tadros, W., Goldman, A. L., Babak, T., Menzies, F., Vardy, L., Orr-Weaver, T., Hughes, T. R., Westwood, J. T., Smibert, C. A. and Lipshitz, H. D.** (2007). SMAUG Is a Major Regulator of Maternal mRNA Destabilization in *Drosophila* and Its Translation Is Activated by the PAN GU Kinase. *Developmental Cell* **12**, 143–155.
- Taieb, F. E., Gross, S. D., Lewellyn, A. L. and Maller, J. L.** (2001). Activation of the anaphase-promoting complex and degradation of cyclin B is not required for progression from Meiosis I to II in *Xenopus* oocytes. *Curr. Biol.* **11**, 508–513.
- Takahashi, M., Iwasaki, H., Inoue, H. and Takahashi, K.** (2002). Reverse genetic analysis of the *Caenorhabditis elegans* 26S proteasome subunits by RNA interference. *Biol. Chem.* 1263–1266.
- Tanaka, K. and Ichihara, A.** (1989). Half-Life of Proteasomes (Multiprotease Complexes) in Rat-Liver. *Biochemical and Biophysical Research Communications* **159**, 1309–1315.
- Tay, J. and Richter, J. D.** (2001). Germ cell differentiation and synaptonemal complex formation are disrupted in CPEB knockout mice. *Developmental Cell* **1**, 201–213.
- Tay, J., Hodgman, R., Sarkissian, M. and Richter, J. D.** (2003). Regulated CPEB phosphorylation during meiotic progression suggests a mechanism for temporal control of maternal mRNA translation. *Genes Dev.* **17**, 1457–1462.
- Teixeira, L. K. and Reed, S. I.** (2013). Ubiquitin Ligases and Cell Cycle Control. *Annu. Rev. Biochem.* **82**, 387–414.
- Thapar, R.** (2015). Structural basis for regulation of RNA-binding proteins by phosphorylation. *ACS Chem. Biol.* **10**, 652–666.
- Thom, G., Minshall, N., GIT, A., Argasinska, J. and Standart, N.** (2003). Role of cdc2 kinase phosphorylation and conserved N-terminal proteolysis motifs in cytoplasmic polyadenylation-element-binding protein (CPEB) complex dissociation and degradation. *Biochem. J.* **370**, 91–100.
- Thomas, J. H.** (2006). Adaptive evolution in two large families of ubiquitin-ligase adapters in nematodes and plants. *Genome Research* **16**, 1017–1030.
- Thompson, B. E., Bernstein, D. S., Bachorik, J. L., Petcherski, A. G., Wickens, M. and Kimble, J.** (2005). Dose-dependent control of proliferation and sperm specification by FOG-1/CPEB. *Development* **132**, 3471–3481.
- Thrower, J. S., Hoffman, L., Rechsteiner, M. and Pickart, C. M.** (2000). Recognition of the polyubiquitin proteolytic signal. *The EMBO Journal* **19**, 94–102.
- Tian, B. and Manley, J. L.** (2017). Alternative polyadenylation of mRNA precursors. *Nat. Rev. Mol. Cell Biol.* **18**, 18–30.
- Topisirovic, I., Svitkin, Y. V., Sonenberg, N. and Shatkin, A. J.** (2010). Cap and cap-binding proteins in the control of gene expression. *Wiley Interdisciplinary Reviews: RNA* **2**, 277–298.
- Trent, C., Purnell, B., Gavinski, S., Hageman, J., Chamblin, C. and Wood, W. B.** (1991). Sex-specific transcriptional regulation of the *C. elegans* sex-determining gene her-1. *Mechanisms of Development* **34**, 43–55.

- Udagawa, T., Swanger, S. A., Takeuchi, K., Kim, J. H., Nalavadi, V., Shin, J., Lorenz, L. J., Zukin, R. S., Bassell, G. J. and Richter, J. D. (2012). Bidirectional Control of mRNA Translation and Synaptic Plasticity by the Cytoplasmic Polyadenylation Complex. *47*, 253–266.
- Uzbekova, S., Arlot-Bonnemains, Y., Dupont, J., Dalbies-Tran, R., Papillier, P., Pennetier, S., Thelie, A., Perreau, C., Mermillod, P., Prigent, C., et al. (2008). Spatio-Temporal Expression Patterns of Aurora Kinases A, B, and C and Cytoplasmic Polyadenylation-Element-Binding Protein in Bovine Oocytes During Meiotic Maturation. *Biology of Reproduction* **78**, 218–233.
- van den Heuvel, S. (2005). Cell-cycle regulation. *WormBook* 1–16.
- Vernet, C. and Artzt, K. (1997). STAR, a gene family involved in signal transduction and activation of RNA. *Trends in Genetics* **13**, 479–484.
- Villaescusa, J. C., Buratti, C., Penkov, D., Mathiasen, L., Planagumà, J., Ferretti, E. and Blasi, F. (2009). Cytoplasmic Prep1 Interacts with 4EHP Inhibiting Hoxb4 Translation. *PLoS ONE* **4**, e5213–12.
- Villalba, A., Coll, O. and Gebauer, F. (2011). Cytoplasmic polyadenylation and translational control. *Current Opinion in Genetics & Development* **21**, 452–457.
- Villeneuve, A. M. and Hillers, K. J. (2001). Whence meiosis? *Cell* **106**, 647–650.
- Vishnu, M. R., Sumaroka, M., Klein, P. S. and Liebhaber, S. A. (2011). The poly(rC)-binding protein alphaCP2 is a noncanonical factor in *X. laevis* cytoplasmic polyadenylation. *RNA* **17**, 944–956.
- Wang, J. T. and Seydoux, G. (2012). Germ Cell Specification. In *Germ Cell Development in C. elegans*. Ed. Schedl, T., pp. 17–39. New York, NY: Springer New York.
- Wang, L., Eckmann, C. R., Kadyk, L. C., Wickens, M. and Kimble, J. (2002). A regulatory cytoplasmic poly(A) polymerase in *Caenorhabditis elegans*. *Nature* **419**, 312–316.
- Wang, Z., Liu, P., Inuzuka, H. and Wei, W. (2014). Roles of F-box proteins in cancer. *Nature Publishing Group* **14**, 233–247.
- Weill, L., Belloc, E., Bava, F.-A. and Mendez, R. (2012). Translational control by changes in poly(A) tail length: recycling mRNAs. *Nature Publishing Group* **19**, 577–585.
- Welcker, M. and Clurman, B. E. (2008). FBW7 ubiquitin ligase: a tumour suppressor at the crossroads of cell division, growth and differentiation. *Nat Rev Cancer* **8**, 83–93.
- Wigington, C. P., Williams, K. R., Meers, M. P., Bassell, G. J. and Corbett, A. H. (2014). Poly(A) RNA-binding proteins and polyadenosine RNA: new members and novel functions. *Wiley Interdisciplinary Reviews: RNA* **5**, 601–622.
- Willems, A. R., Schwab, M. and Tyers, M. (2004). A hitchhiker's guide to the cullin ubiquitin ligases: SCF and its kin. *Biochimica et Biophysica Acta (BBA) - Molecular Cell Research* **1695**, 133–170.
- Winkler, G. S. (2010). The mammalian anti-proliferative BTG/Tob protein family. *J. Cell. Physiol.* **222**, 66–72.
- Wolke, U., Jezuit, E. A. and Priess, J. R. (2007). Actin-dependent cytoplasmic streaming in *C. elegans* oogenesis. *Development* **134**, 2227–2236.
- Wong, L. C., Costa, A., McLeod, I., Sarkeshik, A., Yates, J., Kyin, S., Perlman, D. and Schedl, P. (2011). The functioning of the *Drosophila* CPEB protein Orb is regulated by phosphorylation

- and requires casein kinase 2 activity. *PLoS ONE* **6**, e24355.
- Wood, W. B.** (1988). *The Nematode *Caenorhabditis elegans**. Ed. Wood, W. B. Cold Spring Harbor Laboratory Press.
- Wright, J. E., Gaidatzis, D., Senften, M., Farley, B. M., Westhof, E., Ryder, S. P. and Ciosk, R.** (2011). A quantitative RNA code for mRNA target selection by the germline fate determinant GLD-1. *The EMBO Journal* **30**, 533–545.
- Wu, G., Hubbard, E. J. A., Kitajewski, J. K. and Greenwald, I.** (1998). Evidence for functional and physical association between *Caenorhabditis elegans* SEL-10, a Cdc4p-related protein, and SEL-12 presenilin. *Proceedings of the National Academy of Sciences* **95**, 15787–15791.
- Wu, L., Good, P. J. and Richter, J. D.** (1997). The 36-kilodalton embryonic-type cytoplasmic polyadenylation element-binding protein in *Xenopus laevis* is ElrA, a member of the ELAV family of RNA-binding proteins. *Molecular and Cellular Biology* **17**, 6402–6409.
- Wu, W. K. K., Volta, V., Cho, C. H., Wu, Y. C., Li, H. T., Yu, L., Li, Z. J. and Sung, J. J. Y.** (2009). Repression of protein translation and mTOR signaling by proteasome inhibitor in colon cancer cells. *Biochemical and Biophysical Research Communications* **386**, 598–601.
- Xu, L., Paulsen, J., Yoo, Y., Goodwin, E. B. and Strome, S.** (2001). *Caenorhabditis elegans* MES-3 is a target of GLD-1 and functions epigenetically in germline development. *Genetics* **159**, 1007–1017.
- Xu, L., Wei, Y., Reboul, J., Vaglio, P., Shin, T.-H., Vidal, M., Elledge, S. J. and Harper, J. W.** (2003). BTB proteins are substrate-specific adaptors in an SCF-like modular ubiquitin ligase containing CUL-3. *Nature* **425**, 316–321.
- Yamagishi, R., Tsusaka, T., Mitsunaga, H., Maehata, T. and Hoshino, S.-I.** (2016). The STAR protein QKI-7 recruits PAPD4 to regulate post-transcriptional polyadenylation of target mRNAs. *Nucleic Acids Res* **44**, 2475–2490.
- Yamanaka, A., Yada, M., Imaki, H., Koga, M., Ohshima, Y. and Nakayama, K.-I.** (2002). Multiple Skp1-Related Proteins in *Caenorhabditis elegans*. *Current Biology* **12**, 267–275.
- Yan, X., Hoek, T. A., Vale, R. D. and Tanenbaum, M. E.** (2016). Dynamics of Translation of Single mRNA Molecules *In Vivo*. *Cell* **165**, 976–989.
- Yerlikaya, A., Kimball, S. R. and Stanley, B. A.** (2008). Phosphorylation of eIF2 α in response to 26S proteasome inhibition is mediated by the haem-regulated inhibitor (HRI) kinase. *Biochem. J.* **412**, 579–588.
- Zanetti, S. and Puoti, A.** (2012). Sex Determination in the *Caenorhabditis elegans* Germline. In *Germ Cell Development in C. elegans* (ed. Schedl, T., pp. 41–69. New York, NY: Springer New York.
- Zeke, A., Bastys, T., Alexa, A., Garai, A., Meszaros, B., Kirsch, K., Dosztanyi, Z., Kalinina, O. V. and Remenyi, A.** (2015). Systematic discovery of linear binding motifs targeting an ancient protein interaction surface on MAP kinases. *Molecular Systems Biology* **11**, 837–837.
- Zhang, B., Gallegos, M., Puoti, A., Durkin, E. and Fields, S.** (1997). A conserved RNA-binding protein that regulates sexual fates in the *C. elegans* hermaphrodite germ line. *Nature* **390**, 477–484.
- Zhang, M., Lam, T. T., Tonelli, M., Marzluff, W. F. and Thapar, R.** (2012). Interaction of the histone mRNA hairpin with stem-loop binding protein (SLBP) and regulation of the SLBP-RNA complex by phosphorylation and proline isomerization. *Biochemistry* **51**, 3215–3231.

- Zhang, Y., Yan, L., Zhou, Z., Yang, P., Tian, E., Zhang, K., Zhao, Y., Li, Z., Song, B., Han, J., et al.** (2009). SEPA-1 Mediates the Specific Recognition and Degradation of P Granule Components by Autophagy in *C. elegans*. *Cell* **136**, 308–321.
- Zheng, N., Wang, Z. and Wei, W.** (2016a). Ubiquitination-mediated degradation of cell cycle-related proteins by F-box proteins. *Int. J. Biochem. Cell Biol.* **73**, 99–110.
- Zheng, N., Zhou, Q., Wang, Z. and Wei, W.** (2016b). Recent advances in SCF ubiquitin ligase complex: Clinical implications. *BBA - Reviews on Cancer* **1866**, 12–22.
- Zhong, W., Feng, H., Santiago, F. E. and Kipreos, E. T.** (2003). CUL-4 ubiquitin ligase maintains genome stability by restraining DNA-replication licensing. *Nature* **423**, 885–889.

Acknowledgements

First and foremost, I would like to thank Prof. Dr. Christian R. Eckmann for giving me the opportunity to work in his lab and for being always available and open to discuss scientific problems and ideas. I highly appreciate his expertise and advice that greatly helped in performing the experiments. I am thankful for the support he offered throughout the whole time I spent on the thesis work.

I wish to thank members of my Thesis Advisory Committee, Prof. Dr. Elly Tanaka and Prof. Dr. Tony Hyman for valuable comments on my project, inspiring discussions and advice on shaping the publication.

Special thanks go to Prof. Dr. Eli Knust and Prof. Dr. Christian Dahmann for taking the time to review my thesis.

I am very thankful to Dr. David Drechsel, Dr. Régis Lemaitre and Dr. Barbara Borgonovo for their support and assistance in the protein work.

I would like to greatly thank past and present lab members for introducing me to the work with *C. elegans*, for generating and sharing protocols, worm strains and reagents, and for creating an outstanding working environment.

Last but not least, I wish to thank my family and friends, whose support was, and will always be, absolutely invaluable.

Declaration

Erklärung entsprechend §5.5 der Promotionsordnung

Hiermit versichere ich, dass ich die vorliegende Arbeit ohne unzulässige Hilfe Dritter und ohne Benutzung anderer als der angegebenen Hilfsmittel angefertigt habe; die aus fremden Quellen direkt oder indirekt übernommenen Gedanken sind als solche kenntlich gemacht. Die Arbeit wurde bisher weder im Inland noch im Ausland in gleicher oder ähnlicher Form einer anderen Prüfungsbehörde vorgelegt.

Die Dissertation wurde im Zeitraum vom 01.02.2011 bis 26.01.2017 verfasst und von Prof. Dr. Christian Eckmann, Max-Planck-Institut für molekulare Zellbiologie und Genetik (MPI-CBG), Dresden, derzeit Martin-Luther-Universität Halle-Wittenberg, Halle (Saale), betreut.

Meine Person betreffend erkläre ich hiermit, dass keine früheren erfolglosen Promotionsverfahren stattgefunden haben.

Ich erkenne die Promotionsordnung der Fakultät für Mathematik und Naturwissenschaften, Technische Universität Dresden an.

Date, *Signature*